Myoelectric Controls and Upper Limb Prosthetics Symposium

Symposium Proceedings

August 12-15, 2024

Fredericton, New Brunswick, Canada

MEC24

UNB EST. 1785 UNIVERSITY OF NEW BRUNSWICK | Institute of Biomedical Engineering

TABLE OF CONTENTS

Clinical Practice

A MODULAR SOLUTION TO A UNIQUE DESIGN REQUEST FOR A SHOULDER DISSARTICULATION PROSTHESIS: A CASE STUDY

Heather Daley, CP, Wendy Hill, OT, Dan Dafonseca, RTP

Atlantic Clinic for Upper Limb Prosthetics, Institute of Biomedical Engineering, UNB

ABSTRACT

This case study details the development of a customized myoelectric prosthesis for a patient with a modified shoulder disarticulation level amputation, focusing on the integration of a novel detachable arm feature to enhance user comfort and functionality. By employing additive manufacturing technology and innovative design strategies, a prosthetic solution was crafted to meet the specific needs of the patient, including prolonged wear and ease of use with the most notable quick-disconnect mechanisms. The resulting prosthesis not only fulfilled the patient's request for a modular, lightweight arm but also significantly improved his quality of life by allowing for greater flexibility, versatility, and adaptability in daily activities. This work demonstrates the potential for tailored prosthetic solutions to address complex challenges, highlighting the importance of patient-catered design choices in the field of prosthetics.

INTRODUCTION

Shoulder disarticulation level amputations, constituting only 3% of all traumatic amputations, present distinct challenges in terms of prosthesis fitting and functionality [1]. Unlike more common amputations such as transradial or transhumeral, the limited availability of control sites at the proximal level poses a unique obstacle for achieving optimal functionality in prostheses for shoulder disarticulation amputees. Brachial plexus injuries further complicate matters, as they restrict the use of distal muscles as potential control sites for the prosthesis [2].

Functional prostheses at this level tend to be heavy, bulky, and require control options to operate multiple joints including shoulder, elbow, wrist, and hand motion. Body-powered prostheses for this proximal type of amputation are generally not accepted by patients because of the complexity of cable control for multiple joints and the limited functional grasp given the amount of effort required to activate a terminal device[3]. Body movements required for this level include scapular protraction, retraction, elevation, and rotation which can be particularly challenging or impossible, especially after a brachial plexus injury.

In response to these challenges, powered prostheses emerge as a viable solution for shoulder disarticulation amputees, offering increased functional gripping power with reduced effort from the body [4], [5]. The use of powered prostheses becomes crucial in addressing the limitations associated with body-powered alternatives, providing a more user-friendly and efficient option. This case study outlines a unique design of a powered prosthesis with modular arm sections to meet the functional needs of the patient. The modular design allows for customization and adaptability, addressing the unique complexities associated with this level of amputation and enhancing the overall usability and functionality of the device.

MEDICAL AND PROSTHETIC HISTORY

TC experienced a workplace accident in 1988 when his arm got caught in an industrial bread mixer which resulted in a brachial plexus stretch injury and spasmodic torticollis. After extensive rehab and several surgeries to improve range of motion and hand function, he eventually elected to have his arm amputated at a modified shoulder disarticulation level four years after his original injury. Before his amputation, he experienced significant chronic pain, weakened muscles in the neck and shoulder area, and a non-functional and insensate arm. Due to the high-riding scapula, a major muscle release procedure including trapezius and levator scapulae muscles was performed in conjunction with amputation. The humeral head remained intact. The surgical outcome successfully improved TC's shoulder and neck positioning, enhancing his overall posture. Nevertheless, he continued to experience pain, weakness, and a diminished range of motion in his neck post-surgery.

Following the injury, TC sought care at a different prosthetic clinic for several years. It was at this clinic that he acquired his initial powered prosthesis, which featured a linear transducer for hand open/close control. In an effort to alleviate the burden of the heavy arm while keeping his socket on, TC requested the detachability of the humeral section of the prosthesis. Unfortunately, the clinic expressed skepticism about its feasibility due to the incorporated electronics. Subsequently, TC returned home and took matters into his own hands. He ingeniously incorporated a seatbelt buckle into the shoulder joint and wired an auxiliary ¼" jack to the linear transducer cable, allowing for easy detachment (Fig. 1). This inventive solution not only addressed his desire for a detachable humeral section but also showcased TC's resourcefulness in enhancing the functionality and comfort of his powered prosthesis.

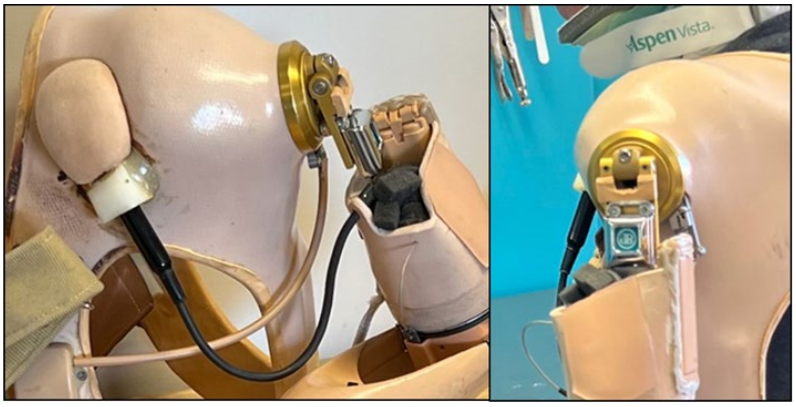

Figure 1: TC's initial adapted powered prosthesis featuring an integrated seatbelt buckle in the shoulder joint and an auxiliary ¼" jack for convenient detachment of the humeral section. This inventive modification was implemented by TC at home to alleviate weight and relieve pain while keeping his socket on.

In 2009 TC received his second powered prosthesis from our clinic with an improved socket design and upgrades to the electronic connections. He returned to our clinic in 2022 requesting a new prosthesis. His previous arm was no longer fitting properly, and the electronics had failed. During our consultation we discussed socket design, materials, terminal devices, and control strategies. TC emphasized his priorities for the design, which included a lightweight structure, a shortened forearm, and a removable arm segment. Our decision to accommodate this request was driven by two primary factors. Firstly, recognizing TC's strong preference for a removable arm, we anticipated that he might attempt self-modifications if not provided with this feature. Secondly, we recognized the intrinsic value of this modification for enhancing his ability to engage in functional activities with reduced pain. Thus, our aim was not only to meet TC's immediate needs but also to contribute to his long-term comfort and functionality.

In order to accomplish this, we needed an easy-to-use locking mechanism that incorporated an electronic pass through, while being able to don and doff without visual feedback due to the limited range of motion in his neck, so that the arm could be removed and reconnected in one swift motion without adding any extra steps for reconnecting electronics.

PROSTHETIC TREATMENT

A lightweight hybrid silicone socket was fabricated with pre-preg carbon-fiber for strength and flexibility. We also incorporated a wide custom silicone axilla strap to distribute the forces and improve comfort. After trials and demos of various components, we decided an Ottobock Ergoarm Hybrid Plus, ETD2, and TASKA hand would best meet his functional needs, with a linear transducer for single site control using chest expansion for excursion. With the use of magnetic Fidlocks, including a boa style Fidlock for the linear transducer cable, this also made donning and doffing far easier than traditional Velcro or buckles.

Designs were drafted for a humeral component that bisected the Axis shoulder joint and the Ottobock elbow joint as the detachable location. This also had to contain the electronic passthrough and lock mechanism all in one unit, while components such as batteries and other heavy parts had to be housed in the detachable portion of the arm. The manufacturing method of choice became 3D printing with the lightest and strongest material available to us at the time, a carbon fiber reinforced Nylon 12 filament (PA12 CF). After several iterations, Fuse Deposition Modeling (FDM) printed PA12 CF worked well as it consequently had a coarse surface finish which bonded well to the carbon

fiber lamination done over the printed parts. A carbon-fiber lamination was necessary to ensure appropriate levels of strength.

This 3D printed design involved non-variable conditions: Locking quick disconnect, anti-rotation, electronic pass through, as well as swift and easy one-handed operation for attachment/detachment. The lock integrated in the design was a smooth pin Icelock 651, and the electronic junction was a spring-loaded pin style connection. Numerous iterations of the modular system were tested with multiple diagnostic fitting stages until a final device was produced (Fig 2).

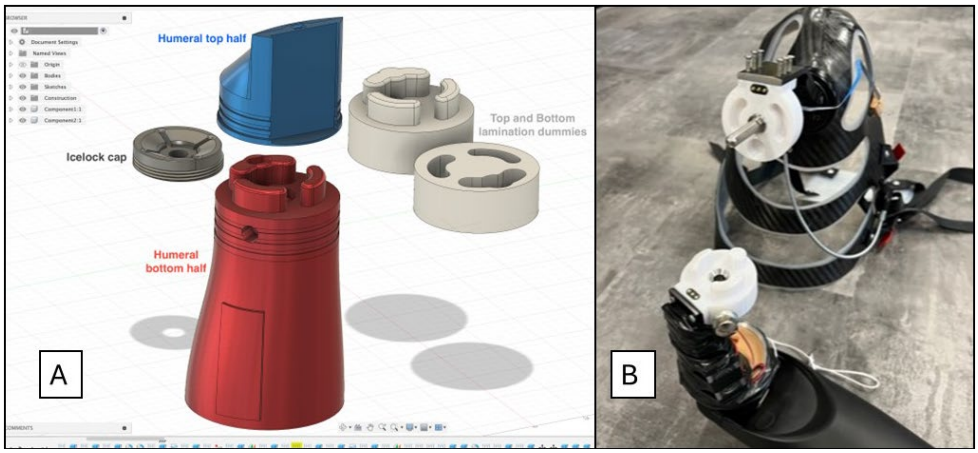

Figure 2: Design process for humeral disconnect. A) CAD drawings B) trial on test socket with components in place

During one of the socket trials, TC mentioned that a second shortened arm segment without an elbow would be useful for some of his applications when using power tools at shoulder level. He also mentioned there were times, especially for doing yard work, that he required a secure grasp with a quick release for tools such as a snow blower, lawnmower and weed trimmer. This conversation led to the design of two additional arm segments (one powered and one passive) that could be used interchangeably with his prosthesis. The final device is shown in Figure 3 below.

Figure 3: Final Prosthesis with three interchangeable arm segments

OUTCOME

The result of this fitting was the creation of a prosthetic device that fulfilled all the patient's criteria: lightweight, flexible, comfortable, and functional. The interchangeable arm segments, designed to address diverse needs, provided significant value. Now, he can maintain his socket for extended periods, thanks to the convenience of the quick-disconnecting arms. Embracing the versatility of his three modular fitting arms, he seamlessly incorporates them into various activities. However, a challenge emerged after several months of use related to the smooth pin lock. The continuous exposure to high vibration power tools led to a gradual loosening of the smooth pin lock, almost resulting in an electronic connection loss. To rectify this issue, the smooth pin Icelock was replaced with the same format ratcheting style Icelock 621.

Through the application of additive manufacturing and an open mind, this project successfully addressed the unique challenges presented by the patient's needs, emphasizing modularity, comfort, and function. The process involved numerous trial fittings and design iterations, particularly in refining the locking mechanism. The final prosthesis significantly improved the patient's quality of life.

*Figure 4: Training with prosthesis A) using power tools as he would at home and B) doing meal prep. *Written consent was obtained for the use of the photos in this paper.*

This case demonstrates the potential of tailored, iterative development processes in advancing prosthetic function and patient satisfaction. The success of this device reinforces the value of continuous improvement and patient involvement in developing prosthetics that not only meet but exceed user expectations.

REFERENCES

[1] T. R. DILLINGHAM, L. E. PEZZIN, and E. J. MACKENZIE, “Limb Amputation and Limb Deficiency: Epidemiology and Recent Trends in the United States,” *South Med J*, 2002, doi: 10.1097/00007611-200208000-00018.

[2] Dr. A. U. S, Dr. D. T. E, and Dr. A. F. E, “Damn Nuisance from brachial Plexus Injury, An Uncommon Indication for Shoulder Disarticulation,” *SAS Journal of Surgery*, vol. 8, no. 5, 2022, doi: 10.36347/sasjs.2022.v08i05.011.

[3] B. Petersen, “Amputations about the shoulder: Prosthetic management,” in *Atlas of Amputations and Limb Deficiencies*, Fourth., vol. 1, I. Krajbich, M. Pinzur, B. Potter, and P. Stevens, Eds., Rosemont: American Academy of Orthopedic Surgeons, 2016, pp. 287–298.

[4] R. D. Lipschutz, B. Lock, J. Sensinger, A. E. Schultz, and T. A. Kuiken, “Use of two-axis joystick for control of externally powered shoulder disarticulation prostheses,” *J Rehabil Res Dev*, vol. 48, no. 6, 2011, doi: 10.1682/JRRD.2010.08.0161.

[5] R. D. Lipschutz, T. A. Kuiken, L. A. Miller, G. A. Dumanian, and K. A. Stubblefield, “Shoulder disarticulation externally powered prosthetic fitting following targeted muscle reinnervation for improved myoelectric control,” in *Journal of Prosthetics and Orthotics*, 2006. doi: 10.1097/00008526-200604000-00002.

BARRIERS AND FACILITATORS TO ADOPTING A CLINICIAN DASHBOARD SUPPORTING UPPER LIMB MYOELECTRIC-CONTROLLED PROSTHESES

Miriam R. Rafferty,[1,2] Paulo Aco,[1] Kristi L. Turner,[3] Laura A. Miller,[3] Blair A. Lock,[4] Zachary A. Wright[4]

[1]Strength+Endurance Lab, Shirley Ryan AbilityLab, Chicago, IL, USA, [2]Departments of Physical Medicine and Rehabilitation and Medical Social Sciences, Northwestern University Feinberg School of Medicine, Chicago, IL, USA; [3]Center for Bionic Medicine, Shirley Ryan AbilityLab, Chicago, IL, USA; [4]Coapt, LLC, Chicago, IL, USA

ABSTRACT

Integrating the use of myoelectric-controlled upper limb prostheses into daily life can be complex. A dashboard reporting data and insights on real-world prosthetic use and performance could improve information available for clinicians to inform care, as well as communication among end-users (prosthesis wearers) and their clinical care providers. The purpose of this project is to blend implementation science and user-centered design methodology to inform the development and refinement of a dashboard that improves efficiency and supports clinical decision-making related to prosthesis training and clinical support. We used a mixed methods approach with a stakeholder advisory panel, semi-structured interviews, and surveys from occupational therapists, prosthetists, end-users, and other technology stakeholders. Interviews reveal clinician and end-user concern related to design, adaptability of the platform to meet the needs, capability, and opportunity of the clinicians, as well as to address motivation of end-users. The dashboard may improve communication but also could create work infrastructure challenges that make the dashboard have a relative disadvantage over other forms of communication. Surveys suggest good usability, acceptability, appropriateness, and feasibility. However, occupational therapists, the primary target population, have the lowest perceived usability and feasibility scores at the current point of dashboard design and conceptualization. In summary, mixed methods data from clinicians and prosthesis wearers provides valuable information that can drive improved development of a dashboard.

INTRODUCTION

Upper limb loss/absence is a significant cause of disability that limits the ability to perform routine daily activities. While prosthetic devices can help restore function of the lost limb, learning to fully incorporate the prosthesis into daily life is a substantial hurdle for many wearers [1]. There are many barriers experienced by people with limb loss/absence, as well as the clinicians (occupational therapists and prosthetists) who help them train to use new prostheses effectively. Improving the quality of prosthesis training is crucial for wearers to achieve optimal function and long-term use.

Unfortunately, insufficient tools exist to inform clinicians about daily prosthesis use and performance outside the clinic. This lack of information makes it difficult for clinicians to make informed decisions to be able to administer effective treatments to improve real-world performance. Consequently, clinicians are “flying blind” once wearers leave the clinic. A clinician-facing dashboard (i.e., a web-based software application) that provides them access to objective, real-world measures and actionable data insights and suggestions could support their intuition and facilitate their decision-making to improve clinical efficiency, and ultimately, rehabilitation outcomes.

Myoelectric-controlled prostheses add technical and clinical complexity [2], which can be a barrier to rehabilitation technology uptake [3]. Many technology developers are comfortable with technology including sensors and software, but prosthesis wearers and clinicians may be less comfortable with these technological advancements. Creating systems, such as a clinician dashboard, that could improve the comfort and competence of clinical and community end-users is essential for the sustained success and uptake of myoelectric controlled devices.

This mixed method study uses implementation science and user-centered design methodology to better understand and address barriers to myoelectric-controlled upper limb prostheses, as well as to develop a clinician dashboard for occupational therapists treating individuals with upper limb loss. First, we engaged a multidisciplinary advisory board to enable partnership between the industry sponsor, clinical and community advisors. Second, we conducted qualitative interviews with occupational therapists, prosthetists, upper limb myoelectric prosthesis wearers, and other

technology stakeholders. Third, we administered a survey to better understand features that would be valued by interview participants, as well as key pre-implementation metrics of usability, feasibility, acceptability, and appropriateness of the dashboard prototype . Our overall hypothesis is that acceptability and future uptake of the dashboard will be enhanced by our application of these user-centered methods.

METHODS

Mixed Methods Design and Multidisciplinary Advisory Board

A convergent parallel mixed methods approach is used including insight from a multidisciplinary advisory board, interviews, and surveys. The advisory board includes five industry representatives, two upper limb myoelectric control wearers, as well as one occupational therapist and one prosthetist on the research team. Key advisory board roles are to provide input on recruitment, interview guides, and data interpretation to ensure that the data is integrated through the lens of practical user experience (clinician and community member). As the results are shared with the advisory board, the co-investigators (MR, ZW) lead collaborative discussions to triangulate data using a convergent parallel approach. Forthcoming think-aloud sessions will guide dashboard refinements.

Interviews

Qualitative research methods include interviewing occupational therapists, prosthetists, upper limb myoelectric control wearers, and other technology stakeholders. Other technology stakeholders could be individuals that work for industry in research and development, sales, or health policy. The goal was at least 12 clinicians and 12 other end-users (prosthesis wearers), as 12 has been shown to be sufficient to reach saturation of themes [4]. Participants are interviewed by someone trained in semi-structured interview techniques who has the same background (*e.g.* occupational therapist (KT), prosthetist (LM), a non-clinician interviews lay/end-user participants (PA)). Informed consent was obtained from each participant under the guidelines and approval of Northwestern University IRB (ID#: STU00219595) prior to study participation.

Semi-structured interviews take 20-40 minutes. They include an initial series of questions about themselves (demographics), their relevant experiences with prostheses, as well as barriers and facilitators to prosthetics rehabilitation. Then all participants watch an approximately 7-minute-long video describing the purpose of the Clinician Dashboard with some visuals suggesting at features that may be included in the Dashboard. Then participants answer another series of semi-structured questions about how they could use the Dashboard, as well as features they would want to see. Probes are used to ask for clarification and additional information when needed.

Interviews are conducted over Zoom. They are audio recorded, transcribed professionally, de-identified, and uploaded into qualitative analysis software (Dedoose, 9.2.005, Los Angeles, CA, USA). Transcripts are coded using a combination of deductive and inductive codes. Coders first use directed content analysis [5] to assign codes related to barriers and facilitators of future implementation based on the constructs defined in the Consolidated Framework for Implementation Research version 2.0 (CFIR), thereby maximizing generalizability for future studies [6]. Each coder (MR, PA, KT, LM) brings unique experience based on their research and clinical backgrounds to share during coding discussions. Each transcript is coded by two raters, blind to the other's codes. Codes are then compared. An additional coder assists with developing consensus as needed when there are discrepancies between coders.

Surveys

Surveys were sent to each interview participants following completion of the interview. Surveys include items selected from previously validated surveys of usability, feasibility, acceptability, and appropriateness. Open ended questions are available but not required to be completed soliciting additional feedback or information. Usability is measured using the System Usability Scale (SUS) [7]. Research indicate that scores over 68% indicates good usability [8]. Participants also complete the Feasibility of Intervention Measure (FIM), Acceptability of Intervention Measure (AIM), and Intervention Appropriateness Measure (IAM) [9]. During survey pretesting with the Advisory Board, surveys were modified to reduce the number of questions and overall study burden. The usability survey was modified to include 6 of 10 questions (scored 0-4). Two of four possible questions were asked about acceptability and feasibility, and only one of four questions on appropriateness was asked (scored 1-5). Survey data is described with sum or means scores based on the convention for that survey, using descriptive statistics.

RESULTS

Multidisciplinary Advisory Board

The advisory board has met 7 times an average of 4 ± 1 weeks apart. Key insights added by the advisory board include the importance of gaining insight from other non-clinician technology stakeholders, recruitment input, and advice on interpretation of suggestions for clinician dashboard design and features.

Interviews and Surveys

At approximately 80% of our recruitment goal, 29 interviews have been completed, including 18 clinicians and 11 non-clinicians (8 individuals with upper limb loss). Table 1 describes the participant demographics and experience within their role and myoelectric control use. 100% of current participants are white and nonhispanic.

Table 1: Participant characteristics

	Occupational Therapist	**Prosthetist**	**End-User**	**Technology Stakeholder**
Number of participants	9	9	8	3
Age (years ± std)	47.6 ± 12.17	46.5 ± 16.8	43.8 ± 12.6	42.3 ± 8.6
Male, n (%) Female, n (%)	0 (0%) 9 (100%)	8 (89%) 1 (11%)	4 (50%) 4 (50%)	1 (33%) 2 (67%)
Experience (# of years as a clinician or with upper-limb loss)	23.4 ± 12.3	26.0 ± 7.4	15.7 ± 13.3	
Congenital limb loss, n (%) Traumatic/Acquired, n (%)			2 (25%) 6 (75%)	
Duration of time training people with upper extremity limb-loss (years)	11.3 ± 7.1	23.3 ± 8.2		
Duration of time working with pattern recognition myoelectric prostheses (years)	6.2 ± 3.3	9.6 ± 3.4	4.4 ± 3.3	8.3 ± 2.4

Barriers and facilitators related to novel technologies were coded to CFIR. Related to the dashboard itself, simple design, adaptability for different patients, and providing relative advantage over other means of data sharing and communication were key considerations. Interviewees commented on the needs, capabilities, and opportunities of the occupational therapists who would be using the dashboard. In contrast, the needs of the end-users were less commonly discussed. Instead, end-user motivators, capability, and opportunity were considered important related to potential barriers to the adoption. Related to organizations that would be adopting the Dashboard (inner setting and processes), interviews indicated the importance of considering communication, engaging users, as well as work infrastructure. Outside of a single organization (outer setting), the dashboard was perceived as potentially facilitating partnerships and connections. However, financing myoelectric controlled devices, health policy and legal ramifications were perceived to be barriers. Clinicians suggested improvements to adaptability and data presentation, while end-users suggested a variety of games and forums to increase communication and connection.

The survey results are described in Table 2. All acceptability and appropriateness values were greater than 80% of the possible score, indicating good pre-implementation potential. However, occupational therapists provided relatively lower scores for usability and feasibility. For this clinician dashboard target population, the average usability score of 40.0 of 60 represents 66.7% of the total possible available score, which is currently below the 68% usability target set by the developers of the System Usability Scale.

Table 2: Pre-implementation scores for the Clinician Dashboard

Construct (Score Type, Range)	**Usability (sum, 0-60)**	**Acceptability (average, 1-5)**	**Feasibility (average, 1-5)**	**Appropriateness (average, 1-5)**
Occupational Therapists (n=9)	40.0 ± 5.0	4.4 ± 0.6	3.9 ± 0.5	4.4 ± 0.5
Prosthetists (n=9)	44.7 ± 8.0	4.2 ± 0.5	4.2 ± 0.6	4.2 ± 0.4
End-Users (n=8)	45.9 ± 7.1	4.4 ± 0.6	4.6 ± 0.4	4.1 ± 0.4
Tech Stakeholders (n=3)	45.8 ± 8.2	5.0 ± 0	5.0 ± 0	5.0 ± 0

DISCUSSION

This work emphasizes the importance of clinical and end-user engagement in the research and development process for novel technologies. We use an innovative approach to combine implementation research methodology and user-centered design. The data highlights the use of pre-implementation outcomes such as usability, feasibility, acceptability, and adoption. Achieving high scores in these domains is thought to facilitate future adoption of technology.

First, our qualitative pre-implementation data corroborate prior research on uptake of novel technologies. Our past research indicates that ease of use, time to set up, and relative advantage are some of the most important barriers [3]. Similarly, we heard in our interviews that simple design was valued and clinicians expressed concern related to the relative advantage of information in the dashboard compared to their current clinical techniques and workflows [3]. The importance of adapting the dashboard to different clinical needs and patient motivators, such as communication preferences, are novel.

Limitations of this research thus far includes the lack of heterogeneity of participants. High proportions of white prosthesis wearers may be indicative of barriers to technology access and cost-related barriers for myoelectric control in underrepresented populations. Additionally, high proportions of end-users with traumatic limb loss may reflect greater prosthesis coverage of myoelectric controlled devices by workers compensation insurance. We are actively recruiting additional interview participants in underrepresented groups.

The interviews and surveys with key stakeholders are the first stage of this research which are being conducted in parallel with development of a dashboard prototype. Occupational therapists who participate in the interviews will be invited back to participate in think-aloud sessions. Think-aloud sessions are a key component of user-centered design that allow the participant to interact with a prototype of the new tool [10]. In these sessions, participants are typically asked to “think-aloud” everything that comes to mind as they navigate through the dashboard prototype and to complete a series of tasks simulating how they might use the dashboard in the real-world. Participants will be asked open-ended questions to reflect on their experience and provide feedback. We plan to complete 3-4 think-aloud sessions between iterative rounds of dashboard refinement and will gather usability, feasibility, acceptability, and appropriateness measures with a goal of reaching 68% usability. The final stage of this work will be real-world implementation where clinicians will use the dashboard in a clinical setting with new myoelectric prosthesis wearers.

ACKNOWLEDGEMENTS

Research reported in this publication was supported by the Eunice Kennedy Shriver National Institute of Child Health & Human Development of the National Institutes of Health under Award Number 1R44HD110334. We thank all our advisors, participants, patients and clinical colleagues who have informed our research focused on improving the experiences of community and clinical technology users.

REFERENCES

[1] E. Biddiss and T. Chau, “Upper-limb prosthetics: Critical factors in device abandonment,” Am J Phys Med Rehabil, vol. 86, no. 12, pp. 977–987, 2007, doi: 10.1097/PHM.0b013e3181587f6c.

[2] E. Scheme and K. Englehart, “Electromyogram pattern recognition for control of powered upper-limb prostheses: State of the art and challenges for clinical use,” J Rehabil Res Dev, vol. 48, no. 6, pp. 643–660, 2011, doi: 10.1682/JRRD.2010.09.0177.

[3] C. Celian *et al.*, "A day in the life: a qualitative study of clinical decision-making and uptake of neurorehabilitation technology," *Journal of neuroengineering and rehabilitation,* vol. 18, no. 1, p. 121, 2021/07/28 2021, doi: 10.1186/s12984-021-00911-6.

[4] G. Guest, A. Bunce, and L. Johnson, "How Many Interviews Are Enough?: An Experiment with Data Saturation and Variability," *Field Methods,* vol. 18, no. 1, pp. 59-82, 2006, doi: 10.1177/1525822x05279903.

[5] H. F. Hsieh and S. E. Shannon, "Three approaches to qualitative content analysis," *Qual Health Res,* vol. 15, no. 9, pp. 1277-88, Nov 2005, doi: 10.1177/1049732305276687.

[6] L. J. Damschroder, C. M. Reardon, M. A. O. Widerquist, and J. Lowery, "The updated Consolidated Framework for Implementation Research based on user feedback," (in eng), *Implement Sci,* vol. 17, no. 1, p. 75, Oct 29 2022, doi: 10.1186/s13012-022-01245-0.

[7] J. Brooke, "SUS: A quick and dirty usability scale," *Usability Eval. Ind.,* vol. 189, Nov 30 1995. [Online]. Available: https://www.usability.gov/how-to-and-tools/methods/system-usability-scale.html.

[8] Technology Transfer Services. "System Usability Scale (SUS)." U.S. General Services Administration. https://www.usability.gov/how-to-and-tools/methods/system-usability-scale.html (accessed March 7, 2024).

[9] B. J. Weiner *et al.*, "Psychometric assessment of three newly developed implementation outcome measures," *Implementation Science,* vol. 12, no. 1, p. 108, 2017/08/29 2017, doi: 10.1186/s13012-017-0635-3.

[10] T. Boren and J. Ramey, "Thinking aloud: Reconciling theory and practice," *Professional Communication, IEEE Transactions on,* vol. 43, pp. 261-278, 10/01 2000, doi: 10.1109/47.867942.

Challenges in restoring prehension following severe brachial plexus injury.

Bowring, Gregory(1,2,3) and Leong, Melissa(1).
Prince of Wales Hospital, Sydney, Australia

Affiliations:
Prince of Wales Hospital (1)
University of NSW (2)
University of Wollongong (3)

Background

Severe brachial plexus injury(BPI) from trauma is an uncommon but devastating injury suffered predominantly by young working-age men involving motor cycles or cars (1,2). The literature on this topic contains many references to other causes of brachial plexus injury, including obstetric and radiation in particular, but I wish to concentrate on the trauma induced variety of severe BPI (i.e. pan-plexus). The Prince of Wales Hospital Rehabilitation Dept, is recognised for its expertise in upper limb amputee management and prosthetic fitting and training, and we have become a referral centre for BPI cases all of whom are treated by the Specialist BPI Reconstructive Surgical Unit in my State of New South Wales (Australia). While Rehabilitation, by its nature, involves an holistic multidisciplinary approach to the wide variety of problems resulting from such a devastating injury, it became clear that our expertise in providing prehension might add significant value to the functional outcomes sought by our Surgical colleagues.

According to 2 large reported series from Brazil and the USA, in those requiring surgical reconstruction, half have panplexus injuries, 30-40% have upper plexus injuries, and a small minority have lower plexus injuries (1,2). Our experience at POWH concurs with these reports.

A myriad of surgical techniques are used to attempt to restore function to the arm - decompression and repair, nerve transfers, free functional muscle transfers, tendon transfers, joint arthrodesis, rotation osteotomy, and more recently, targeted muscle reinnervation (3). The literature is not clear on which technique is superior in any particular case, and the variability of approaches reported makes this hardly surprising. What is clear is that the surgery should only be carried out be experts and the situation in NSW is precisely that.

Rehabilitation is multidisciplinary, person-centred and goal oriented. It seeks to optimise function - physical, functional, psycho-social and vocational. In doing so it seeks to optimise quality of life in persons who have suffered disability from injury (or illness). In treating a patient with BPI this may include: to maintain joint range of motion, protect the flail limb from secondary injury, address pain management, provide psychological support, teach personal care independence, and provide vocational support to return to their existing employment or retrain.

In the early years of my career at another teaching hospital I received occasional referrals of such patients, usually from their General Practitioners, often many years after their original injury and treatment. Typically I found them seeking help with intractable neuropathic pain, carrying a flail upper limb supported via a variety of methods including nothing, hand in pocket, collar and cuff, or triangular sling. Invariably they had severe gleno-humeral subluxation. They had often undergone surgical repair years earlier but seemed to have no understanding of what that had been intended to achieve, and whether it had been successful or not. They had rarely returned to work, and often asked if I could help them to obtain an amputation believing (or at least hoping) it might help their pain. Of course, the surgical options are complex, often requiring multiple procedures, and the recovery times e.g. after nerve transfers, can be much longer than patients anticipate, leading to a loss of engagement, and uncertainty about achievable outcomes. I observed that what rehabilitation had occurred, was generally predominantly physiotherapy delivered by Specialty Hand physiotherapists. The patients seemed not to understand that there was generally no expectation that hand function could be recovered.

Restoring prehension

In the past prehension was addressed through body powered(BP) or externally powered(EP) orthoses or combined gleno-humeral arthrodesis and transhumeral amputation (THA) and BP or

EP prostheses. Many examples are readily found in old textbooks often from Specialty centres in the UK like Roehampton and Stanmore. My 1980s training had taught me that 1. None of these orthoses were used, 2. That THA might be performed for a flail arm which was suffering from repeated trauma but it should never be contemplated early and to beware of the patient believing it would help their pain, and 3. THA prostheses fitted after THA were rarely used as function was so poor. In Australia these approaches have largely fallen out of favour.

Our recent experience confirms that The RNSH BPI surgical unit in Sydney has a reliable expectation of providing a stable shoulder with limited abduction/flexion and good biceps function following nerve and or tendon transfers +/- humeral rotation osteotomy. They explicitly state that they have no ability to restore intrinsic hand function though some finger function via tendon transfers or muscle grafts combined with wrist fusion can restore some grasp. What patients lack is fine prehension. I was inspired by Aszman's innovative work combining TMR and Trans Radial Amputation(TRA).

Current approach to restoring prehension
We have since developed an approach which, following surgical reconstruction, involves a patient centred choice between TRA and prosthetic fitting, or exoskeleton, both of which can be activated by auxiliary switching technology if necessary, in the absence of sEMG signals in the arm. I will present examples of each from cases which we have treated at The Prince of Wales Hospital in Sydney Australia.

Exoskeleton
The exoskeleton is the option for those who do not want amputation. This is the majority of our cohort and tends to be the younger aged. Preserving passive hand function is important in this group. The rigid exoskeleton fitted (Myopro) required a patient who could tolerate a bulky heavy unit suspended from a shoulder saddle resting on their wasted shoulder girdle. The hand module demanded a flexible wrist and hand, with a fully preserved thumb web space or the risk of trauma was significant. The exoskeleton utilised the reinnervated biceps sEMG signal to provide enhanced elbow flexion power. The hand close/open relied upon a single site switching approach using sEMG e.g. rhomboids, or a linear transducer or alternative. The decision was based on a team discussion between patient, Occupational Therapist and Orthotist/Prosthetist, and testing of various options for the most reliable. Fitting was difficult and successful positioning of the electrode could only be achieved by an assistant. The patient could successfully open and close the hand reliably but usage in functional tasks was not achieved.

Trans Radial Amputation (TRA) and prosthetic fitting
In those willing to undergo TRA, a prosthetic socket was fitted and initially supported by attachment to the Wilmer BPI orthosis. A myoelectric TD was added and single site activation via a linear transducer attached to a chest strap was reliably demonstrated. Over time, as the biceps became stronger, the Wilmer support was removed. Reliable holding of an object in the Prosthetic TD supports functional task performance but weak shoulder flexion limits the range of tasks.

Decision pathway
1. Financial options known
2. Pt preferences re amputation understood.
3. Pt beliefs about pain relief recognised and cautioned.
4. Psychological evaluation (esp re amputation)
5. Precluding injuries excluded e.g. severe TBI, skeletal injuries (harness tolerance and motion)
6. Surgical plan for G-H stability & Elbow Flexion reinnervation agreed and/or underway.
7. Shoulder and elbow function achieved.
8. TRA amputation undertaken and prosthesis fitted OR exoskeleton trialled.

Future plans
1. A more suitable exoskeleton is needed. The soft orthotic glove type exoskeleton appeals as a better alternative, although none of the existing commercially available models have proved to be suitable for the needs of this patient group.
2. Alternative activation systems are needed. The limited sEMG signals available suggests that linear transducers will be relied upon despite their own limitations. BCI technology may ultimately solve this problem.

1. Faglioni et al 2013
2. Kaiser et al, Neurosurgical Review, 2020-04, Vol 43(2). P442-453.
3. Hruby et al, J Neurosurgery, Vol 127, issue 5, 2017, p.1163-1171.

EXPLORING THE PERSPECTIVES OF DIFFERENT PROFESSIONS ON TASK-BASED UPPER-LIMB PROSTHESIS ASSESSMENT TECHNIQUES

Joshua R. Siegel[1], and Jonathon S. Schofield[1]
[1]*Department of Mechanical and Aerospace Engineering, University of California, Davis, Davis, CA, United States*

ABSTRACT

Upper limb prostheses can significantly enhance independence and functionality for individuals with limb differences, offering them renewed independence, functionality, and quality of life. Task-based evaluation measures, which involve patients directly manipulating objects with their prosthesis, are crucial for accurately assessing performance. However, these measures must meet the needs of various stakeholders, including researchers, clinicians, and insurers, who rely on this data for patient care and technological advancements. Yet, the specific demands of these groups can vary widely and remain underexplored, creating a gap in developing universally applicable evaluation methods. Our study aims to investigate these differences by conducting an online survey targeting a broad spectrum of professionals, including physical and occupational therapists, certified prosthetists/orthotists, medical practitioners, and academic researchers. This approach aims to gather a comprehensive understanding of current evaluation practices and identify areas in need of refinement, ultimately contributing to enhanced precision in prosthetic evaluations and improved patient outcomes.

INTRODUCTION

Task-based metrics, which involve the patient directly manipulating test objects with their prosthesis, offer a myriad of benefits as they provide an immediate assessment of a patient's real-time performance operating their device. Some of these benefits include: the potential to help inform clinical decision making including the selection of appropriate prosthetic solutions for individual patients; enabling precise monitoring of patient progress either as indications of care effectiveness or the need for adjustments; and helping provide an evidence base for decision making in the contexts of insurance coverage and public health systems, collectively helping foster transparency among stakeholders including patients, clinicians, researchers, and regulatory bodies. Additionally, standardized task-based evaluations allow for consistent comparisons across different prosthetic technologies, contributing to innovation by minimizing variability from diverse and often disparate evaluation methodologies. Finally, when paired with patient self-reported data, task-based assessments can also help mitigate common biases, such as response fatigue, social desirability, and central tendency biases, offering an additional objective and supplementary perspective on patient functionality [1], [2], [3]. Collectively, task-based evaluation tools are foundational to progress in upper-limb prosthetics, ensuring advancements are both significant and quantifiable.

Despite their clear importance, there is a notable research gap in this area. While mechatronic technology for upper-limb prosthetics has seen significant advancements, we have found in our recent literature review that only 25 task-based evaluation measures have been reported in literature, and crucially, validated since 1948 [4]. This disparity between the rapid rate of technological advancement and the blunted evolution of standardized measures to assess their performance emphasizes the growing need for more universally accepted and consistently updated assessment frameworks. The challenge of addressing this issue is compounded by the differing priorities of professionals across clinical environments and research laboratories. Clinical settings, which are often under time constraints, may prefer more rapid tests for their efficiency in assessing patient outcomes. However, this may come at the expense of the depth of data collected. On the other hand, research settings may opt for more comprehensive tests which, despite their thoroughness, face challenges in wider spread adoption due to their extensive setups, accessibility of testing materials, significant costs, and more complex protocols.

Our goal was to gather insights on current task-based evaluation methods in the context of the unique needs and expectations across the diversity of practitioners that may interact with individuals prescribed upper limb prostheses. We employed an online survey and contacted a wide array of individuals across the professional spectrum, including physical and occupational therapists, prosthetists, medical practitioners, and academic researchers.

METHODS

Survey Design

Our online survey was strategically designed to gather data on professionals' experiences, preferences, and practices related to upper-limb prostheses and task-based functional measures. Our study was approved by the University of California,

Davis Institutional Review Board. Recruitment was performed though email via our team's professional networks. Once participants agreed to take part in the study, they were provided with a link to an anonymous survey hosted on Qualtrics. This began with an introduction outlining the study's objectives, confidentiality assurances, detailed instructions, and contact information for any follow-up questions. Consent to proceed led participants through a questionnaire that require no more than 15 minutes to complete. The survey incorporated a variety of question types, including multiple-choice, checkboxes, and questions that allowed respondents to order their preferences. This design facilitated the easy and efficient capture of detailed responses across a range of topics. The questionnaire was structured to progress through a series of questions aimed at anonymously characterizing each participant's profession, experience, training, and exposure to individuals with upper-limb prostheses. Following this initial characterization, the survey focused on identifying which validated task-based measures participants were aware of and actively used in their practice. Finally, participants were asked to prioritize a list of factors they deem most important in a task-based measure for upper-limb prosthetic assessment.

Data Analysis

We employed binning and response counts as our primary analytical methods. Data collected from the survey were first separated (binned) by profession, allowing for a detailed analysis of the perspectives of different professional. Response counts were utilized to quantify the prevalence of specific views and practices among the participants, providing a straightforward method to identify the most used task-based measures and the factors considered most important in upper-limb prosthetic measures.

RESULTS

In this paper, we present data from N=30 participants, whose professional backgrounds are outlined in Table 1. The distribution of participants by profession was as follows: 5 physical/occupational therapists (PT/OTs), 4 certified prosthetist/orthotists (CPOs), 14 medical doctors (MD/DOs), and 7 who are primarily researchers (PRs). Additionally, we documented the median duration of practice in their respective fields by having them select from a list of time ranges: PT/OTs and CPOs professionals had a median range of experience between 10 to 15 years of experience; MD/DOs participants reported a median range of 12.5 to 17.5 years; and for those primarily involved in research (PRs), the median experience ranged from 15 to 20 years. The survey also required participants to select from a list highlighting the frequency range they interact with upper limb prosthesis users, the median rate of patient interactions revealed a spectrum of engagement frequencies: PT/OTs and PRs typically interacted with patients once every 2 to 5 months; CPOs reported at least one patient interaction per week; and MD/DOs professionals engage with patients at least once per month.

Table 1: Respondent Background

Profession	Respondents	Median Time Practicing	Median Patient Interaction Rate
Physical/Occupational therapist	5	10 – 15 years	Once every 2-5 months
Certified Prosthetist/Orthotist	4	10 – 15 years	At least once per week
Medical Doctor	14	12.5 – 17.5 years	At least once per month
Primarily Researcher	7	15 – 20 years	Once every 2-5 months

Table 2 highlights the results from a survey question that prompted participants to select task-based measures, from a list of 25 (identified in [4]), that they were familiar with and would likely use with patients in their professional practice. The Box and Block Test (BBT) was identified as the most favored test across all professions for patient use. This finding is particularly significant considering the test's brevity and limited scope in assessing functional capabilities. Despite these constraints, the Box and Block Test is valued for its comprehensive validation with numerous patient populations, endorsement through peer review, straightforward administration, affordability, and ease of learning. Conversely, more involved evaluations such as the Southampton Hand Assessment Procedure (SHAP), Activities Measure for Upper-Limb Amputees (AM-ULA), and Gaze and Movement Assessment (GaMA) were primarily chosen for research purposes. It is important to note that a significant portion of the MD/DOs reported a lack of familiarity with many of the tests listed. Several doctors indicated in their responses that they would prefer to delegate the responsibility of administering these tests to PT/OTs.

Table 2: Perspectives on Currently Available Tests

Profession	Top Rated Tests to be used with a Patient – Percentage of Respondents * Indicates tie
Physical/Occupational therapist	1: Box and Block Test (BBT) – 71.43%
	2*: Action Research Arm Test (ARAT) – 50.00% 2*: Jebsen Hand Function Test (JHFT) – 50.00% 2*: Nine-Hole Peg Test – 50.00%
Certified Prosthetist/Orthotist	1: Box and Block Test (BBT) – 50.00%
	2*: Assessment of Capacity for Myoelectric Control (ACMC) – 33.33% 2*: University of New Brunswick Test of Prosthetic Function (UNBT) – 33.33%
Medical Doctor	1*: Box and Block Test (BBT) – 21.42% 1*: Jebsen Hand Function Test (JHFT) – 21.42% 1*: Nine-Hole Peg Test (NHPT) – 21.42%
	2*: Purdue Pegboard Test (PPT) – 14.29% 2*: Unilateral Below Elbow Test (UBET) – 14.29%
Primarily Researcher	1*: Southampton Hand Assessment Procedure (SHAP) – 44.44% 1*: Box and Block Test (BBT) – 44.44%
	2*: Activities Measure for Upper-Limb Amputees (AM-ULA) – 42.86% 2*: Gaze and Movement Assessment (GaMA) – 42.86%

Table 3 shows the results when participants selected from a list of maximum time ranges they felt was acceptable to administer a task-based measure in their practice. Additionally, Table 3 highlights the top three criteria they viewed as important when selecting a task-based measure, underscoring a universal preference for validated and peer-reviewed tools. Clinical practitioners report a significantly shorter maximum testing time compared to their research-focused peers, highlighting a prioritization of efficiency in clinical settings. This emphasis on time efficiency is reflected in the ranking of the total administration time as a key factor for its selection among clinical professionals. Despite these differences, there's a unanimous agreement on the importance of using tests that effectively monitor patient progress, illustrating a common objective to employ assessments that are both practical and beneficial for patient care across diverse professional landscapes.

Table 3: Desired Characteristics for Evaluation Methods

Profession	Median Max Time for Test	Ranking of Most Important Factors
Physical/ Occupational therapist	Between 10-20 minutes	1: The test has been validated and peer-reviewed
		2: Efficacy of monitoring patient progress
		3: Total administration time
Certified Prosthetist/ Orthotist	Between 15-25 minutes	1: The test has been validated and peer-reviewed
		2: Total administration time
		3: Comprehensive analysis of multi-grasp dexterity and impact of varying control systems
Medical Doctor	Between 5-10 minutes	1: The test has been validated and peer-reviewed
		2: Total administration time
		3: Efficacy of monitoring patient progress
Primarily Researcher	Between 30-60 minutes	1: The test has been validated and peer-reviewed
		2: Efficacy of monitoring patient progress
		3: Comprehensive analysis of multi-grasp dexterity and impact of varying control systems

DISCUSSION

Our study unveiled insightful findings regarding the prevailing views on task-based evaluation methods for upper-limb prosthetics. We observed notable variations in how frequently different professional groups engage with patients equipped with upper-limb prosthetics. It is essential to mention that these interactions ranged from weeks to months, highlighting a considerable variance among professionals. However, a potential limitation of our study was the methodology used to contact respondents—email outreach within our network of researchers and clinicians specializing in upper-limb absence care. This approach might have led to an overestimation of interaction frequency, as it may not accurately represent the engagement levels of the average practitioner. Despite this limitation, the importance of addressing the prosthetic needs and managing patient expectations cannot be overstated, especially considering the challenges posed by the advancing technology in upper-limb prosthetics. These challenges are compounded by the mobility requirements of the upper-limb and the vital role that hands and arms play in our daily activities. Our findings also shed light on the "upper extremity dilemma [5]," where prosthetics are becoming more technologically advanced and specialized. However, the relatively infrequent encounters with upper-limb prosthetic users make it difficult for many clinicians to expand their knowledge and expertise [6]. This gap necessitates a high level of specialized care for a group of patients seen less frequently by practitioners, leading to potential challenges in meeting their specific needs [7]. To bridge this gap, validated task-based measures and a more universally applicable analysis framework could play a crucial role. Such tools would provide practitioners with objective data, facilitating more informed decision-making and ultimately enhancing care for patients using upper-limb prosthetics.

Our results revealed many intriguing insights about current perspectives on available task-based evaluation methods used for upper-limb prostheses. Categorizing the data from 30 participants by profession revealed distinct preferences in testing goals and methods. Although all groups emphasized the necessity of validated and peer-reviewed tests, notable differences emerged: clinical settings prioritize quick evaluations next, with the box and block test— likely favoured for its sub-5-minute completion time—ranking high among physical and occupational therapists, prosthetists/orthotists, and medical doctors [4]. Notably, the maximum time reported for testing report in these clinical groups was significantly shorter than that for research-focused professions. Furthermore, professionals across these fields consistently rank the total time required to administer a test as one of the top three criteria for determining its effectiveness. In contrast, research environments valued the comprehensive analysis which likely explains the preference for the more intensive Southampton Hand Assessment Procedure, though the box and block test does remain in use for this group. Nevertheless, professionals unanimously agree on the importance of tests that effectively monitor patient progress. These findings highlight the shared and unique priorities across professions, underscoring the need for a balanced approach in developing and selecting upper-limb prosthetic evaluation methods to accommodate the quick assessment preferences of clinical practitioners and the detailed analytical needs of researchers.

ACKNOWLEDGEMENTS

This work was supported by a 2024 University of California Noyce Initiative Research Award and 2024 UC Davis Next Lever Research Award. The authors would also like to thank Jedidiah Harwood for his statistical expertise. Finally, the authors would like to thank Peyton Young, Eden Winslow, Marcus Battraw, Matthew Siegel, and Erica Siegel for their support and general guidance.

REFERENCES

[1] B. C. K. Choi and A. W. P. Pak, “A Catalog of Biases in Questionnaires,” *Prev. Chronic. Dis.*, vol. 2, no. 1, p. A13, Dec. 2004.

[2] S. Salminger *et al.*, “Current rates of prosthetic usage in upper-limb amputees – have innovations had an impact on device acceptance?,” *Disabil. Rehabil.*, vol. 44, no. 14, pp. 3708–3713, Jul. 2022, doi: 10.1080/09638288.2020.1866684.

[3] F. Virginia Wright, S. Hubbard, J. Jutai, and S. Naumann, “The prosthetic upper extremity functional index: Development and reliability testing of a new functional status questionnaire for children who use upper extremity prostheses,” *J. Hand Ther.*, vol. 14, no. 2, pp. 91–104, Apr. 2001, doi: 10.1016/S0894-1130(01)80039-9.

[4] J. R. Siegel, M. A. Battraw, E. J. Winslow, M. A. James, W. M. Joiner, and J. S. Schofield, “Review and critique of current testing protocols for upper-limb prostheses: a call for standardization amidst rapid technological advancements,” *Front. Robot. AI*, vol. 10, 2023, Accessed: Nov. 14, 2023. [Online]. Available: https://www.frontiersin.org/articles/10.3389/frobt.2023.1292632

[5] C. Lake and R. Dodson, “Progressive upper limb prosthetics,” *Phys. Med. Rehabil. Clin. N. Am.*, vol. 17, no. 1, pp. 49–72, Feb. 2006, doi: 10.1016/j.pmr.2005.10.004.

[6] C. Brenner, “Wrist disarticulation and transradial amputation: prosthetic management.,” in *Atlas of amputations and limb deficienciesd surgical, prosthetic and rehabilitation principles*, 3rd ed., Rosemont: American Academy of Orthopaedic Surgeons, 2004, pp. 223–230.

[7] J. S. Schofield, K. R. Schoepp, H. E. Williams, J. P. Carey, P. D. Marasco, and J. S. Hebert, “Characterization of interfacial socket pressure in transhumeral prostheses: A case series,” *PLOS ONE*, vol. 12, no. 6, p. e0178517, Jun. 2017, doi: 10.1371/journal.pone.0178517.

RETHINKING THE SHOULDER DISARTICULATION PROSTHESIS: LET'S STOP THINKING OUTSIDE THE BOX AND MAKE THE BOX BIGGER

Christopher Fink, CPO; Timothy Bump, CPO; Debra Latour, OTD, OTR/L

Handspring Clinical Services

ABSTRACT

In this article, authors explore how reducing the amount of technology and modifying the traditional shoulder disarticulation prosthesis design can lead to an improvement in task completion, device satisfaction, and reduced prosthetic abandonment. While new devices demonstrate potential for improved function, appearance, and control, there is a lack of translation of these advancements to actual daily functional improvements for the upper limb population. Prosthetic abandonment continues to be extremely high in the upper limb population even with improvements in the latest technology.

Persons with shoulder disarticulation/ interscapular thoracic occupy less than 0.1% of the total population. With such a small population of potential users, many prosthetists default to caring for these individuals in a very traditional manner as they lack the experience to do so differently. Traditionally, shoulder disarticulation prostheses have consisted of a prosthetic shoulder, elbow, wrist, and terminal device. While these devices may be successful for some users, they are heavy and require an extensive amount of positioning before operating the terminal device. In a typical shoulder level prosthesis, there are six degrees of freedom to control and position prior to terminal device actuation. With current technology these degrees of freedom are typically sequentially controlled and may be positioned multiple times prior to attempting to operate the terminal device. The cognitive burden of positioning these movements and the time to do so are routine complaints of users. While offering access to function once correctly positioned, achieving the correct position is time consuming and fatiguing. The increased complexity and degrees of freedom for control in more proximal level users requires more cognitive load and could explain the higher level of abandonment with higher levels of limb difference.

To combat this, the practitioners explored a novel design to reduce the complexity of operating the shoulder level external powered prosthesis and combat the common issues of function, comfort, and weight. The novel prosthesis was designed around the criteria of access to function at multiple levels (seated at a table and standing at a counter) and be able to complete bimanual activities of daily living (ADLs) such as meal preparation, household chores, stabilizing paper to write with the contralateral limb, and eating with a knife and fork.

INTRODUCTION

The authors of this paper explore how reducing the amount of technology and modifying the traditional shoulder disarticulation prosthesis design can lead to an improvement in task completion, device satisfaction, and reduced prosthetic abandonment. Society continues to be enamoured with technology. From the latest smart phone or watch to self-driving cars, we have become people that love technology for the sake of innovation. This infatuation is not independent from the field of prosthetics. Innovations are developed daily, with a substantial amount of that technology concentrated to the upper limb. While new devices demonstrate potential for improved function, appearance, and control, there is a lack of translation of these advancements to actual daily functional improvements for the upper limb population.

Persons with upper limb absence (ULA) continue to derive a small percentage of the overall limb-different community. There are an estimated 2.2 million persons living with limb difference, with 185,000 persons with new loss each year [1,2]. Partial hand difference makes up a large majority of the upper limb population (92%) followed by trans radial/ wrist disarticulation, and trans humeral/ elbow disarticulation. Persons with shoulder disarticulation/ interscapular thoracic occupy less than 0.1% of the total population [1,2,3]. With such a small population of potential users, many prosthetists default to caring for these individuals in a very traditional manner as they lack the experience to do so differently. Many work under the pretext that a prosthesis needs to replace the anatomical limb in a mimicking manner such as a hand for a hand, an elbow for and elbow, etc. Development in technology has been driven around making the prosthesis more human-like. While this may be appropriate in some instances, it may not be the best course of action in all circumstances. For instance, many machines and robots have been developed to replace humans in manufacturing jobs that do not operate under this pretext.

Prosthetic abandonment continues to be extremely high in the upper limb population even with improvements in the latest technology [4]. More proximal amputation levels also show higher levels of abandonment [4]. Reasons included weight, temperature, sweating, durability, and aesthetics with a consensus of comfort and function being the leading factors [4,5,6]. The prosthetist is responsible to create well-fitting sockets, but prosthetic comfort can be influenced by factors such as weight or control mechanism. Function is extremely multifaceted and includes the tasks that are meaningful to the user, technology design and selection, control mechanisms, occupational therapy/ training, and socket fit/ comfort. Additionally, the increased cognitive load associated with using an upper limb prosthesis may lead to greater abandonment [7]. The increased complexity and degrees of freedom (DOF) for control in more proximal level users requires even more cognitive load and could explain the higher level of abandonment with higher levels of limb difference.

Traditionally, shoulder disarticulation prostheses have consisted of a prosthetic shoulder, elbow, wrist, and terminal device. For individuals requiring active elbow motion and grasp, body powered prostheses are less preferred compared to external powered prostheses due to the lack of excursion available at this level of limb loss [8]. A typical external powered shoulder level prosthesis (Fig. 1) consists of a locking shoulder joint (mechanical or electric) to control shoulder flexion and extension with a friction ab/adduction setting to allow positioning of the shoulder in abduction; an external powered elbow joint that allows for flexion and extension of the elbow joint; a mechanical friction turntable on top of the elbow joint to mimic humeral rotation; an electric wrist rotator to supinate/ pronate the terminal device; and an external powered terminal device that could be in the form of a hook, simple prehension hand, or multi-articulating hand. Many terminal devices also have the option for changing the wrist flexion position as well.

While these devices may be successful for some users, they are heavy and require an extensive amount of positioning before operating the terminal device. In a typical shoulder level prosthesis, there are 6 DOF to control and position prior to terminal device actuation. With current technology these DOF are typically sequentially controlled and may be positioned multiple times prior to attempting to operate the terminal device. The cognitive burden of positioning these 6 DOF as well as the time to do so are routine complaints of users. While offering access to function once correctly positioned, achieving the correct position is time consuming and fatiguing. To combat this, the practitioners explored a novel design to reduce the complexity of operating the shoulder level external powered prosthesis and combat the common issues of function, comfort, and weight. Participants gave written consent to use of their images.

Figure 1: Example of a traditional external powered shoulder disarticulation style prosthesis

Figure 2: Novel shoulder disarticulation style prosthesis in its shortest position to function while seated at a table

Figure 3: Novel shoulder disarticulation prosthesis in its extended position to work at a countertop height while standing

The novel prosthesis was designed around the criteria of access to function at multiple levels (seated at a table and standing at a counter) and be able to complete bimanual activities of daily living (ADLs) such as meal preparation, household chores, stabilizing paper to write with the contralateral limb, and eating with a knife and fork. The device needed to be lighter weight, easier to operate and more functional than the typical shoulder level prosthesis. The novel prosthesis (Fig. 2 and Fig. 3) consisted of a universal friction shoulder joint to control elbow flexion/ extension, ab/ adduction, and humeral rotation; a telescoping “elbow joint” to provide a short operating position and long operating position; a standard electronic quick disconnect wrist unit to allow for passive wrist rotation; and an external powered multi-articulating hand.

CASE STUDY 1

Case study 1 (CS1) is a 28-year-old male who presents with acquired shoulder disarticulation of the right dominant upper limb due to a work-related accident. He demonstrates limited movement and has extensive scarring at the residuum and dorsal/lateral trunk and volar clavicular areas. Sensation is described as hypersensitive in the right anterior axilla. He experiences phantom and residual limb but denies pain in the left sound upper limb. Since January 2023, CS-1 has been using an externally powered device that includes a body powered locking shoulder joint, powered elbow joint, a powered wrist rotator, ETD2 with wrist flexion and FLAG, waterproof collar, and waterproof sleeve, 2 site touch pad control, electric switch, and chest straps for suspension harnessing. He received OT for prosthetic training and was able to use the device for some ADLs but continued to experience some limitations. Prior to his accident, CS-1 led an active life, working full time in construction at an asphalt company. He lived in the family home with his parents and siblings, contributing to home and property maintenance, and enjoyed diverse activities in his free time, including sports, working out, camping, fishing, and hunting. He also played musical instruments such as piano, trumpet and drums. He hoped that prosthetic technology would enable him to return to these activities. CS-1 expressed interest in trialling the idea of the novel prosthesis using the telescoping feature that could offer access to tasks at diverse heights more efficiently.

In October 2023, CS-1 was fitted with the novel prosthesis. He noted that the adjustable length feature of the forearm/ humeral section was at a perfect length for tasks while seated at a table and extended an appropriate length to work at a countertop while standing. He was able to change the arm length quickly and was happy with the added and improved features of the new prosthesis. His control continues to be excellent and ability to use the prosthesis. Initial measures show improved his perception of disability, work, and recreation scores (QuickDASH) and prosthetic satisfaction (McGann Feedback Form). CS-1 continues to be monitored for ADLs via performance measures, however he has demonstrated improvements in ability to complete many bimanual tasks such as cutting food, preparing meals, and carrying heavy objects.

CASE STUDY 2

Case study 2 (CS-2) presents as a 42-year-old male with a right shoulder disarticulation amputation with full root avulsion that occurred in 2013 from a traumatic motorcycle injury. He continues to experience pain, anxiety, PTSD, and depression. CS-2 was initially fitted in 2015 with a passive activity-specific prosthesis, and then with an externally powered prosthesis in 2017. He has since lost the passive device during relocation and the externally powered device no longer fits due to weight gain. CS-2 complains of limited function with his device because of the weight complexity to operate the components.

In October 2023, prosthetists discussed the novel prosthesis with a telescoping locking elbow instead of a flexing/extending elbow. CS-2 was interested and discussed the potential for control using touch pads at the right shoulder. Following trials with a developing prototype, a device with single-site, posterior motion to open/close; elbow with 2 telescoping positions, and an i-limb quantum with power grip was delivered to CS-2 in January 2024. He was able to operate the device and to initiate bimanual tasks such as zip up a jacket, manipulate a knife and fork to cut food, and manage a wallet and mobile phone. CS-2 stated, “It has been a long time since I had this much hope to accomplish tasks.”

Initial measures show improved his perception of disability, work, and recreation scores (QuickDASH) and prosthetic satisfaction (McGann Feedback Form). CS-2 continues to be monitored for ADLs via performance measures, however he has demonstrated improvements in ability to complete many bimanual tasks such as cutting food, preparing meals, and carrying heavy objects.

DISCUSSION

These case studies demonstrate that the novel prosthesis has several advantages over the traditional prosthesis including decreased overall weight, decreased weight perceived by the user, improved function to complete tasks at table (seated) and counter (standing) heights, and increased wear time. Additionally, the users were able to correctly position the TD faster and more efficiently compared to the traditional prosthesis. Once the user adjusted the telescoping “elbow joint” at the proper length, the TD was positioned by moving the universal shoulder joint and rotating the wrist unit. This resulted in a total of 3 actions before operating the TD in the novel prosthesis (positioning the telescoping elbow joint, the universal shoulder joint, and the wrist rotator) compared to five actions required to actuate the traditional prosthesis (positioning the shoulder for flex/ extension, abduction, humeral rotation, elbow flexion, and wrist rotation).

Users of this device were able to complete tasks they could not perform or struggled to perform with the traditional prosthesis. Seated at a table the novel prosthesis outperformed the traditional prosthesis because the angle and position of the

prostheses allowed the user to interact with items on the table. With a traditional prosthesis the subjects were unable or struggled to use the prosthesis to grasp objects from the tabletop, hold a water bottle or cup and cut with a fork and knife. The novel prosthesis, however, easily permitted access to complete these tasks. The lack of a traditional elbow joint allows the TD on the novel prosthesis to access objects on the tabletop in a more intuitive, efficient, and easier strategy to control motion.

Currently there is no knowledge of any other prosthesis that has been designed with the characteristics of the novel prosthesis. While both subjects found value in the novel prosthesis, one of the subjects continues to use his traditional prosthesis on occasion because both prostheses serve purposes to his daily life. This action coincides with the findings that no one prosthesis can replace the human arm/hand and that multiple devices are required to achieve the vast array of functions of the human arm. Further examination of this prosthesis design is required to further determine its merits for the wider shoulder level prosthetic community. Future design considerations will include other tasks beyond household chores, eating, meal preparation and writing.

ACKNOWLEDGEMENTS

Thank you to our patients for their patience, dedication, and critical feedback to create the best prostheses for them and others, and acknowledge Tom Passero CP, Handspring Clinical Services, for his support in this process.

REFERENCES

[1] K. Ziegler-Graham, E.J. MacKenzie, P.L. Ephraim, T.G. Travison, R. Brookmeyer. “Estimating the Prevalence of Limb Loss in the United States: 2005 to 2050,” *Archives of Physical Medicine and Rehabilitation,* vol. 89(3), pp. 422-9, 2008.

[2] M. Owings, L.J. Kozak. National Center for Health S. “Ambulatory and Inpatient Procedures in the United States, 1996”. Hyattsville, Md.: U.S. Dept. of Health and Human Services, Centers for Disease Control and Prevention, National Center for Health Statistics; 1998.

[3] T.R. Dillingham, L.E. Pezzin, E.J. MacKenzie. “Limb amputation and limb deficiency: epidemiology and recent trends in the United States”, *South Med J*, vol. 95(8), pp. 875-883, 2002.

[4] S. Salminger, H. Stino, L. Pichler, C. Gstoettner, A. Sturma, J. Mayer, M. Szivak, O. Aszmann. “Current rates of prosthetic usage in upper-limb amputees – have innovations had an impact on device acceptance?”, *Disability and Rehabilitation, v*ol. 44:14, pp. 3708-3713, 2022.

[5] E. Biddiss, T. Chau. “Upper-limb prosthetics: critical factors in device abandonment”, *Am J Phys Med Rehabil*, vol. 86:977, 2007.

[6] L. Smail, C. Neal, C. Wilkins, T. Packham. “Comfort and function remain key factors in upper limb prosthetic abandonment: findings of a scoping review”, *Disability and Rehabilitation: Assistive Technology*, 2020.

[7] D.S. Childress. “Closed-loop control in prosthetic systems: historical perspective”, *Ann Biomed Eng*, vol. 8(4-6), pp. 293-303, 2008.

[8] J. Miguelez, M. Miguelez, R. Alley. Chapter 21: Amputations about the shoulder: prosthetic management. In Smith D, Michael J, Bowker J (eds): *Atlas of Amputations and Limb Deficiencies, ed 3*, American Academy of Orthopaedic Surgeons, pp 263-274, 2004.

Clinical Research

AFFECTED MUSCLES RETAIN DEXTROUS MOTOR CAPABILITIES IN CHILDREN BORN WITH UPPER-LIMB DEFICIENCIES

Eden Winslow[1], Marcus Battraw[2], Justin Fitzgerald[1,3,4], Michelle James[5,6], Anita Bagley [5,6], Wilsaan M. Joiner[1,4,7], Jonathon Schofield[2]

[1]Department of Biomedical Engineering, University of California, Davis, Davis CA, USA
[2]Department of Mechanical and Aerospace Engineering, University of California, Davis, Davis CA, USA
[3]Clinical and Translational Science Center, University of California Davis Health, Sacramento CA, USA
[4]Department of Neurobiology, Physiology, and Behavior, University of California, Davis, Davis CA, USA
[5]Shriners Children's Hospital, Northern California, Sacramento CA, USA
[6]Department of Orthopedic Surgery, University of California Davis Health, Sacramento CA, USA
[7]Department of Neurology, University of California Davis Health, Sacramento CA, USA

ABSTRACT

Children with Unilateral Congenital Below-Elbow Deficiencies (born without a hand, UCBED) have a high rate of prosthetic abandonment, pointing to unresolved challenges that may be distinct from those faced by adults with limb loss. There is limited knowledge of the motor control these children have over their affected muscles, a highly relevant question for effective dextrous prosthetic control. Our research aims to measure the extent of volitional muscle activation that exists in the residuum when children attempt moving their missing hand, with the goal of creating highly functional pediatric-specific prosthetic devices. In this work, we recruited 28 pediatric UCBED patients across four Shriners Hospital locations. We measured muscle activity using ultrasound imaging and surface electromyography while children attempted 10 missing-hand movements, then used machine learning to analyze the patterns of the affected and unaffected sides. Our algorithms predicted hand movements from residual muscle activity at over 80% accuracy in most cases, and well above chance in all participants. This indicates inherent muscular control which may be leveraged to develop more functional prosthetic devices tailored towards pediatric UCBED patients.

INTRODUCTION

Approximately 1 in 500 live births will present with an upper limb deficiency, the most common reason for limb absence in children [1]. Children born with a unilateral, congenital, below-elbow deficiency (UCBED) are typically amenable to a prosthesis, but prosthetic abandonment rates for pediatric users reach as high as 45%, compared to approximately 25% for adults with limb loss [2], indicating these devices are not providing the necessary functionality or improved quality of life that the users require [3]. Although there have been significant advancements in dextrous prosthesis development and availability for adults and children, with this increased dexterity comes the need for more sophisticated control systems to pilot the newly available movements. Toward this goal, advanced machine learning-based control systems such as myoelectric pattern recognition approaches have demonstrated significant promise for adult prosthesis users, but have seen limited to no adoption among children born with their limb deficiency [4].

Encouragingly, we have shown in small cohorts of children with UCBED (N= 6-9) that they retain a degree of control over their affected muscles, despite having never actuated a hand before [5-6]. These studies were performed using surface electromyography (sEMG) and the emerging technique of sonomyography (ultrasound imaging) respectively to capture muscle activity. We found that it is possible to decode intended movements of the missing hand from the patterned behavior of the affected muscles using either measurement modality. These results indicate that, like adults with acquired limb absence, these children have a significant potential to benefit from advanced prosthetic control systems.

In the current work, we present our findings from a cohort of N=28 children with UCBED whose data was collected from 4 Shriners Children's Hospital locations across the United States. Participants were asked to attempt simultaneously moving their intact and missing hands into a variety of positions while EMG and ultrasound imaging

recorded the corresponding forearm muscle activity. We hypothesized that, like our prior work, each participant would produce distinct patterns of muscle activity that were unique to each intended hand movement. We further hypothesized that classification accuracies of these patterns would be similar, albeit slightly reduced, when comparing the affected to the unaffected sides. This work provides a deeper understanding of the motor capabilities of children with UCBED and points to the potential for these children to benefit from advanced prosthesis control systems.

METHODS

Study Design: We recruited N=28 pediatric participants (ages 5-20 years old, 16 males and 12 females) with UCBED from 4 Shriners Children's Hospital locations (Northern California, Portland, Greenville, Chicago). Exclusion criteria include those with sensorimotor, cognitive, or developmental differences aside from the absence of an upper limb. All research protocols were approved by the Shriners Hospitals for Children Western Institutional Review Board (WIRB). Participants or their legal guardians provided written, informed consent (and assent as necessary) prior to the study.

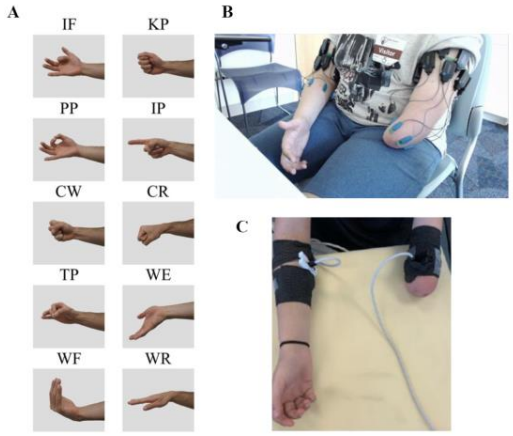

Figure 1: A) Hand grasp configurations used in the experimental procedures B) sEMG sensor placement example C) Ultrasound sensor placement example

We employed ultrasound imaging and sEMG to capture the simultaneous muscle activity of participants affected and unaffected limbs while they attempted different missing-hand movements (Figure 1). Our methodology then used machine learning (ML) algorithms to analyze the consistency of the recorded muscle activity, based either on patterns of electrical activity across sEMG electrodes or the spatiotemporal motion patterns of the muscles. Therefore, participants performed two repetitions of the same experimental paradigm, once while wearing ultrasound sensors, and once while wearing sEMG sensors. Here, they were asked to perform ten different grasp and wrist motions from among the most commonly used grasps in daily living (index flexion (IF), key pinch (KP), pulp pinch (PP), index point (IP), cylindrical wrap (CW), cylindrical wrap wrist rotate (CR), tripod pinch (TP), wrist extension (WE), wrist flexion (WF), and wrist rotation (WR)) [7]. Participants were prompted to begin in a relaxed state, then maintain the designated position for 3 seconds before returning to a relaxed state. Five to 10 trials worth of data were collected for each hand movement dependent on the child's attention span and reports of mental or physical fatigue.

Ultrasound setup: Following our previously established protocol [6], a clinical ultrasound imaging system (Terason uSmart 3200T, Terason, Tetratech Corporation, Pasadena) with a linear array transducer (16HL7 transducer, Terason, Tetratech Corporation, Pasadena) was used to capture tissue deformation in the participants' affected and unaffected forearms. The transducers were positioned on the anterior side of each arm, below the elbow, at a location that maximized observed tissue deformation when participants contracted and relaxed their muscles. Image data was sent to a laptop computer through a video capture card (DVI2USB 3.0, Epiphan Systems, Incorporated, Ottawa, CA) at 30 frames per second, and processed in MATLAB (MathWorks, Inc., Natick). Here, the image frames were down-sampled from the raw size of 1048x1048 pixels to 128x128 pixels. The first frame and last five frames of the trial were taken to represent the beginning and final state of the muscles respectively. We calculated the Pearson correlation coefficient between each image frame to the initial muscle state, and used a K-nearest neighbor algorithm to classify the end muscle states of the movement patterns. Leave-one-out cross-validation was used to calculate the classification accuracy and assess the performance of the classifier.

sEMG setup: Consistent with our prior work [5], a 16-channel Delsys Trigno surface EMG System (Delsys Inc., Natick) was used to capture affected and unaffected forearm electrical activity. Seven wireless Trigno Mini Sensors were placed on each limb, equally spaced around the circumference of the forearm muscle bulk. sEMG data was sampled at 2000Hz, bandpass filtered at 20-450 Hz, and passed to a National Instruments USB 6210 data acquisition system (National Instruments Corp., Austin), which sampled the data at 6000 Hz and stored it in MATLAB. To examine the accuracy to which hand movements could be classified, we used 60-40 cross-validation analysis with a

Linear Discriminant Analysis classifier that was trained on five sEMG features (correlation coefficient, multi-channel energy ratio, log detector, Hjorth mobility parameter, and integrated absolute value).

RESULTS

All N=28 participants produced ultrasound imaging and sEMG muscle activity data that was classifiable well above chance (10%). In Figure 2, we present results from two participants (age 11 and age 8) demonstrating the spectrum of the highest-performing through lowest-performing classification accuracies found in our sEMG data. Participant 3's sEMG data was classified with 88.3% ±10.0% accuracy and Participant 2's data was classified with 56.5% ±8.7% accuracy, demonstrating the potential variability across children with UCBED. However, the classification accuracies of the ultrasound data for these same two participants were much higher at 98.7% ±2.4% and 96.4% ±4.6%, respectively.

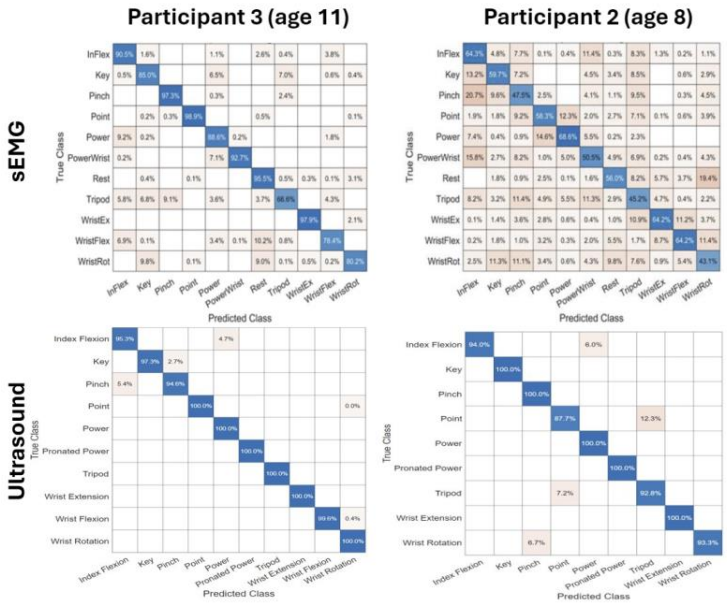

Figure 2: Confusion matrices for sEMG (top) and ultrasound (bottom) classifiers for the affected limbs of two study participants

In Figure 3, we use a polar plot to compare accuracies of affected and unaffected limbs for each grasp within the same two participants. Prediction accuracies for the affected limbs were either comparable or slightly diminished compared to the unaffected side, a phenomenon observed across all participants. The average classification accuracies for all 28 participants were 80.80% ±10.32% (sEMG, affected), 92.76% ±4.79% (sEMG, unaffected), 88.27% ±19.25% (ultrasound, affected), and 97.26% ±4.20% (ultrasound, unaffected). Thus, generally, across participants, classification accuracies for the ultrasound data exceed those of the sEMG data. Across our cohort, we observed that classifying muscle activity from the unaffected side resulted in higher classification accuracies; however, even the values for the affected side were far above chance, with the lowest results coming from participant 2's sEMG data at an average 56.5% ± 8.7% accuracy, and the best performance seen in the ultrasound data with accuracies nearing 100%.

DISCUSSION AND FUTURE DIRECTIONS

The design of effective dextrous prosthetic control systems requires a clear understanding of the motor capabilities of the user and the ability of the user to elicit clear, consistent patterns of muscle activation that can be reliably decoded. The results from the study indicate that children with UCBED have a robust level of motor control over their residual muscles, and that using multiple measurement modalities paired with machine learning, we can decode motor intent from the resulting muscle activity. Here, we found that all N=28 participants were able to elicit consistent patterns of muscle activity that were classifiable well above chance and, in many cases, achieving accuracy values consistent with adult myoelectric pattern recognition literature [8]. Though we must recognize the need for diligence in adapting adult-based techniques to serve the unique conditions a child with UCBED may present, this work emphasizes that children possess innate potential to effectively use ML-based control systems.

It should be noted that most participants had no prior training or experience with myoelectric prosthetics, and all participants did not have any prior experience with motor imagery to practice envisioning and moving their missing hand. Like any motor skill, we suggest moving a missing hand requires learning and training to reach high levels of proficiency. We believe there are exciting possibilities in this population of children to not only amplify their functional abilities with advanced control systems, but also to study human motor learning and development in a truly unique model. For example, most participants' affected muscles did produce consistent and unique patterns of muscle

activation with each attempted missing hand movement. This occurred across all ages of participants which spanned 5-20 years old. Our findings suggest that aspects of hand motor representations are retained despite the child never developing a hand. Further work to understand how affected muscle activity correlates to activity in higher control centers can provide a much deeper understanding of motor development and build up the foundations for effective control of advanced prostheses in this population.

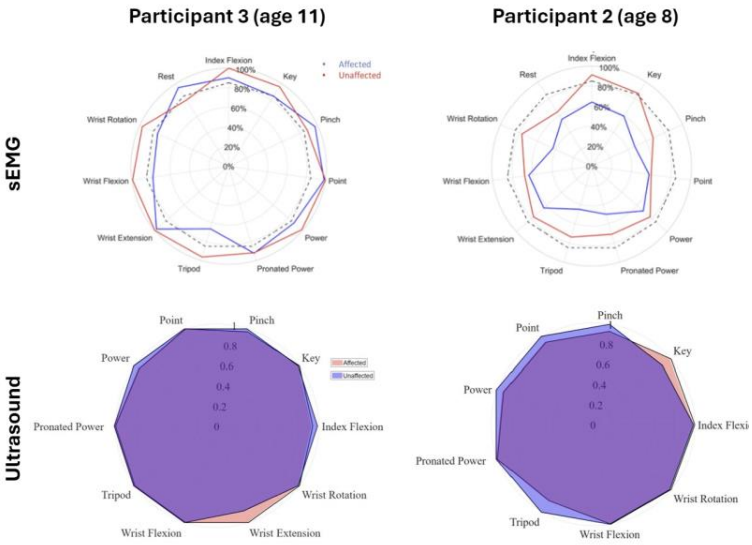

Figure 3: Polar plots for sEMG (top) and ultrasound (bottom) classifiers for both limbs of two study participants

The higher performance seen in the ultrasound data compared to the sEMG is interesting to note. Here, each measurement modality captures different muscular phenomenon: muscular displacement across the depths of the residuum or electrical activation measured at the surface of the skin. We believe there is a strong likelihood that sEMG and ultrasound are identifying distinct yet complementary information in the muscles. Examining fusion techniques or identifying use cases and conditions most amenable to each modality in future work would prove powerful insight to maximizing the classification performance of control systems for children with UCBED. The work presented here is a subset of a large multi-center research effort collecting data from children with UCBED across the United States. Here, the goal is to examine how patient-specific factors such as age, gender, limb characteristics, and prosthetic use may influence their abilities to control affected muscles and the control techniques that may be most amenable to serve patients given these factors. Together this work begins to build the foundations to better understand the muscle motor capabilities of children with UCBED, as well as put down the necessary groundwork that must first be in place to effectively adapt dextrous control techniques for this population.

ACKNOWLEDGEMENTS

This work was supported by the National Science Foundation (2133879), Shriners Children's Clinical Research Award (79139), and EJW is supported by a NIAMS funded training program in Musculoskeletal Health Research (T32 AR079099) and by NSF NRT Award #2152260. Additional thanks to Josh Siegel.

REFERENCES

[1] H. Giele, C. Giele, C. Bower, M. Allison, "The incidence and epidemiology of congenital upper limb anomalies: a total population study," *The Journal of Hand Surgery,* vol 26, no. 4. pp. 628–634, 2001.

[2] E. Biddiss, T.Chau, "Upper limb prosthesis use and abandonment: a survey of the last 25 years," *Prosthetics and Orthotics International,* vol. 31, no. 3. *Prosthetics and Orthotics International*, pp. 236–257, Sep. 2007.

[3] M. James, A. Bagley, K. Brasington, C. Lutz, S. McConnell, F. Molitor, "Impact of prostheses on function and quality of life for children with unilateral congenital below-the-elbow deficiency," *J Bone Joint Surg Am,* vol. 88, no. 11, pp. 2356-65, 2006.

[4] M. Battraw, J. Fitzgerald, W. Joiner, M. James, A. Bagley, J. Schofield, "A review of upper limb pediatric prostheses and perspectives on future advancements," *Prosthetics and Orthotics International,* vol. 46, no. 3, pp. 267-273, 2022.

[5] M. Battraw, J. Fitzgerald, M. James, A. Bagley, W. Joiner, J. Schofield, "Understanding the capacity of children with congenital unilateral below-elbow deficiency to actuate their affected muscles," *Scientific Reports,* vol. 14, no. 1, p. 4563, 2024.

[6] J. Fitzgerald, M. Battraw, M. James, A. Bagley, J. Schofield, W. Joiner. "Moving a missing hand: children born with below elbow deficiency can enact hand grasp patterns with their residual muscles," *J NeuroEngineering Rehabil,* vol 21, no. 1, p. 13, 2024.

[7] J. Zheng, S. De La Rosa, & A. Dollar, "An investigation of grasp type and frequency in daily household and machine shop tasks," *IEEE Int. Conf. Robot. Autom,* pp. 4169-4175, 2011.

[8] M. Simão, N. Mendes, O. Gibaru, P. Neto, "A Review on Electromyography Decoding and Pattern Recognition for Human-Machine Interaction," *IEEE Access,* vol. 7, pp. 39564-582, 2019.

EFFECTS OF AUGMENTED REALITY TRAINING ON PATTERN RECOGNITION CONTROL IN MYOELECTRIC PROSTHESES USERS: A CASE STUDY

Salma Soliman[1], Anna Rita Moukarzel[1], InHwa Lee[2], Megan C. Hodgson[2], Christopher L. Hunt[2], Rahul R. Kaliki[2], Ahmed W. Shehata[1,3], Jacqueline S. Hebert[1,3]

[1]Department of Biomedical Engineering, University of Alberta, Canada, [2]Infinite Biomedical Technologies, USA, [3]Department of Medicine, University of Alberta, Canada

ABSTRACT

Myoelectric prosthesis control has seen significant advancements, with pattern recognition (PR) standing out as one of the key innovations. However, achieving a consistent level of control using PR demands extensive training. In this work, we present a case study to explore an augmented reality (AR) system for myoelectric control training. An individual with a transradial amputation underwent nine training sessions using an AR system over a month, and we assessed his progress by analyzing metrics collected during functional tasks. Throughout the training sessions, performance consistently improved, as indicated by completion rates and average task completion times. This improvement was accompanied by a reported decrease in mental workload, as measured by the PROS-TLX. These results suggest that training using AR systems has the potential to enhance myoelectric prosthesis control.

INTRODUCTION

Upper limb loss can significantly impact an individual's life and often lead to decreased life satisfaction [1]. Choosing the appropriate type of prosthesis and receiving adequate training is crucial. Advances within the field have resulted in the development of prostheses with higher degrees of motion [2]. Novel control strategies, such as pattern recognition (PR), have been introduced to provide access to these advanced devices. PR-based control is expected to lead to more intuitive operation of advanced prostheses compared to direct myoelectric control [3]. Training to use these control strategies involves both pre-prosthetic and prosthetic training. Pre-prosthetic training is done before the prosthesis fitting; it includes signals, physical strength, range of motion, and visualization training [4]. Studies suggest that users who commence myoelectric prosthesis training before prosthesis fitting have better rehabilitation outcomes [5]. Therefore, pre-prosthetic training is an essential component of the overall training process. However, there are some challenges with the current pre-prosthetic training methods, including the absence of feedback about their progress, poor motivation, and lack of training modules that directly relate to prosthesis use. These challenges can lead to prosthesis abandonment due to dissatisfaction with prosthetic control and function [4].

One of the current solutions explored is game-based training, which can increase patient motivation and provide feedback on progress through levels and scores. Other approaches expand the game-based training by integrating immersive platforms, which can further enrich motivation and feedback [6]. These tools enable patients to use a virtual arm instead of just visualizing their hand movements. Augmented reality (AR) training is an emerging rehabilitation technology that combines virtual objects with a real-world view. It involves displaying a virtual prosthesis controlled by electromyograph (EMG) signals and virtual objects manipulated by this prosthesis, all combined with the physical environment of the user. This training method has advantages over virtual reality training because the incorporation of real-world cues leads to a more accurate depth perception and reduced risk of virtual reality sickness [5]. Recent research has developed various AR systems for pre-prosthetic training [5,6]. However, the specific aspects of improvement and the optimal number of sessions required remain unclear. This case study aims to monitor and evaluate the effects of AR training on individuals with upper limb loss. The study uses AR prosthesis training with the newly developed Myoelectric Augmented Reality Training and Assessment (MARTA) system. The progress will be evaluated through the MARTA training sessions, and the training effects will be assessed using a pre-test and post-test protocol.

METHODS

Participant: The participant was a 56-year-old male with a right transradial amputation (1991; trauma). He had a corrected to normal vision and experienced phantom limb sensation with limited control. He had experience with a one-degree-of-freedom direct myoelectric control prosthesis. The participant attended the Bionic Limbs for Improved Natural Control (BLINC) lab for the training and testing sessions. Study protocols were approved by the University of Alberta Health Research Ethics Board (PRO00103131), and the participant provided written informed consent. The participant's measurements were recorded during the first visit, including his height of 187.96 cm, intact hand circumference of 23.88 cm, residual limb length of 23 cm, and circumference of 7 cm.

Equipment: The MARTA system required the participant to perform tasks in which virtual entities were rendered in the real-world environment through the Hololens (Microsoft, USA), a binocular head-mounted display. This device rendered virtual objects and a two-degrees-of-freedom prosthesis in real-time at 60 Hz, where the virtual prosthesis was overlayed on the participant's residual limb (Figure 1). Three VIVIE trackers (HTC Corporation, Taiwan) were used as a reference to map the virtual task objects in the AR environment to real-world locations. An additional VIVE tracker was placed on the participant's residual limb to allow real-time tracking of the virtual prosthesis. The virtual prosthesis hand movements were controlled by the participant using an EMG PR system (Infinite Biomedical Technologies, USA). For the real-time control of this prosthesis, the participant was fit with a Myo armband (Thalmic Labs, Canada) on their residual limb, 6 cm from the lateral epicondyle, which captured the signals from the arm and then sent them to the EMG PR system to command this virtual prosthesis.

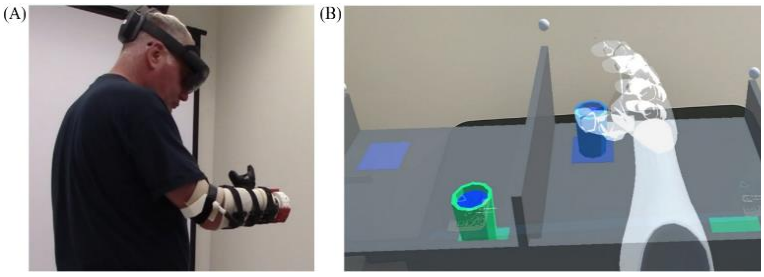

Figure 1: Experimental setup illustrating A) The participant wearing the equipment. B) The Augmented Reality task as observed from the participant's viewpoint.

AR tasks: The MARTA system consisted of three tasks: Dog Puzzle, Cup Transfer task, and Pasta Box task. The Dog Puzzle involved organizing and orienting cone-shaped objects into a 3-D dog shape. There were five levels in this task, with each level increasing the puzzle height for increased difficulty. Both the Cup Transfer task and the Pasta Box task were modelled in MARTA from the standardized tasks of the Gaze and Movement Assessment (GaMA) protocol [7]. In the Cup Transfer task, the participant was asked to move two cups over a barrier with specific grasps and then bring them back to their starting position using the same grasps. In the Pasta Box task, the participant moved a pasta box from a side table and placed it on a lower shelf in front of them, then to a higher shelf in front of them, and then back to its starting position. The Cup Transfer and Pasta Box tasks each had two levels of difficulty.

Training procedure: The MARTA system was used to train the participant, and training effects were assessed using a pre-test and post-test experimental design. Between the assessments, the participant completed nine training sessions over a period of three weeks, practicing the Dog Puzzle and the Pasta Box task. Weight was added throughout these sessions to improve the transferability of the training [5]. In session one, the socket weight was 379 g; in session four, we increased the weight to 521 g, and then to 671 g in session eight. Each training session was capped at two and a half hours, including the breaks and technical setup. For each session, the AR training tasks involved up to five trials of the Dog Puzzle, where each trial comprised a different level. Additionally, there were up to ten trials of each level of the Pasta Box task, where at least ten trials of level one were completed in any of the sessions before proceeding to level two. Each training session involved recording the placement of the Myo armband on the participant's residual limb to ensure consistency across sessions. The session started with PR calibration, where four different movements (open, close, pronation, supination) were recorded twice. After that, the recorded classifications were reviewed with the participant to confirm that he could successfully activate the classes. If not, the calibration was repeated. The participant then performed the Target Achievement Control (TAC) test to assess his control and evaluate how quickly and accurately he could achieve a specific movement. After completing this test, the participant watched demonstrational videos explaining the task, and then started the AR task. The participant wore the AR headset and practiced using the system for a maximum of ten minutes to get familiar with the AR environment, after which he proceeded with the training. After training, the participant filled out the Prosthesis Task Load Index (PROS-TLX) [8], a self-report measure designed to measure the physical and mental workload often experienced during tasks.

Assessment procedure and outcome measures: There were two assessment sessions, the baseline and the post-training. Each assessment session was capped at three hours, including breaks and technical setup time. The AR evaluations included up to 20 trials of the Cup Transfer task and ten trials of the Pasta Box task. The setup used for these sessions was similar to the training sessions, with the same calibration process. The TAC test and the two testing tasks (Cup Transfer and Pasta Box tasks) were performed after calibration, followed by the PROS-TLX at the end of each session. The study's primary outcome measures included the number of attempted and successful trials and the completion time of the successful trials for all tasks. For the Dog Puzzle, the number of object drops and attempted grips (how many times the hand completely closed) were also recorded. The results were compared across the sessions, and the averages and medians were calculated for different outcome measures.

RESULTS

Training progress: On average, the participant's active training time was one hour and 20 minutes. In the first training session, the participant had a 20% completion rate for the Dog Puzzle then his performance ramped up until he achieved a 100% completion rate by the fourth training session. The average trial completion time for the Dog Puzzle decreased from 7 minutes (one trial) in session one to 4 ± 1 minutes in session five, then to 3.60 ± 1.14 minutes in session eight. The participant started with a median of 51 grips and four drops in session two. The goal for the number of drops is zero and is ten for the number of attempted grips, as there are ten puzzle pieces in the Dog Puzzle. The participant's performance improved until it reached its peak at session five, with a median of 22 grips and zero drops. However, there was a decline in his performance during session six due to an unusual time gap between the fifth and sixth training sessions. For the Pasta Box task, the participant was unable to complete any trials in the first four training sessions due to the session time limit. He started with one successful trial of level one in session five, and then the number of completed trials and successful trials gradually increased (Figure 2A). By session eight, the participant had completed ten trials at level one, out of which eight were successful, and moved on to level two in this session and the following session. However, the participant's performance decreased in the last training session, with fewer completed and successful trials. This decrease in performance is also reflected in the average trial completion time, which increased from 1.28 ± 0.21 minutes at session eight to 3.39 ± 2.69 minutes at session nine (Figure 2B). The PROS-TLX score started at 47.99 in the first training session. It decreased until it reached the lowest point of 35.99 in session eight, demonstrating less load. The highest score was in the last training session, where it reached 64.86.

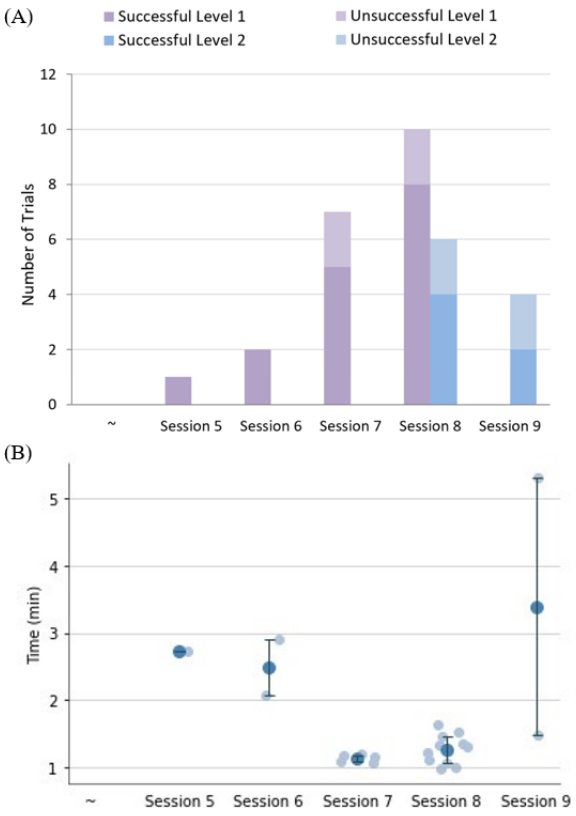

Figure 2: Outcomes of the Pasta Box task; the participant began progressing to the task starting from the fifth training session. A) Breakdown of the number of trial successes across different levels over the training duration. B) The dark colour represents the mean time taken per session. The error bars represent the standard deviation.

Pre- versus Post-training: For the Cup Transfer task, the participant's completion rate increased from 0% at the baseline to 80% at the post-training session. The average trial completion time was 1.40 ± 0.30 minutes during the post-training session. For the Pasta Box task, the performance improved as well, where the completion rate increased from 0% at the baseline to 70% at the post-training session. The average trial completion time was 1.69 ± 0.32 minutes for the post-training session. The PROS-TLX score was 56.32 at the baseline assessment, decreasing to 40.25 at the post-training assessment.

DISCUSSION

This work investigated the impact of the MARTA system on myoelectric PR control within the AR environment through metrics collected during functional virtual tasks. The results of our case study indicated that AR training positively influenced both control and motor learning aspects. Specifically, improvements were observed across the training sessions in the completion rates and times for both tasks, in addition to the number of grips and drops for the Dog Puzzle. Moreover, performance during the post-training assessment session was highly improved compared to the baseline assessment. The participant also reported a motivational and positive user experience with the system, this could be due to several factors, including the novelty of AR technology.

The participant demonstrated rapid progress during the training. As a result, in session five, we decided to increase the challenge of the Dog Puzzle by adjusting its height to keep the participant engaged and help continue his skill development. The results show that the performance achieved a peak twice during the training, in the fifth and eighth sessions. However, there was a decrease in performance between these sessions, followed by a gradual increase. We noticed a gap of four days between sessions five and six, which may have disrupted the continuity of skill acquisition, leading to fluctuations in performance during the following sessions. The PROS-TLX score of the final training session aligned with the performance outcomes, providing valuable insights into the participant's training experience.

The main limitation of this study was the prolonged technical setup time, which may have affected the participant's engagement and experience. Another limitation was the potential difficulty in perceiving objects correctly in the AR environment, which influenced the controller utilization. For instance, issues with visual perception in AR can lead to unintentional actions, such as air gripping instead of grasping the object or dropping the object through the table instead of placing it on the table, which happened during the first few training sessions. This could affect the study's results, as the number of grips in the Dog Puzzle won't be solely determined by the controller but also by the AR perception. These preliminary results are part of an ongoing study in which the number of participants and outcome metrics are expanded to explore more aspects as well as examine skill transferability to physical prosthesis function.

CONCLUSION

This preliminary data has shown that AR is promising for improving the control features important to myoelectric prosthetic training. The results demonstrated that the training was influential, as there was an improvement in performance at the end of the training. Additionally, the PROS-TLX revealed a notable reduction in mental workload throughout the training sessions, indicating a positive user experience. The study serves as a basis for the use of AR in pre-prosthetic training. A more extensive study with more participants and outcome measures is underway to allow for the exploration of the transferability to real-world prosthesis usage in the target population.

ACKNOWLEDGEMENTS

This work was supported by the department of defense under Award no. W81XWH-19-DMRDP-CRMRP-RESTORE.

REFERENCES

[1] K. Østlie, P. Magnus, O. H. Skjeldal, B. Garfelt, and K. Tambs, “Mental health and satisfaction with life among upper limb amputees: a Norwegian population-based survey comparing adult acquired major upper limb amputees with a control group,” *Disabil. Rehabil.*, vol. 33, no. 17–18, pp. 1594–1607, Jan. 2011, doi: 10.3109/09638288.2010.540293.

[2] A. Marinelli *et al.*, “Active upper limb prostheses: a review on current state and upcoming breakthroughs,” *Prog. Biomed. Eng.*, vol. 5, no. 1, p. 012001, Jan. 2023, doi: 10.1088/2516-1091/acac57.

[3] T. A. Kuiken, L. A. Miller, K. Turner, and L. J. Hargrove, “A Comparison of Pattern Recognition Control and Direct Control of a Multiple Degree-of-Freedom Transradial Prosthesis,” *IEEE J. Transl. Eng. Health Med.*, vol. 4, pp. 1–8, 2016, doi: 10.1109/JTEHM.2616123.

[4] C. Widehammar, K. Lidström Holmqvist, and L. Hermansson, “Training for users of myoelectric multigrip hand prostheses: a scoping review,” *Prosthet. Orthot. Int.*, vol. 45, no. 5, pp. 393–400, Oct. 2021, doi: 10.1097/PXR.0000000000000037.

[5] C. L. Hunt *et al.*, “Limb loading enhances skill transfer between augmented and physical reality tasks during limb loss rehabilitation,” *J. NeuroEngineering Rehabil.*, vol. 20, no. 1, p. 16, Jan. 2023, doi: 10.1186/s12984-023-01136-5.

[6] A. Boschmann, D. Neuhaus, S. Vogt, C. Kaltschmidt, M. Platzner, and S. Dosen, “Immersive augmented reality system for the training of pattern classification control with a myoelectric prosthesis,” *J. NeuroEngineering Rehabil.*, vol. 18, no. 1, p. 25, Dec. 2021, doi: 10.1186/s12984-021-00822-6.

[7] A. M. Valevicius *et al.*, “Characterization of normative hand movements during two functional upper limb tasks,” *PLOS ONE*, vol. 13, no. 6, p. e0199549, Jun. 2018, doi: 10.1371/journal.pone.0199549.

[8] J. V. V. Parr *et al.*, “A tool for measuring mental workload during prosthesis use: The Prosthesis Task Load Index (PROS-TLX),” *PLOS ONE*, vol. 18, no. 5, p. e0285382, May 2023, doi: 10.1371/journal.pone.0285382.

THE EFFECTIVENESS OF VIRTUAL REALITY TRAINING FOR ARM PROSTHESIS CONTROL COMPARED WITH PROSTHESIS SIMULATOR TRAINING

Bart Maas[a], Jack Tchimino[a], Bram van Dijk[a], Alessio Murgia[a], Corry K. van der Sluis[b], Raoul M. Bongers[a]

[a] *University of Groningen, University Medical Center Groningen, Department of Human Movement Sciences, Groningen, The Netherlands*
[b] *University of Groningen, University Medical Center Groningen, Department of Rehabilitation Medicine, Groningen, The Netherlands*

ABSTRACT

Background: It would be beneficial for people with an upper limb amputation to be able to start prosthesis training at an early stage during their rehabilitation process. Virtual reality can be used to provide early access to training. The current paper evaluates the differences in effectiveness of training using virtual reality and training using a prosthesis simulator.

Method: Twenty able-bodied participants were included and randomly divided into two groups, the VR (virtual reality) and the SIM (prosthesis simulator) group. Both groups completed a pre-test / post-test design with five training sessions in between. The effectiveness of the training was measured during the pre-test and post-test by using 3 standardized tests, the Box and Blocks test, the Southampton Hand Assessment Procedure (SHAP) and the Cylinder test.

Results: Both groups improved from pre-test to post-test and almost no statistical differences between groups were found. Only in a bimanual task from the SHAP the SIM group significantly outperformed the VR group.

Conclusion: No distinct differences between both groups were found in the majority of the tests, which shows that virtual reality training does not differ in effectiveness from prosthesis simulator training. However, virtual reality training is novel which is why motivational aspects and patient training should be explored in future research.

INTRODUCTION

Prosthesis training would preferably start at an early stage during rehabilitation to practice functional skills and to experience actual prosthesis use. Incorporating a virtual reality environment in rehabilitation practice can offer such an early training. A virtual environment where people with a recent amputation experience what it is like to use a prosthesis in daily tasks could prepare them for when they receive their personal device. Such an environment can also have variable difficulty settings to ensure motivation for training. Furthermore, in virtual reality individual feedback can be given to the user to assist during training. However, the question needs to be asked whether virtual reality and real life training provide different experiences and might be different in their effectiveness. The research question in the current paper is what the difference in the improvement of functional prosthesis control is between training in a virtual reality environment and training with a prosthesis simulator.

METHOD

Design

A pre-test post-test design with two experimental groups, the Virtual Reality (VR) group and the Simulator (SIM) group, was used. Before the start of the experiment, participants provided written informed consent. Participants were randomly assigned to one of the two groups before the start of the experiment. Each group trained for five training sessions on consecutive days between the pre-test and post-test. The pre-test and post-test were identical and included three tests which measured how skilled participants were in using the upper limb prosthesis simulator (Figure 1A), which resembled actual prosthesis use. The simulator consisted of a brace with an elbow joint which was connected to the upper arm and forearm using Velcro straps. The prosthesis, a Bebionic hand (Ottobock

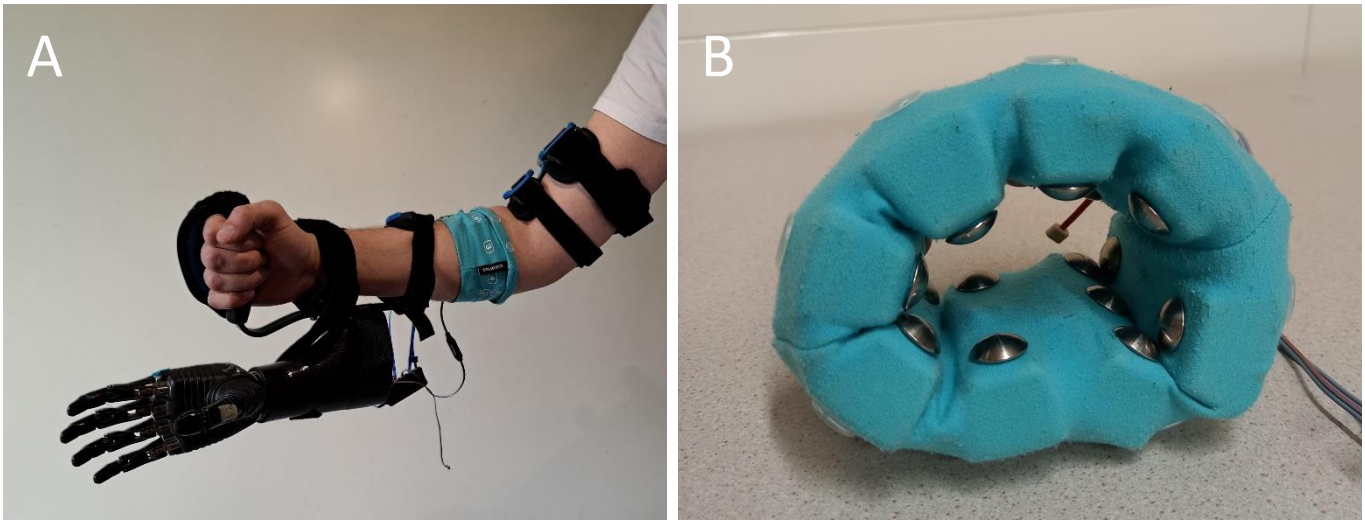

Figure 1. A: The prosthesis simulator controlled by the MyoPlus system which uses pattern recognition control. B: The cuff comprising the Ottobock MyoPlus system used to control the virtual prosthesis in the virtual reality environment

Healthcare Products GmbH, Austria), was attached underneath the brace of the forearm. The hand was controlled using the MyoPlus system (Ottobock Healthcare Products GmbH, Austria), which operates using pattern recognition. The virtual prosthesis was controlled using the same control scheme as the real prosthesis using the MyoPlus system from Ottobock (Figure 1B).

The tests included in the pre-test and post-test were the Box and Blocks test [1], the Jar Lid task and the Zipper task from the SHAP [2] and the Cylinder test [3], [4].

Training protocol

The VR group trained for five sessions within the virtual immersive environment, which was designed to be game-like. The setting of the game was that the user plays as a barista in a Mediterranean coffee shop. Participants had to complete a waitress's orders by choosing the correct cup and the correct button on the machine using the virtual prosthesis (Figure 2). They then needed to move the cup to the tray while trying not to spill any liquid. After an order was completed, the participants received a reward based on their performance in the form of coins. Dependent on the type of cup, the gasping force could deform or break the cup when too much force was applied. The game provided the user with relevant feedback on the amount of force they applied when a cup was grasped. This force feedback was provided in the form of a horizontal bar with a slider which indicated the amount of force applied by the prosthesis (Figure 2B).

The SIM group also trained for five training sessions performing a task similar to the VR group except using the prosthesis simulator in a real world setting, mimicking the virtual environment. A training set-up was built closely resembling the outlay of the VR coffee shop. Participants had to use the prosthesis simulator to grasp the correct cups following an order, move them under a coffee machine and move them to a tray.

Statistical analysis

For the Box and Blocks test a repeated measures ANOVA was conducted with Group as between-subjects factor and Test Moment as within-subjects factor. This was done after testing for normality with a Kolmogorov-Smirnoff test. For the Jar Lid and Zipper task of the SHAP we only analysed the post-test scores because many participants were unable to complete the task in the pre-test. After the missing values and outliers were removed the total number of included participants for the Jar Lid task was 17 (9 in SIM, 8 in VR) and for the Zipper 13 (7 in SIM, 6 in VR). With this limited number of participants the decision was made to test non-parametrically which was done with a Mann-Whitney U test. For the Cylinder test the normalized aperture was analysed using a linear mixed effect model with Group, Cylinder size and Test moment as fixed effects and individual participants as random effect. Interaction effects were also tested in this model.

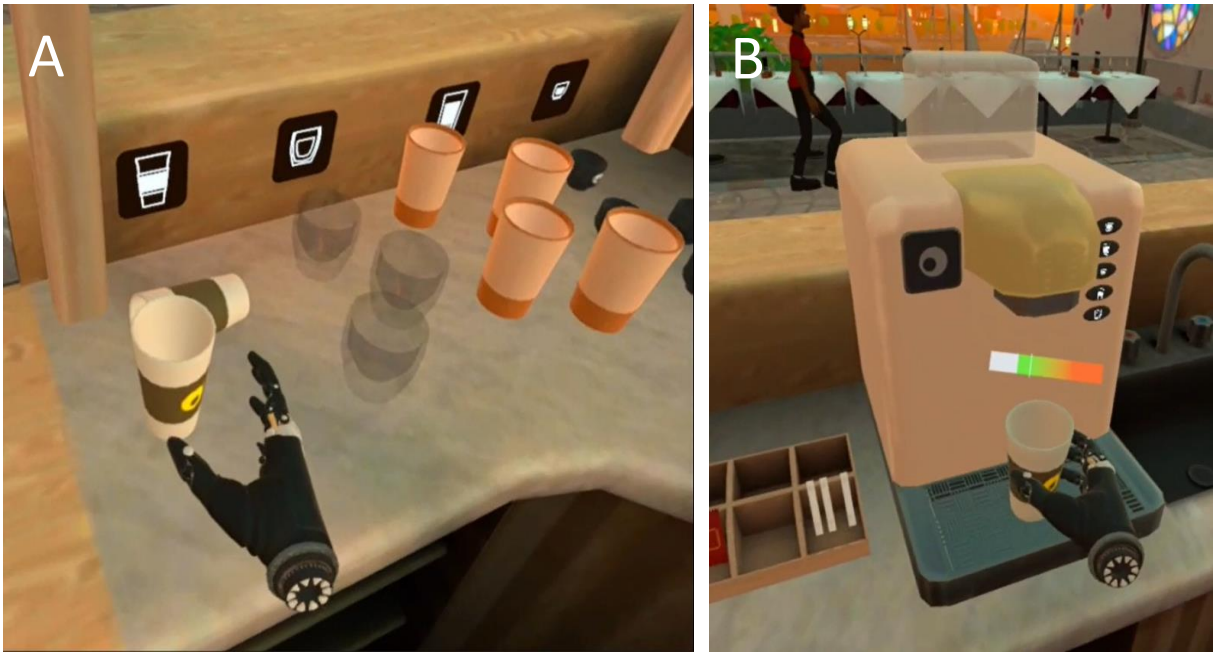

Figure 2. The virtual environment. A: The virtual prosthesis grabs a compressible cup (other cups can be seen on the right). Each cup had different properties, from left to right these were: the white cups were compressible, the transparent cups had glass cup properties and broke when grasped too hard, the brown cups were rigid and the black cups were small. B: The cup is placed underneath the coffee machine. The different coffee options are depicted on the right side of the machine by different buttons. The horizontal bar above the cup provides feedback on the grasping force. The colors of the bar indicate different ways the hand is interacting with the cup: white when the cup is not grasped, green when the cup is grasped and red if the cup is compressed or crushed.

RESULTS

A total of 20 participants were included, 8 males and 12 females with a mean age of 21.2 ±1.9 years. Ten participants were assigned to the VR group, 4 males and 6 females and ten participants were assigned to the SIM group, 4 males and 6 females.

For the Box and Blocks test a significant main effect of Test Moment was found, $F(1, 17) = 10.66$, $p = .005$. No significant effect for group or interaction effect was found. See figure 3A for the mean scores and standard error of the mean (SEM). Regarding the Jar Lid and Zipper tasks of the SHAP, a significant difference between groups was found for the Jar Lid task. The simulator group outperformed the VR group, $z = -2.5$, $p = 0.01$ (see figure 3B). The analysis on the aperture in the Cylinder test revealed a significant fixed effect of Test moment ($\chi^2(1) = 6.82$, $p = .009$) and of Cylinder size ($\chi^2(2) = 126$, $p < .001$), see figure 3C and 3D respectively.

DISCUSSION AND CONCLUSION

The main finding of this study is that the improvement of participants in the VR group was not different from the improvement of the participants in the SIM group in most tests. Therefore, it seems like both training methods are both effective in improving functional prosthesis control.

This is a relevant finding due to the fact that the VR group had to transfer the skills they learned in a virtual environment to actual use with a prosthesis simulator. Additionally, the VR group improved functionality at a similar rate with the SIM group, who trained with the prosthesis simulator and had thus an advantage.

The only test in the current study that does not support the equivalence claim between VR and SIM, is the result of the Jar Lid task of the SHAP where the SIM group outperformed the VR group in the post-test. Further research is necessary to explain this deviating finding.

One point that should be made is that VR training presents a number of advantages compared to the SIM group that are not analyzed in the current paper. Factors such as motivation, effects of individualized feedback and less fatigue due to the missing weight of the simulator could have a major impact on training effectiveness.

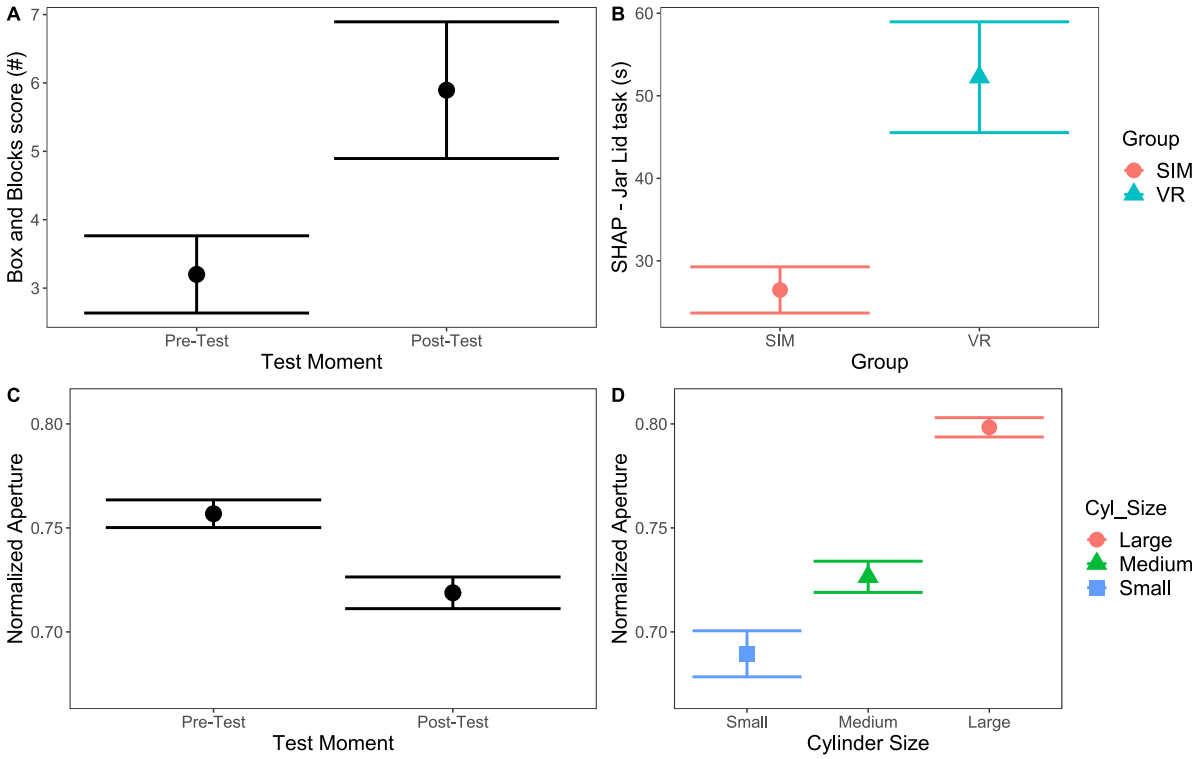

Figure 3. A) The scores Box and Blocks test for the Pre-Test and the Post-Test. The mean and SEM are presented. B) The completion time for the Jar Lid task from the SHAP for the VR group and the SIM group. The mean time and SEM are presented C) The normalized aperture of the Cylinder test for the Pre-Test and the Post-Test. The mean and SEM of the normalized aperture are presented. D) The normalized aperture of each individual cylinder size, Small, Medium and Large. The mean and SEM of the normalized aperture are presented.

To conclude, there seem to be no major differences between training in a virtual reality environment and training with an actual prosthesis simulator based on our results. That is why our conclusion is that there is no difference in improvement on effectivity between virtual reality and prosthesis simulator training. However, the current study used able-bodied individuals which is why future research should expand on the current design by including patients and also explore the motivational aspects of training with VR.

REFERENCES

[1] Mathiowetz, Virgil & Volland, Gloria & Kashman, Nancy & Weber, Karen. (1985). Adult Norms for the Box and Block Test of Manual Dexterity. The American journal of occupational therapy : official publication of the American Occupational Therapy Association. 39. 386-91. 10.5014/ajot.39.6.386.

[2] C. M. Light, P. H. Chappell, and P. J. Kyberd, “Establishing a standardized clinical assessment tool of pathologic and prosthetic hand function: Normative data, reliability, and validity,” *Arch Phys Med Rehabil*, vol. 83, no. 6, pp. 776–783, 2002, doi: 10.1053/apmr.2002.32737.

[3] L. Van Dijk, C. K. Van Der Sluis, H. W. Van Dijk, and R. M. Bongers, “Learning an EMG controlled game: Task-specific adaptations and transfer,” *PLoS One*, vol. 11, no. 8, pp. 1–14, 2016, doi: 10.1371/journal.pone.0160817.

[4] L. Van Dijk, C. K. Van Der Sluis, H. W. Van Dijk, and R. M. Bongers, “Task-Oriented Gaming for Transfer to Prosthesis Use,” *IEEE Transactions on Neural Systems and Rehabilitation Engineering*, vol. 24, no. 12, pp. 1384–1394, 2016, doi: 10.1109/TNSRE.2015.2502424.

Myoelectric Controls Algorithms

3-STAGE NEURAL NETWORK TRAINING PROTOCOL FOR GENERALISABLE MYOELECTRIC CONTROL

Chenfei Ma, Xinyu Jiang, Kianoush Nazarpour

School of Informatics, The University of Edinburgh, United Kingdom

ABSTRACT

Myoelectric control methods have undergone rapid evolution since the pre-1960s era. However, a longstanding challenge has been the variability of myoelectric signals across individuals, which impedes the development of universally applicable myoelectric control models. Researchers and companies in the field have been active in exploring various aspects such as different control strategies, pattern recognition methods, signal processing, and decoding. For instance, Meta recently reported a common model for a database of 6700 able-bodied participants. Development of such datasets with people with limb difference, in the higher education sector is unrealistic. But what we believe could be helpful is a scheme to guide researchers in addressing different stages of the process, with the aim of collectively developing a general-purpose, pre-trained, and generalisable myoelectric model. In this paper, we propose a 3-stage neural network training paradigm. Experiments were conducted with able-bodied participants to demonstrate the significance and necessity of each stage in the proposed scheme. Work is in progress to further enhance and verify the method. We aim to share this approach at MEC to receive feedback and invite collaborations for standardising data collection and pulling together our resources.

INTRODUCTION

The increasing popularity of technology-enabled human-machine interfacing research and commercialisation has been significantly strengthened by the emergence of a wide array of wearables [1]. This surge is primarily driven by the demand for devices that prioritise intuitiveness, efficiency, portability, and wearability, thus placing myoelectric signals at the forefront of attention. Notably, the advancement of methods for myoelectric control has accelerated rapidly, particularly with the advent of deep learning techniques and the remarkable growth in computational power. Various deep learning architectures such as convolutional neural networks [2], recurrent neural networks [3], and deep belief networks [4] have been applied extensively in both discrete movement classification and continuous regression tasks with varying success.

While many studies have demonstrated outstanding performance in movement estimation, their direct application in practical settings remains challenging. This difficulty arises primarily from end-to-end training methodologies, which often results in overfitting. Additionally, factors such as privacy concerns, substantial individual differences among users, and the inherent complexity of human movement further contribute to these challenges. Furthermore, the opaque nature of neural networks poses additional hurdles, as it complicates efforts to calibrate or adapt models when accommodating new users who may not share similar data distributions with the original training set. These limitations curtail the applicability and scalability of neural networks in real-world contexts, highlighting the need for further refinement and innovative approaches in addressing these constraints.

This paper introduces a novel 3-stage neural network training scheme, with blocked referred to as Pretraining, Localisation, and Self-calibration. Each stage employs the simplest method to provide a clear and comprehensive explanation while demonstrating the viability of the proposed protocol. Through a series of multi-stage experiments conducted over a 2-day period with 28 participants, the need for each stage is demonstrated, thus validating the efficacy of the proposed approach.

We intend to present this approach at MEC with the objective of soliciting feedback and fostering collaborations aimed at standardising data collection practices and pooling our resources.

METHOD

Pretraining

As extensively utilised in deep learning methodologies, pretraining [5] serves as an efficient means to extract and organise prior knowledge from existing data. This approach facilitates the development of robust models and therefore is an integral component of the increasingly prevalent transfer learning paradigms. As previously mentioned, the scarcity of training data in myoelectric control scenarios underscores the critical importance of carefully selecting neural network structures for the pre-training stage of the proposed paradigm.

The Temporal Convolutional Network (TCN) structure [6] has proven to be effective in processing time-sequence data, as demonstrated in various applications such as action segmentation [6] and network traffic prediction [7]. In this paper, we employ a single shallow TCN structured as depicted in Figure 1. The utilisation of dilated and causal convolutions within the TCN significantly expands the receptive field of the network. This modification directs the network's focus towards information preceding the current time step, contrasting with the typical convolutional neural network approach, which tends to distribute attention across the entire input. These characteristics align well with the requirements of processing and classifying myoelectric signals. For further details, please refer to [6].

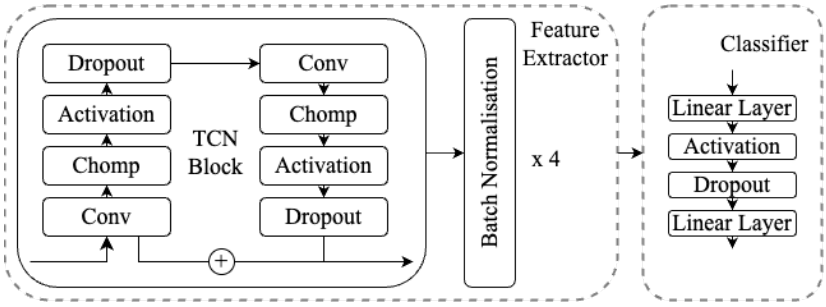

Figure 1: The TCN structure employed in the pretraining part, which is unified across all stages

Localisation

While the pretrained model demonstrates robust convergence on the pretraining dataset, the significant individual diversity poses challenges, occasionally resulting in complete failures when the myoelectric signal distribution from a new user diverges from the pretraining dataset. However, the limited size of the data collected from the new subject prohibits the establishment of a fair distribution or comprehensive representation within the model. Consequently, achieving proper calibration at this stage is impractical. Instead, a localisation approach will be implemented, which involves using a minimal amount of data to adapt the pretrained model to the new user. While one trial per movement of data may not provide sufficient information for precise adjustment of the pretrained model to the new user, experimental results demonstrate its efficacy in reducing total failures.

To localise the pretrained model, we employ fine-tuning [8]. We relax the weights for each layer of the TCN network and utilise the Adam optimizer [9] to decrease the gradient, which is calculated based on cross-entropy loss [10]. This approach is facilitated by the availability of one trial of data and its corresponding label, both of which are recorded during data collection from the new subject.

Self-calibration

Following the localisation process, the neural network begins to adapt to the distribution of the new subject's data. However, the second challenge mentioned earlier persists: the continuously evolving patterns over time within a user. This leads us to the third stage: self-calibration. Unlike the previous two stages, self-calibration utilises unlabelled myoelectric data. Its objective is to ensure the model remains adaptable to the ongoing changes in the distribution of myoelectric signals from the user. To achieve this, we propose a clustering-based semi-supervised learning approach, illustrated in Figure 2.

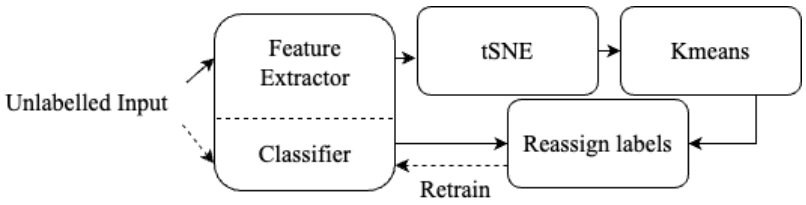

Figure 2: Schematic diagram for the proposed clustering-based pseudo labelling method

The TCN model, as described above, consists of two components: the feature extractor (FE) and the classifier. The feature extraction stage extracts high-level features from the input and passes them to the classifier. During the self-calibration process, the FE remains frozen, and its output is subjected to t-distributed Stochastic Neighbour Embedding (t-SNE) [11] for unsupervised non-linear dimensionality reduction. Subsequently, the low-dimensional embedding undergoes clustering via K-means. Although initial labels are generated, they may not align perfectly with the pre-set values. Therefore, the output of the classifier, representing predictions from the localised model, is utilised to reassign labels through comparison. Specifically, the majority label from the classifier for each sample cluster in the K-means output is reassigned to match the classifier's prediction. This process ensures uniform labelling, with the final step involving the combination of the new labels and input data to retrain the localised model. It is important to note that this self-calibration process occurs each time a certain number of samples is obtained for each label, thereby ensuring the continuous adaptability of the model to users.

Experiment design

All participants signed an informed consent form approved by the local ethics committee at the University of Edinburgh (reference number: 2019/89177), in accordance with the Declaration of Helsinki. The experiment comprised six movements: power, lateral, tripod, pointer, open, and rest. A total of 28 participants aged between 21 and 43 years, including 13 males and 15 females, were recruited. Upon informed consent, first, each participant performed one trial per movement, during which 15-channel Delsys electrodes were placed around the forearm near the elbow to collect data. Following this data collection phase, participants completed 10 blocks of tests consisting of five randomly ordered trials for each movement. During each trial, participants were instructed to mimic a gesture displayed on a computer screen for 2 seconds, with data and labels recorded during the latter 1-second interval to account for reaction time. No feedback was provided to participants to prevent bias in user behaviour. The test of the proposed scheme is illustrated in Figure 3, with each part involving the model from the preceding section. All tests were conducted using the last two trials of each block to ensure fair comparison. Furthermore, all three examinations were conducted as leave-one-out tests, wherein the same process was repeated 28 times, with each subject serving as the test subject while pretraining was conducted on the remaining subjects.

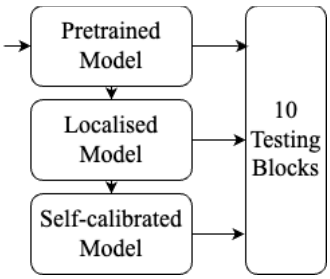

Figure 3: 3 Testing protocol

Feature extraction and processing

We extracted time-domain (waveform length, log variance, zero crossing, slope sign changes, and skewness) and frequency-domain (mean frequency, peak frequency, and variance of central frequency) features. The feature set was validated during the pretraining phase as the most reliable, yielding optimal performance. Additionally, data augmentation was performed by calculating averages between neighbouring channels to create virtual channels in between. Empirical analysis showed that this augmentation improved model performance by two percentage points.

RESULTS

The evaluation of model performance involved comparing the accuracy of the model outputs to the ground truth labels. As depicted in Figure 4(a), across all 10 blocks, the localised model consistently outperformed the pretrained model in terms of accuracy, and the self-calibrated model exhibited superior performance compared to the localised model. Although both the pretrained and localised models experienced a decline in performance during the second block, the localised model ultimately demonstrated better performance than the pretrained model, as illustrated in

Figure 4(b). Notably, the performance of the pretrained model became significantly more unstable during the last three blocks, possibly due to users forgetting the correct gesture movements. In contrast, the self-calibrated model's performance remained stable throughout all 10 blocks, beginning with a satisfactory accuracy of 79% and consistently maintaining an accuracy above 80% for most of the duration.

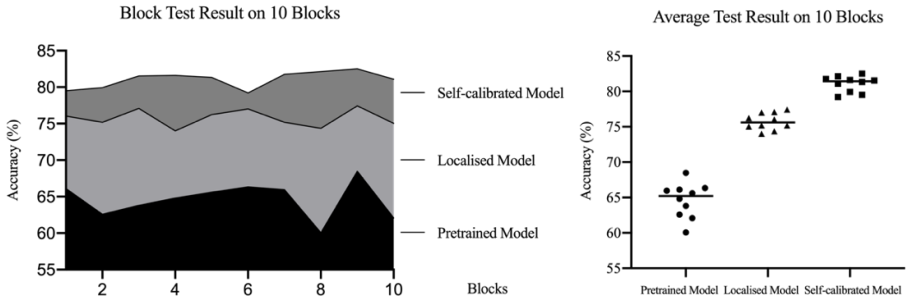

(a) (b)

Figure 4: (a) The test accuracy results on each block (b) The average test accuracy results on 10 blocks

DISCUSSION

The proposed training method offers a versatile approach that can be applied to any modern neural network architecture. Through three stages [pretraining, localisation, and self-calibration], it extracts information from existing datasets, personalises the network for new users, and continuously updates the model to accommodate changing myoelectric behavior. The methods chosen for each stage are intentionally simple and straightforward to facilitate clear communication of ideas and concepts. It is undeniable that machine learning based methods will increasingly dominate conventional approaches in myoelectric control. However, the way we train the neural networks in this field is equally important. The protocol outlined in this paper represents a starting point for segmenting the myoelectric signal processing pipeline and moving away from end-to-end training. In future research, we plan to explore transfer learning, aiming to apply it with a modest amount of data to fully leverage information from existing databases.

REFERENCES

[1] J. Cannan and H. Hu, "Human-Machine Interaction (HMI): A Survey," *Technical Report: CES-508*, 2011.

[2] A. Ameri, M. A. Akhaee, E. Scheme, and K. Englehart, "Real-time, simultaneous myoelectric control using a convolutional neural network," *PLoS One*, vol. 13, no. 9, 2018, doi: 10.1371/journal.pone.0203835.

[3] C. Ma *et al.*, "A Bi-Directional LSTM Network for Estimating Continuous Upper Limb Movement from Surface Electromyography," *IEEE Robot Autom Lett*, vol. 6, no. 4, 2021, doi: 10.1109/LRA.2021.3097272.

[4] J. Zhang, C. Ling, and S. Li, "EMG Signals based Human Action Recognition via Deep Belief Networks," in *IFAC-PapersOnLine*, 2019. doi: 10.1016/j.ifacol.2019.12.108.

[5] D. Hendrycks, K. Lee, and M. Mazeika, "Using pre-training can improve model robustness and uncertainty," in *36th International Conference on Machine Learning, ICML 2019*, 2019.

[6] C. Lea, M. D. Flynn, R. Vidal, A. Reiter, and G. D. Hager, "Temporal convolutional networks for action segmentation and detection," in *30th IEEE Conference on Computer Vision and Pattern Recognition, CVPR 2017*, 2017. doi: 10.1109/CVPR.2017.113.

[7] J. Bi, X. Zhang, H. Yuan, J. Zhang, and M. C. Zhou, "A Hybrid Prediction Method for Realistic Network Traffic With Temporal Convolutional Network and LSTM," *IEEE Transactions on Automation Science and Engineering*, vol. 19, no. 3, 2022, doi: 10.1109/TASE.2021.3077537.

[8] K. He, R. Girshick, and P. Dollar, "Rethinking imageNet pre-training," in *Proceedings of the IEEE International Conference on Computer Vision*, 2019. doi: 10.1109/ICCV.2019.00502.

[9] D. P. Kingma and J. L. Ba, "Adam: A method for stochastic optimization," in *3rd International Conference on Learning Representations, ICLR 2015 - Conference Track Proceedings*, 2015.

[10] C. E. Shannon, "A Mathematical Theory of Communication," *Bell System Technical Journal*, vol. 27, no. 4, 1948, doi: 10.1002/j.1538-7305.1948.tb00917.x.

[11] G. Hinton and S. Roweis, "Stochastic Neighbor Embedding," in *NIPS 2002: Proceedings of the 15th International Conference on Neural Information Processing Systems*, 2002. doi: 10.1007/978-3-031-10602-6_16.

A RESPONSIVE MYOELECTRIC CONTROL SIGNAL PROCESSING TECHNIQUE USING MUSCLE EXCITATION-CONTRACTION MODELING

Barathwaj Murali, MS[1] and Richard F. *ff.* Weir, PhD[1,2]

[1] Department of Bioengineering, University of Colorado Anschutz Medical Campus, Aurora CO USA, [2] Rocky Mountain Regional VA Medical Center, Aurora CO USA

ABSTRACT

Existing myoelectric controllers operate in a sequential fashion and use a state machine architecture to select grip postures. Direct control interfaces that seek to map individual muscles with joints in a prosthesis can provide a greater ability to perform individuated movements but require users to selectively activate their muscles to prevent unintended motion from natural muscle co-activations. Musculoskeletal modeling offers a possibility to estimate joint motion from muscle co-activation patterns themselves but require significant computational resources to run in real time. A major source of delay in a myoelectric system that reduces the amount of time available for advanced signal decoding schemes such as a musculoskeletal model is the low-pass filtering of rectified EMG signals. To minimize these delays, we explore the low-pass filtering properties of skeletal muscle using a simplified excitation-contraction dynamics model, applying a thresholded EMG signal and the rectified EMG profile itself as model inputs. Our results indicate that passing these signals through a biomechanical model of muscle can produce a usable myoelectric control signal while introducing a physiologically appropriate amount of delay between EMG onset and muscle force estimation.

INTRODUCTION

Approximately 541,000 individuals live with an upper limb deficiency in the United States [1]. Myoelectric control options for these individuals typically include two-site myo (the standard of care), pattern recognition, and postural control [2-4]. These systems operate in a sequential open-close fashion as users can switch between grip postures but are unable to modify their motions in real-time or combine postures simultaneously. The state machine architecture used by these controllers also reduces the capability of multi-articulated prosthetic hands to simple grasping mechanisms. Direct control schemes seek to achieve simultaneous joint motion using targeted EMG electrode placement to provide a greater number of control sites. Cipriani et al. [5] demonstrated the ability of intact individuals to produce individuated and simultaneous thumb, index, and middle finger motions through a direct control interface using intramuscular EMG measured from the extrinsic finger flexors. However, mapping joint motion to EMG activity produced by individual muscle compartments required users to selectively activate their targeted muscles and avoid producing natural muscle co-activations that play an important role in producing dexterous motions. Musculoskeletal simulation provides an appealing option to estimate joint motion produced by muscle co-activations that ultimately result in complex and intuitive limb motion.

Using a musculoskeletal model as a signal decoding interface requires significant computational overhead to run in real-time [6]. A real-time myoelectric control system must acquire, process, and decode EMG data at a rate faster a human operator can perceive. Users can largely tolerate controller update rates of 100ms before complaining of sluggish performance [7]. The low-pass filtering (or enveloping) of EMG activity can introduce delays between the onset of muscle contraction and prehensor motion ranging between 50-250ms [8]. Larger filtering time constants reduce the overall system bandwidth along with the proportion of the controller update rate available for more sophisticated signal decoding schemes. Childress et al. [9] developed a highly responsive control signal by thresholding the EMG amplitude profile and pulse modulating a motor within a myoelectric prehensor to leverage its inherent dynamics for low-pass filtering. Skeletal muscle performs a similar role in the body by producing a force response from pulsed motor unit action potentials that closely follows a minimum-jerk smoothness profile [10]. In this work, we apply a thresholded (or myopulse) EMG signal in addition to the rectified EMG amplitude profile as inputs to a physiological model of muscle excitation-contraction dynamics to demonstrate its ability to produce a smooth output response while introducing a physiologically appropriate delay between EMG onset and muscle contraction.

METHODS

Muscle Excitation-Contraction Dynamics

A simplified model of muscle excitation dynamics based on the model in Krylow et al. [10] consisted of two coupled first-order ODEs to estimate the active state of the muscle, defined as the rate at which calcium-bound troponin exposes actin binding sites for cross-bridge formation [11]. The amount of free calcium $r(t)$ in Eqn. 1 is proportional to pulsed input $x(t)$ and offset by the reabsorption of free calcium. The proportion of bound calcium $y(t)$ in Eqn. 2 provides the active state of the muscle, bounded between 0 and 1. The coefficients $C_1 = 100$, $C_2 = 107$, $C_3 = 99$, and $C_4 = 94$ were determined by fitting Eqns. 1 and 2 to match muscle activation and deactivation time constants of 10ms and 40ms recommended for human muscle [12].

$$\dot{r}(t) = C_1 x(t) - C_2 r(t) \tag{1}$$

$$\dot{y}(t) = \begin{cases} C_4 r(t) - C_3 y(t), & y(t) \le 1 \\ -C_3 y(t), & y(t) > 1 \end{cases} \tag{2}$$

The active state estimated by Eqn. 2 drove a simplified two-element model [10], illustrated in Figure 1a, consisting of a contractile element representing the muscle body and a series elastic element representing the tendon. The contractile element followed Hill's force-velocity relation [13], expressed in Eqn. 3

$$V_{CE} = \frac{b_0 (P_0 y - F_M)}{F_M + a_0} \tag{3}$$

where V_{CE} is the muscle shortening velocity, $a_0 = 0.3$ and $b_0 = 0.04\ m/s$ are Hill model constants, $P_0 = 24.1\ N$ is the maximum isometric muscle force, F is the contractile element force, and y is the muscle active state [10].

The force developed by the series elastic tendon in Eqn. 4 is equal to contractile element force F_M and can be expressed in terms of total muscle length L_M and contractile element length L_{CE}

$$F_{SE} = k L_{SE} = k(L_M - L_{CE}) \tag{4}$$

where F_{SE} is the force on the tendon, $k = 1800\ N/m$ is the tendon stiffness [10], and L_{SE} is the tendon length.

Scaling the model constants a_0, b_0, and k using an empirical isometric force-length curve from Krylow et al. [10] introduces length-dependence to the force-velocity and tendon stiffness equations in Eqns. 3 and 4. Differentiating Eqn. 4 yields the ordinary differential equation governing contractile element force production

$$\frac{dF_M}{dt} = k(V_M - V_{CE}) \tag{6}$$

In Eqn. 6, the velocity of the muscle-tendon endpoint (V_M) is set to zero to represent an isometric force scenario. The system of ODEs formed by Eqns. 1-3 and 6 were solved using a fourth-order Runge-Kutta integrator.

Experimental Protocol

Eight subjects (6M/2F, all right-handed, age 28.6 ± 7.6 yrs.) performed a set of steady-state isometric contraction tasks consisting of a single isometric force trial at Maximum Voluntary Contraction (MVC) followed by a series of sub-maximal contraction tasks in increments of 20-percent MVC. Subjects provided informed consent for their participation and the protocol was approved by the Colorado Multiple Institutional Review Board (COMIRB). Subjects produced isometric forces by gripping a Jamar hand dynamometer instrumented with a pressure transducer (Honeywell, Charlotte NC) while a single differential electrode (Delsys, Natick MA) placed on the medial surface of the forearm recorded EMG activity from the extrinsic finger flexors. Data was acquired at 2000 Hz while a custom graphical interface developed provided visual cues of target grip force levels to participants.

Data Analysis

Surface EMG data was bandpass filtered (6th order Butterworth, 30 Hz high-pass, 480 Hz low-pass) and notch filtered (2nd order IIR bandstop, 60 Hz stopband frequency). After normalizing EMG data to MVC values for each subject, the myopulse signal was computed for each isometric force trial using a threshold value of three standard

deviations above the mean quiescent EMG amplitude. The muscle excitation-contraction dynamics model estimated muscle force using the myopulse signal and the rectified EMG amplitude profile as separate inputs. The average steady-state isometric forces estimated by the model were used to determine the relationship between estimated muscle force and measured muscle contraction level.

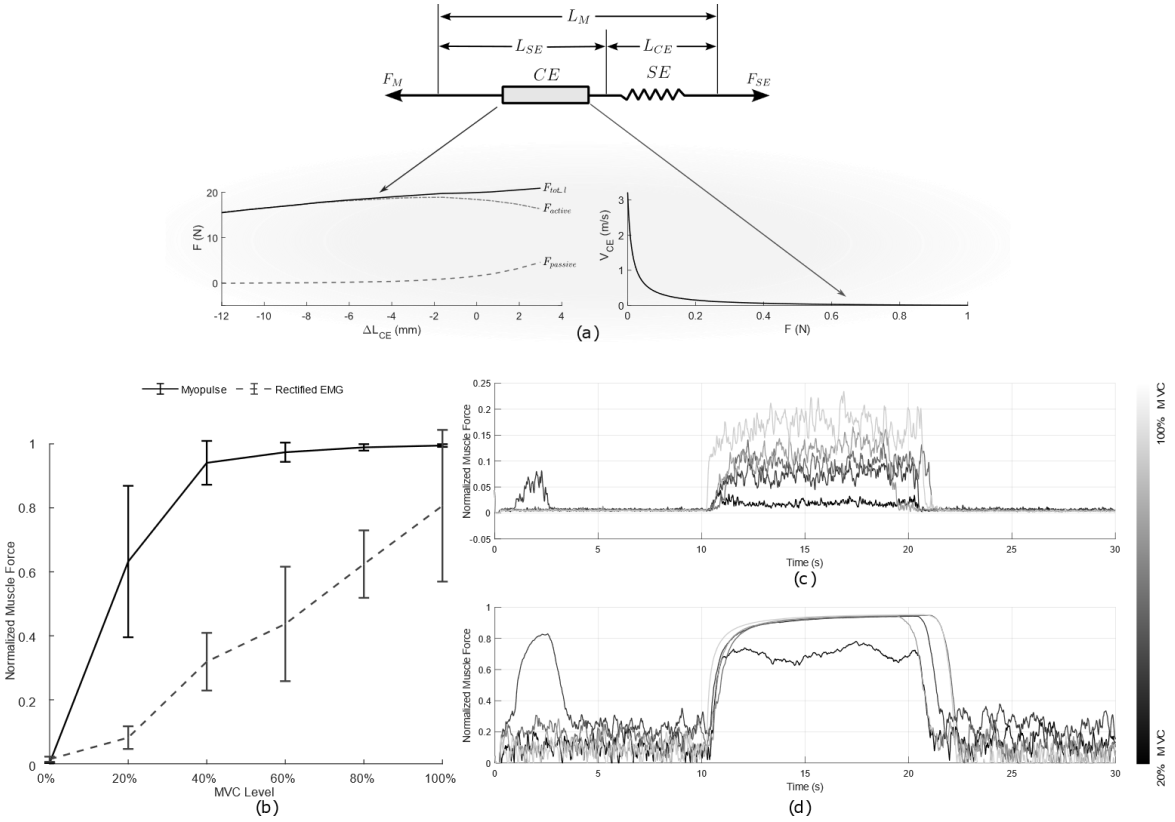

Figure 1: (a) Two-element Hill model from Krylow et al. [10] and force-length and force-velocity relations. (b) Normalized muscle forces plotted against steady state MVC contraction level. (c) Time series plot of estimated muscle forces from excitation-contraction dynamics model from rectified EMG signal. (d) Time series plot of estimated muscle forces from myopulse signal.

RESULTS

The forces estimated from the myopulse signal produced a hyperbolic relationship with muscle contraction level, (Figure 1b), while the forces estimated from rectified EMG amplitudes produced a linear relationship with muscle contraction level. The myopulse signal produced a smoother force response at steady-state isometric contraction levels and reached higher force magnitudes (Figure 1c), but also produced noisier forces during the quiescent portions of the isometric force trials. The opposite was true for the force profiles produced by the rectified EMG signal (Figure 1d) characterized by smoother quiescent forces and noisier steady state values.

DISCUSSION

We explored the ability of a physiological model of muscle excitation-contraction dynamics to avoid introducing large time constants associated with EMG low-pass filtering. The system of equations governing the model essentially act a cascaded fourth-order filter that successively smooths the input signal and constrains the delays introduced at each stage within a physiologically appropriate range. From Figure 1, the forces estimated from the quiescent myopulse signal are noisier than those estimated from the rectified EMG signal. This result is most likely due to the on-off nature of the myopulse signal which would cause noticeable force production depending on the time constants used by the excitation dynamics equations. In contrast, the rectified EMG signal produced a noisier steady-state force

profile but a smoother quiescent period. Since the rectified signal retains its amplitude information, the active state estimated from low EMG amplitudes will also be small in magnitude. Although the magnitudes of the estimated muscle forces vary between the myopulse and rectified EMG inputs, proper scaling and normalization will produce sufficient output signal magnitudes to drive a myoelectric system. The selection of excitation dynamics coefficients and tendon stiffness values influences the rise time of the muscle force profiles, as an inverse relationship exists between the amount of delay introduced to the output signal and the degree of smoothing performed by the excitation-contraction dynamics model.

The steep increase in output force produced by the myopulse signal at low muscle contraction levels and force saturation at higher contraction levels may be a result of the interaction between the force-velocity curve with the response of the myopulse signal with increasing muscle contraction. As these relationships are both hyperbolic but inverse to each other [9, 13], it is likely that these quantities cancel at higher MVC levels while remaining either linear or hyperbolic at lower contraction levels given a mismatch in slopes. Combining the myopulse and rectified EMG signals may produce an improved force response across all muscle contraction levels. Multiplying the myopulse signal with the rectified EMG signal would produce a thresholded signal that retains amplitude information. The corresponding muscle force behavior would most likely display high sensitivity at low contraction levels from the myopulse signal content and high linearity across contraction levels from the rectified EMG amplitudes.

CONCLUSION

We evaluated the ability of thresholded and rectified EMG data to produce a responsive myoelectric control signal using simplified model of muscle excitation-contraction dynamics. These results further confirm the physiological role of muscles as a biological low-pass filter and establish the ability of a muscle model to sufficiently filter rectified EMG activity while introducing physiologically appropriate delays to the output signal. Additionally, from observing the properties of the estimated force profiles produced using thresholded and rectified EMG signals, we believe that combining both signals will produce a robust myoelectric control signal that displays high sensitivity at lower contraction levels favorable to myoelectric control use while producing a linear response at higher contraction levels.

ACKNOWLEDGEMENTS

This work was supported by the National Science Foundation Graduate Research Fellowship (GRFP) Grant No. 230762.

REFERENCES

[1] K. Ziegler-Graham, E. J. MacKenzie, P. L. Ephraim, T. G. Travison, and R. Brookmeyer, "Estimating the Prevalence of Limb Loss in the United States: 2005 to 2050,", *Arch. Phys. M*, vol. 89, no. 3, pp. 422-429, 2008.

[2] J. L. Segil and R. F. f. Weir, "Novel postural control algorithm for control of multifunctional myoelectric prosthetic hands," *J Rehabil Res Dev*, vol. 52, no. 4, pp. 449-466, 2015.

[3] K. Englehart and B. Hudgins, "A robust, real-time control scheme for multifunction myoelectric control," (in en), *IEEE Transactions on Biomedical Engineering*, vol. 50, no. 7, pp. 848-854, 2003.

[4] N. Berger and C. R. Huppert, "The use of electrical and mechanical muscular forces for the control of an electrical prosthesis," (in eng), *Am J Occup Ther*, vol. 6, no. 3, pp. 110-114, 1952.

[5] C. Cipriani, J. L. Segil, J. A. Birdwell, and R. F. f. Weir, "Dexterous Control of a Prosthetic Hand Using Fine-Wire Intramuscular Electrodes in Targeted Extrinsic Muscles," *IEEE Trans Neural Syst Rehabil Eng*, vol. 22, no. 4, pp. 828-836, 2014.

[6] A. J. van den Bogert, D. Blana, and D. Heinrich, "Implicit methods for efficient musculoskeletal simulation and optimal control," *Procedia IUTAM*, vol. 2, pp. 297-316, 2011.

[7] T. R. Farrell and R. F. Weir, "The Optimal Controller Delay for Myoelectric Prostheses," *IEEE Trans Neural Syst Rehabil Eng*, vol. 15, no. 1, pp. 111-118, 2007.

[8] R. Merletti and P. Di Torino, "Standards for reporting EMG data," *J Electromyogr Kinesiol*, vol. 9, no. 1, pp. 3-4, 1999.

[9] D. S. Childress, D. W. Holmes, and J. N. Billock, "Ideas on myoelectric prosthetic systems for upper-extremity amputees," *The control of upper-extremity prostheses and orthoses*, pp. 86-106, 1974.

[10] A. M. Krylow and W. Z. Rymer, "Role of intrinsic muscle properties in producing smooth movements," *IEEE Transactions on Biomedical Engineering*, vol. 44, no. 2, pp. 165-176, 1997.

[11] A. M. Gordon, A. F. Huxley, and F. J. Julian, "The variation in isometric tension with sarcomere length in vertebrate muscle fibres," (in en), *The Journal of Physiology*, vol. 184, no. 1, pp. 170-192, 1966.

[12] F. E. Zajac, "Muscle and tendon: properties, models, scaling, and application to biomechanics and motor control," (in eng), *Crit Rev Biomed Eng*, vol. 17, no. 4, pp. 359-411, 1989.

[13] A. V. Hill, "The heat of shortening and the dynamic constants of muscle," *Proc. Roy. Soc.*, vol. B126, pp. 136-195, 1938.

BIOPOINT: SINGLE-SITE, MULTI-SENSOR COMPOUND GESTURE RECOGNITION

Félix Chamberland, Xavier Isabel, Evan Campbell, Gabriel Gagné, Benoit Gosselin, Erik Scheme, Gabriel Gagnon-Turcotte †, Ulysse Côté-Allard †

ABSTRACT

EMG-based gesture recognition tasks have received a lot of attention in recent years, mostly focused on multi-channel EMG sensors, leading to issues in ease of use and computational requirements of such systems. The present study leveraged the BioPoint, a smartwatch-like device, to proceed to multi-sensor deep-learning based gesture recognition. 3 hand gestures in 3 wrist orientations were targeted by measuring the EMG, PPG and IMU waveforms on able-bodied subjects (n=10). Preprocessing and feature extraction allowed the modalities to be used in a two-head neural network trained for the simultaneous classification of hand gestures and wrist rotation. During evaluation, the model obtained an average classification accuracy for hand gestures of $83.5 \pm 12.4\%$ and $94.3 \pm 9.7\%$ for wrist position. Overall, this study showed the potential of single-site, multi-sensor approaches for compound gesture recognition.

INTRODUCTION

Upper extremity musculoskeletal disorders, motor impairments, and amputations profoundly affect millions of individuals worldwide, leading to diverse challenges and significant lifestyle changes [1]. Myoelectric prostheses represent a significant advancement in upper-limb assistive technology to address these issues. These sophisticated robotic devices harness electromyographic (EMG) signals from the muscles in the amputated limb to enable control. Recent progress in robotics has significantly enhanced the capabilities of these prostheses, particularly in achieving various grasp shapes [2]. This enhanced functionality owes much to the integration of multi-channel surface EMG (sEMG) sensor setups, which allow for high-accuracy recognition of multiple concurrent gestures [3], [4]. However, such advancements have primarily been confined to laboratory environments [5].

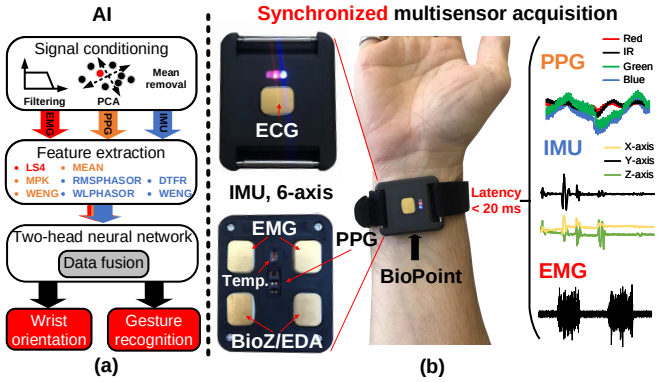

Fig. 1: Concept: (a) The BioPoint provides low-latency synchronized data from up to 6 sensors, (b) the PPG, IMU and EMG signals are processed by a two-head neural network to extract wrist orientation and gesture.

Despite their impressive performance in gesture recognition, multichannel EMG systems face several limitations, including increased complexity, cost and computational requirements, and tend to reduce comfort due to their size [6]. These drawbacks can substantially affect their practicality and user experience.

Moreover, effective prosthetic control encompasses more than just the recognition of diverse grasping actions; it crucially includes the management of wrist dynamics, integral for performing a wide range of activities of daily living [7]. Despite its importance in reducing compensatory movements, which can be a cause for prosthesis rejection [8], the concurrent modulation of grip and wrist motions remains a significant challenge. Studies such as those conducted by Connan et al., exploring the online myocontrol of combined hand and wrist actions, exemplify efforts to overcome these obstacles [9]. Nevertheless, the intricate nature of these challenges underscores the necessity for further innovation and research in signal acquisition, processing, and control algorithms to achieve truly seamless and intuitive control of both grasp and wrist motion simultaneously to enable users to perform a wider array of tasks effortlessly.

Consequently, this work introduces the simultaneous classification of grasp and wrist movements from a single-point, single-channel EMG device as shown in Figure 1(a). This advancement, made possible by the integration of an inertial measurement unit (IMU) and a photoplethysmograph (PPG) within the EMG device, leverages a multi-head deep neural network to perform sensor fusion. The proposed approach is designed to offer a more streamlined, efficient, and user-friendly solution, whilst providing high-level functionality and ultimately improving user experience in prosthetic control.

†U. Côté-Allard and G. Gagnon-Turcotte may be considered co-last authors.

F. Chamberland is the corresponding author (Email: felix.chamberland.1@ulaval.ca). F. Chamberland, X. Isabel, G. Gagné, B. Gosselin, and G. Gagnon-Turcotte are with the Dept. of ECE, Laval University, Québec, Canada. E. Campbell and E. Scheme are with the Department of ECE, University of New Brunswick, Fredericton, NB, Canada, E3B 5A3. U. Côté-Allard is with the Dept. of Technology Systems, University of Oslo, Oslo, Norway.

METHODS

System Hardware

Figure 1(b) illustrates the collection of EMG, PPG, and IMU data conducted throughout the study using the BioPoint [10], a compact and wireless device with the capability of simultaneously recording and streaming EMG, ECG, PPG, IMU, BioZ/EDA, and skin temperature data. Within the context of this study, we focused on three out of the six modalities provided by BioPoint: PPG (Blue, Green, Red, and Infrared) sampled at 50 Hz, a 6-axis IMU sampled at 100 Hz, and EMG sampled at 2 kHz. Figure 1 presents the BioPoint device alongside examples of data captured for various gestures. An important advantage offered by the BioPoint for this study is the synchronization of all sensors using a common clock, eliminating the need for additional processing as all modalities are inherently aligned with each other.

Pre-processing

During the post-acquisition pre-processing phase, the raw data obtained from EMG, PPG, and IMU sensors undergo initial standardization filtering. This filtration process involves removing the mean and adjusting signal magnitudes based on their respective standard deviations, which are derived from the subject's training data. This step ensures a consistent range of values across all three modalities. Additionally, for EMG data, a 60 Hz notch filter is applied to attenuate powerline interference, followed by a 20-450 Hz band-pass filter to eliminate motion artifacts and component noise. PPG data undergoes further processing with a 0.66-3 Hz band-stop filter to mitigate cardiac pulse influences. Moreover, as suggested in [11], a Principal Component Analysis (PCA) is conducted specifically on the Infrared and Red channels. These channels are targeted due to their longer wavelengths, facilitating better penetration into the arm tissue and heightened sensitivity to changes in arm geometry. Regarding IMU data, the approach directly utilizes the standardized signals' 3-axis accelerometer data.

In the context of real-time human-computer interaction, latency is a crucial consideration. To optimize system usability while minimizing input delay, selecting an appropriate window size for data processing is essential. While longer window sizes are associated with enhanced performance in myoelectric control [12], research suggests that the optimal window size to mitigate input latency falls within the range of 150 to 250 ms [13]. Consequently, this study adopts a 200 ms window for classification, supplemented with a 20 ms incremental update, to effectively capture the dynamic nature of the sensor data.

Sensor Fusion Classification Algorithm

A preliminary feature selection was performed for PPG and IMU on pilot subjects to determine appropriate features for each of the modalities. Selection was performed on a per modality basis with the criterion of individual classification accuracy. Subsequently, maximum (MPK), wavelet energy (WENG), and mean (MEAN) features were selected for PPG, and waveform length phasor (WLPHASOR), discrete Fourier transform representation (DTFR), wavelet energy (WENG), and root mean square phasor (RMSPHASOR) features were selected for IMU. The EMG gesture recognition literature was consulted and the LS4 feature set was used, composed of l-score (LS), maximum fractal length (MFL), mean squared ratio (MSR), and Willison's amplitude (WAMP) [14].

The feature vectors are concatenated to form a single input vector, which is then fed into a fully connected neural network. This network comprises three hidden layers, containing 64, 128, and 64 neurons respectively. For each layer, we apply batch normalization, which is then followed by the Scaled Exponential Linear Unit (SELU) activation function as the non-linearity function [15]. Additionally, we employ Alpha Dropout (with a rate of 0.5) after each activation function to reduce overfitting and improve robustness under different input distributions, as suggested by the SELU activation's design principles [15].

The network utilizes a dual fully connected output layer strategy (dual heads), tailored for multitasking. One layer focuses on predicting the three grasps, while the other is dedicated to the wrist movements. The softmax function is applied as a the final layer of non-linearity for both heads.

AdamW [16] is employed with a learning rate of 0.01 to optimize the weights of the network. Learning rate scheduling is used with a step size of 5 epochs and a decay factor (gamma) of 0.1, to adjust the learning rate during training. Furthermore, to prevent overfitting and ensure generalization, we apply early stopping, using 10% of the training dataset as a validation set and a patience parameter set to 30 epochs. Finally, the loss is calculated using cross-entropy, assigning equal importance to both grasp and wrist movement predictions.

Data Collection

In this study, data collection involved ten able-bodied participants, including four women and six men, with ages ranging from 21 to 59 years (Mean: 32.4, SD: 14.8 years). Four participants had no prior experience with biosignal-based collection, and all were new to IMU and PPG data collection methods. The data acquisition protocol received approval from the ethics committee for sectorial research in readaptation and social integration of the *CIUSSS de la Capitale-Nationale* (project 2023-2639). Ethical compliance was ensured through obtaining informed consent from all participants.

Each participant was instructed to execute 3 hand gestures (Neutral grasp (NG), Open hand (OH) and Power grip (PG)) in sequence for three wrist positions: supination (Su), neutral wrist (NW), and pronation (Pr) as shown in Figure 2. Each gesture was recorded for six repetitions lasting 5 seconds each. Only the isometric portions of the contraction were utilized to train the classifier.

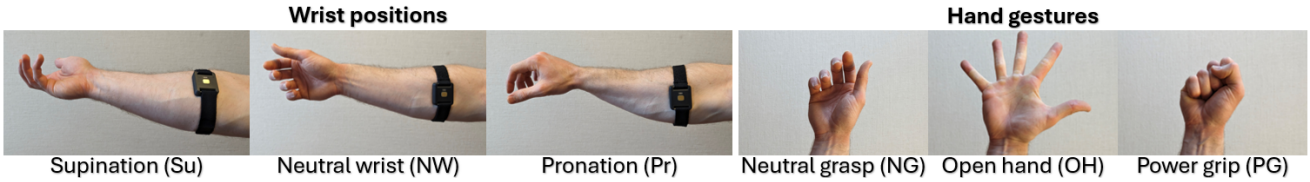

Fig. 2: Gesture set collected during the experiment composed of three hand gestures taken in each of the three wrist positions. The figure illustrates the positioning of the BioPoint sensor on the participant's forearm, located between the brachioradialis and flexor carpi radialis, distal to the elbow joint.

RESULTS AND DISCUSSION

Figure 3 showcases an example of how raw signals from EMG, IMU and PPG differ when comparing different wrist positions and different hand gestures. Neutral grasp, which is used during transitions, has the lowest EMG activity and generally keeps the IMU and PPG signals stable. Open hand causes a slight rise in EMG activity, which is explained by the activation of extensor muscles located on the opposite side of the sensor placement. However, IMU signals have high frequency oscillations similar to the ones obtained with the power grip which have the highest EMG activity due to the recruitement of flexor muscles located right under the sensor. To differentiate between wrist positions, EMG visually seems to play a much smaller role compared to IMU and PPG. The DC levels of the IMU are quite different between the orientations and the shape of the PPG signals are consistent for the same wrist position. These two sensors provide reliable metrics to differentiate amongst the wrist rotations.

Further analysis through feature extraction and neural network training was conducted to obtain quantitative results. The confusion matrix of figure 4(a) shows the results for combined hand grasping and wrist rotation. Both network's heads had to be accurate for the sample to be compiled in the good classification diagonal. One result of note is the generally lower accuracies for the neutral grasp compared to the other active hand gestures. It could be explained by users activating their muscles to maintain pronation or supination which are the two lowest wrist positions for this hand grasp.

Next, by isolating the hand grasps and wrist rotations, classification accuracy with an average of $83.5 \pm 12.4\%$ was obtained for the hand grasps and an average of $94.3 \pm 9.7\%$ for the wrist positions. Figure 4(b) shows the spread of the distribution across the 10 users. Hand grasp was harder to classify due to its reliance on EMG signals which was taken only at a single site far away from the hand. It is to note that the variation in performance across users is significant and the average is skewed downwards by less experienced users. On the other hand, wrist rotations had much higher accuracies except for one outlier user as denoted by the dot under the boxplot at around 67%. Wrist orientations were easier for new users to perform as they do not require the same level of muscular control and practice as finger gestures. Moreover, IMU and PPG sensors were very sensitive to those rotations.

Overall, this experiment showed that separating the hand and wrist motions using multiple sensors on a single-site already obtains great results. Therefore, performing a similar compound movement experiment using sensor fusion and multi-site EMG is a promising next step to hopefully enhance control of the newer generation of fully articulated prosthesis.

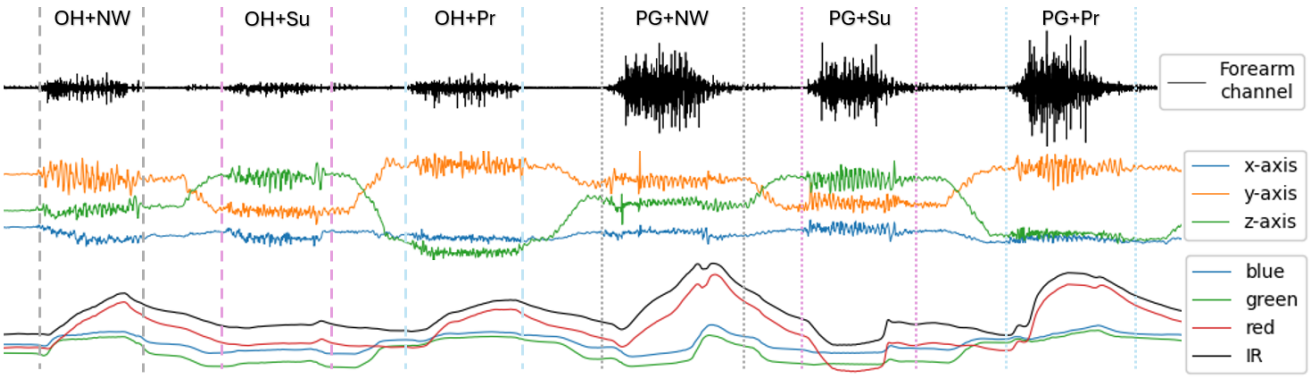

Fig. 3: A sequence was performed to showcase how the EMG, IMU and PPG raw signals affected by hand and wrist motion. 6 combinations of active hand gestures and wrist positions were performed. Transition periods were used to change wrist orientation while keeping the hand in a neutral grasp (passive).

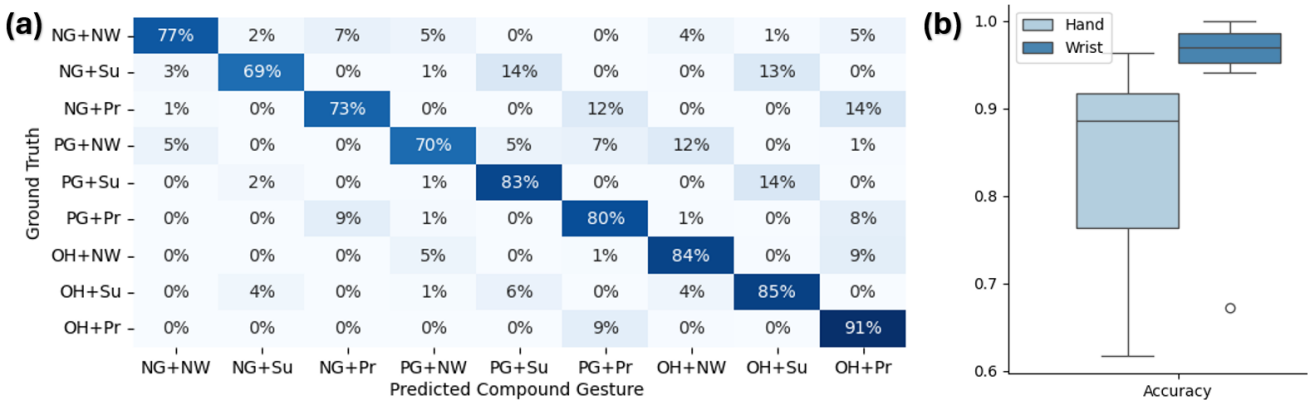

Fig. 4: (a) shows the confusion matrix for the grasps and wrist motions considered simultaneously as predicted by the dual-head deep neural network utilizing sensor fusion in the proposed classification pipeline. (b) provides the box plots, showcasing the distribution of the participants' accuracies for both grasp (hand) and wrist motions predicted separately.

CONCLUSION

In this study, the BioPoint, a single-site multi-modal acquisition device, was used to implement a two-head neural network for simultaneous classification of hand gestures and wrist rotations, laying the groundwork for integrating wrist dynamics into gesture recognition systems. Following preprocessing of EMG, IMU, and PPG waveforms, features supported by literature and experiments were extracted. The network's performance was evaluated with common offline metrics and showed near-perfect performance for wrist rotations and high accuracy for hand gestures. While these results are promising, further experiments should capitalize on online classification and on evaluating the system's effectiveness with upper-limb amputees, both of which are crucial aspects for the practicality of myoelectric prostheses control.

REFERENCES

[1] K. Ziegler-Graham, E. J. MacKenzie, P. L. Ephraim, T. G. Travison, and R. Brookmeyer, "Estimating the prevalence of limb loss in the united states: 2005 to 2050," *Archives of physical medicine and rehabilitation*, vol. 89, no. 3, pp. 422–429, 2008.

[2] J. T. Belter, J. L. Segil, and B. SM, "Mechanical design and performance specifications of anthropomorphic prosthetic hands: a review," *Journal of rehabilitation research and development*, vol. 50, no. 5, p. 599, 2013.

[3] F. Chamberland, É. Buteau, S. Tam, E. Campbell, A. Mortazavi, E. Scheme, P. Fortier, M. Boukadoum, A. Campeau-Lecours, and B. Gosselin, "Novel wearable hd-emg sensor with shift-robust gesture recognition using deep learning," *IEEE Transactions on Biomedical Circuits and Systems*, 2023.

[4] U. Côté-Allard, G. Gagnon-Turcotte, F. Laviolette, and B. Gosselin, "A low-cost, wireless, 3-d-printed custom armband for semg hand gesture recognition," *Sensors*, vol. 19, no. 12, p. 2811, 2019.

[5] E. Campbell, A. Phinyomark, and E. Scheme, "Deep cross-user models reduce the training burden in myoelectric control," *Frontiers in Neuroscience*, vol. 15, p. 657958, 2021.

[6] M. Tavakoli, C. Benussi, and J. L. Lourenco, "Single channel surface emg control of advanced prosthetic hands: A simple, low cost and efficient approach," *Expert Systems with Applications*, vol. 79, pp. 322–332, 2017.

[7] F. Cordella, A. L. Ciancio, R. Sacchetti, A. Davalli, A. G. Cutti, E. Guglielmelli, and L. Zollo, "Literature review on needs of upper limb prosthesis users," *Frontiers in neuroscience*, vol. 10, p. 209, 2016.

[8] A. J. Metzger, A. W. Dromerick, R. J. Holley, and P. S. Lum, "Characterization of compensatory trunk movements during prosthetic upper limb reaching tasks," *Archives of physical medicine and rehabilitation*, vol. 93, no. 11, pp. 2029–2034, 2012.

[9] M. Connan, R. Kõiva, and C. Castellini, "Online natural myocontrol of combined hand and wrist actions using tactile myography and the biomechanics of grasping," *Frontiers in Neurorobotics*, vol. 14, p. 11, 2020.

[10] G. Gagnon-Turcotte, U. Côté-Allard, Q. Mascret, J. Tørresen, and B. Gosselin, "Photoplethysmography-based derivation of physiological information using the biopoint," in *2023 45th Annual International Conference of the IEEE Engineering in Medicine & Biology Society (EMBC)*. IEEE, 2023, pp. 1–5.

[11] Y. Ruan, X. Chen, X. Zhang, and X. Chen, "Principal component analysis of photoplethysmography signals for improved gesture recognition," *Frontiers in Neuroscience*, vol. 16, p. 1047070, 2022.

[12] N. Parajuli, N. Sreenivasan, P. Bifulco, M. Cesarelli, S. Savino, V. Niola, D. Esposito, T. J. Hamilton, G. R. Naik, U. Gunawardana *et al.*, "Real-time emg based pattern recognition control for hand prostheses: A review on existing methods, challenges and future implementation," *Sensors*, vol. 19, no. 20, p. 4596, 2019.

[13] L. H. Smith, L. J. Hargrove, B. A. Lock, and T. A. Kuiken, "Determining the optimal window length for pattern recognition-based myoelectric control: balancing the competing effects of classification error and controller delay," *IEEE transactions on neural systems and rehabilitation engineering*, vol. 19, no. 2, pp. 186–192, 2010.

[14] A. Phinyomark, R. N. Khushaba, and E. Scheme, "Feature extraction and selection for myoelectric control based on wearable emg sensors," *Sensors*, vol. 18, no. 5, p. 1615, 2018.

[15] G. Klambauer, T. Unterthiner, A. Mayr, and S. Hochreiter, "Self-normalizing neural networks," *Advances in neural information processing systems*, vol. 30, 2017.

[16] I. Loshchilov and F. Hutter, "Decoupled weight decay regularization," *arXiv preprint arXiv:1711.05101*, 2017.

ENABLING MYOELECTRIC CONTROL TRAINING USING CONTINUOUS DATA THROUGH SELF-SUPERVISED REPRESENTATION LEARNING

Shriram Tallam Puranam Raghu[1], Dawn MacIsaac[1], and Erik Scheme[1]

[1]*Institute of Biomedical Engineering, University of New Brunswick, Canada*

ABSTRACT

In this work, we explore the potential of integrating continuous transition data into the training process for pattern recognition-based myoelectric control. We use a set of steady-state and continuous transition performance metrics to compare the performance of classifiers trained with continuous data versus the traditional ramp contraction approach. We further compare the performance of the popular LDA classifier with that of a deep gated recurrent unit (GRU) classifier capable of leveraging the temporal dynamics. We also introduce a novel self-supervised contrastive representation learning approach with augmentations that significantly improves the offline steady-state and transition performance. This work provides compelling early evidence of the potential for semi-supervised learning approaches to leverage temporal dynamics in continuous training data to improve the performance of pattern recognition-based myoelectric control.

INTRODUCTION

Pattern recognition (PR) based myoelectric control has been heavily explored due to its ability to provide intuitive control via learned patterns of surface electromyography (sEMG) signals from multiple channels [1]. Its susceptibility to various sources of noise and confounding factors, however, has encouraged researchers to continue to improve its robustness through various algorithmic and training approaches.

Previous works have shown that training PR classifiers with ramp data, where users increase their contraction intensity from rest, rather than static contractions provides improved online (usability) performance [2]. This is likely because ramp data offer a fuller representation of the motion classes through their inclusion of contraction dynamics. While these dynamics help the classifier to learn about how to transition from no movement to each motion class, they don't offer much help in learning about transitions from one motion class to another. This is an important area of exploration, since studies have indicated that errors during transition impact usability [3], [4]. It is conceivable that including examples of these 'continuous transitions' in training data may further inform PR models beyond what is achieved through ramp data alone, especially if they are able to better inform temporal models like long short-term memory networks (LSTMs) or gated recurrent units (GRUs), which are capable of exploiting time series dynamics. The purpose of this work was to explore this possibility.

Training with data that includes continuous transitions from one motion class to another, however, presents new challenges. Besides increased burden on users to collect more training data, supervised classifiers like the conventional LDA, LSTM, and GRU all require labeled training data, and it is not clear how to label regions of transition, or even identify region bounds. Until a robust EMG-based algorithm for marking transition bounds between active classes is established, a secondary source such as a motion sensor could be used. Even when the bounds are identified, a labeling scheme must be chosen; for example, a naive scheme could label all frames within a transition as the next motion class, hoping to drive the decision stream to the next class quickly. Alternatively, self-supervised learning approaches could offer a possible solution, eliminating the need for pre-established labels altogether.

Self-supervised approaches do not require labels to train the model, and instead rely on augmentations to learn the structure of the data [5]. The model learns to maximize similarity of two augmented views of the same sample; for example, during training, two scaled-amplitude versions of a frame would be tagged as matches so the model could be updated accordingly. This makes them robust to perturbations and particularly interesting for learning useful information from hard-to-label dynamic data. They construct a latent space that drives similar samples closer together, which may have the effect of 'clustering' motion classes in a way that includes transition frames appropriately. Once the feature vectors from the latent space are established, a strategy that focuses on those members of each cluster that are easily classed with their pre-established labels (i.e. a group of steady state members) can be used to establish the motion classes of latent space feature vectors so they can be properly classified during inference.

In this work, we explore the potential of leveraging such a semi-supervised representation learning approach to leverage dynamics in continuous transition training data to inform PR-based myoelectric control. We show that the proposed approach significantly improves offline steady-state and transition performance compared the traditional ramp approach using a set of steady-state and continuous transition performance metrics [6].

METHODS

A dataset collected from 43 able-bodied participants, fully described in [7] and approved by the UNB Research Ethics Board (REB #2021-116), was used in this study. Briefly, each participant completed 5 ramp trials and 6 continuous transition trials, following screen prompts of 6 motion classes: Wrist Flexion (WF), Wrist Extension (WE), Wrist Pronation (WP), Wrist Supination (WS), Chuck Grip (CG), and Hand Open (HO), and a No Motion (NM) class. Ramp contractions always began in the No Motion class and gradually increased in intensity to reach the steady state contraction of a motion class (about $3\,\mathrm{s}$). Continuous transition trials started in the No Motion class and then randomly transitioned between classes continuously, holding the steady between each transition for about $3\,\mathrm{s}$, until all transitions between each class and every other (including No Motion) were complete. All 42 transitions were captured in a random order each trial.

All data were collected using six channels of sEMG sampled at a rate of 2kHz using Delsys Trigno ®electrodes spaced equidistantly around the circumference of the participant's right forearm. Each trial was segmented into overlapping frames with a length of $162\,\mathrm{ms}$ and an increment of $13.5\,\mathrm{ms}$. Then, the Low-Sampling Frequency 4 (LSF4) feature set [8] was extracted from each frame, as this feature set has been shown to robust and generalizable. Kinematic data were also collected with a Leap Motion Controller (LMC) infrared sensor positioned below the hand so that transitions between motion classes could be identified through movement.

Two classifiers – a Linear Discriminant Analysis (LDA) classifier, and a deep Gated Recurrent Unit (GRU) classifier – were evaluated across the two training conditions (ramp and continuous). Both conditions were *evaluated* on continuous transition data using the following offline performance metrics: steady-state Active Error Rate (SS-AER), steady-state Total Error Rate (SS-TER), and steady-state Instability (SS-INS), and transition: Offset Delay (T_{OFF}), Onset Delay (T_{ON}), Transition Duration (T_{TD}), Instability (INS), Tertiary Class Error (TER), and Percent No Movement (PNM) [6].

All five trials of *the ramp data* were used to train the LDA classifer, which was evaluated using all six trials of the continuous transition data. When using the GRU, one random trial was used for validation and the remaining four trials were used for training. When training with *the continuous data*, a leave-one-trial-out approach was used for evaluation. For each participant, after removing one trial for evaluation, the remaining 5 were used to train the LDA. Again, for the GRU, one of the five trials was held out for validation, and the remaining four were used for training. This process was repeated six times so that trained models could be evaluated on all six trials of the continuous transition data. To establish the labels required for supervised learning of the continuous data, the frames were re-labelled according to a modified version of the prompts. The start of each transition was identified as the first frame after a prompt change that coincided with the initiation of movement (as identified by the LMC). All the frames after this frame were labeled as belonging to the prompted motion class.

A conventional cross-entropy loss function was used to train the *supervised* GRUs described above. Additionally, a novel *self-supervised* contrastive loss function called VICReg [9] was investigated to avoid the need for the LMC-dependent re-labeling approach when using the continuous transition data. Although many augmentations have been proposed in the literature for use in self-supervised learning [10], random feature scaling, additive white Gaussian noise, and time shifting were used in this work. Two augmented views of the frames in the training data were generated, and these augmented views were then used train the self-supervised GRU. Once the model was trained, the prompt-labeled latent space feature vectors were used to determine the centroid of each motion class, so that a Nearest Centroid (NC) classifier could be applied on the test trials during evaluation.

RESULTS

Figure 1 show box plots of the steady-state and transition metrics for each of the models. One-way ANOVA ($\alpha = 0.05$) comparing training conditions (ramp vs continuous transition) for *supervised* models showed significant differences in all three steady-state metrics ($p < 0.0001$) regardless of the classifier. For transition metrics, four of the six metrics showed significant differences ($p < 0.02$). The classifiers had significantly shorter transition duration when trained with continuous data, but at the expense of slight but significantly longer T_{OFF}. INS also showed a significant difference, but a post-hoc multiple comparison test with Šidák correction ($\alpha = 0.05$) revealed that only GRU[R] had statistically lower values ($p < 0.0001$).

One-way ANOVA ($\alpha = 0.05$) comparing the classifiers trained with continuous transition data showed significant differences in SS-INS ($p < 0.0001$). For transition metrics, T_{OFF}, INS, and TCE also showed significant differences. A post-hoc multiple comparison test with Šidák correction ($\alpha = 0.05$) revealed that VICReg had statistically lower values ($p < 0.0001$) for SS-INS, INS and TCE, but a statistically higher value for T_{OFF} ($p < 0.0001$).

Figure 2 shows an example of the decision and probability streams of nearest centroid classifiers trained using the original, unmodified feature space, and that of the VICReg latent space. Figure 3 shows an example of the latent space learnt by VICReg for the ramp and continuous training data compared to that of a continuous testing trial.

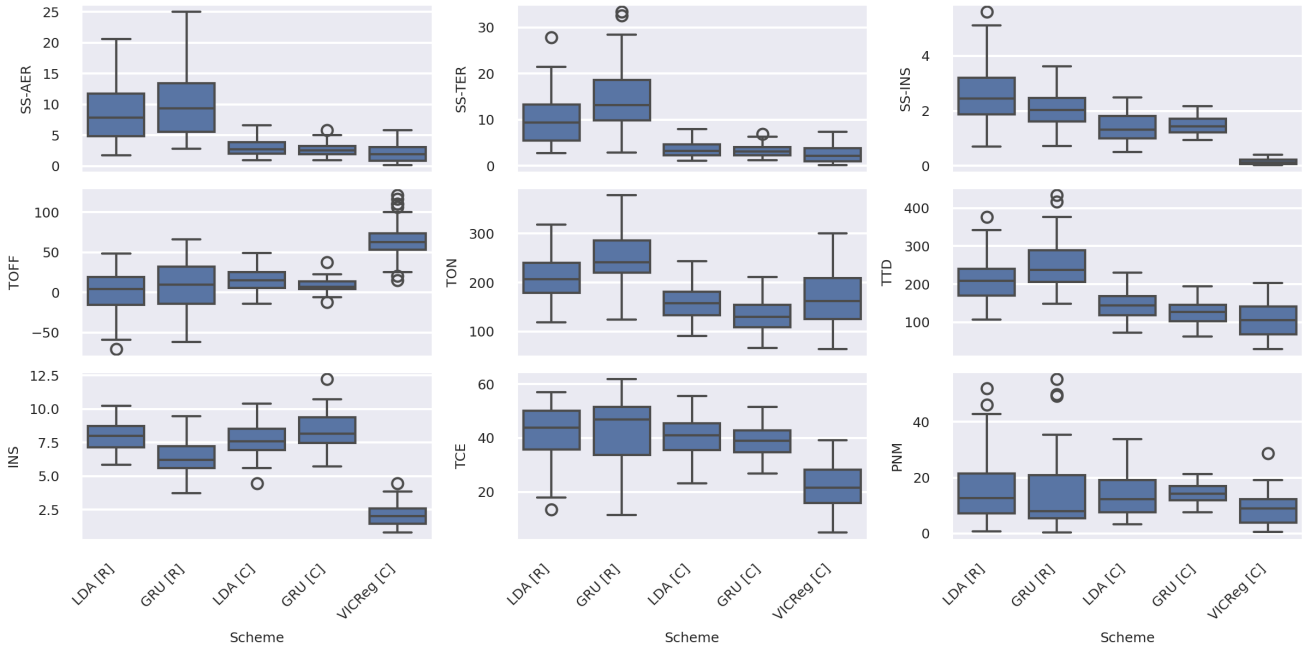

Fig. 1: Comparison of the performance of the different classifiers. The top row shows steady-state metrics, whereas the bottom two rows show transition metrics. Classifier schemes denoted as [R] were trained with Ramp data and [C] were trained with continuous data.

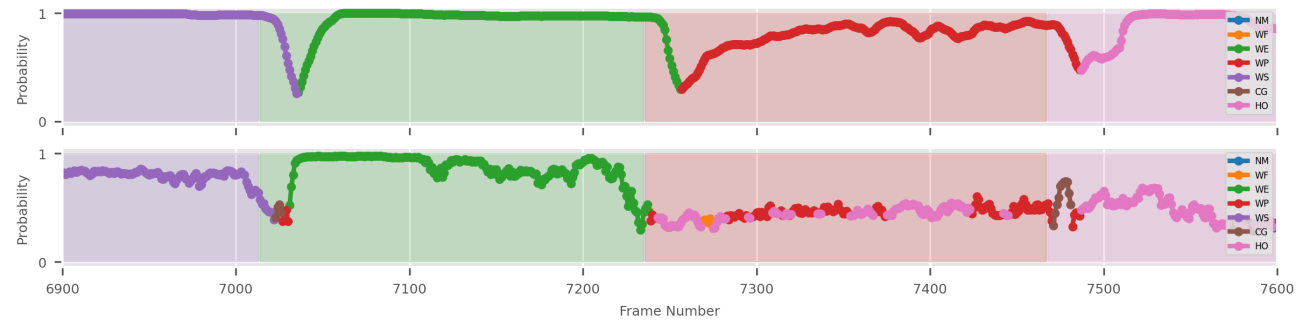

Fig. 2: An example of the nearest centroid classifier probability and decision streams when using the original, unmodified feature space (Bottom) and when using the VICReg latent space (Top). The color of the lines represents the classifier output, whereas the background color denotes the prompted class.

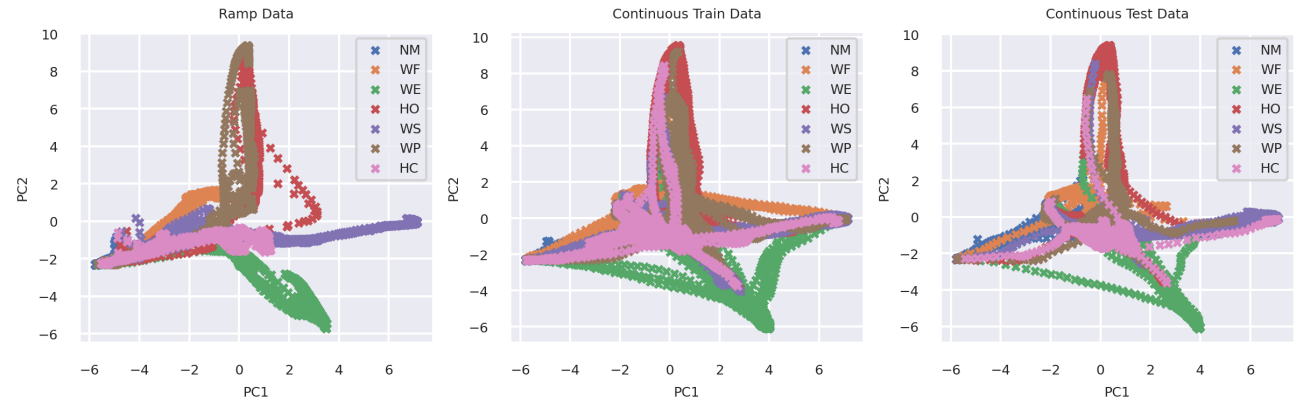

Fig. 3: A visualization of the VICReg latent space for an example participant, projected into a 2 dimensional space using PCA. Left: Ramp Training Data, Middle: Continuous Training Data, Right: Continuous Testing Data

DISCUSSION

Results indicate that classifiers trained with continuous data performed better than those trained with ramp data, according to most of the offline metrics. However, we observed that LDA and GRU performed on par in all metrics except T_{ON}. This was surprising given that the GRU is a temporal classifier and should be better at exploiting temporal information in the data compared to the LDA. It may be that the naive labeling strategy prevented the GRU from fully exploiting its capacity to learn dynamics. This is supported by the fact that VICReg, which was designed to avoid the need for labelling, showed significantly improved performance in terms of INS, SS-INS, and TCE. Regardless, to fully exploit training supervised classifiers with continuous transition data, more work is required regarding how best to label transitions. In particular, in a closed-set classification problem such as this, the data during transitions does not truly belong to any of the prescribed labels. Consequently, labelling them as belonging to an 'unknown' class or applying label smoothing [11] may be more appropriate. Also, requiring the use of an LMC device to mark the bounds of transition regions is undesirable and even infeasible for persons with limb differences. Furthermore, EMG activity precedes kinematic movement [12], which was not accounted for in this work. Consequently, a segmentation technique that works directly with the raw EMG data in real-time would be more more desirable, though more work is required to solve this challenging problem.

Resistant to these labeling issues, the self-supervised VICReg classifier also yielded considerably better performance across many of the metrics, particularly in instability and transition errors. The generated latent spaces shown in Figure 3 suggests that the embedding not only clusters points belonging to the same class together (even though the model had never seen any class labels), but that it also encodes transitions into narrow corridors travelling between those clusters in a seemingly repeatable way. The two figures with continuous data also show the better population of these transition regions. This behavior is further evidenced by the probability decision stream when using VICReg in Figure 2, whose probability is more consistent while in steady state and transitions directly from the previous class to the target class.

While the self supervised VICReg improves the stability of the decision stream, however, it appears to do so at the expense of a slight increase in onset lag. If this lag isn't perceptible to device users during online use, the improved stability and transitions may substantially improve usability. However, if this lag is perceivable, it may cause the control to feel sluggish. Subsequent work should continue to explore this effect and if other augmentations may overcome this trade-off. Ongoing work is testing these models in an online Fitt's law test and seeking to correlate the offline and online metrics.

Even with the noted benefits of using continuous transition training data, the increased burden on the users to collect these data is a critical disadvantage. Fortunately, techniques that rely on transfer learning and domain adaptation are emerging and may be leveraged to mitigate this issue [13]. Such techniques may be able to shift the burden of collecting most training data away from the end user while still providing most, if not all, of the observed benefits of training with continuous data. Further research into such strategies may be necessary to make training with continuous data practical.

REFERENCES

[1] M. Asghari Oskoei and H. Hu, "Myoelectric control systems—A survey," *Biomedical Signal Processing and Control*, vol. 2, no. 4, pp. 275–294, Oct. 2007.

[2] L. Hargrove, Y. Losier, B. Lock, K. Englehart, and B. Hudgins, "A Real-Time Pattern Recognition Based Myoelectric Control Usability Study Implemented in a Virtual Environment," in *2007 29th Annual International Conference of the IEEE Engineering in Medicine and Biology Society*, Aug. 2007, pp. 4842–4845, iSSN: 1558-4615.

[3] J. W. Robertson, K. B. Englehart, and E. J. Scheme, "Effects of Confidence-Based Rejection on Usability and Error in Pattern Recognition-Based Myoelectric Control," *IEEE Journal of Biomedical and Health Informatics*, vol. 23, no. 5, pp. 2002–2008, Sep. 2019.

[4] A. M. Simon, L. J. Hargrove, B. A. Lock, and T. A. Kuiken, "A Decision-Based Velocity Ramp for Minimizing the Effect of Misclassifications During Real-Time Pattern Recognition Control," *IEEE Transactions on Biomedical Engineering*, vol. 58, no. 8, pp. 2360–2368, Aug. 2011.

[5] R. Balestriero, M. Ibrahim, V. Sobal, A. Morcos, S. Shekhar, T. Goldstein, F. Bordes, A. Bardes, G. Mialon, Y. Tian, A. Schwarzschild, A. G. Wilson, J. Geiping, Q. Garrido, P. Fernandez, A. Bar, H. Pirsiavash, Y. LeCun, and M. Goldblum, "A Cookbook of Self-Supervised Learning," Jun. 2023, arXiv:2304.12210 [cs].

[6] S. Tallam Puranam Raghu, D. MacIsaac, and E. Scheme, "Analyzing the impact of class transitions on the design of pattern recognition-based myoelectric control schemes," *Biomedical Signal Processing and Control*, vol. 71, p. 103134, Jan. 2022.

[7] S. T. P. Raghu, D. MacIsaac, and E. Scheme, "Decision-Change Informed Rejection Improves Robustness in Pattern Recognition-Based Myoelectric Control," *IEEE Journal of Biomedical and Health Informatics*, vol. 27, no. 12, pp. 6051–6061, Dec. 2023.

[8] A. Phinyomark, R. N. Khushaba, and E. Scheme, "Feature Extraction and Selection for Myoelectric Control Based on Wearable EMG Sensors," *Sensors*, vol. 18, no. 5, p. 1615, May 2018.

[9] A. Bardes, J. Ponce, and Y. LeCun, "VICReg: Variance-Invariance-Covariance Regularization for Self-Supervised Learning," Jan. 2022, arXiv:2105.04906 [cs].

[10] X. Zhang, Z. Zhao, T. Tsiligkaridis, and M. Zitnik, "Self-Supervised Contrastive Pre-Training For Time Series via Time-Frequency Consistency," *Advances in Neural Information Processing Systems*, vol. 35, pp. 3988–4003, Dec. 2022.

[11] R. Müller, S. Kornblith, and G. E. Hinton, "When does label smoothing help?" in *Advances in Neural Information Processing Systems*, vol. 32. Curran Associates, Inc., 2019.

[12] G. L. Gottlieb, "Muscle Activation Patterns During Two Types of Voluntary Single-Joint Movement," *Journal of Neurophysiology*, vol. 80, no. 4, pp. 1860–1867, Oct. 1998.

[13] X. Chen, Y. Li, R. Hu, X. Zhang, and X. Chen, "Hand Gesture Recognition based on Surface Electromyography using Convolutional Neural Network with Transfer Learning Method," *IEEE Journal of Biomedical and Health Informatics*, vol. 25, no. 4, pp. 1292–1304, Apr. 2021.

EXPLORATION OF FUZZY LOGIC AS A MEANS TO HANDLE IMPRECISE EMG SIGNALS IN PATTERN RECOGNITION CLASSIFIERS

Stephanie A. Lorelli & Richard F. *ff*. Weir

University of Colorado Denver: Department of Bioengineering

ABSTRACT

Myoelectric pattern recognition systems have the potential to offer intuitive selection and nearly seamless switching between different prosthetic hand grip patterns. This is made possible by using surface electromyogram (sEMG) signals to decode the user's intent each moment in time instead of the user sequentially switching between pre-programmed patterns via a unique motion. However, despite many advances in machine learning algorithms, myoelectric hands face numerous clinical barriers which prevent widespread user acceptance and adoption [2]. These clinical barriers include accuracy declines from sEMG signal shifts, imprecise control, operation lag times, and daily retraining time burdens [3,2].

Fuzzy Logic is a powerful tool which can transform ranges of numerical values into linguistic variables for performing mathematical approximations much like how we use language to describe subsets of populations without having exact numbers [4,5]. Therefore, since sEMG signals are notoriously noisy and have imprecise ranges, Fuzzy Logic may offer a way to account for this inherent signal property yet still be able to decipher the overall control signal command. This quality has the potential to address some of the clinical challenges of being able to reliably differentiate between active contraction and rest states, even if the sEMG signal has shifted due to fatigue or untrained arm positions which other machine learning algorithms seem to struggle with handling [3,7].

Based on promising results from Ajiboye & Weir, we seek to re-explore Fuzzy Logic as a rule-based pattern recognition system [1]. Our preliminary data shows that a Fuzzy C-Means (FCM) system is able to maintain higher accuracies across multiple bin sizes with averages ranging from 76-82% for the resting & momentary "OFF" data compared to a Linear Discriminant Analysis (LDA) system with averages ranging from 53-73%. Therefore, progress from a control perspective seems to have been made as it is easier to reliably return to a resting state before making a desired posture again instead of waiting for the control system to determine if the desired state is actually "OFF". While this is intriguing, more optimization still needs to be done to have this FCM system obtain higher "ON" postural contraction accuracies closer to the clinical standard-of-care LDA system.

INTRODUCTION

Clinical Problem

Machine Learning is a powerful tool for finding underlying patterns in large quantities of data. This has led to impressive technologies such as facial recognition, computer vision, AI speech technology, and other forms of data analysis in the medical research fields. Despite the best advances in machine learning, there is still a low adoption rate for myoelectric prosthetic hand systems [2]. However, this is not due to producing low accuracy rates. In fact, greater than 95% "ON" classification rates have been produced since the 1980s [2]. So the puzzling thing is, why do people prefer to not use myoelectric pattern recognition hands? One answer points toward the fact that these high accuracies achieved in a lab setting decrease significantly when the system is used in daily life with many other external factors to account for [3]. Even training neural networks with more extensive data does not necessarily solve these clinical problems as many would have hoped for. To date, researchers are still struggling to find a machine learning algorithm that presents a robust solution for dealing with changing noise and EMG patterns in daily use while minimizing the training burden on the user.

Research Rationale

Humans produce muscle contractions to perform different hand postures. When our brains are forming, we learn how to produce repeatable muscle patterns reliably. Therefore, the same neuron connections for muscle memory are strengthened every time we produce the same action, acting almost like a rule. However, each time the muscles

contract to produce a posture, there will be some slight variation in the final signal due to human imprecision. In addition, myoelectric signals fluctuate throughout the day and as a result, produce patterns that are different from initial training data. These factors challenge pattern recognition systems as it is difficult to account for all possible scenarios of fatigue, accumulation of sweat, and different arm positions without requiring a person to spend hours training and recalibrating each day.

We hypothesize that FCM may offer more robustness in the face of imprecise EMG signals compared to the standard-of-care LDA system since Fuzzy Logic offers a way to handle noisy data by not needing to calculate exact numerical values and can accept values that are within similar rules, memberships, and ranges. This is done by transforming hard numbers into linguistic variables which is similar to how we utilize adjectives to refer to portions of populations without performing computations to reduce brain energy consumption [4,5]. Therefore, we are exploring how an FCM system can classify hand postures with imprecise sEMG ranges while reliably separating those from momentary rest states and minimizing the amount of data that is necessary to train the system.

METHODS

How Fuzzy Logic and Clustering Works

There are two parts to the FCM system. First, there is the Fuzzy Clustering where multiple centers are spread across a feature's data cloud to capture the whole space instead of reducing it to one point like how an LDA system works. This is done by sharing the membership (U) of each point as a percentage based on the relative closeness to each center. The data then pulls the centers apart through an iterative process such that each data point tries to obtain the highest U possible [8].

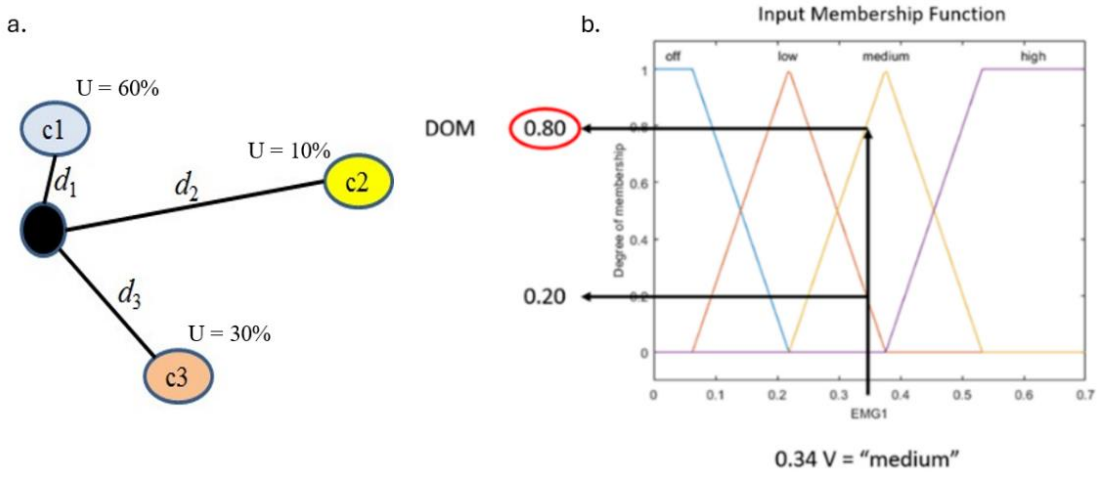

Figure 1:(a.) Fuzzy Clustering membership is shared between all cluster centers based on the relative distance to each center [8]. (b.) Converting cluster center numeric values into linguistic values via a membership function. Here we have 0.34 Volts being inputted into the membership function which is converted into "MEDIUM" via the highest degree of Degree of Membership (DOM) [8].

The second part is the Fuzzy Logic System where each center is transformed into a linguistic variable. Once the locations of the feature centers are determined, then their numeric values are converted into linguistic variables such as "OFF", "LOW", MEDIUM", or "HIGH" via an input membership function. Once we have converted each cluster center into a linguistic variable, we can now create rules that describe what each sEMG channel is doing when a certain posture is being performed. Such as, *If* [EMG_1 is "LOW" & EMG_2 is "HIGH" & EMG_3 is "OFF"] *then* Posture = "Hand Close", to describe a Root Mean Square (RMS) feature's center. Then we determine how well a new point matches to the rule via a degree of membership (DOM). The highest DOM produces the final hand posture's classification. While Ajiboye only used RMS, we are also exploring the use of a common time-domain (TD) feature set of RMS, zero-crossings (ZC), slope-sign-change (SSC), and wavelength (WL) paired with this approach.

Once we have a rule base of "IF/THEN" rules, we have a computationally inexpensive way to see how well each new numeric value matches to a rule within a posture's EMG set [1]. Ultimately, this can decrease controller delay times and potentially decrease the amount of data required to initially train the system since all that is required is a mean and range of data which can be produced by even one EMG contraction. In practice, multiple contractions

would be beneficial for reproducibility purposes. Also once set up, membership functions can accommodate EMG shifts due to already being trained on a spread of data for each posture.

"ON" vs. "OFF" Total Real-Time Controller Accuracy Testing

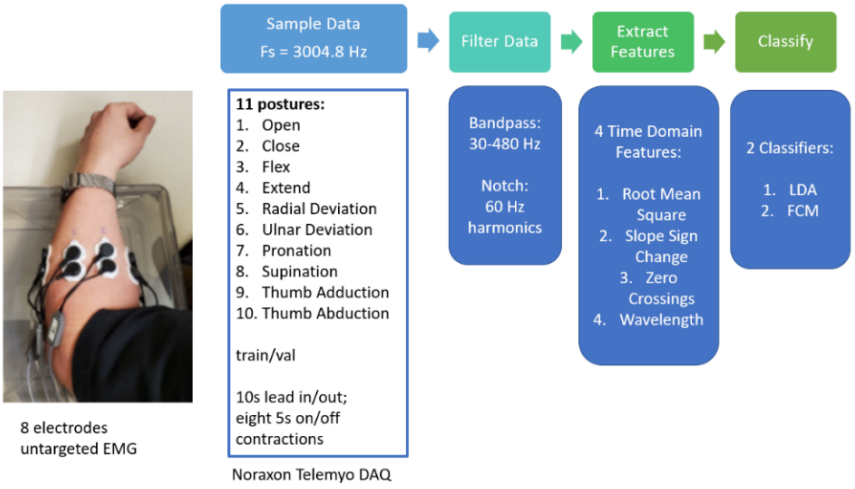

Figure 2: Data Acquisition Protocol for the CU Denver Weir Biomechatronics Development Lab covered under COMIRB No: 14-0838.

The first part of creating a controller is to see if it can reliably differentiate between multiple grasp patterns. These "ON" contractions are typically the ones reported in the literature and achieve very high accuracies within a lab setting [2]. However, in a real-time controller the person is switching between active grasp patterns and resting patterns. Unfortunately, the accuracies reported in literature do not include an overall accuracy comprised of how well the controller switches between a posture and back to a brief resting pattern between contractions. Therefore, we are researching how to report both the "ON" and "OFF" accuracies for any given controller to obtain information on how well each system can reliably and quickly differentiate between active contraction and momentary rest states as a user would experience the system.

We have tested, built, and acquired data (Figure 2) for two control systems and are using cluster computing to fine tune hyperparameters and compare the Fuzzy Logic system to the clinical standard-of-care LDA system.

PRELIMINARY DATA & OBSERVATIONS

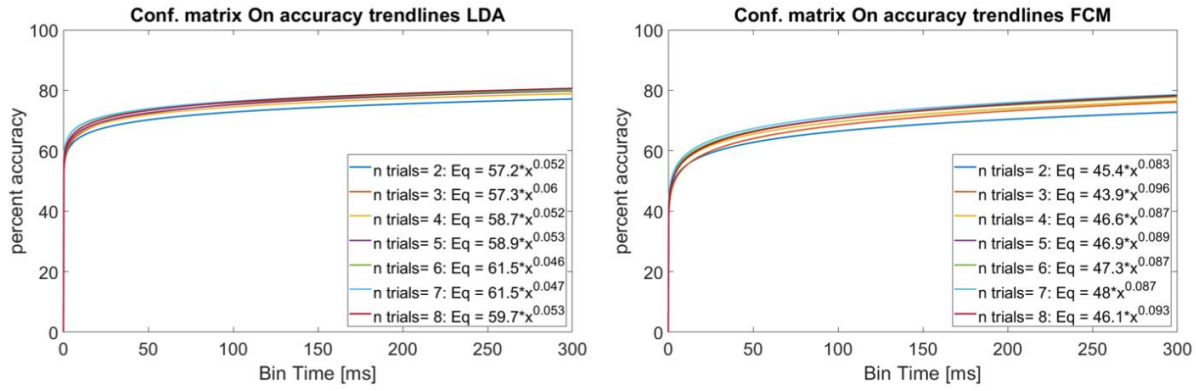

Figure 3: LDA & FCM "ON" Data testing across different bin time sizes and numbers of contractions to train each posture. From 7 people, LDA averages range from 60-80% while FCM averages range from 43-78%. We reach a tight accuracy band after 100ms bins generally agreeing with Ajiboye & Weir and Smith, Hargrove, Lock, & Kuiken and if "n trials" is greater than four [6, 1]. However, minimal accuracy improvements happen even if more contractions are included all the way up to 8 contractions per posture in training data. Therefore, we may be able to reduce the training time burden on the users by requiring only 5 or 6 contractions per posture instead of 8 or more.

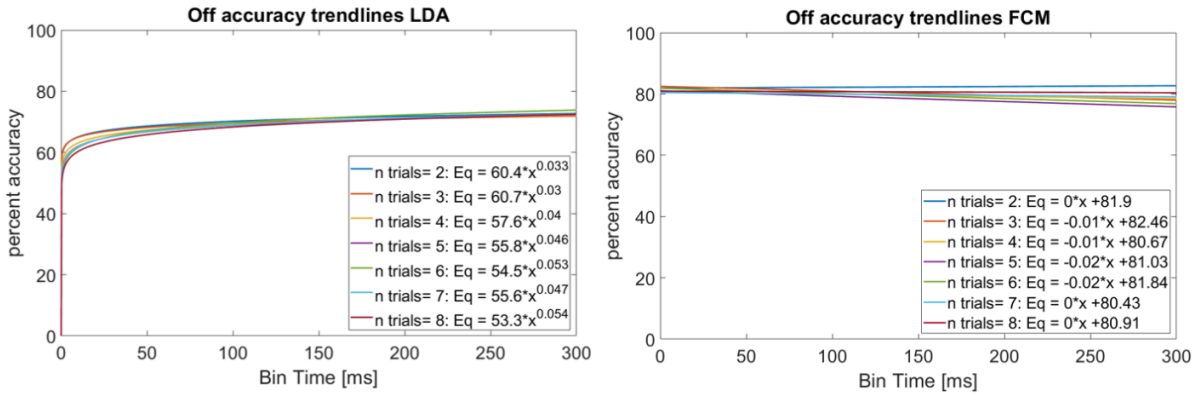

Figure 4: Averages from 7 people range from 53-73% for the LDA "OFF" Data testing across different bin time sizes and numbers of contractions to train each posture. We reach a tight accuracy band with minimal improvement after 100ms bins. For the FCM "OFF" Data testing, averages range from 76-82%. We reach a declining accuracy after 50ms bins, however overall FCM "OFF" accuracies start out higher than the LDA "OFF" accuracies.

This work used the computing resources at the Center for Computational Mathematics, University of Colorado Denver, including the Alderaan cluster, supported by the National Science Foundation award OAC-2019089. The averages for each of the "n trials" are from using 7 people's sEMG data, each run with varying numbers of bin sizes and numbers of contractions per posture to train the algorithms. Trendlines with explanations are plotted in Figures 3 & 4.

CONCLUSION

We see that the Fuzzy Logic system may offer ways to reliably control a prosthetic hand by making it easier to differentiate between active contractions and momentary rest states. In addition, it may be possible to reduce the obligations on the amount of data and time required by the user to train the system. For example, only needing the user to train the system on 6 contractions per posture instead of 8 or more.

While this is useful, "ON" accuracies for the FCM across the board need to be improved by around 10% to be comparable to the LDA "ON" accuracies. Therefore, further research will be done to continue to optimize the FCM algorithm and test different feature combinations in hopes of providing a future controller that is intuitive, robust, and responsive for prosthetic hand users.

REFERENCES

[1] A. Ajiboye, R. Weir, "A Heuristic Fuzzy Logic Approach to EMG Pattern Recognition for Multifunctional Prosthesis Control," *IEEE Transactions on Neural Systems and Rehabilitation Engineering*, vol. 13, issue. 3, pp. 280-291, 2005.

[2] B. Peerdeman, D. Boere, H. Witteveen, R. Veld, H. Hermens, S. Stramigioli, H. Rietman, P. Veltink, S. Misra, "Myoelectric forearm prostheses: State of the art from a user-centered perspective," *Journal of Rehabilitation Research & Development*. vol. 48. no. 6, pp. 719-738, 2011.

[3] I. Kyranou, S. Vijayakumar, M. S. Erden, "Causes of Performance Degradation on Non-invasive Electromyographic Pattern Recognition in Upper Limb Prostheses," *Frontiers in Neurorobotics*. vol. 12. article 58, 2018.

[4] L. A. Zadeh, "Fuzzy Logic – Computing with Words," *IEEE Transactions on Fuzzy Systems*, vol.4, no. 2, 1996.

[5] L. A. Zadeh, "Is There a Need for Fuzzy Logic?" *Information Sciences*, vol. 178, pp. 2751-2779, 2008.

[6] L. Smith., L. Hargrove, B. Lock, T. Kuiken, "Determining the Optimal Window Length for Pattern Recognition-Based Myoelectric Control: Balancing the Competing Effects of Classification Error and Controller Delay," *IEEE Transactions on Neural Systems and Rehabilitation Engineering*, vol. 19, no. 2, 2011.

[7] O. Samuel, M. Asogbon, Y. Geng, A. Al-Timemy, S. Pirbhulal, N. Ji, S. Chen, P. Fang, G. Li, "Intelligent EMG Pattern Recognition Control Method for Upper-Limb Multifunctional Prostheses: Advances, Current Challenges, and Future Prospects," *IEEE Access*. vol. 7, pp. 10150-10165, 2019.

[8] S. Lorelli, "Predicting Prosthetic Finger Postures Via Parallel Fuzzy C-Means Classification," *ProQuest Dissertations Publishing*, 2020.

FEASIBILITY OF SPATIO-TEMPORAL LINEAR FEATURE LEARNING FOR MYOELECTRIC CONTROL: A SMALL WINDOW SIZE APPROACH

Seyedeh Nadia Aghili and Kianoush Nazarpour

School of Informatics, University of Edinburgh, UK

ABSTRACT

Numerous research papers have delved into spatio-temporal analysis for myoelectric control, yielding meaningful outcomes, often employing window sizes ranging from 100 to 300 milliseconds. However, the industry is interested in achieving robust performance within smaller window sizes, more applicable to real-world scenarios. This study introduces a novel approach, Spatio-Temporal Linear Feature Learning (STLFL), with a robust trade-off between high performance and compact window size. Our investigation primarily focused on five classes within the state-of-the-art DB5 dataset—rest, abduction of all fingers, pointing index, power sphere grasp, and prismatic pinch grasp. Comparative analyses with two established methods, namely support vector machine (SVM) and convolutional neural network (CNN), revealed that STLFL consistently outperformed, achieving an impressive average accuracy of 84.6±3.9% across 10 subjects within an 80-millisecond window in a 16-channel electromyography signal. These results highlight the efficiency of STLFL in achieving myoelectric control within a limited timeframe, demonstrating promising outcomes for multiclass applications in both future contexts and real-world scenarios.

INTRODUCTION

Spatio-temporal analysis is extensively utilised in recent electromyography (EMG)-based literatures due to its capacity to leverage optimal features in both spatial and temporal domains [1-3]. This preference stems from recognised limitations in traditional EMG feature extraction methods, which encounter challenges such as the inability to extract inter-temporal dependencies between feature extraction windows and a limitation in capturing synergistic and spatial muscle patterns [1]. Advanced approaches such as spatio-temporal-based techniques are thus warranted to address these shortcomings. However, in many cases, there is a critical aspect that is often overlooked, and that pertains to the window size.

Various studies indicate that the choice of window size significantly influences classification accuracy and control delay in real-world scenarios [4]. Many research papers have explored window sizes ranging from 100 to 300 milliseconds, although this may lead to increased computational time [5, 6]. In contrast, recent literature [4] has shown promising outcomes with smaller window sizes for the first time, demonstrating accelerated processing in high-dimensionality EMG decoding systems. In light of this, we are inspired to adopt a smaller window size (below 100 milliseconds) for our spatio -temporal linear feature learning approach, focusing specifically on a 16-channel EMG signal. The primary objective of our work is as follows:

- Presenting a new version of the spatio-temporal linear analysis in multi classes objective, yielding promising outcomes when applied to raw state-of-the-art EMG signals.
- Adopting a small window size with the objective of reducing delay in controlling myoelectric signals for future real-world scenarios.

METHODS

Dataset

To assess the effectiveness of our proposed method, we utilised a widely recognised EMG dataset obtained from the Ninapro website (DB5) [7]. The dataset captures the EMG activity of ten healthy participants' hands, recorded through 16 surface electrodes (utilizing two Thalmic Myo Armbands). Participants performed 53 distinct hand

gestures, which included periods of rest. Each hand gesture was repeated six times, with each repetition lasting approximately 5 seconds, followed by a 3-second rest interval. The sampling frequency of the recorded EMG signals was set at 200 Hz. In our study, we focused on five classes: rest, abduction of all fingers, pointing index, power sphere grasp, and prismatic pinch grasp. These classes were chosen for our primary investigation into the application of the proposed spatio-temporal linear method in myoelectric control.

Pre-processing

Prior to initiating the classification process, we employed a 6th-order high-pass Butterworth filter with a cutoff frequency set at 10 Hz. For extracting input, we adopted an overlapped segmentation approach with a window length of 80 ms and a 10 ms incremental step. In our approach, we opted to utilise raw EMG data rather than extracting predefined feature sets. This decision guided us to represent the input as overlapped windows of 2D arrays (time-by-channel) in the format of $R^{16\times16}$ for our proposed method.

Spatio-Temporal Linear Feature Learning (STLFL)

The STLFL was introduced in our prior work on binary classification [8]. Here, we extended the method to accommodate multiple classes using a one-vs-one approach and implemented it on the raw EMG signal. The primary objective of this algorithm is to identify the most relevant spatial and temporal features from raw data. To achieve this, the algorithm adjusts two weights associated with the spatial and temporal dimensions of the raw dataset. This adjustment aims to enhance the between-class distribution while minimizing the within-class distribution.

The optimization process is iterative and continues until the error, defined as the minimum difference between the weights in the current iteration and the preceding iteration, reaches a threshold of 0.0001. In our present study, the number of final features is determined by the smaller value between the number of channels and temporal features. Subsequently, the more informative features are inputted into Linear Discriminant Analysis for the purpose of classification.

Convolutional Neural Network (CNN)

In our research, we employed a CNN to compare with STLFL, the parameters of which were chosen through heuristic methods for optimal performance. The model comprises six layers: batch normalization, two convolutional layers, another batch normalization, fully connected, and a final softmax layer for classification. ReLU is used as the activation function throughout and the learning rate for our model is set to 0.001.

For the convolutional operation, three crucial parameters—size, number of kernels, and stride—are considered. Our approach used a convolutional layer with 20 kernels of size [Ch × 1], where Ch is the number of channels (16), and a stride of 1 was applied. Furthermore, we applied a second convolutional layer with 20 kernels of size [1 × 2] and a stride of 1 subsequent to the initial convolutional layer.

RESULTS

In this research, we assessed the effectiveness of our proposed STLFL model in comparison to two other methods: CNN, a conventional deep learning model, and support vector machine (SVM), a traditional machine learning algorithm. We used classification accuracy as our evaluation criterion, maintaining a uniform preprocessing approach across all methods.

For statistical validation of the accuracy values, we employed a Wilcoxon sign-rank test with Bonferroni correction using MATLAB software, considering p-values less than 0.05 as indicative of significant differences. This nonparametric test enabled us to assess paired data (classification accuracy of the STLFL versus the SVM and the CNN), thereby enhancing the robustness of our research findings.

Figure 1 presents a box-plot depicting average accuracy values across all subjects for STLFL, CNN, and SVM. Notably, STLFL and CNN exhibit a significant performance advantage over SVM, with average accuracy values of approximately 84.6±3.9% and 78.3.30±6.0%, respectively. This visual representation underscores the superior performance of the STLFL compared to other methods.

Furthermore, in the comparison between STLFL and CNN, a substantial improvement of approximately 6% is evident in favour of STLFL. Our introduced STLFL model not only outperforms CNN but also demonstrates a statistically significant enhancement in accuracy (p-value = 0.002) when compared to the conventional CNN model.

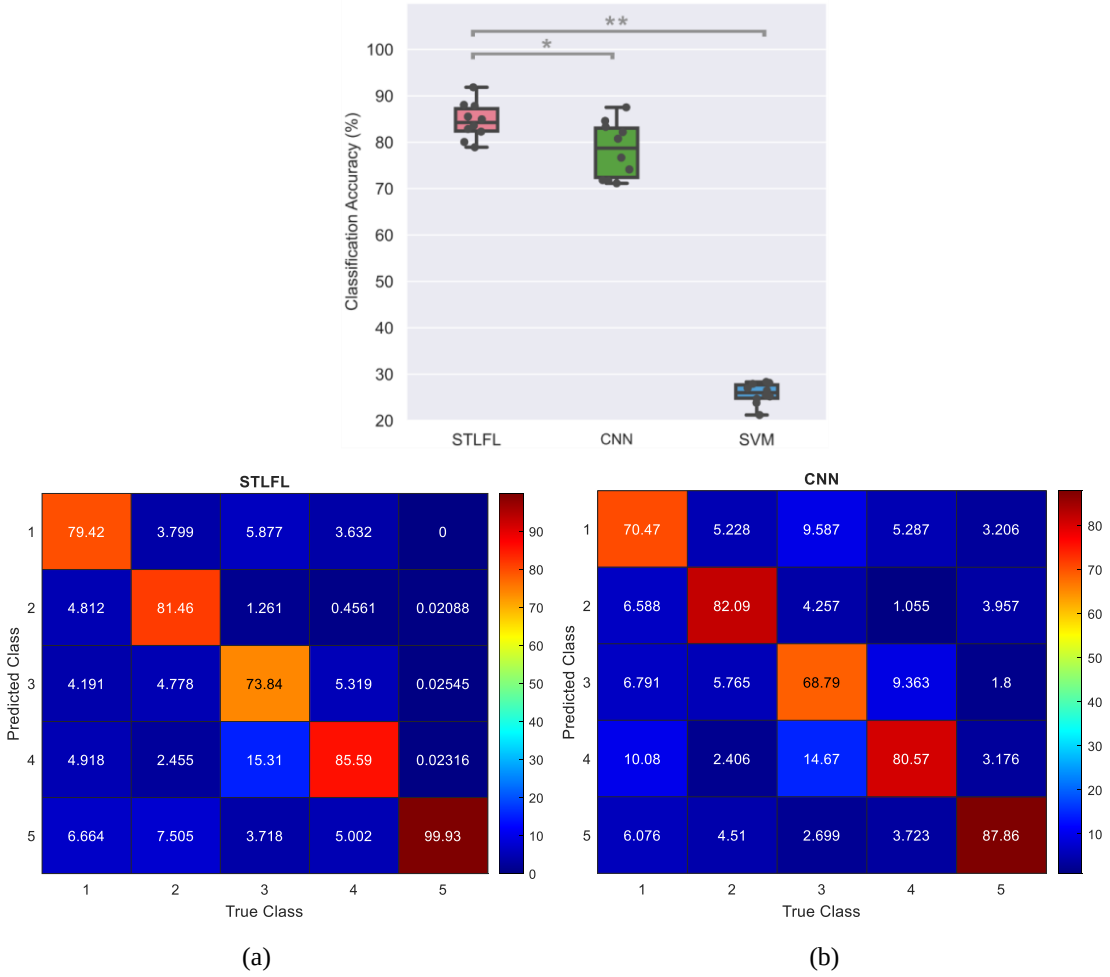

(a) (b)

Figure 1: Box-plot depicts average classification accuracy values across 10 participants using different methods including STLFL, CNN, and SVM models and represent their individual accuracy by grey point. Significant differences are denoted with stars (* for p <0.005 and ** for p <0.001). Figures (a) and (b) display the average confusion matrix for STLFL and CNN, respectively.

DISCUSSION

This paper introduces an innovative spatio-temporal linear feature learning approach for myoelectric control. Our method is intentionally designed with a minimal number of parameters, ensuring its practical suitability for real-world applications. The simplicity of our approach is particularly advantageous, especially in comparison to more intricate analyses such as deep learning techniques.

Upon evaluating our method alongside existing methodologies, including deep learning models like CNN, we have observed superior performance under similar conditions. These results underscore the potential effectiveness of linear approaches in myoelectric applications, highlighting the practical advantages in real-world implementation.

Our study also contributes significantly to the exploration of raw EMG signals in small window sizes, opening way for further investigations in this field. However, it is recognised that specific spatio-temporal convolutional neural networks (STCNN) [9] have achieved favourable results in real-world scenarios. By clarifying the approaches employed in both current proposed STLFL and other relevant STCNN models, and outlining their respective contributions, we aspire to obtain more thorough and informative results. This effort is anticipated to significantly advance our comprehension of the dynamics inherent in myoelectric control.

Moreover, the outcomes, particularly in small window lengths (less than 100 milliseconds), reveal promising advancements for EMG-driven systems, emphasizing enhanced system speed. Previous literature exploring small window lengths often concentrated on high-dimensional signals across numerous channels. In contrast, our study demonstrates these positive results using only a 16-electrode recorded EMG signal. Looking ahead, our method should be implemented in a real-time scenario, and efforts should be directed towards to increasing performance by developing the model.

ACKNOWLEDGEMENTS

This work is supported by funding from Engineering and Physical Sciences Research Council (EPSRC) under grant (EP/R004242/2).

REFERENCES

[1] M. Jabbari, R. Khushaba, and K. Nazarpour, “Spatio-temporal warping for myoelectric control: an offline, feasibility study,” *J. Neural Eng.*, vol. 18, no. 6, p. 066028, 2021.

[2] S. O. Williams, *et al.*, “Spatio-temporal based descriptor for limb movement-intent characterization in EMG-pattern recognition system,” in *proceeding IEEE EMBC*, pp. 2637-2640, 2019.

[3] R. Khushaba, A.H. Al-Timemy, and O.W Samuel, E. Scheme, “Myoelectric Control with Fixed Convolution-Based Time-Domain Feature Extraction: Exploring the Spatio–Temporal Interaction,” *IEEE Trans. Hum. Mach. Syst.*, vol. 52, no. 6, pp. 1247 – 1257,2022.

[4] R. Khushaba, and K. Nazarpour., “Decoding HD-EMG Signals for Myoelectric Control - How Small Can the Analysis Window Size be?” *IEEE robot. autom. lett.*, vol. 6, no. 4, p. 8569 – 8574, 2021.

[5] L. H. Smith, L. J. Hargrove, B. A. Lock, and T. A. Kuiken, “Determining the optimal window length for pattern recognition-based myoelectric control: Balancing the competing effects of classification error and controller delay,” *IEEE Trans. Neural Syst. Rehabil. Eng*., vol. 19, no. 2, pp. 186–192, 2011.

[6] A. Krasoulis, S. Vijayakumar, and K. Nazarpour, “Multi-grip classification-based prosthesis control with two EMG-IMU sensors,” *IEEE Trans. Neural Syst. Rehabil. Eng*., vol. 28, no. 2, pp. 508–518, Feb. 2020.

[7] S. Pizzolato, *et al.*, “Comparison of six electromyography acquisition setups on hand movement classification tasks,” *PLoS One*, vol. 12, no. 10, p. e0186132, 2017.

[8] S.N. Aghili, S. Kilani, R. Khushaba, E. Rouhani, “A spatial-temporal linear feature learning algorithm for P300-based brain-computer interfaces,” *Heliyon.,* vol.9, no.4, 2023.

[9] M Jabbari and K. Nazarpour, “Spatio-temporal convolutional networks for myoelectric control,” *submitted to MEC 2024*.

FEASIBILITY OF THE GLIDE MYOELECTRIC CONTROL ALGORITHM TO PARTIAL HAND PROSTHESIS CONTROL

Christopher L. Hunt[1], György M. Lévay[1], Megan C. Hodgson[1], Damini Agarwal[1], and Rahul R. Kaliki[1]

[1]*Infinite Biomedical Technologies, LLC, Baltimore, MD*

ABSTRACT

While the number of individuals with partial hand limb loss is ten times greater than all other upper limb amputation categories combined, the state of available technology for this underserved patient population is relatively poor. Even though studies report preference towards myoelectric partial hand prostheses, patient adoption of myoelectric devices has been stunted by the limitations of the only control methodology commercially available, direct control. To address this challenge, we suggest the novel application of the *Glide* myoelectric control strategy to individuals with partial hand limb loss. In this work, we describe preliminary investigations with two individuals with partial hand limb loss, one with standard, intrinsic musculature of the residual hand and another who has undergone state-of-the-art surgical interventions.

INTRODUCTION

Approximately 600,000 people live with partial hand amputations in the United States, with an estimated 14,500 new cases occurring each year [1], [2]. The level of impact on the functionality of the limb after amputation depends on which finger or fingers are affected. For example, loss of both the index and middle fingers results in 40% and 36% impairments of the hand and upper extremity respectively, and 22% impairment of the whole body [3]. In fact, individuals with partial hand limb loss (PHLL) self-report a higher level of disability compared to individuals with other major unilateral upper limb loss (ULL) [4]. But while the number of individuals with PHLL is 10 times greater than all other upper limb amputation categories combined, the state of available technology for this underserved patient population is relatively poor [5]. Prosthetic solutions for partial hand amputations are considered only after reconstructive surgical procedures have failed [6]. If prostheses are an option, individuals with PHLL have three main options for prosthetic care: 1) passive prostheses; 2) body powered prostheses operated by flexing the proximal joints; and 3) myoelectric prostheses operated by electronic input from the patient's residual limb [7], [8], [9]. While some studies report preference towards myoelectric devices [10], prosthetic selection should be based on a patient's individual needs and include personal preference, prosthetic experience, and functional needs [11]. Advantages of myoelectric prostheses include increased comfort, natural control, greater range of motion, reduced compensatory movements, perceived sensory feedback, and more cosmetic acceptance [10], [12].

Despite the above potential advantages of myoelectric prostheses, the adoption of such devices is poor. The primary reason for this is related to the control methodology. Current myoelectric systems are typically limited to operating one degree-of-freedom (DOF) using 2 electrodes from intrinsic myoelectric signals. The only available control strategy for partial hand myoelectric prostheses is Direct Control (DC), wherein the activity of a single electromyography (EMG) electrode is correlated directly with the actuation of a single DOF. However, because DC requires isolated control signals, the close proximity of intrinsic hand muscle sites creates significant cross-talk from sensors and limits the number of sensors that can be used [13]. Although recent variations of DC have allowed users to directly map "discrete" electrode functionality to individual or coupled finger motions, these strategies still require signal isolation (some even suggesting surgical intervention). To get around this limitation, manufacturers have created other methods of switching between grasps using mobile apps, EMG triggers, or accelerometer-based switching features, techniques that have not been well received by individuals with PHLL.

In this work, we explore the feasibility of a directional control algorithm (i.e., *Glide*) as an alternative control strategy for myoelectric partial hand prostheses. Originally designed for individuals with above-wrist amputation,

the *Glide* control strategy uses the vector summation of the amplitude of EMG signals from multiple electrodes to navigate a *Glide* cursor to angular positions within a circular map (i.e., the *Glide* domain) [14], [15], [16]. The *Glide* domain can be partitioned into user-adjustable slices, each correlated with a specific motion of the user's prosthesis. By modulating the relative amplitude across EMG channels, users drive the *Glide* cursor to a desired slice of the *Glide* domain, resulting in volitional prosthesis movement. In contrast to DC, the *Glide* algorithm allows patients to control multiple DOFs even when individual electrodes suffer from crosstalk and co-activation. Due to the custom partitioning of the *Glide* domain, the *Glide* algorithm can leverage synergistic co-activity to provide additional dimensions of control. Here we explore the suitability of the *Glide* control strategy to individuals with PHLL

METHODS

This study was conducted in accordance with a protocol approved by the Johns Hopkins University School of Medicine Institutional Review Board. Two individuals with PHLL were recruited by study team members to trial the use of a commercial equivalent *Glide* system, driven by the residual musculature of their partial hand.

Participant 1 (P1) is a woman in her mid-30s who underwent amputations of the middle, ring, and little digits of her left hand due to a workplace accident. Since her amputation, she has operated a set of passive positional prosthetic digits (GripLock Fingers®, Naked Prosthetics, Olympia, Washington) in her daily life; she had no experience with myoelectric devices.

Participant 2 (P2) is a man in his early-50s who underwent amputations of the middle, ring, and little digits of his right hand due to a workplace accident. During his amputation surgery, his clinical care team performed a double Starfish transfer [17] of his second and third dorsal interossei muscles in the hopes of providing him with independent digital control of myoelectric partial hand prostheses. While P2 was prescribed externally powered myoelectric digits (i-digits® quantum, Össur hf., Reykjavík, Iceland), he has not used them regularly in his daily life due to his inability to generate consistent EMG patterns.

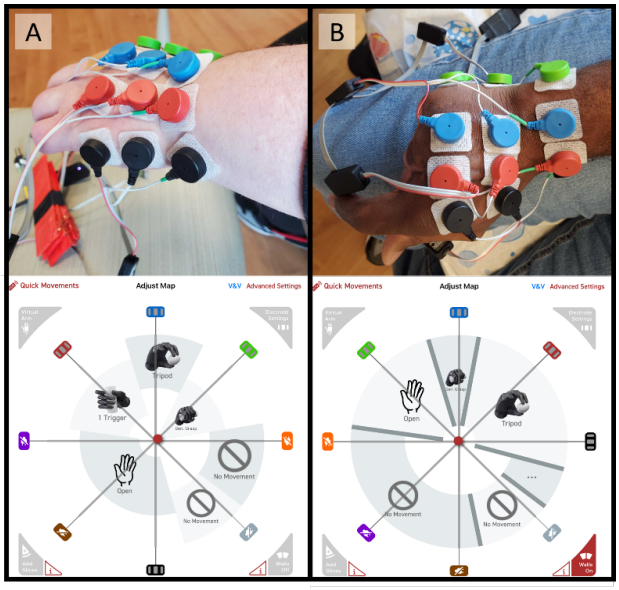

Figure 1. Pilot evaluations of the *Glide* control strategy with individuals with PHLL. (A) P1 had undergone amputations of her middle, ring, and little digits of her left hand and was naïve to myoelectric control strategies. After an hour, she was able to achieve four separate functions given the *Glide* map shown, left. (B) P2 had undergone amputations of his middle, ring, and little digits of his right hand as well as a double Starfish transplantation of his interossei. P2 had abandoned daily use of his myoelectric device due to an inability to generate consistent, distinct EMG patterns of activity. After a single evaluation session, P2 was able to elicit three separate functions given the *Glide* map shown below, right.

During the feasibility study, participants were fit with four pairs of bipolar, surface EMG electrodes (Infinite Biomedical Technologies, Baltimore, MD), targeted over the first, second, and third dorsal interossei muscles as well as the abductor digiti minimi of their partial hand (Figure 1). After electrode placement, participants were trained on the use of the *Glide* system and were prompted to attempt to activate each recorded myosite independently by flexing the targeted, underlying intrinsic muscle. To prompt activation, participants were shown a cue of which electrode to activate (Black, Red, Blue, or Green) in a random order with the cue being presented for 1 s before data collection began. During data collection, the root-mean-square (RMS) of each electrode channel was recorded for 5 s. Kernel density estimates of the observed RMS values for each electrode were then used to define an activation profile for each prompted flexion (Figure 2). These activation profiles were useful in determining how many individual movements participants should aim to begin with for a specific electrode configuration. Using the observed activation profiles, a *Glide* map was constructed for each participant. Over the course of the evaluation period, algorithm parameters (i.e., electrode gains, EMG smoothing, onset delay, etc.) were tuned to balance each participant's control stability and performance.

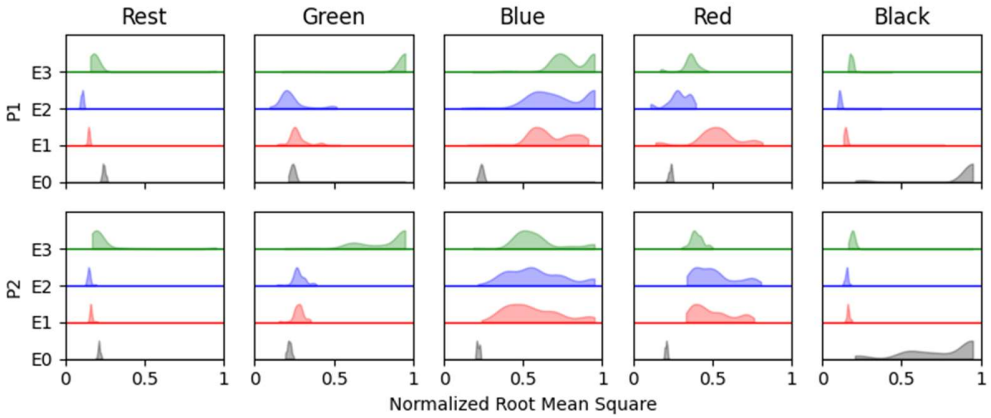

Figure 2. Activation profiles of each participant. Each electrode subplot represents the distribution of RMS values recorded while attempting to activate each electrode independently. (Top) P1 exhibits good separation for the Green and Black electrodes with severe to moderate co-activity present when attempting to isolate the Blue and Red electrodes. (Bottom) P2 exhibits similar intrinsic muscle activation profiles, albeit with greater co-activation between the Blue and Red electrodes.

RESULTS

Attempts at individual muscle flexions revealed that both P1 and P2 were prone to co-activation of neighbouring interossei (observed most prominently in the Blue and Red electrodes, Figure 2). In the case of P1, this is unsurprising as they were naïve to myoelectric control and therefore had difficulty isolating individual myosites. Similarly, prior to this evaluation with the *Glide* control algorithm, P2 was historically unable to elicit discriminable activity on more than two sets of electrodes (i.e., the abductor digiti minimi and all dorsal interossei), allowing only two available functions in an agonist-antagonist pairing. The activation profiles of P2 seem to support these limited independent control axes, with the Red and Blue electrodes exhibiting highly correlated activity.

Despite both participants being prone to interossei co-activity, after adjusting the gain of each individual electrode to fine-tune and bias their responses, both participants were able to consistently control multiple distinct movements via the *Glide* user interface. While both participants began with the simplest *Glide* map (an agonist-antagonist movement pairing), both were able to achieve a more complex, functional map by the end of evaluation (Figure 1). P1 was able to control four movements (one for each electrode): three synergistic hand grasps and one antagonistic movement mapped to Hand Open. P2 was able to control three movements: two synergistic hand grasps and one antagonistic movement mapped to Hand Open. Continued testing with these *Glide* maps over the course of 1 hr confirmed that each participant was able to reliably reproduce each assigned movement, even without the visual feedback of the user interface.

DISCUSSION

The results from this preliminary study highlight several strengths of the *Glide* control strategy when applied to individuals with PHLL. Primarily, results suggest that *Glide* allows individuals to independently control multiple DOF, despite existing co-activations inherent to the intrinsic muscle activity. In contrast, DC requires completely independent control sites free from co-activity [18], [19], [20], [21]. And while emerging surgical interventions, such as the Starfish procedure [17], may alleviate some limitations by increasing the separation between muscle sites, the size of the patient population who have received such interventions ($\leq$ 20 [22]) is dwarfed by the total amount of patients living with a partial hand amputation. The *Glide* system does not require the independence of control sites (or surgical interventions) expected by DC.

Additionally, these results suggest that a progressive training regimen with the *Glide* system may help individuals with PHLL attain greater functionality as they become accustomed to their control capabilities. Both participants had initial difficulties eliciting independent myosite activations, despite one participant even having undergone the aforementioned Starfish procedure. Despite these challenges, we were able to begin with a simplified *Glide* map, focusing on just a pair of agonist-antagonist movements, increasing the complexity of their maps as they

became more comfortable. This scalable nature of the *Glide* system contrasts with DC, wherein an additional electrode would need to be added for each desired additional DOF.

Of course, this work is not without its limitations. For one, as a preliminary investigation, the sample size is small; a subsequent study will require greater participant recruitment. Additionally, these investigations are motivated by the assumption that access to more DOFs will result in greater functionality for individuals with PHLL. And while this assumption has largely held true for individuals with other upper limb amputations, it has not been shown in this patient population (largely due to the lack of available myoelectric control strategy options). Follow-up studies should directly compare the effect the choice of myoelectric control strategy (i.e., DC or *Glide*) has on partial hand prosthesis functionality. However, as a preliminary investigation, this work demonstrates the feasibility of successfully applying the *Glide* control strategy to the partial hand myoelectric control problem.

ACKNOWLEDGEMENTS

The authors would like to thank Dr. Ajul Shah, MD, FACS, Alta Fried, CHT, OTR/L, and their colleagues at the Center for Amputation Rehabilitation Medicine and Surgery in Neptune, NJ for their help in participant identification and recruitment for this study.

REFERENCES

[1] K. Ziegler-Graham, E. J. MacKenzie, P. L. Ephraim, T. G. Travison, and R. Brookmeyer, "Estimating the Prevalence of Limb Loss in the United States: 2005 to 2050," *Arch. Phys. Med. Rehabil.*, vol. 89, no. 3, pp. 422–429, Mar. 2008, doi: 10.1016/j.apmr.2007.11.005.

[2] T. R. Dillingham, L. E. Pezzin, and E. J. MacKenzie, "Limb amputation and limb deficiency: epidemiology and recent trends in the United States," *South. Med. J.*, vol. 95, no. 8, pp. 875–883, Aug. 2002.

[3] R. D. Rondinelli, "Commentary on Reliability of the AMA Guides to the Evaluation of Permanent Impairment," *J. Occup. Environ. Med.*, vol. 52, no. 12, pp. 1204–1205, Dec. 2010, doi: 10.1097/JOM.0b013e31820061f3.

[4] J. Davidson, "A comparison of upper limb amputees and patients with upper limb injuries using the Disability of the Arm, Shoulder and Hand (DASH)," *Disabil. Rehabil.*, vol. 26, no. 14–15, pp. 917–923, Aug. 2004.

[5] Committee on the Use of Selected Assistive Products and Technologies in Eliminating or Reducing the Effects of Impairments, Board on Health Care Services, Health and Medicine Division, and National Academies of Sciences, Engineering, and Medicine, *The Promise of Assistive Technology to Enhance Activity and Work Participation*. Washington, D.C.: National Academies Press, 2017. doi: 10.17226/24740.

[6] C. Lake, "Partial Hand Amputation: Prosthetic Management," in *Atlas of Amputations and Limb Deficiencies: Surgical, Prosthetic, and Rehabilitation Principles*, Rosemont: American Academy of Orthopaedic Surgeons, 2004.

[7] M. Lang, "Challenges and solutions in control systems for electrically powered articulating digits," Myoelectric Symposium, 2011.

[8] C. Lake, "Experience With Electric Prostheses for the Partial Hand Presentation: An Eight-Year Retrospective," *JPO J. Prosthet. Orthot.*, vol. 21, no. 2, p. 125, Apr. 2009, doi: 10.1097/JPO.0b013e3181a10f61.

[9] J. E. Uellendahl and E. N. Uellendahl, "Experience Fitting Partial Hand Prostheses with Externally Powered Fingers," in *Grasping the Future: Advances in Powered Upper Limb Prosthetics*, United Arab Emirates: Bentham Science Publishers, 2012.

[10] S. G. Millstein, H. Heger, and G. A. Hunter, "Prosthetic Use in Adult Upper Limb Amputees: A Comparison of the Body Powered and Electrically Powered Prostheses," *Prosthet. Orthot. Int.*, vol. 10, no. 1, pp. 27–34, Apr. 1986, doi: 10.3109/03093648609103076.

[11] S. L. Carey, D. J. Lura, M. J. Highsmith, CP, and FAAOP, "Differences in myoelectric and body-powered upper-limb prostheses: Systematic literature review," *J. Rehabil. Res. Dev.*, vol. 52, no. 3, pp. 247–262, 2015, doi: 10.1682/JRRD.2014.08.0192.

[12] R. B. Stein and M. Walley, "Functional comparison of upper extremity amputees using myoelectric and conventional prostheses," *Arch. Phys. Med. Rehabil.*, vol. 64, no. 6, pp. 243–248, Jun. 1983.

[13] P. Parker, K. Englehart, and B. Hudgins, "Myoelectric signal processing for control of powered limb prostheses," *J. Electromyogr. Kinesiol.*, vol. 16, no. 6, pp. 541–548, Dec. 2006, doi: 10.1016/j.jelekin.2006.08.006.

[14] J. L. Segil, M. Controzzi, R. F. ff. Weir, and C. Cipriani, "Comparative study of state-of-the-art myoelectric controllers for multigrasp prosthetic hands," *J. Rehabil. Res. Dev.*, vol. 51, no. 9, pp. 1439–1454, 2014, doi: 10.1682/JRRD.2014.01.0014.

[15] J. L. Segil, S. A. Huddle, and R. F. ff. Weir, "Functional Assessment of a Myoelectric Postural Controller and Multi-Functional Prosthetic Hand by Persons With Trans-Radial Limb Loss," *IEEE Trans. Neural Syst. Rehabil. Eng.*, vol. 25, no. 6, pp. 618–627, Jun. 2017, doi: 10.1109/TNSRE.2016.2586846.

[16] J. Segil, R. Kaliki, J. Uellendahl, and R. Weir, "A Myoelectric Postural Control Algorithm for Persons with Transradial Amputation: A Consideration of Clinical Readiness," *IEEE Robot. Autom. Mag.*, pp. 0–0, 2019, doi: 10.1109/MRA.2019.2949688.

[17] R. G. Gaston, J. W. Bracey, M. A. Tait, and B. J. Loeffler, "A Novel Muscle Transfer for Independent Digital Control of a Myoelectric Prosthesis: The Starfish Procedure," *J. Hand Surg.*, vol. 44, no. 2, p. 163.e1-163.e5, Feb. 2019, doi: 10.1016/j.jhsa.2018.04.009.

[18] F. R. Finley and R. W. Wirta, "Myocoder-computer study of electromyographic patterns," *Arch. Phys. Med. Rehabil.*, vol. 48, no. 1, pp. 20–24, Jan. 1967.

[19] R. N. Scott, "Myoelectric control of prostheses and orthoses," *Bull. Prosthet. Res.*, vol. 7, p. 93, 1967.

[20] J. H. Lyman, A. Freedy, and R. Prior, "Fundamental and applied research related to the design and development of upper-limb externally powered prostheses," *Bull Prosthet. Res*, vol. 13, pp. 184–195, 1976.

[21] J. T. Belter and A. M. Dollar, "Performance characteristics of anthropomorphic prosthetic hands," in *2011 IEEE International Conference on Rehabilitation Robotics*, Jun. 2011, pp. 1–7. doi: 10.1109/ICORR.2011.5975476.

[22] S. K. Denduluri, A. Rees, K. M. Nord, B. J. Loeffler, and R. G. Gaston, "The Starfish Procedure for Independent Digital Control of a Myoelectric Prosthesis," *Tech. Hand Up. Extrem. Surg.*, vol. 27, no. 1, pp. 61–67, Mar. 2023, doi: 10.1097/BTH.0000000000000412.

IMPROVING USER-IN-THE-LOOP MYOELECTRIC CONTROL USING CONTEXT INFORMED INCREMENTAL LEARNING

Evan Campbell[1], Ethan Eddy[1], Ulysse Côté-Allard[2], and Erik Scheme[1]
[1]*Institute of Biomedical Engineering, University of New Brunswick, Canada*
[2]*Department of Technology Systems, University of Oslo, Norway*

ABSTRACT

Screen or prosthesis guided training is typically used to train pattern recognition-based myoelectric control by providing controlled calibration samples with known labels. When these models are used with a user-in-the-loop, however, the observed patterns are much more variable, resulting in poor model extrapolation to these conditions and thus poor usability. Incremental and reinforcement learning approaches can continue learning from user-in-the-loop settings, but are limited in their reliability due to the lack of supervised labels and increased training times. In this work, we propose context informed incremental learning (CIIL), which adapts by drawing contextual information from the control task, to solve these issues. We test our claims across two conditions: a short training data scenario and a simulated electrode shift scenario. With only one second of initial training data per class, CIIL achieves similar throughput as SGT in a Fitts' law-style usability test after only two minutes of adaptation (the same amount of time taken for SGT). In the harder electrode shift scenario, CIIL significantly outperformed the pre-shifted SGT model after 5 minutes of adaptation, offering a promising direction for future clinical validation of user-in-the-loop training.

INTRODUCTION

Screen guided (or prosthesis guided) training (SGT) has become the standard practice for pattern recognition-based myoelectric control, achieving reasonable classification accuracy with acceptable effort and time invested by the user. By directing users through a sequence of motions to collect a representative dataset of electromyography (EMG) signals corresponding with known motion labels, models can be trained via supervised learning. An ongoing challenge, however, is how to make this data collection more representative of the data produced while the user is actively controlling their device, called the closed-loop/user-in-the-loop/online control setting. Solutions like collecting "ramp" contractions and known confounding factors like variable limb position have improved the performance in the online setting [1]; however, SGT still has meaningful shortcomings because of behavioural variability that arises from the online control setting (compensatory motions, proportional control, and error correction) which ultimately degrades model transfer to the online setting [2].

While strategies that continue to learn with the user-in-the-loop have tried to bridge this gap and produce more representative intent recognition models, these approaches have their own challenges. Among these strategies, unsupervised adaptation and reinforcement learning have been successful in addressing behavioural variability. Unsupervised adaptation, or incremental learning, continues to update the model in a weakly supervised learning process with the assumption that the model's prediction can be taken as a substitute for true labels. Approaches generally filter these predictions to only reincorporate highly confident [3], or representative [4] predictions to improve the robustness of the adaptation. Nevertheless, unsupervised incremental learning is generally not viable when the model's output is not trustworthy, such as after electrode-shift [5], and thus is not a reliable strategy when adaptation is arguably needed the most. Reinforcement learning leverages an environmental reward signal that truthfully describes the appropriateness of its actions for the situation, irrespective of classifier performance. Unfortunately, reinforcement learning is sample inefficient, which consequently increases the training burden to an unaffordable amount ($\sim$10-30 minutes [6]) as a standalone strategy employed online. Correspondingly, the challenge of all incremental learning and reinforcement learning approaches for incorporating user-in-the-loop behaviours is that they fail to simultaneously address the need for guaranteed performance improvements while ensuring sample efficiency.

Our proposed approach, context informed incremental learning (CIIL), aims to achieve the positives of both approaches. By using an environmental reward-like signal through context (similar to reinforcement learning), CIIL can reliably improve performance.Further, by using supervised learning to update model weights, CIIL can rapidly improve performance while minimizing the training burden on users. Across two simulated scenarios, including a short training data initialization and an introduced electrode shift, the proposed CIIL approach is compared to unsupervised high-confidence adaptation – the established baseline adaptation approach [3]. The results corroborate that CIIL quickly improves the model by incorporating user-in-the-loop patterns, irrespective of starting performance, which may lead to more robust long-term models.

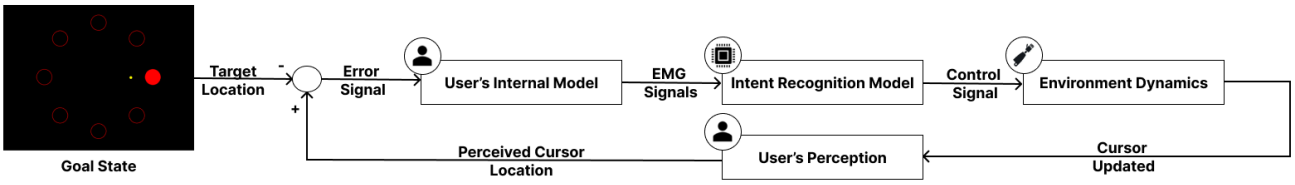

Fig. 1: Diagram of closed-loop myoelectric control. In this depiction, the user tries to direct a small yellow cursor to the red goal using myoelectric control. While the user is in-the-loop, they uses their internal model of the task and visual feedback to produce the necessary EMG to bring the cursor to the target. Consequently, produced EMG signals can be much more variable in this scenario compared to open-loop control that does not contain feedback.

METHODS

A. Hardware, Gestures, and Data Processing

The commercial Myo Armband was used to collect EMG data at 200Hz from 8 channels. Wrist flexion/extension and hand open/close gestures, plus a rest class, were mapped to left/right, up/down, and no movement of the cursor. To recognize the five gestures, all EMG data were first split into windows of 200ms with 100ms increments. Next, Hudgins' time domain features (Mean Absolute Value, Slope Sign Changes, Zero Crossings, and Waveform Length) were extracted from each window. All data processing was done using LibEMG, an open source Python library for myoelectric control [7]. Finally, all features were passed through an adaptive Linear Discriminant Analysis (aLDA) classifier [8].

B. Incremental Learning Strategies

The purpose of incremental learning is to gather behaviours that arise during the closed-loop setting. In this setting, subjects vary their contractions to move the cursor to a target position. The patterns produced are dependent on several factors, including the user's internal model and task-specific behaviours (Figure 1), and consequently are more variable than signals observed during SGT. Within this study, we evaluated an established incremental learning approach, Unsupervised High Confidence (UHC) compared to our proposed approach Context Informed Incremental Learning (CIIL).

Unsupervised High-Confidence (UHC): As proposed by Sensinger et al. [3], UHC adaptation involves updating a classifier based on predictions whose probability are above a predefined threshold.

Context Informed Incremental Learning (CIIL): Our proposed method makes use of a novel source of information returned from the environment: *context*. Context contains *suitability* information related to whether the actions taken at this time step were aligned with goal-seeking behaviour or not (binary value), and can be instrumented within many scenarios, such as the target acquisition environment shown in Figure 2. The control actions that are viable *options* for goal-seeking behaviour are also returned at each time step, which realistically can be inferred even from complex environments like prosthesis control using detection of proximal objects to curate likely classes of motion. Context is then used to inform the selection of labels that were suitable for the environment given the task, reinforcing positive actions. For unsuitable actions, wherein the classifier prediction disagrees with all viable options, the most viable option is used to relabel the sample for adaptation. This promotes the prediction of more viable alternatives the next time similar EMG patterns appear, adapting the model behaviour in this uncertain region.

C. Experimental Overview

Both experiments followed the same experimental structure, outlined as follows, with minor modifications outlined in the individual experimental sections. Both experiments were approved by the University of New Brunswick Research Ethics Board and are on file as REB 2022-122. Further details can be found in [9].

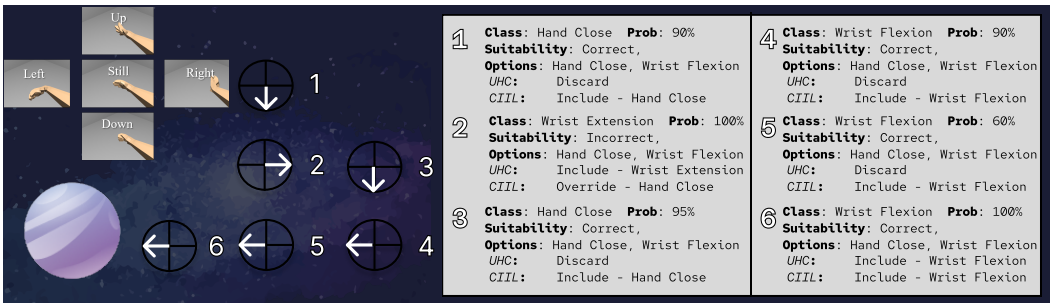

Fig. 2: Diagram of how adaptation strategies filter or correct pseudo-labels from within the gamified environment. The gesture mapping to cursor movement map is given in the top left. Crosshairs and arrows indicate cursor position at a given timestep and intent recognized. A table is given that provides information available to the incremental learning approaches, and how the sample is ultimately used in future model updates.

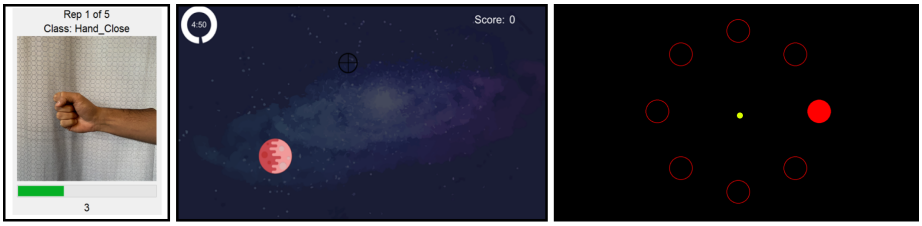

Fig. 3: (Left) Shows the SGT environment. (Middle) Shows Myo Shoot — the gameplay environment where adaptation took place. Users controlled the black cross-hair, and the planet represented the target. (Right) Shows the adapted ISO 9241-9 Fitt's law test. The circles represent targets, and the smaller yellow icon represents the cursor.

1) *Armband Placement:* The Myo Armband was placed 2/3 up the participant's right forearm, proximal to the elbow.
2) *Initial Model Training:* The initial model was trained. For experiment scenario one, one second of training data for each class was acquired. For experiment scenario two, 5 reps of 3 seconds were recorded for each gesture using SGT (see Figure 3, Left).
3) *Initial Model Evaluation:* The initial model was evaluated as per *Step 5 - Online Assessment*.
4) *Adaptive Gameplay:* Participants played the Myo-Shoot game (Figure 3, Middle), whereby real-time adaptation occurred in ten-second batches. The goal during this game was to acquire as many targets (planets) as possible. To successfully acquire a target, users had to hover the cross-hair within the planet's bounds and hover on top of it for three seconds. After successfully acquiring a planet, another was randomly re-generated at another position on the screen. Models were updated during this phase based on the given adaptation strategy. The order of adaptation strategies was randomized across participants.
5) *Online Assessment:* Using the adapted model from step 4, participants completed an ISO 0241-9 inspired Fitt's law test (Figure 3, Right), whereby they had to hover a cursor over a set of targets and hover within their bounds for three seconds. Once acquired, the user was prompted to move the cursor to a different target. This continued until the participant acquired all eight targets in the ring. During this evaluation, no adaptation occurred.
6) *Offline Assessment:* To enable offline testing of the adapted model with representative data, two additional three-second repetitions of each gesture were acquired.

Experimental Scenario 1: Limited Training Data Eleven participants took part in this initial study on the use of a limited amount of training data (1 second per class). The adaptive gameplay phase lasted for 2 minutes. A constant velocity was employed, meaning the cursor moved at a fixed speed, regardless of contraction intensity. Finally, due to the high confidence profile of LDA classifiers, a UHC threshold of 100% was leveraged. Even at this seemingly high threshold, approximately 50% of decisions were used to adapt the model [10].

Experimental Scenario 2: Electrode Shift In a subsequent study, 21 individuals evaluated the adaptation strategies after a severe 45° electrode shift. After training the initial model via SGT, participants were instructed to rotate the Myo Armband clockwise by one electrode. The adaptive gameplay phase lasted 5 minutes. Due to the decreased confidence profile of the aLDA classifier, a lower confidence threshold of 99% was selected for UHC adaptation. Additionally, a proportional control scheme was adopted, meaning harder contractions resulted in faster cursor speeds meaning subjects could generally achieve higher throughput [1].

RESULTS

The results across the online assessment and offline assessment of both experiments were compiled into Table I. In the limited training data scenario, all incremental learning approaches led to improved performance across all metrics when compared to the model seeded with only one second of calibration data. CIIL performed comparably to a full SGT protocol for online metrics, despite only beginning with one second of calibration data. In the same setting, UHC performed marginally worse than CIIL, with a 12.5% relative difference in throughput. In the electrode shift scenario, the offline accuracy of the model dropped from 87.8% to 48.3%, demonstrating the severity of the degradation introduced by the electrode shift. After a 5 minute adaptation phase, CIIL was able to significantly outperform the UHC approach, which was unable to recover to a usable state. CIIL also significantly outperformed the pre-shift SGT, tested before the shift was introduced, and the unusable post-shift SGT.

DISCUSSION

In the limited training data scenario, a single second of calibration data per class was sufficient for both UHC and CIIL adaptation to positively influence the throughput of the model. Past work has evaluated UHC under favourable conditions, where model performance is extremely high when adaptation begins; however, this study shows that UHC can improve performance for a distinguishable gesture set when classification accuracy begins as low as 65.7%. Regardless, CIIL was

TABLE I: Summary of performance for the two experimental scenarios. Bold values indicate the best value of the metric across the approaches within an experiment. Dashes denote the fact that the SGT Post-Shift model was unusable and thus no acquisitions were completed. An asterisk (*) indicates a significant difference with CIIL determined through a Friedman test with Finner posthoc correction.

Model	Accuracy (%)	Active Error (%)	Instability (%)	Overshoots (#)	Efficiency (%)	Throughput (bit/s)
Experiment 1: Limited Training Data						
SGT	**91.3 ± 8.6**	**6.2 ± 5.7**	**5.0 ± 3.8**	4.5 ± 3.7	68.5 ± 6.8	**0.41 ± 0.06**
1 Second	65.7 ± 14.2 *	32.6 ± 12.3 *	19.9 ± 6.0 *	13.6 ± 19.4	42.6 ± 18.8 *	0.24 ± 0.10 *
UHC	79.1 ± 12.8	18.2 ± 12.0 *	12.1 ± 7.3 *	6.1 ± 7.5	60.6 ± 14.1	0.35 ± 0.08
CIIL	85.3 ± 11.0	10.5 ± 8.0	8.1 ± 6.2	**3.6 ± 3.9**	**70.1 ± 8.2**	0.40 ± 0.06
Experiment 2: Electrode Shift						
SGT Pre-Shift	**87.8 ± 7.6**	**10.0 ± 6.2**	7.8 ± 4.6	7.9 ± 7.9	61.6 ± 13.6	0.50 ± 0.18 *
SGT Post-Shift	48.3 ± 15.5 *	61.5 ± 18.4 *	11.4 ± 5.3 *	–	–	–
UHC	45.2 ± 17.8 *	65.1 ± 22.5 *	**6.5 ± 4.5**	9.6 ± 12.4 *	11.6 ± 21.7 *	0.09 ± 0.18 *
CIIL	79.5 ± 17.2	21.0 ± 20.4	7.3 ± 4.3	**5.0 ± 7.0**	**66.0 ± 15.8**	**0.61 ± 0.21**

shown to improve throughput more than UHC in the limited training data setting, where both models were provided the same one second calibration and two minute adaptation phase. This outcome suggests that CIIL can quickly reduce epistemic errors through adaptation, and with a higher ceiling than UHC, even when beginning with a correctly trained model.

In the second experiment, both adaptation approaches began with an abrupt and intentional concept shift that degraded classifier accuracy from 87.8% to 48.4%. With this lower starting accuracy, UHC was unable to recover to a usable state post-adaptation. Further, despite filtering predictions using high confidence, UHC marginally decreased accuracy and active error compared to the initialization; indicating the lack of reliability of current adaptation approaches to address large concept shifts. Conversely, CIIL was shown to reliably improve performance irrespective of classifier performance and even outperformed the pre-shift SGT model's throughput. This outcome suggests that CIIL can reliably improve the model regardless of initial classifier performance using context from the environment. Correspondingly, CIIL warrants future work exploring the numerous other confounding factors that introduce concept shifts, such as limb position [11].

This study was an initial validation of CIIL, with future work needed to make the approach viable for clinical populations. If used as a training environment, the proposed CIIL approaches are viable in their current state. However, if leveraged during real-time use, future work on how to gather context within a prosthesis use-case, and how frequently it can be incorporated, is required. The benefits of using CIIL would need to merit the cost of creating advanced prostheses with the ability to perceive the environment to recognize nearby objects and grasps suitable for the situation. Once fully instrumented, it could be possible to rely on the environmental context alone for semi-autonomous gesture elicitation, however, this would decrease the user's agency over their device [12]. Consequently, the proposed CIIL approach may offer a favorable tradeoff for improved control. Ultimately, CIIL enables the incorporation of user-in-the-loop training data with context-based pseudo-labels. The ability to integrate user behaviours, confounding factors, and changes over time based on situational context is promising, and warrants further research.

REFERENCES

[1] E. Scheme, B. Lock, L. Hargrove, W. Hill, U. Kuruganti, and K. Englehart, "Motion normalized proportional control for improved pattern recognition-based myoelectric control," *IEEE Transactions on Neural Systems and Rehabilitation Engineering*, vol. 22, no. 1, pp. 149–157, 2013.

[2] L. Hargrove, Y. Losier, B. Lock, K. Englehart, and B. Hudgins, "A real-time pattern recognition based myoelectric control usability study implemented in a virtual environment," in *2007 29th Annual International Conference of the IEEE Engineering in Medicine and Biology Society*. IEEE, 2007, pp. 4842–4845.

[3] J. W. Sensinger, B. A. Lock, and T. A. Kuiken, "Adaptive pattern recognition of myoelectric signals: exploration of conceptual framework and practical algorithms," *IEEE Transactions on Neural Systems and Rehabilitation Engineering*, vol. 17, no. 3, pp. 270–278, 2009.

[4] K. Szymaniak, A. Krasoulis, and K. Nazarpour, "Recalibration of myoelectric control with active learning," *Frontiers in Neurorobotics*, vol. 16, p. 277, 2022.

[5] D. Yeung, I. M. Guerra, I. Barner-Rasmussen, E. Siponen, D. Farina, and I. Vujaklija, "Co-adaptive control of bionic limbs via unsupervised adaptation of muscle synergies," *IEEE Transactions on Biomedical Engineering*, vol. 69, no. 8, pp. 2581–2592, 2022.

[6] A. L. Edwards, A. Kearney, M. R. Dawson, R. S. Sutton, and P. M. Pilarski, "Temporal-difference learning to assist human decision making during the control of an artificial limb," *arXiv preprint arXiv:1309.4714*, 2013.

[7] E. Eddy, E. Campbell, A. Phinyomark, S. Bateman, and E. Scheme, "LibEMG: An open source library to facilitate the exploration of myoelectric control," *IEEE Access*, vol. 11, pp. 87 380–87 397, 2023.

[8] H. Zhang, Y. Zhao, F. Yao, L. Xu, P. Shang, and G. Li, "An adaptation strategy using LDA classifier for EMG pattern recognition," in *2013 Annual International Conference of the IEEE Engineering in Medicine and Biology Society (EMBC)*, 2013, pp. 4267–4270.

[9] E. Eddy, E. Campbell, S. Bateman, and E. Scheme, "Leveraging task-specific context to improve unsupervised adaptation for myoelectric control," in *2023 IEEE International Conference on Systems, Man, and Cybernetics (SMC)*. IEEE, 2023, pp. 4661–4666.

[10] E. Scheme and K. Englehart, "A comparison of classification based confidence metrics for use in the design of myoelectric control systems," in *2015 Annual International Conference of the IEEE Engineering in Medicine and Biology Society*. IEEE, 2015, pp. 7278–7283.

[11] E. Campbell, A. Phinyomark, and E. Scheme, "Current trends and confounding factors in myoelectric control: Limb position and contraction intensity," *Sensors*, vol. 20, no. 6, 2020.

[12] J. W. Sensinger and S. Dosen, "A review of sensory feedback in upper-limb prostheses from the perspective of human motor control," *Frontiers in Neuroscience*, vol. 14, p. 345, 2020.

SPATIO-TEMPORAL CONVOLUTIONAL NETWORKS FOR MYOELECTRIC CONTROL

Milad Jabbari and Kianoush Nazarpour

School of Informatics, University of Edinburgh, UK

ABSTRACT

Utilising both within-channel temporal and between-channel spatial dependencies of the surface Electromyographic (sEMG) signals improves the accuracy of machine learning-based models of myoelectric control. Here, we introduce the Spatio-Temporal Convolutional Network (STCN) to decode five hand gestures from eight EMG signals recorded from the forearm of eight able-bodied subjects. We compared our proposed STCN model with a combination of a conventional convolutional neural network (CNN) and a Long Short-Term Memory (LSTM) deep learning model, as well as the Linear Discriminant Analysis (LDA). The results show that STCN model can outperform both CNN-LSTM and LDA methods at a much lower computational complexity.

INTRODUCTION

For decades, conventional machine learning models have served as the gold-standard models in EMG -based hand gesture classification [1]. Despite providing reliable results, they suffer from a lack of generalisation and robustness. Furthermore, they depend extremely on the distribution and separability of the feature set. Therefore, to achieve higher performance, they need high-quality hand-crafted and separable features. Extracting such features is not trivial and may lead to complex computations, posing difficulties in translating the system into a real-time experience [2].

Deep learning models possess the ability to extract insightful features from raw data, thereby obviating the necessity for manual hand-crafted feature extraction. Moreover, through hierarchical representation, non-linear decision boundaries, and regularization techniques, they enhance the robustness of performance [3]. These inherent advantages position such models as exceptional candidates for mapping raw EMG signals or basic low-level features to a notably enriched informative space with maximal separability.

In EMG-based hand gesture classification system, extracting both temporal and spatial features can enhance the performance in terms of accuracy and generalisation. For instance, in hybrid CNN-LSTMs models, CNN and LSTM extract spatial and temporal dependencies, respectively [4-5]. However, the substantial computational cost of this approach renders hardware implementation challenging. Recently, Temporal Convolutional Networks (TCN) have proved effective in sequence modelling. By implementing the concept of dilation, TCNs demonstrates their superiority in capturing temporal dependency, while maintaining significantly lower computational cost compared to other deep learning models [6].

In this work, we introduce the Spatio-Temporal Convolutional Network (STCN) model to enable simultaneous extraction of temporal and spatial components. We compare this network with the CNN-LSTM structure as well as the LDA method, which serves a benchmark.

METHODS

Participants and EMG Recording

A schematic experimental setup from the experiment is shown in Figure 1. The experimental protocol was in accordance with the ethical approval granted by the local committee at the University of Edinburgh (reference number: 2019/89177). Eight participants took part in the experiment after signing an informed consent. During the experiment, participants performed five hand gestures including Open, Power, Pointer, Tripod, and Rest. The EMG signals were recorded using eight OY Motion EMG electrodes at a sampling frequency of 1000 Hz. Before the start of the

experiment, electrodes were placed on the participants' arm and secured using an armband. During the experiment, participants sat in front of a screen which instructed the gestures. We recorded fifteen examples for each gesture, ech 2 seconds long.

Utilised Models

In this study, to conduct spatial convolution, we aimed to use a *depthwise* convolution layer to extract spatial features from the channels. Following a spatial block, a temporal block containing 4 dilated temporal convolutional layers captured the temporal dependencies. Figure 2(A) presents the proposed STCN concept. A simplified block diagram representation of STCN model is presented in Figure 2(B). In addition to the proposed STCN, we deployed a hybrid CNN-LSTM model and a conventional LDA classifier to perform 5-movement classification. For both models, spatial part consists of two 1-Dimensional CNN layer followed by a batch normalization and a dropout layer. Utilized CNN-LSTM model benefits from an LSTM layer consists of 100 units, whereas TCN block in STCN is a single-stack basic TCN.

Feature set and statistical analysis

We fed these three models with six features called spatio-temporal feature set (STFS), which were in line with [7]. This feature set consists of integral square descriptor, normalised root square coefficient of first and second differential derivatives, mean log-kernel, an estimate of mean derivative of the higher-order moments, and a measure of spatial muscle information. To evaluate statistical significance of the obtained findings, Wilcoxon rank signed test was employed. The Bonferroni correction method was used to adjust the *p*-values and re-balance the compounding risks.

RESULTS

To assess the proposed STCN model and provide comparison with CNN-LSTM and LDA methods, we calculated classification accuracy using:

$$\mathrm{CA} = \frac{correctly\ classified\ samples}{total\ classified\ samples} \times 100\% \quad (1)$$

Furthermore, averaged confusion matrixes over all participants were calculated to demonstrate between class variation of the performance. Figure 3(A) illustrates boxplot presentation of CA values for STCN, CNN-LSTM, and LDA methods. The results show that using STCN can significantly outperform both CNN-LSTM and LDA with $p<0.05$ and $p<0.001$ and average CA about 95.21±0.01%. Moreover, averaged confusion matrixes over all participants for LDA and STCN is shown in figure 3(B) and figure 3(C), respectively. It is visible that performance of STCN in terms of between classification variation is better than LDA.

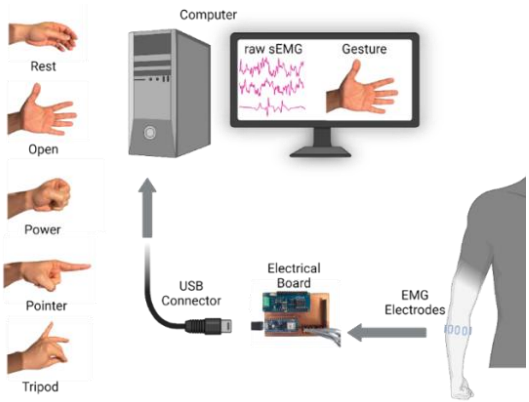

Figure 1: Schematic experimental setup. Participant generates the illustrated gestures including Rest, Open, Power, Pointer, and Tripod, while is sitting on a chair and with a fixed position arm.

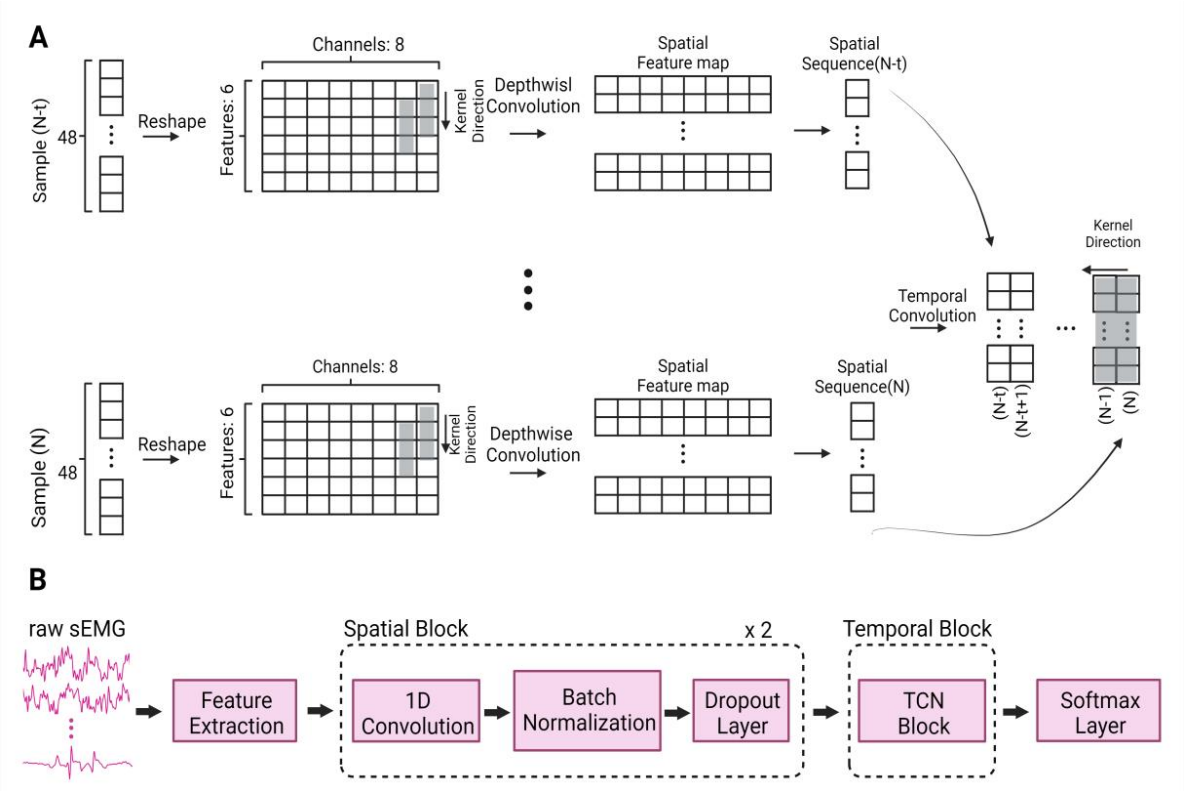

Figure 2: Schematic representation of the utilized Spatio-Temporal approach and overall block diagram of the STCN model shown in A and B.

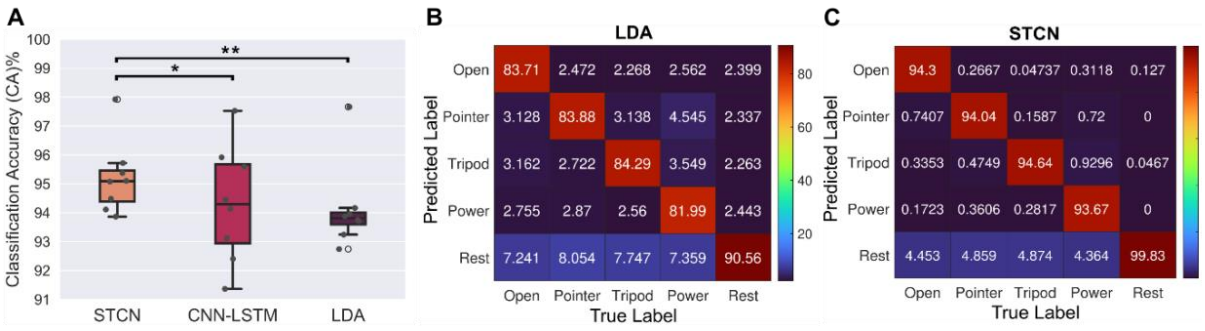

Figure 3: Boxplot representing of averaged CA values over all subjects for STCN, CNN-LSTM, and LDA and averaged confusion matrices of LDA and STCN are illustrated in A, B, and C, respectively.

DISCUSSION

This study presents a novel spatio-temporal model designed to capture both the spatial and temporal dependencies of sEMG signals. Inspired by the convolution concept and moving the kernel in spatial and temporal directions in separated blocks, we show that a reliable performance can be achieved. Deploying a spatial convolutional layer by using CNNs reveals the spatial flow of information and connectivity between muscles signals. These spatially distributed components of information can be fed into a TCN block after appropriately reshaping of timesteps and result in higher accuracy compared to conventional ML models. Previous studies have demonstrated the excellence of hybrid CNN-LSTM models in conducting EMG based hand gesture classification, however, in this study we show that using dilated convolution may lead to better performance compared to cell state concept in LSTM.

Our findings demonstrate that employing a deep learning-based model with low-level representation of sEMG signal as feature may lead to reliable classification. An important consideration in the STCN model is the choice of kernel shape and size. In this study we utilised 1D kernels. An alternative approach can involve switching to 2D kernels of different size. Considering how electrodes are distributed in distal/proximal and lateral directions, selecting the kernel type and size will also be a crucial parameter.

ACKNOWLEDGEMENTS

This work is supported by funding from Engineering and Physical Sciences Research Council (EPSRC) under grant (EP/R004242/2).

REFERENCES

[1] E. Scheme, and K. Englehart, "Electromyogram pattern recognition for control of powered upper-limb prostheses: state of the art and challenges for clinical use," *J. Rehabil. Res. Dev.*, vol. 46, no. 6, 2011.

[2] M. Jabbari, R. N. Khushaba, and K. Nazarpour, "Spatio-temporal warping for myoelectric control: an offline, feasibility study," *J. Neural Eng.*, vol. 18, no. 6, p. 066028, 2021.

[3] J. Ye, N. Jiangqun, and Y. Yang, "Deep learning hierarchical representations for image analysis," *IEEE Trans. Inf. Forensics Secur.*, vol. 12, no. 11, pp. 2545-2557, 2017.

[4] Y. Hu, *et al.*, "A novel attention-based hybrid CNN-RNN architecture for sEMG-based gesture recognition," *PLoS One.*, vol. 13, no. 10, p. e0206049, 2018.

[5] T. Bao, *et al.*, "A CNN-LSTM hybrid model for wrist kinematics estimation using surface electromyography," *IEEE Trans. Instrum. Meas..*, vol. 70, pp. 1-9, 2020.

[6] U. Cote-Allard, *et al.*, "A transferable adaptive domain adversarial neural network for virtual reality augmentation EMG-based gesture recognition," *IEEE Trans. Neural Syst. Rehabil. Eng.*, vol. 29, pp. 546-555, 2021.

[7] S. O. Williams, *et al.*, "Spatio-temporal based descriptor for limb movement-intent characterization in EMG-pattern recognition system," in *proceeding IEEE EMBC*, pp. 2637-2640, 2019.

TOWARD SELF-CALIBRATING PLUG-AND-PLAY MYOELECTRIC CONTROL

Xinyu Jiang, Chenfei Ma, and Kianoush Nazarpour

School of Informatics, The University of Edinburgh, Edinburgh, United Kingdom.

ABSTRACT

Myoelectric control enables users to interact with diverse devices. However, electromyographic (EMG) signals change over time due to diverse factors, e.g., user behaviour variation, and other. These variations lead to a substantial reduction in performance of machine learning-based myoelectric control model, which in turn necessitate frequent re-calibration. In this paper, we report the results of our "self-calibrating" and "plug-and-play" random forest model. We pre-train the model and then calibrate it on new participants via one-shot calibration. The model then calibrate itself autonomously . We validated this model on 18 testing participants. Work is on-going to expand our database and study the effectiveness of the approach with people with limb difference.

INTRODUCTION

Myoelectric control systems enable users to interact with diverse devices, e.g. exoskeleton and prosthesis [1] by recognizing different patterns of the EMG signals. Diverse known or unknown factors, such as the behaviour variation of users, noises, electrode shift, muscle fatigue, limb position and other physiological factors jointly lead to the variability of EMG patterns [2], [3]. The EMG variability leads to substantially degraded performance of a model, even within a short period of time.

Training a machine learning model that can account for the variability of EMG characteristics requires a large amount of labelled data. Previous attempts to address the above issues by taking the best advantages of both labelled or unlabelled data. For instance using the notion of domain adaptation, Vidovic et al. proposed a covariate shift adaptation algorithm to adapt the basic statistical metrics of training and testing data [4]. Other studies that utilised semi-supervised learning enabled the self-training or self-calibration of a deep neural network [5], [6]. A very recent study applied a domain-adversarial neural network to generalise a model between multiple days [7].

However, these studies mostly performed one-time calibration of the model each time it was used or evaluated the model performance by pooling the testing data collected in each session together to give an overall accuracy. In practical applications, even within the same experimental session, the EMG characteristics can change [8]. This continuous change in EMG pattern causes a major challenge for myoelectric control in real-life settings. We see this challenge as an opportunity to capture intermediary data which serves our model to gradually track the change and generalise to the new EMG patterns.

We developed a self-calibrating random forest (RF) common model, which can (1) be pre-trained on data from many people and easily adapt to a new user via one-shot calibration, and (2) second, keep calibrating itself once in a while in a statistically meaningful way. The effectiveness of our method has been validated on 18 participants.

DATA COLLECTION

All participants signed an informed consent form approved by the local ethics committee at the University of Edinburgh (reference number: 2019/89177), in accordance with the Declaration of Helsinki. All settings and details of data collection are the same as our previous study [9]. Here we briefly introduce the data collection experiments.

We conducted 2 experiments. In experiment 1, we recruited 20 participants (aged 22--43 years, 12 males, 8 females). Eight electrodes were placed across the circumference of the forearm. Delsys Trigno sensors with a 2000 Hz sampling rate and 10--500 Hz passband were used for data collection. Each participant performed six hand grips ("power", "lateral", "tripod", "pointer", "open" and "rest", the same as our previous study [9]). For each hand gesture, 10 repetitions (6s each) were performed in 10 trials. Data recorded in the first 2s reaction and transition period of each trial were removed, with the last 4s retained. A 5s inter-trial resting period was provided.

In experiment 2, we recruited new participants (aged 22--28 years, 11 males, 7 females). The experiment consisted of two sessions, the calibration and the testing sessions. In the calibration session, participants performed only one repetition per gesture in a 2s trial. Only signals during the latter 1 second were retained (the same for the testing session) and used in our analyses. The testing session comprised 5 testing blocks. In each testing block, participants performed five repetitions per gesture (30 repetitions in total), with a pseudo-randomised order. Participants had 2 seconds and 5 minutes for inter-trial and inter-block rest, respectively.

METHODS

Feature Extraction

Features in each channel were extracted via a sliding window with 200 ms length and 100 ms sliding step. The following ten types of features were extracted: root mean square (RMS), mean absolute value (MAV), waveform length (WL), slope sign changes (SSC), zero crossings (ZC), skewness, mean frequency (MNF), median frequency (MDF), peak frequency (PKF), and variance of central frequency (VCF). The final length of feature vector is 80 (8 channels × 10 features).

Pre-training and Fine-tuning a RF Model

The RF model for each user was first pre-trained on data from other users. The pre-trained RF model consists of 200 decision trees. All pre-trained decision trees were then pruned using the calibration data (collected in the calibration section) from the new user. A bottom-up pruning strategy was applied. Details on decision tree pruning can be found in [9]. After pruning each pre-trained decision tree, we trained 200 new decision trees from scratch, using only the calibration data from the new user. These new decision trees were appended to the pre-trained and pruned RF model. The pre-trained and fine-tuned RF consists of 400 decision trees (200 pre-trained and pruned trees and 200 appended trees). All other details are the same as our previous work [9].

Self-calibration

When using the model, we applied a data buffer to save the latest testing samples. The size of the data buffer was set to 1500 windowed samples (about 500 KB for float32 precision). The data buffer was updated after each testing block and used to self-calibrate the model. When the data buffer reached its maximum size, the oldest sample corresponding to the gesture label (determined as pseudo-labels) with the most samples would be deleted.

To assign reliable pseudo-labels on high-dimensional EMG features, we performed t-Distributed Stochastic Neighbor Embedding (t-SNE) [10] to map the original 80-dimensional EMG feature space into a 3-dimensional subspace, and at the same time preserve the local distribution structure in the original space. After that, K-Means clustering was performed on the 3-dimensional data. The initialised labels of all testing samples before clustering were assigned as the predictions directly given by the current model.

After the pseudo-label assignment, both data in the data buffer with pseudo-labels and the calibration data (used in the fine-tuning stage) with ground-truth labels were combined together to train new decision trees and replace the original ones. We kept those pruned decision trees fixed and only replaced those appended decision trees. Each time we only replaced 80 (40% of 200) randomly selected appended decision trees.

Validation

All data from the 20 participants in experiment 1 were allocated to the pre-training dataset. For data from the 18 participants in dataset 2, each participant was in turn viewed as the target testing participant, with data from the other 17 participants used as additional pre-training data. Accordingly, for each of the 18 testing participants, data from 37 participants were available for model pre-training. Given the pre-trained RF model, data collected from the testing participant in the calibration session were used to fine-tune the RF model via pruning and appending decision trees. Self-calibration was performed after each testing block. In addition to the above models, we further implemented standard user-specific linear discriminant analysis (LDA) and random forest (RF) models to provide baseline performances. The standard LDA and RF models were trained using only the data collected in the calibration session for each target testing participant.

RESULTS AND DISCUSSION

Results are presented in Figure 1. According to Figure 1 (a) and Figure 1 (b), the accuracy of pruned and appended RF model achieved a higher accuracy compared with standard RF and LDA models. With self-calibration, the accuracy of pruned and appended RF could be further improved. Specifically, as presented in Figure 1 (a), the accuracy with self-calibration showed a slowly increased trend, demonstrating that the self-calibrating model can progressively adapt to the data distribution in the testing process.

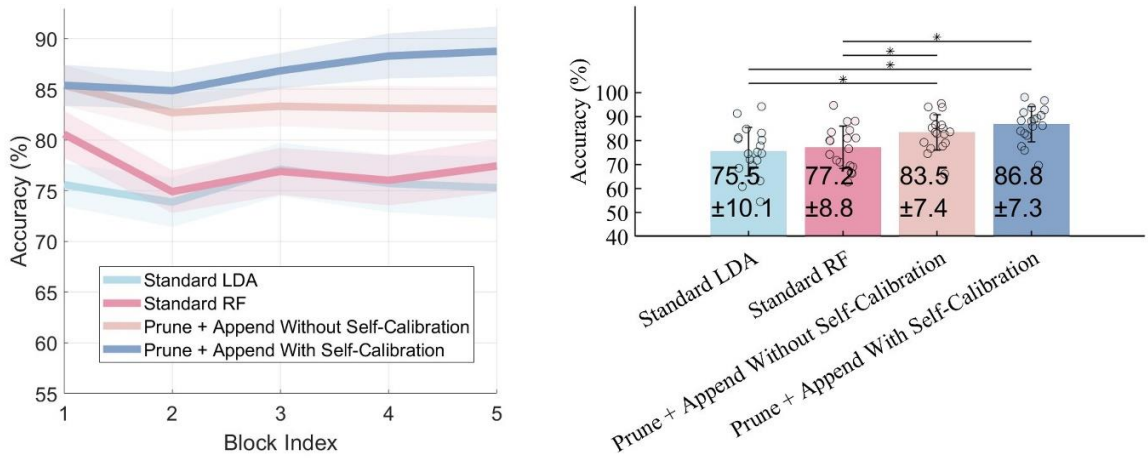

(a) Accuracy-Block Curve

(b) Error Bar of Different Models

Figure 1: Results of Different Models. In (a), standard error (SE) was presented as the shaded area for the figure clarity. In (b), standard deviation (STD) was presented.

The pre-training and self-calibration steps could progressively improve the model performance compared with the standard RF model. It does so by learning more general knowledge from much more data from other participants, therefore the model generalise better with only a few calibration samples from each new participant. The self-calibration step improves the model performance by estimating a more precise data distribution using more testing data. The assigned pseudo-labels may not be 100% accurate but can still provide useful information on the overall distribution of data belonging to each class.

In our method, the pseudo-labels were assigned by integrating manifold learning via t-SNE and clustering via K-Means. EMG features are normally of high dimensions, distributed on a curved manifold in the feature space. The motivation to apply manifold learning is to simply the data distribution in the high-dimensional feature space. Through manifold learning, the curved manifold can be flattened in a low-dimensional space. The motivation for applying clustering is to jointly consider (1) the knowledge learned by the current model (for the initialisation of pseudo-labels before clustering) and (2) the statistical information and distribution structure of a batch of saved data. Without these components (i.e., directly assigning pseudo-labels using the predictions of the current model), the model would be more likely to fall into a loop to learn biased knowledge given by itself. With the joint contribution from all modules, the final self-calibrating model achieved the highest accuracy compared with all baseline methods.

CONCLUSION

We proposed a self-calibrating RF common model. The RF common model can be first pre-trained on data from many users and then fine-tuned using only one-repetition per gesture from a new target user. The RF common model would then self-calibrate itself once in a while during long-term applications. Analyses on data from 18 testing

participants demonstrate the effectiveness of our model. Our work promotes the use of a plug-and-play model in real-world applications.

REFERENCES

[1] M. A. Garenfeld, M. Strbac, N. Jorgovanovic, J. L. Dideriksen, and S. Dosen, "Closed-Loop Control of a Multifunctional Myoelectric Prosthesis With Full-State Anatomically Congruent Electrotactile Feedback," *IEEE Trans. Neural Syst. Rehabil. Eng.*, vol. 31, pp. 2090–2100, 2023, doi: 10.1109/TNSRE.2023.3267273.

[2] L. Wang, X. Li, Z. Chen, Z. Sun, and J. Xue, "Electrode Shift Fast Adaptive Correction for Improving Myoelectric Control Interface Performance," *IEEE Sens. J.*, vol. 23, no. 20, pp. 25036–25047, Oct. 2023, doi: 10.1109/JSEN.2023.3312403.

[3] S. A. Stuttaford, M. Dyson, K. Nazarpour, and S. S. G. Dupan, "Reducing Motor Variability Enhances Myoelectric Control Robustness Across Untrained Limb Positions," *IEEE Trans. Neural Syst. Rehabil. Eng.*, vol. 32, pp. 23–32, 2024, doi: 10.1109/TNSRE.2023.3343621.

[4] M. M.-C. Vidovic, H.-J. Hwang, S. Amsuss, J. M. Hahne, D. Farina, and K.-R. Muller, "Improving the Robustness of Myoelectric Pattern Recognition for Upper Limb Prostheses by Covariate Shift Adaptation," *IEEE Trans. Neural Syst. Rehabil. Eng.*, vol. 24, no. 9, pp. 961–970, Sep. 2016, doi: 10.1109/TNSRE.2015.2492619.

[5] K. Wang, Y. Chen, Y. Zhang, X. Yang, and C. Hu, "Iterative Self-Training Based Domain Adaptation for Cross-User sEMG Gesture Recognition," *IEEE Trans. Neural Syst. Rehabil. Eng.*, vol. 31, pp. 2974–2987, 2023, doi: 10.1109/TNSRE.2023.3293334.

[6] U. Côté-Allard *et al.*, "Unsupervised Domain Adversarial Self-Calibration for Electromyography-Based Gesture Recognition," *IEEE Access*, vol. 8, pp. 177941–177955, 2020, doi: 10.1109/ACCESS.2020.3027497.

[7] D. Lee *et al.*, "EMG-based hand gesture classifier robust to daily variation: Recursive domain adversarial neural network with data synthesis," *Biomed. Signal Process. Control*, vol. 88, p. 105600, Feb. 2024, doi: 10.1016/j.bspc.2023.105600.

[8] A. Krasoulis, S. Vijayakumar, and K. Nazarpour, "Effect of User Practice on Prosthetic Finger Control With an Intuitive Myoelectric Decoder," *Front. Neurosci.*, vol. 13, Sep. 2019, doi: 10.3389/fnins.2019.00891.

[9] X. Jiang, C. Ma, and K. Nazarpour, "One-shot random forest model calibration for hand gesture decoding," *J. Neural Eng.*, vol. 21, no. 1, p. 016006, Jan. 2024, doi: 10.1088/1741-2552/ad1786.

[10] L. van der Maaten and G. Hinton, "Visualizing Data using t-SNE," *J. Mach. Learn. Res.*, vol. 9, no. 11, pp. 2579–2605, 11/1/2008 2008.

Myoelectric Controls Implementations

A PRELIMINARY INVESTIGATION INTO BIO-INSPIRED DATA COLLECTION FOR TRANSHUMERAL TARGETED MUSCLE REINNERVATION PROSTHETIC CONTROL

Laura C. Petrich[1,5], Heather E. Williams[2,5], Matthew E. Taylor[1,5], Jacqueline S. Hebert[2,4], Pierre Lemelin[3], Ahmed W. Shehata[2], and Patrick M. Pilarski[4,5]

[1]*Dept. of Computing Science,* [2]*Dept. of Biomedical Engineering,* [3]*Dept. of Surgery, and* [4]*Dept. of Medicine, University of Alberta, Edmonton, AB, Canada;* [5]*Alberta Machine Intelligence Institute (Amii), Edmonton, AB, Canada.*

ABSTRACT

For persons with transhumeral amputation, targeted muscle reinnervation (TMR) has unlocked the potential for innovative and intuitive control of myoelectric prostheses. There are many open source datasets available for training machine learning (ML) models for transradial and transhumeral prosthetic control. However, to the best of our knowledge, no datasets have been gathered *in different limb positions* with the intent of training models specifically for *persons with transhumeral amputation who have undergone TMR surgery*. Moreover, such a dataset is challenging to curate as TMR is still a relatively new surgical technique and there are few people with TMR. In this work we present a novel biologically-inspired protocol for collecting data from *persons both with and without upper-limb amputations* that can be used to train generalized ML models for this growing population of users. Our results from a three-participant pilot study suggest that by choosing targeted sensor placements that correspond to specific limb nerve/muscle compartment associations post-TMR surgery, we can potentially capture control-relevant muscle activation patterns from persons without limb difference that closely resemble expectations of anatomical prime movers. We expect this collection protocol to provide further utility in studying the relationship between limb positions and myocontrol signals, and differences between isotonic and isometric muscle contractions during prosthesis use, leading to a new generation of TMR-ready control solutions.

INTRODUCTION

Most commercially available motorized prostheses are controlled via electromyogram (EMG) signals from a pair of residual agonist-antagonist muscles [1]. Conventional control strategies map the acquired EMG signal amplitude to operate each joint of the prostheses [2]. For example, EMG signals from the contraction of the biceps brachii and triceps brachii muscles can be mapped to operate elbow flexion and extension, respectively. However, myoelectric control with only two signals is slow and unintuitive [3]. In contrast, targeted muscle reinnervation (TMR) is a surgical technique that reroutes nerves that would innervate forearm and hand muscles to alternative muscle sites in the residual limb [4]. As a result, persons with TMR and transhumeral amputations (hereafter simply termed *users*) can have up to five distinct muscle sites, allowing for advanced ML solutions to control multiple joints simultaneously. TMR has been shown to improve myoelectric prosthesis control for persons with transhumeral amputations or shoulder disarticulations [5, 6].

Machine learning (ML) models for prosthetic control can be trained to recognize patterns in the acquired signals related to their physiologically appropriate joint action [7]. However, training a personalized ML model capable of making accurate predictions in different limb positions and conditions of use requires a substantial amount of labelled data from the user, which is time consuming and prohibitive during daily use [8]. Furthermore, these models tend to suffer from lack of generalizability both across and within participants, due to inter- and intra-participant variability, as well as differences in sensor placement and environmental conditions [2, 9]. Being able to augment the training set with data from persons without limb differences—or a TMR user's other limb without amputation—may contribute to both increasing the initial generality of learned controllers and reducing re-training effort. Our preliminary study demonstrates that data collected using our proposed protocol reflects anatomically-based expectations of muscle activation patterns for a non-amputated upper limb during various actions. This will enable future work to analyze the effect of limb positions on muscle activation signals and capture the differences between isotonic and isometric muscle contractions in the arm and forearm.

METHODS

Our proposed data collection protocol provides an anatomically-inspired sensor placement guide designed to acquire signals from muscles that align with a residual limb post-TMR. We first describe an overview of the data collection protocol and then present the results of a three-person pilot study.

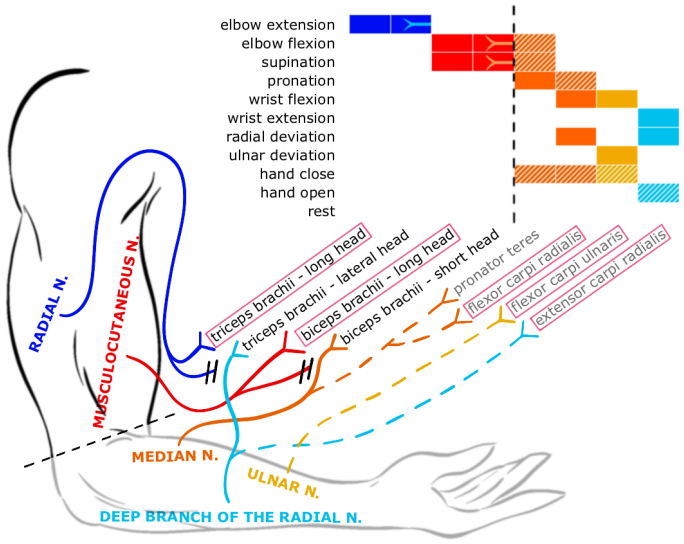

Figure 1: The five nerves responsible for providing motor innervation to muscles of the residual limb after transhumeral TMR. Note: N. denotes *nerve*; this figure is best viewed in colour.

Bio-inspired Sensor Placement

Since we were interested in creating a data collection protocol that can be used on both prosthesis users and persons without limb difference, we took inspiration from our own underlying anatomy. While humans show some variation in the location of individual nerves, we all share the same basic innervation patterns, originating from the development of the limb buds, with each terminal nerve always innervating the same muscles [10]. The intermuscular septum divides the limb bud into anterior and posterior compartments, with flexor muscles developing in the former and extensor muscles in the latter [11]. The brachial plexus provides innervation to the upper limb and follows the same division, with trunks separating into anterior and posterior divisions before ending as five terminal branches. The axillary and radial nerves supply the posterior compartment while the musculocutaneous, median, and ulnar nerves supply the anterior compartment. For our protocol, we positioned sensors on specific muscles based on their nerve supply. In other words, muscles are viewed as a conduit for collecting motor signals from the brain, which we can then use as input features for training ML models. It is because of this novel perspective that we will be able to collect data from both users and persons without limb differences.

Figure 1 shows the five nerves responsible for providing motor signals to muscles in the residual limb after TMR surgery. The radial nerve natively innervates the long and lateral heads of the triceps brachii (marked by the dark blue lines in Figure 1); for users, the lateral head is denervated from the radial nerve (demarked by black slanted lines through the dark blue line) with the deep branch of the radial nerve re-routed to provide supply to the muscle belly (solid light blue line). Since the deep branch of the radial nerve natively supplies most of the posterior compartment of the forearm, for a person without limb differences, we can choose any muscle from this compartment to position the relevant sensor. We chose the extensor carpi radialis longus and brevis (dashed light blue line) due to its proximity to the surface and because it contributes to both wrist flexion and radial deviation. We follow the same reasoning for the remaining four nerves. The musculocutaneous nerve natively innervates the long and short heads of the biceps brachii (solid red line); for users, the median nerve is re-routed to the short head of the biceps brachii (solid orange line), which in turn natively supplies the pronator teres and flexor carpi radialis (dashed orange lines). The ulnar nerve provides native innervation to the flexor carpi ulnaris muscle (dashed yellow line) and gets mapped to the brachialis muscle for users, if their residual limb is long enough. Note that there is a line missing from Figure 1 that would be solid yellow leading from the ulnar nerve to the brachialis muscle; for persons without limb difference, we are unable to place a sensor on the brachialis muscle because it lies deep to the biceps brachii. However, this does not have a negative effect on the data: during model training, we would compose the input feature vector from the signals matching up to the five nerves. For persons without limb difference, these channels are marked with pink boxes in Figures 1 and 2; for users we simply replace the flexor carpi radialis, flexor carpi ulnaris, and extensor carpi radialis features with signals from the short head of the biceps brachii, brachialis, and lateral head of the triceps brachii, respectively. For each column in Figure 1, a solid-colored square marks that the muscle is a prime mover for the corresponding action along the y-axis. A hatched square denotes that the muscle is either a synergist or there is anticipated noise due to its proximity to the prime mover for the given action.

Data Collection Protocol

Three participants without limb difference, two males (26 years old, 193 cm, 104 kg, right-handed; 33 years old, 178 cm, 100 kg, left-handed) and one female (40 years old, 170 cm, 70 kg, right-handed), provided informed consent and were recruited for this pilot study (P1, P3, and P2 in Figure 2, respectively). We used the Delsys Trigno Wireless Biofeedback System with the Trigno Avanti sensors (Delsys) set to broadcast EMG signals at 1926 Hz and accelerometer data at 74 Hz. Eight sensors were placed on each arm in the middle of the muscle belly for each muscle in Figure 1 (x-axis); the solid-coloured actions in each column can be used to help find the correct muscle belly. The participants' dominant arm was then braced with the elbow bent at approximately 70°, forearm at mid-pronation, and wrist straight. This bracing position was chosen to lock the arm approximately in the middle of each joint's range of motion. This was to elicit isometric contractions to capture a higher amplitude from the signal for a longer duration, which we expect to be more similar to the type of muscle contractions a person with limb difference has. On the unbraced side, isotonic contractions are elicited as the participants moved actively through the range of motion, producing concentric contractions in the prime mover and synergist muscles.

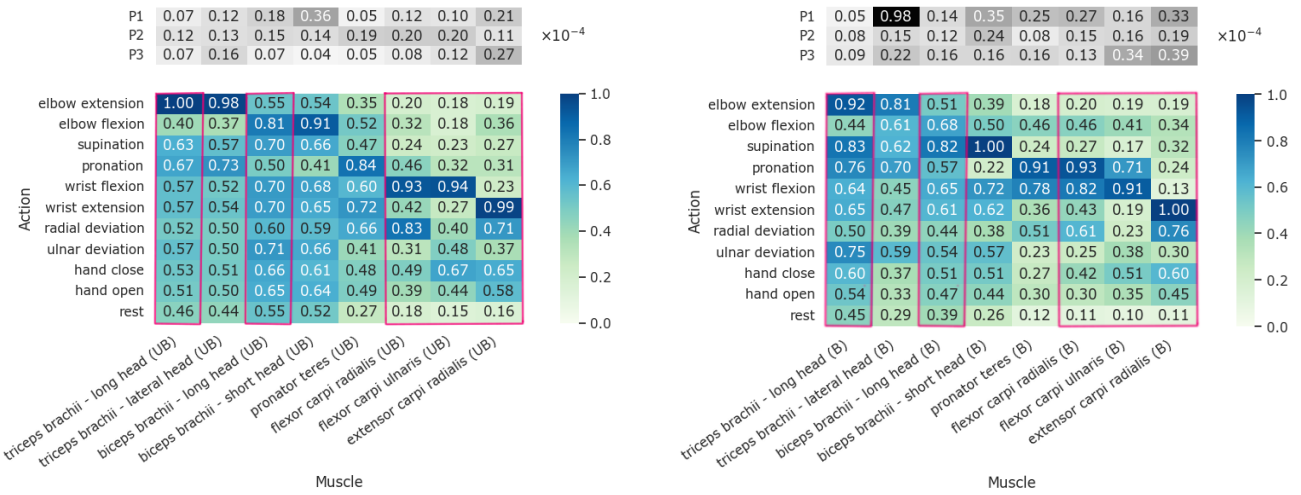

(a) Unbraced arm (isotonic contractions)

(b) Braced arm (isometric contractions)

Figure 2: Consolidated muscle activation heatmap showing the results of our pilot study. In each column, activation is ranked with the highest number (normalized mV) denoting a given muscle as the prime mover for the corresponding action and lower numbers denoting lesser/minimal involvement in the action.

An interactive video played on a monitor in front of the participant to visually guide them through the data collection process. Participants follow a series of 11 actions (Figure 2, y-axis) in 13 limb positions to curate a dataset that covers the functional workspace of the human arm, including positions above the shoulder and behind the back. Three cross-body positions were also included but were found to be awkward to perform and their removal had minimal effect on the results. Once the participant was ready, a random limb position was presented on the monitor, and they were guided through a pre-ordered set of actions in that position. Each action was held for five seconds. Each participant carried out one training session guiding them through all 11 actions in one limb position before starting the full data collection process. After each limb position the participant was allowed to rest before continuing to the next limb position or redoing the last. To prepare the raw data for analysis, a bandpass filter from 20–450 Hz and a notch filter at 60 Hz was applied. The mean absolute value feature was then extracted using a sliding window of size 50 in increments of 10 samples. The participant data was aggregated into unbraced and braced groups to compare the difference bracing (i.e., isotonic vs. isometric) has on the muscle signals, and to account for differences in handedness. For clear visualization in Figure 2, each action-sensor pair were normalized by the greatest mean activation signal (mV) obtained for that sensor across all actions and limb positions.

RESULTS

The heatmaps shown in Figure 2 highlight the potential of our new data collection protocol to provide meaningful signals for each action across all limb positions. Figures 2a and 2b show the data from all three participants consolidated and normalized by sensor for the unbraced and braced arms, respectively. Each column provides a ranked order of activation strengths for the muscle, with the highest number reflecting the highest contractile strength for that action relative to all the other actions. The grey mini-maps contain the highest mean activation signal obtained for each sensor. Despite its normal overall activation pattern, the lateral head of the triceps brachii muscle value for P1 was an order of magnitude higher than all other mean activation signals. Further investigation suggests this may have been due to the participant activating this muscle to counteract the weight of the brace during elbow flexion in limb positions above the shoulder line. We focus our analysis on the five muscles marked with pink boxes in Figures 1 and 2 as these are the signals we would use for training a TMR prosthesis control model. In a ML model, the input would be the vector of EMG signals (e.g., the five signals from one row of the heatmap) and the output would be the action label (i.e., one of the y-axis labels).

Comparing Figure 2 with the anatomical expectations in Figure 1, a similar activation pattern emerges. Note that, as expected, the unbraced arm more closely matches the expected pattern as these predictions are based off anatomical muscle tables [12]. For the unbraced arm (Figure 2a), results reflect that the triceps brachii is the prime mover for elbow extension, the biceps brachii for elbow flexion, the flexor carpi radialis and flexor carpi ulnaris for wrist flexion, and the extensor carpi radialis for wrist extension. Interestingly, when compared with the isometric contractions elicited in the braced arm (Figure 2b) we see less distinct signals for each action as muscles close to the prime mover are also activated during the sustained contraction. This is shown in similar activation patterns of the pronator teres, flexor carpi radialis, and flexor carpi ulnaris during both pronation and wrist flexion. The biceps brachii also exhibits higher activation during supination than elbow flexion when braced, compared to unbraced. Both the unbraced and braced results reflect the effect of limb

position on muscle contractions, as seen in the high activation signals for all forearm, wrist, and hand actions for the triceps and biceps brachii muscles. In fact, further investigation across individual limb positions show that EMG signals from the triceps and biceps brachii muscles begin to activate at a higher level across all actions as the participants raised their arms.

DISCUSSION AND CONCLUSION

Targeted muscle reinnervation (TMR) is a promising avenue for opening new and intuitive methods for myoelectric control. This work offers three key contributions to the field of advanced prosthetic control. Firstly, we introduce a bio-inspired protocol for collecting data in thirteen different limb positions targeted at training ML models for persons with transhumeral amputation that have undergone TMR surgery. We present results from a three-person pilot study using our proposed data collection protocol, highlighting its potential utility. Data from this limited sample mirrors what would be expected from anatomical predictions of which muscles should be active during each given action; this is most noticeable in the unbraced arm and provides validation for our choice of sensor placement. By analyzing muscle activation patterns for different upper limb actions, we can anticipate which actions ML models should be able to accurately predict for users. These actions are elbow flexion and extension, forearm supination and pronation, wrist flexion and extension, and radial and ulnar deviation. A model would have trouble predicting hand open and close accurately if included in this set of labels. Secondly, this study also touches on the limb position effect (c.f., Williams et al. [8]), which is reflected in the data and enables us to further analyze the effect of limb position on muscle contractions. Future work will include a more detailed analysis of this effect across all thirteen limb positions. Thirdly, our protocol captures the differences between isotonic (unbraced) and isometric (braced) muscle contractions, which will be of particular interest when comparing with data from users in future investigations. Looking ahead, we plan to streamline training processes by exploring ML-based transfer learning techniques as well as identifying the minimal number of limb positions and sensors needed during data collection to capture the full set of arm actions. In conclusion, this work presents a novel data collection protocol for TMR prosthesis control that uniquely reveals the interplay between limb position and muscle activation, while capturing the differences between isotonic and isometric contractions. This research sets the stage for training limb-position-aware prosthetic control models, offering the flexibility to use data from persons without amputations or a TMR user's non-amputated limb. Our approach has the potential to help streamline the development of a new generation of TMR-ready control solutions designed to improve the lives of persons with transhumeral amputations.

ACKNOWLEDGEMENTS

This work was supported by Amii, NSERC, Alberta Innovates, the Canada CIFAR AI Chairs Program, and the department of defense, Peer Reviewed Orthopaedic Research Program (PRORP) under Award no. HT9425-23-1-0398. This study was approved by the University of Alberta Research Ethics Board (Pro00077893). We thank Dylan Brenneis, Michael R. Dawson, Justin Francis, and Johannes Günther for their support and feedback. Special thanks to Shaylee Lorrain for graphical design assistance.

REFERENCES

[1] J. E. Cheesborough, L. H. Smith, T. A. Kuiken, and G. A. Dumanian, "Targeted muscle reinnervation and advanced prosthetic arms," *Seminars in Plastic Surgery*, vol. 29, no. 01, pp. 062–072, 2015.

[2] E. Scheme and K. Englehart, "Electromyogram pattern recognition for control of powered upper-limb prostheses: state of the art and challenges for clinical use," *Journal of Rehabilitation Research & Development*, vol. 48, no. 6, 2011.

[3] F. Cordella, et al., "Literature review on needs of upper limb prosthesis users," *Frontiers in Neuroscience*, vol. 10, p. 209, 2016.

[4] T. A. Kuiken, et al., "Targeted muscle reinnervation for real-time myoelectric control of multifunction artificial arms," *Jama*, vol. 301, no. 6, pp. 619–628, 2009.

[5] T. A. Kuiken, G. A. Dumanian, R. D. Lipschutz, L. A. Miller, and K. Stubblefield, "The use of targeted muscle reinnervation for improved myoelectric prosthesis control in a bilateral shoulder disarticulation amputee," *Prosthetics and Orthotics International*, vol. 28, no. 3, pp. 245–253, 2004.

[6] T. A. Kuiken, et al., "Targeted reinnervation for enhanced prosthetic arm function in a woman with a proximal amputation: a case study," *The Lancet*, vol. 369, no. 9559, pp. 371–380, 2007.

[7] L. J. Hargrove, L. A. Miller, K. Turner, and T. A. Kuiken, "Myoelectric pattern recognition outperforms direct control for transhumeral amputees with targeted muscle reinnervation: a randomized clinical trial," *Scientific Reports*, vol. 7, no. 1, p. 13840, 2017.

[8] H. E. Williams, et al., "Composite recurrent convolutional neural networks offer a position-aware prosthesis control alternative while balancing predictive accuracy with training burden," *2022 Int. Conf. on Rehabilitation Robotics (ICORR)*, Rotterdam, Netherlands, pp. 1-6, 2022.

[9] A. W. Shehata, H. E. Williams, J. S. Hebert and P. M. Pilarski, "Machine learning for the control of prosthetic arms: Using electromyographic signals for improved performance," *IEEE Signal Processing Magazine*, vol. 38, no. 4, pp. 46–53, 2021.

[10] H. Shinohara, H. Naora, R. Hashimoto, T. Hatta, and O. Tanaka, "Development of the innervation pattern in the upper limb of staged human embryos," *Acta Anatomica*, vol. 138, no. 3, pp. 265–269, 1990.

[11] H. H. Srebnik, "Innervation of upper limbs," *Concepts in Anatomy*, ch. 20, pp. 135–142, New York, NY: Springer, 1 ed., 2002.

[12] F. H. Netter, "Upper limb muscle tables," *Atlas of Human Anatomy*, ch. 6, pp. 6-1–6-4, Philadelphia, PA: Saunders/Elsevier, 6 ed., 2014.

A VIRTUAL REALITY TRAINING ENVIRONMENT FOR MYOELECTRIC PROSTHESIS GRASP CONTROL WITH SENSORY FEEDBACK

Mitchell A. Dumba[1], Michael R. Dawson[2,3], Glyn Murgatroyd[4], Patrick M. Pilarski[2,3], Jacqueline S. Hebert[1,2,4], Ahmed W. Shehata[1]

[1]Department of Biomedical Engineering, University of Alberta, Edmonton, Alberta, Canada; [2]Department of Medicine, University of Alberta, Edmonton, Alberta, Canada; [3] Alberta Machine Intelligence Institute, Edmonton, Alberta, Canada; [4]Glenrose Rehabilitation Hospital, Alberta Health Services, Edmonton, Alberta, Canada

ABSTRACT

Upper limb myoelectric prosthesis control is difficult to learn. Virtual reality has seen increased deployment in recent years for prosthesis training because it is repeatable, engaging, and can be implemented in the home. While most virtual reality prosthesis simulators do not challenge grasp function, this paper presents the Virtual Prosthesis Emulator (ViPEr), a virtual reality environment for prosthesis grasp control with sensory feedback. For sensory feedback in ViPEr, we have derived data-driven transfer functions that best approximate the applied force from a physical prosthesis and integrated them into a sensory feedback system. This system allows us to relay the interaction force using mechanotactile tactors and recreate realistic interactions, including objects' specific lift, crush, and deformation characteristics. We will use ViPEr in an upcoming study to evaluate the skill transfer to physical prosthesis performance and the effect of providing sensory feedback in virtual reality training.

INTRODUCTION

Myoelectric control for prostheses is complex and often proves challenging due to its learning curve [1]. The difficulty is compounded because prosthesis fitting can take several months following an amputation. This prolonged period of disuse of the residual limb can lead to muscle atrophy and intact arm compensation [2], further complicating the learning process of operating the prosthesis once fit. As a result, individuals can experience dissatisfaction with their prostheses and abandon them [3]. Current training methods typically involve pre-fitting muscle contraction visualizations, training with physical hardware at the clinic [4], and intensive post-fitting daily training sessions [2], which can be logistically demanding.

In response to these challenges, researchers have begun to explore the potential of Virtual Reality (VR) environments as a tool for prosthesis training [5-7]. Their purpose is to supplement the current training methods in conjunction with occupational therapists to mitigate travel and scheduling barriers [5]. Virtual environments are complex, immersive, three-dimensional prosthesis simulators. VR training platforms can offer several benefits over current training methods. They allow users to experiment with the prosthesis without fear of causing damage — are engaging, and efficient, making them ideal for use in TeleHealth, i.e. remote community health centers and at-home rehabilitation settings [5,7,8]. VR training has also been shown to be beneficial for managing Phantom Limb Pain [9]. However, it is important to note that while these platforms offer many advantages, most currently have “snap-on” object grasping [5-7] and do not challenge prosthesis grasp control. For this, we have developed the Virtual Prosthesis Emulator (ViPEr) that focuses on grasp control and incorporates sensory feedback. Sensory feedback can enhance the performance of novice users of myoelectric prostheses, as it allows them to make minor adjustments in real-time [10]. However, sensory feedback may become less useful as users gain proficiency in controlling their prostheses since they can create more precise control [10]. Therefore, sensory feedback may be most effective during the training phase, when users are inexperienced. This paper presents an overview of ViPEr and the methods for the implementation of real-time touch and force feedback for virtual object interactions.

METHODS

Virtual Prosthesis Emulator (ViPEr). ViPEr is a virtual reality training platform for prosthesis control with up to 3 degrees of freedom (hand, wrist rotation, elbow). Developed in the Unity Game Engine Version 2019.3.2f1, based on feedback from clinicians, persons with transradial, and persons with transhumeral amputation, ViPEr is an intermediary training platform for use prior to prosthetic fitting (**Figure 1a**). Its current configuration utilizes

commercially available computer equipment and myoelectric sensors, including a desktop computer, a Vive VR headset, a Vive Tracker (HTC, Taiwan), a Myo armband (Thalmic Labs, discontinued, Canada), and a mechanotactile feedback system [11]. In ViPEr, the virtual prosthetic hand is the PowerHand [11], a one-degree-of-freedom, sensorized, 3D-printed hand that operates by opening and closing at a velocity proportional to the strength of the input signals (**Figure 1b**). Muscle signals acquired by the Myo Armband are linearly mapped to the opening and closing velocity of the PowerHand via the brachI/Oplexus software [12]. This emulator offers a training environment where participants progress through successively more challenging and gamified training tasks. These tasks are goal-oriented to maximize user engagement [7]. The platform also incorporates mechanotactile sensory feedback to enhance the training experience. As the training scene represent rooms of a house, ViPEr is a versatile prosthesis training tool for activities of daily living.

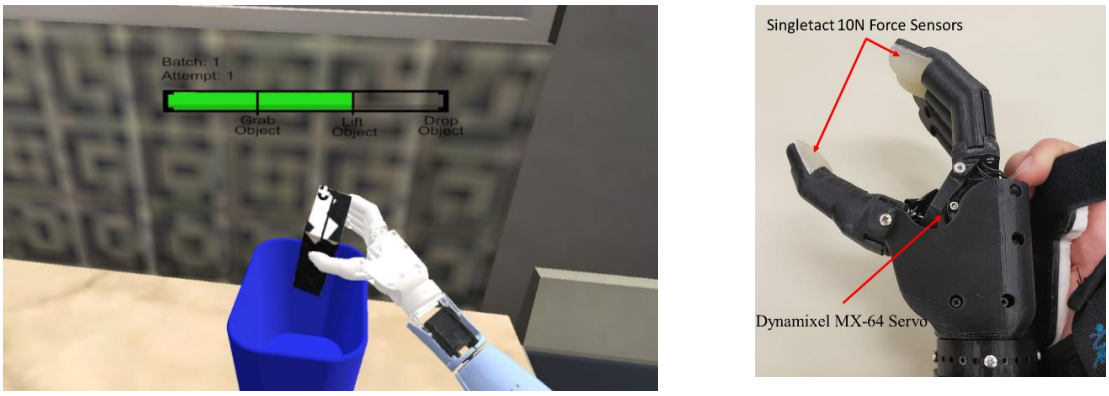

a) **b)**

Figure 1: a) User's point of view in ViPEr moving a milk carton into the stew recycling bin, **b)** PowerHand 1 DoF prosthesis with fingertip sensors and servo locations.

Force Approximation. We created custom interaction physics for the PowerHand in ViPEr to simulate object interactions and deliver grasp control training. While we used Unity's physics engine in ViPEr, it was not sufficient in an unmodified form for our intended grasp force deployment setting. We recorded hundreds of physical object interactions using fingertip force sensors, embedded in the PowerHand, to identify transfer functions from myoelectric inputs and contact duration to prosthesis force. Four objects were recorded interacting with the PowerHand, which had identical dimensions and were categorized by their deformations under a 1 kg mass into soft, medium, hard, and rigid compliances (**Figure 2a**). To limit mechanical variation and ensure consistent grasping, we fixed the position of the PowerHand and objects. Given the unsteady nature of myoelectric signals, we gave steady input signals across the myoelectric range for repeatability. These recorded inputs are ratios from 0 to 1 in increments of 0.05, corresponding to the percentage of maximum voluntary contraction (%MVC). Once recorded, we removed some of the electromechanical dead zones created by the silicone fingertips, delay in data acquisition, fingertip sensors, and object compliance. Dead zone removal was implemented to create responsive force profiles to relay real-time touch feedback. We then averaged, calibrated for aperture, filtered by batch of input %MVC, and combined the raw data into a training set. We used a polynomial regression to derive smooth transfer functions that best approximated the force profiles of the PowerHand, with the extracted feature being the sum of the %MVC at 64 Hz after object contact (Eq. 1-4). The instant the user attempts to grasp an object in ViPEr, we sum the provided %MVC inputs from their muscle signals (**Figure 2b**).

$$\text{Rigid: } f(x) = \frac{12.56}{1+e^{(-0.666\sum|\text{contact}|(\%MVC)+3.181)}} - 0.50 \quad (1)$$

$$\text{Hard: } f(x) = \frac{26.25}{1+e^{(-0.391\sum|\text{contact}|(\%MVC)+0.022)}} - 13.0 \quad (2)$$

$$\text{Med: } f(x) = \frac{26.70}{1+e^{(-0.277\sum|\text{contact}|(\%MVC)+0.031)}} - 13.20 \quad (3)$$

$$\text{Soft: } f(x) = \frac{25.75}{1+e^{(-0.212\sum|\text{contact}|(\%MVC)+0.090)}} - 12.30 \quad (4)$$

The rigid profile was unexpected and didn't follow the stiffness trend, which we attribute to the dampening effect of the compliant object on the onset of applied force. We intentionally aimed to simulate this behaviour. These TFs are implemented in ViPEr to simulate grasp forces and provide sensory feedback.

Feedback Implementation. The mechanotactile feedback system in ViPEr is designed to enhance the immersive experience by providing feedback on object interactions, typically limited in VR. The emulator utilizes a

mechanotactile tactor connected to Unity via a UDP connection. The tactor relays the virtual force values, based on the TFs, proportionally extending or retracting the tactor head. The design of the mechanotactile tactors is a rack and pinion mechanism detailed in [11].

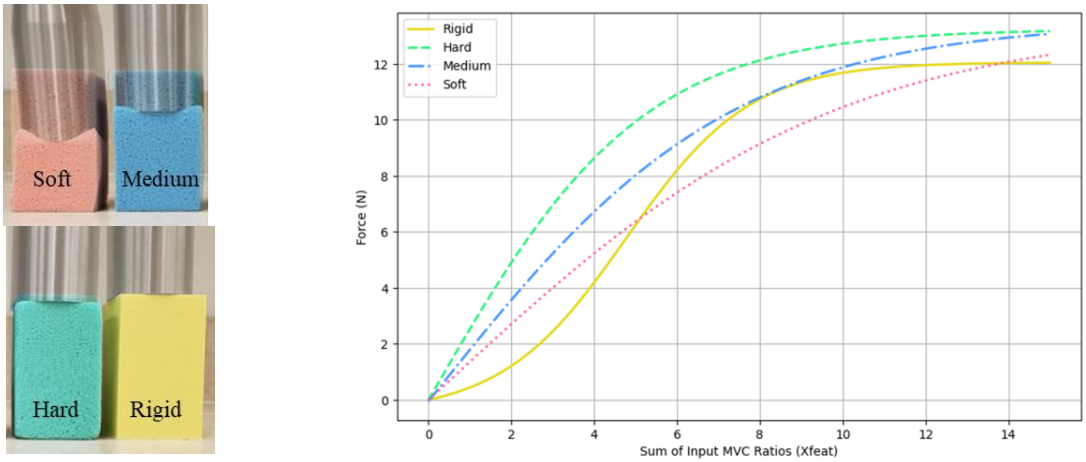

a) **b)**

Figure 2: a) (Left to right, top to bottom) Soft, medium, hard, and rigid objects and their deformation under a 1 kg compressive load, **b)** TFs for applied force from the sum %MVC ratios after contact by compliance.

Tasks. Participants with upper limb amputation and clinicians informed task development and constraint identification for ViPEr. ViPEr's levels span a virtual house, including kitchen, living room, and bedroom scenes. To progress through the levels, users must achieve a prespecified success rate on the current level before advancing to the next. The progressive difficulty and success rate only allow users with higher prosthesis grasp control to attempt advanced levels. All tasks in ViPEr are object relocation tasks. In the kitchen, there are two tasks: the recycling task — where the user moves empty common household cartons into a recycling bin - and the stew-making task (**Figure 1a**) — where users move six food objects into a pot. In the living room scene, users move books and small objects around and on a bookshelf. Finally, in the bedroom scene, users put away clothes and other small objects into designated drawers in a dresser. There are four ways to increase the difficulty level. First, we start varying the mass of the objects, affecting how much virtual force the user must put on the object before it can be picked up. Next, we add object fragility by setting the maximum allowable applied virtual force. Interactions with these objects require precise grasp force modulation; too little force causes the object to slip out of the virtual hand, while too much force crushes the object. **Figure 3a)** shows the lift and crush thresholds of the objects in the stew-making task. Third, we add object compliance. The objects in this difficulty level deform along the imaginary line between the fingers and thumb of the virtual prosthesis, as shown in **Figure 3b)**, to the same degree as the soft, medium, and hard objects used to develop the TFs in **Figure 2a)**. Finally, we increase the number of controllable DoFs.

DISCUSSION

A main contribution of the present work and the pilot study with two able-bodied participants is initial evidence that ViPEr should be explored as a training platform by evaluating the skill transfer to wearable prosthesis performance, which is crucial for future clinical translation. Our study design involves recording participants' baseline physical prosthesis performance, followed by three one-hour training sessions in ViPEr, and then repeating the physical prosthesis evaluation to assess skill transfer. We hypothesize participants will improve their myoelectric grasp control after the training. We also examine the effect of training with sensory feedback on the evolution of skill level throughout the training sessions by randomly assigning participants to either a feedback or no-feedback group in ViPEr. We periodically probe the feedback groups' understanding of the grasp force control throughout their training with no-feedback trials. We expect to gain insight into the learning curve of both groups and the role of sensory feedback in training. Finally, we are comparing the post-training performance of the groups with the no-feedback physical prosthesis to evaluate the effect of using sensory feedback as a training tool. We hypothesize that sensory feedback in ViPEr will improve training efficacy and skill transfer. Written informed consent was obtained

from participants prior to conducting the pilot study as approved by the University of Alberta's Research Ethics Board (PRO0007893).

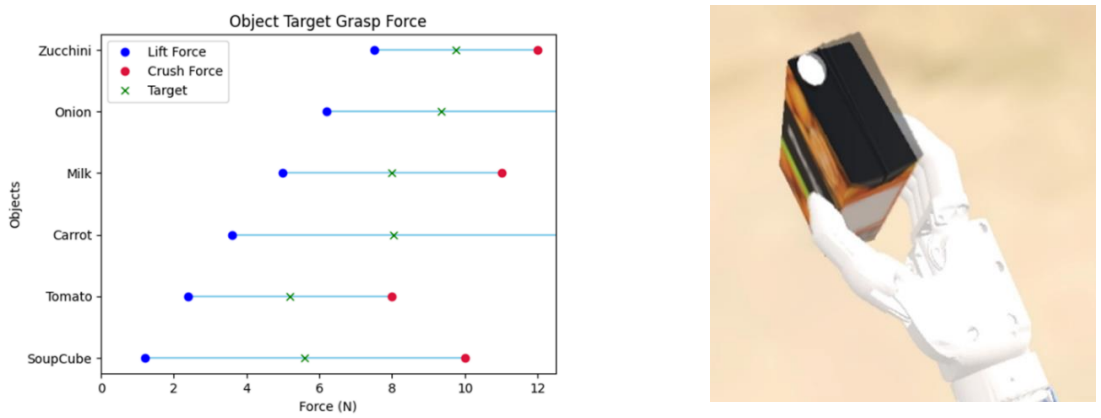

a) **b)**

Figure 3: a) Grasp force ranges for the food items used in the stew making task, with blue, green, and red markers representing the required lift, target, and crush forces respectively, **b)** Deformed juice carton when grabbed in the recycling task with a semi-transparent overlay of the undeformed shape, equivalent to the medium object.

ACKNOWLEDGEMENTS

M. A. D. received support from the NSERC SMART CREATE Program at the University of Alberta. We would like to acknowledge Quinn Boser, Riley Dawson, Cyrus Diego, Taylor Bulbuc, Eric Beaudry, Alexander Nichols, and Zahra Hamilton for their contributions to the development of ViPEr.

REFERENCES

[1] H. Bouwsema, C. K. van der Sluis, & R. M. Bongers, "Changes in performance over time while learning to use a myoelectric prosthesis," *Journal of NeuroEngineering and Rehabilitation*, vol. 11, pp. 1-16, 2014. doi:10.1186/1743-0003-11-16F.

[2] L. N. Hermansson & K. Turner, "Occupational therapy for prosthetic rehabilitation in adults with acquired upper-limb loss: Body-powered and Myoelectric Control Systems," *JPO Journal of Prosthetics and Orthotics*, vol. 29, no. 4S, Oct. 2017. doi:10.1097/jpo.0000000000000154

[3] E. A. Biddiss & T. T. Chau, "Upper limb prosthesis use and abandonment," *Prosthetics & Orthotics International*, vol. 31, no. 3, pp. 236–257, Sep. 2007. doi:10.1080/03093640600994581

[4] M. R. Dawson, J. P. Carey, F. Fahimi, "Review of Myoelectric Training Systems," *Expert Reviews of Medical Devices*, vol.8, no.5, pp. 581-589, 2011. doi:10.1586/erd.11.23

[5] W. Li, P. Shi, S. Li, & H. Yu, "Current status and clinical perspectives of extended reality for myoelectric prostheses: review," *Frontiers in Bioengineering and Biotechnology*, vol 11, 2024. doi:0.3389/fbioe.2023.1334771

[6] L. van Dijk, C. K. van der Sluis, H. W. van Dijk, & R. M. Bongers, "Task-oriented gaming for transfer to prosthesis use," *IEEE Transactions on Neural Systems and Rehabilitation Engineering*, vol. 24, no. 12, pp. 1384-1394, 2016. doi:10.1109/tnsre.2015.2502424

[7] Y. Sun et al. "A comparison between virtual reality and augmented reality on upper-limb prosthesis control," *2021 International Symposium on Electrical, Electronics and Information Engineering*, Feb. 2021. doi:10.1145/3459104.3459189

[8] L. Resnik, K. Etter, S. L. Klinger, and C. Kambe, "Using virtual reality environment to facilitate training with advanced upper-limb prosthesis," *The Journal of Rehabilitation Research and Development*, vol. 48, no. 6, p. 707, 2011. doi:10.1682/jrrd.2010.07.0127

[9] T. Rutledge et al. "A virtual reality intervention for the treatment of phantom limb pain: development and feasibility results," *Pain Medicine*, vol. 20, no. 10, pp. 2051-2059, 2019. doi:10.1093/pm/pnz121

[10] J. Sensinger & S. Dosen, "A review of sensory feedback in upper-limb prostheses from the perspective of human motor control," *Frontiers in Neuroscience*, vol. 14, 2020. doi: 10.3389/fnins.2020.00345

[11] E. Wells et al. "Development of a modular simulated prosthesis and evaluation of a compliant grip force sensor," *MEC symposium*, Jul. 2020. https://conferences.lib.unb.ca/index.php/mec/article/view/74

[12] M. Dawson, H. Williams, G. Murgatroyd, J. Hebert, & P. Pilarski, "BrachIOplexus: myoelectric training software for clinical and research applications," MEC symposium, Jul. 2020. https://conferences.lib.unb.ca/index.php/mec/article/view/40

COMPARATIVE KINEMATIC ANALYSIS OF TWO KINESTHETIC INTERFACES FROM DISTINCT RECORDING METHODOLOGIES

Charles H. Moore[1,2], B. Ulgen Kilic[1,2], Federico Masiero[3,4], Marta Gherardini[3,4], Christian Cipriani[3,4], and Paul Marasco[1,2]

[1]*Department of Biomedical Engineering, Lerner Research Institue, Cleveland Clinic, Cleveland OH*

[2]*Charles Shor Epilepsy Center, Cleveland Clinic, Cleveland OH*

[3]*The Biorobotics Institute Scuola Superiore Sant'Anna, 56127, Pisa, Italy*

[4]*Department of Excellence in Robotics and AI, Scuola Superiore Sant'Anna, 56127, Pisa, Italy.*

ABSTRACT

This study compares kinesthetic percepts from two different kinesthetic prosthetic interfaces and features a new method to obtain kinematic grasp data from standard video footage. Video data recorded from a participant with an intramuscular myokinetic kinesthetic interface was processed and compared to kinematic data from two participants with targeted reinnervation for kinesthesia (TRk) interfaces. Correlations of rate of change in digit joint angles of hand close percepts were obtained, revealing kinematic similarities between the two interface types. The myokinetic kinesthetic interface participant's first day elicited hand close grip percept and a TRk interface participant's first day elicited hand close grip percept were found to be similar with respect to the rates of joint angle movement. Similarities disappeared between the two interfaces after the TRk interface participant underwent a week of training with the percept. This relationship between the two interfaces provides evidence that elicited kinesthetic grip percepts share similar features when the participant is first introduced to the intervention.

Introduction

The exploration of sensory feedback through regenerative and implanted neural interfaces has progressed significantly in recent decades [1]. In particular, kinesthesia—defined as the sensation of active movement—has been induced with considerable success in individuals with upper limb TRk interfaces [2,3,4,5]. Targeted reinnervation interfaces are created with surgical nerve redirection techniques that rewire nerves to new skin and muscle sites, enabling a biological neural-machine interface for prosthetic control and feedback. Vibrating muscle tissue in TRk interfaces at 90 Hz induces synergistic kinesthetic percepts that have been shown to enable near able-bodied performance during grasping tasks [3].

Direct comparisons of different regenerative and implanted neural interfaces can be difficult, particularly when different research entities have collected data through distinct tools and data types. This is also the case when attempting to quantify the similarities and differences between the complex synergistic grip percepts generated across emerging kinesthetic interfaces. Here, we provide a methodology for quantitatively comparing reported synergistic kinesthetic grip percepts between different kinesthetic feedback interfaces for upper limb prosthetics.

Methods

Written informed consent from the participant was obtained under the guidelines and approval of the Ethical Committee of Azienda Ospedaliero Universitaria Pisana (ClinicalTrials.gov Identifier: NCT06176482). We modified and repurposed Google's publicly available machine learning model (available at https://developers.google.com/mediapipe) to extract hand kinematic data from video recording of a participant using their sound hand to express perceived kinesthetic sensations during residual intramuscular stimulation. We leveraged this machine learning model to detect and draw hand landmarks on each frame of a video input. The hand landmarks detected on each frame are stored and output as three-dimensional world coordinates.

We then transformed the relative positions of the landmark coordinates to calculate digit kinematic joint angles. The angles between the joints in the hand are calculated using a function that operates on the geometric principle that the dot product of two vectors is equal to the product of their magnitudes and the cosine of the angle between them.

This function takes the indices of three landmark points as input: a base point that serves as the vertex of the angle, and two additional points that, along with the base point, define the angle in question. The coordinates of these points are extracted from the list of detected hand landmarks. Vectors are then constructed from the base point to each of the other two points by subtracting their coordinates. The angle between these two vectors is calculated by first finding the dot product of the vectors, then dividing this by the product of their norms to find the cosine of the angle, and finally applying the arc cosine function to determine the angle in radians. This calculated angle quantifies the bend between two segments of the hand, allowing for the analysis of hand movement patterns based on the relative positions of hand landmarks.

Next, we segmented the video data, converting the continuous repetition of the participant opening and closing their sound hand into eleven distinct hand close percepts. We identified local minima and maxima across each joint angle, representing the points of highest degree of finger movement within each cycle of hand closure. Minima and maxima were identified by searching for points where the angle's rate of change transitions from positive to negative, indicating a peak, while adhering to predefined criteria such as minimum height and distance between peaks to filter out insignificant fluctuations.

We performed these transformations on the video data to allow a direct comparison to a kinematic dataset from two TRk interface participants recorded using a 22-sensor CyberGlove II data glove (CyberGlove Systems LLC, www.cyberglovesystems.com). Written informed consent was obtained from these two participants under the guidelines and approval of the Institutional Research Ethics Board at Cleveland Clinic (Protocol #13-1349). Each participant was recorded during 30 trials of 90Hz stimulation applied to their TR interface that induced the sensation of hand close. These trials were performed on each participant’s first day of experimentation, as well as their fourth (last) day of experimentation, resulting in 30 trials for each day for each participant. We then interpolated the data glove data to account for the differing framerates between the video and data glove, and normalized each trajectory to a common, unified scale ensuring that the data points for each movement cycle segment were directly comparable. See Figure 1 for averaged and normalized hand close trajectories for both kinematic interface type datasets.

Finally, comparative analysis of digit kinematic joint angles was performed to evaluate the correlation of perceived kinesthetic sensations across participants. We obtained differential data for both datasets, focusing the analysis on changes in the angle measurements over time that reflect the dynamics of the hand movement patterns. See Table 1 for the correlations of rate of change in digit joint angles during hand close percepts across our two kinematic interface datasets.

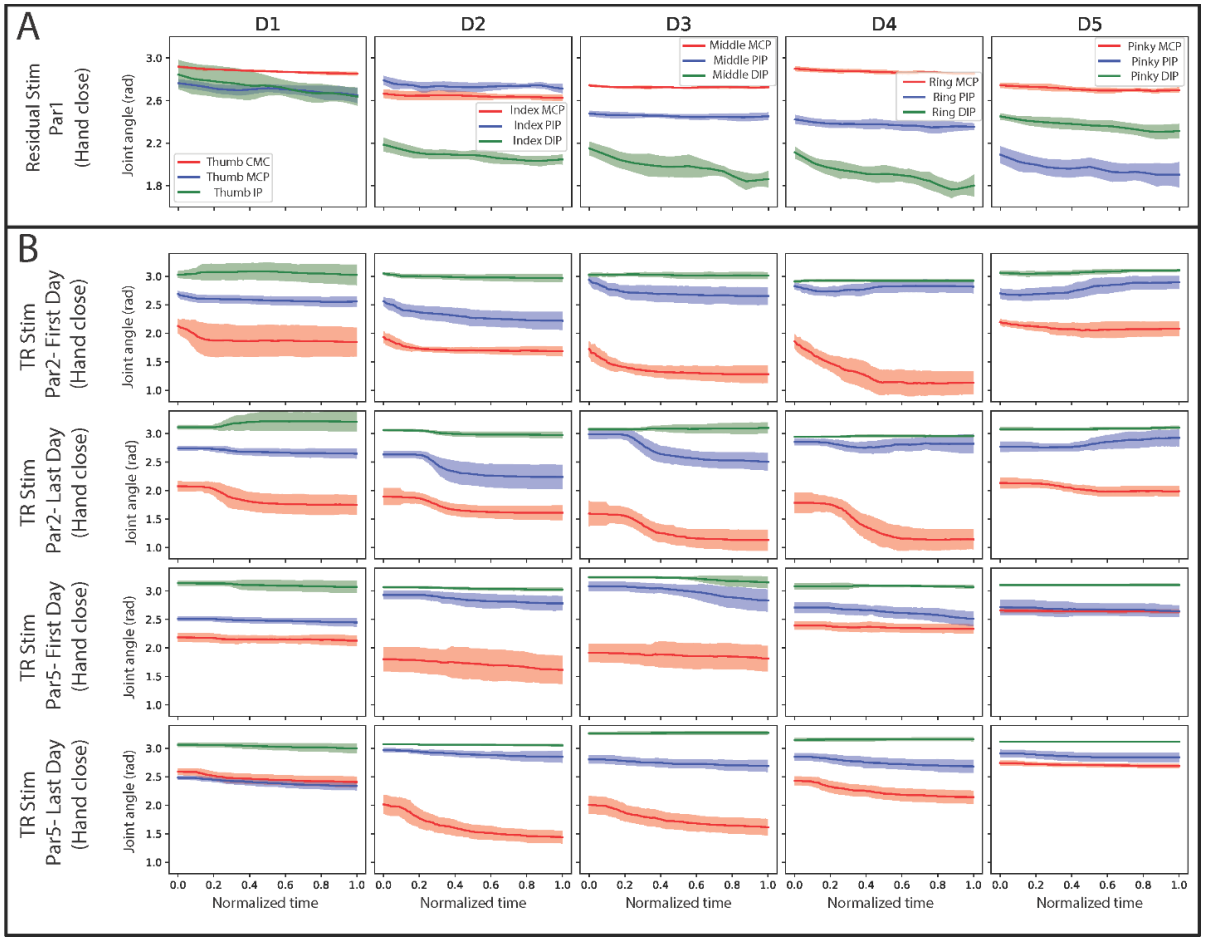

Figure 1: Averaged and normalized digit joint angle trajectories during hand closure recorded from A) Kinematic data extraction of video recording during 90Hz residual intramuscular stimulation and B) data glove recordings of two participants during 90Hz TR interface stimulation on their first and last days of participation.

Results

Initial analysis revealed multiple correlations in many of the finger kinematic joint angles between one of the two TRk amputees (Participant 2) on their first day of experiencing the stimulus and the participant who received residual intramuscular stimulation. However, these correlations turned negative after the TRk participant experienced three days of contextually relevant training, suggesting a significant shift in the perception and integration of kinesthetic feedback when used to complete tasks.

Table 1: Pearson's correlations of rate of change in digit joint angles during hand close percepts in response to vibration-induced kinesthetic sensations between one participant with residual intramuscular stimulation and two participants with TR interface stimulation.

	Participant 2				**Participant 5**			
	Day 1		***Day 4***		***Day 1***		***Day 4***	
Joint Name	**Pearson's r**	**p-value**	**Pearson's r**	**p-value**	**Pearson's r**	**p-value**	**Pearson's r**	**p-value**
Thumb CMC	**0.62**	**<0.001*****	-0.054	0.089	-0.083	0.79	0.055	0.084
Thumb MCP	**0.080**	**0.012***	0.0085	0.786	-0.021	0.52	0.0039	0.91

Thumb IP	**-0.070**	**0.027***	**0.11**	**<0.001*****	-0.051	0.11	**-0.073**	**0.021***
Index MCP	**0.41**	**<0.001*****	**-0.31**	**<0.001*****	0.012	0.71	**-0.085**	**0.007****
Index PIP	**0.29**	**<0.001*****	**-0.24**	**<0.001*****	**-0.13**	**<0.001*****	-0.022	0.48
Index DIP	**0.27**	**<0.001*****	**-0.10**	**0.002****	**-0.086**	**0.007****	0.0027	0.93
Middle MCP	**0.40**	**<0.001*****	-0.046	0.142	0.032	0.31	0.024	0.45
Middle PIP	**0.32**	**<0.001*****	-0.024	0.443	-0.057	0.071	0.0036	0.91
Middle DIP	**-0.10**	**<0.001*****	0.034	0.280	-0.054	0.087	-0.014	0.66
Ring MCP	**0.23**	**<0.001*****	**-0.073**	**0.020***	-0.0014	0.96	0.061	0.052
Ring PIP	**0.36**	**<0.001*****	**-0.087**	**0.006****	**-0.11**	**<0.001*****	-0.036	0.25
Ring DIP	**-0.11**	**<0.001*****	**0.069**	**0.028***	-0.023	0.47	-0.036	0.26
Pinky MCP	**0.20**	**<0.001*****	**0.22**	**<0.001*****	0.061	0.056	0.042	0.18
Pinky PIP	**0.27**	**<0.001*****	**0.071**	**0.025***	0.014	0.66	0.025	0.42
Pinky DIP	**0.089**	**0.005****	**0.10**	**<0.001*****	-0.0031	0.92	-	-

Conclusion

These findings showcase an effective quantitative method for comparing different neural interfaces providing similar sensory stimulation. Despite kinematic datasets comprising different measures and data types, we demonstrated a sound methodology to enable a quantified analysis of their similarities that detected a number of moderate correlations with very high statistical significance.

We found that kinematics were similar across kinesthetic interfaces for one of the two TR interface participants, but only on initial exposure to kinesthetic stimulation. The negative shift in correlations following task-specific training underscores the adaptability of kinesthetic perception and its integration for motor control.

These methodologies can facilitate extraction and re-examination of recorded video data sets containing previously unidentifiable kinematic data.

REFERENCES

[1] S. Bensmaia and L. Miller, “Restoring sensorimotor function through intracortical interfaces: progress and looming challenges” *Nature Reviews Neuroscience*, 2014

[2] P. Marasco et al., “Illusory movement perception improves motor control for prosthetic hands” *Science translational medicine*, 2018

[3] P. Marasco et al., "Neurorobotic fusion of prosthetic touch, kinesthesia, and movement in bionic upper limbs promotes intrinsic brain behaviors" *Science robotics*, 2021

[4] M. Gherardini, et al., "The myokinetic interface: Implanting permanent magnets to restore the sensory-motor control loop in amputees" *Current Opinion in Biomedical Engineering*, 2023

[5] J. Montero et al., "The myokinetic stimulation interface: activation of proprioceptive neural responses with remotely actuated magnets implanted in rodent forelimb muscle" *Journal of Neural Engineering*, 2022

COMPARISON OF DIFFERENTIAL SURFACE EMG CIRCUITS AND INTERELECTRODE SPACING FOR USE WITH REGENERATIVE PERIPHERAL NERVE INTERFACES

Amber Bollinger and Richard F. *ff.* Weir

University of Colorado Denver: Department of Bioengineering

ABSTRACT

Surface electromyography (sEMG) studies how to detect electrical signals produced by muscles from the surface of the skin [1]. However, the noise and crosstalk from nearby muscles are some of the drawbacks to using a surface EMG system [1]. Single and double differential (SD and DD) surface electrode systems were designed to minimize these drawbacks. Still, sEMG systems have not yet been optimized to detect deep and/or small signals from within the body [1]. This is particularly an issue when considering regenerative peripheral nerve interfaces (RPNIs) for controlling a myoelectric prosthesis because EMG signals from RPNIs are usually too small for surface level detection (approximately 100μV – 2mV) [4].

Since interelectrode spacing and pick-up volume have a direct relationship [6] these therefore pose an interesting avenue for designing a surface electrode system that can detect EMG signals from RPNIs. Through a model in Maxwell 3D by Ansys, we aim to explore how varying the interelectrode distance from 8mm-40mm can change the spatial pick-up volume of electrodes, and further examine how the SD and DD circuits process the information to determine the best approach for surface detection of an RPNI. In the future, these results will then be validated through human subject testing.

INTRODUCTION

Surface electromyography (sEMG) studies how to detect electrical signals produced by muscles from the surface of the skin [1]. Passive surface electrodes typically consist of a metal plate and have not changed much in design since 1912 when they were first used by Piper in the detection of EMG signals [1]. Active surface electrodes have been redesigned over the years to increase the input impedance of the electrode to better reduce noise from the body and other power sources (ex. Mains Noise at 60Hz). This improves the quality of the detected signals [1]. One of the biggest disadvantages of surface electrodes is that they can only effectively be used to detect signals from superficial and/or larger muscles [1]. To minimize noise and crosstalk, differential circuits were designed as part of the active electrode. A bipolar or single differential (SD) circuit uses 2 electrodes and a reference electrode. It subtracts, filters, and amplifies the inputs to produce a usable signal for control, as shown in equation 1, where V_a and V_b are the inputs, G is the gain of the system, and V_{out} is the final output.

$$V_{out} = G(V_a - V_b) \quad (1)$$

A double differential (DD) circuit performs similar functions as a single differential circuit, but with 3 electrodes and a reference electrode, giving equation 2, where V_a, V_b, and V_c are the inputs, G is the gain of the system, and V_{out} is the final output. Both SD and DD circuits have been shown to reduce noise compared to a monopolar EMG system, but the DD circuit is better able to reduce noise and crosstalk than the SD system. [2]

$$V_{out} = G(V_a - 2V_b + V_c) \quad (2)$$

The inability to effectively detect signals from smaller and/or deeper muscles is a disadvantage for using sEMG for myoelectric control of a prosthesis as it limits the sites available for control of a device, thereby reducing its potential for control.

Clinical Problem

Regenerative peripheral nerve interface (RPNI) is a surgical technique developed by a multidisciplinary team led by Dr. Paul Cederna and Cindy Chestek at the University of Michigan in 2012. In this surgery, the severed end of a peripheral nerve is implanted into a free muscle graft. This technique can treat symptomatic neuroma formation of the severed nerve [3] while also creating additional sites for myoelectric control of a prosthetic device [4]. Currently these new sites generate EMG signals on a scale of approximately 100μV – 2mV [4]. These signals are too small for normal surface electrode detection so, the signal is collected through needle EMG (nEMG) which requires placing needle electrodes into the respective grafts. This

intramuscular placement allows for increased specificity in the control but lacks real world application as these needles are invasive, must be placed by a specialized professional and cause the user discomfort [5].

While RPNI creates new sites for myoelectric control, the ability to detect the signals using sEMG is extremely difficult due to the size of the signals generated by these muscle grafts. Adjusting the active sEMG electrodes to detect deeper and/or smaller signals will allow the surface electrode systems to be used in conjunction with the RPNIs. This could improve control for prostheses by providing additional control sites for a user to operate the device.

Research Rationale

In practice, surface EMG systems use an interelectrode spacing of 10mm-20mm depending on the system used. With the direct relationship between pick-up volume and interelectrode spacing [6], our research aims to study how changing the interelectrode spacing may allow for detection of EMG signals from deeper within the body or detection of smaller signals without introducing excessive noise or crosstalk that could render the EMG signal useless in a control paradigm.

METHODOLOGY AND PRELIMINARY DATA

Preliminary testing was conducted using a DD circuit designed by Federico N. Guerrero et. al. using 4 operational amplifiers, shown in figure 1 [7]. An instrumentation amplifier was added to the end of the circuit to allow for the collection and processing of the EMG Data. Figure 1 also shows the red boxed area of the circuit that was removed as a modification to create a SD circuit from the proposed DD circuit.

Pilot testing was conducted on 3 individuals under the CU Denver Weir Biomechatronics Development Laboratory covered under COMIRB No. 14-0838. The SD and DD circuits were tested in tandem. The electrode array in figure 2 was affixed to the subject's dominant arm using a tie bandage. The array was placed over the wrist flexor muscles in the forearm. The subjects performed 2 tasks for each interelectrode spacing. The tasks were conducted as follows:

Task 1: Wrist Flexions

1. 10s lead in – Rest
2. [2s Wrist Flexion, 3s Rest] – repeat 10x
3. 10s lead out – Rest

Task 2: Individual Finger Movements

1. 10s lead in – Rest
2. [2s Flexion, 3s Rest] for each of the following movements in this order
    a. Wrist Flexion
    b. Index Finger Flexion
    c. Middle Finger Flexion
    d. Ring Finger Flexion
    e. Pinky Finger Flexion
    f. Index + Middle Finger Flexion
    g. Middle + Ring Finger Flexion
    h. Ring + Pinky Finger Flexion
    i. All 4 Fingers Flexion
    j. Wrist Flexion
3. 10s lead out - Rest

The EMG data was collected, filtered, and analyzed to determine the Signal-to-Noise Ratio (SNR) and the appearance of crosstalk. The data from the three individuals was inconclusive regarding the trends in the SNR due to multiple sources of error. This is thought to be a result of the circuits being tested in tandem and the common-mode rejection ratio (CMRR) affecting each system differently when the systems were tested in tandem. Due to these results, an electrode simulation model is being developed using Maxwell 3D on the Ansys Electronics Desktop Program. After the results of the simulations are processed, the results will be validated through human subject testing.

The model is currently designed as an idealized cylinder to provide a simplified representation of an arm. Later, the model will be updated to better reflect the actual geometry of an arm using real-life scans if an arm. These models are based on two papers by Madeline Lowery et. al. from 2002 and 2004 with all material parameters matching the models described in these references [8, 9]. Figure 3 shows the idealized cylindrical model with the three electrode bars for reading out the EMG signal, two electrode disks to act as excitation electrodes in the model, and a muscle fiber currently located 14.5mm below the surface of the skin. The muscle fiber will have a sinusoidal wave passed through to simulate a muscle signal in the body. Using finite-element analysis, the EMG signals will be analyzed to determine the expected spatial pick-up volume for each scenario and

how this changes with different interelectrode spacing. The muscle fiber depth is also variable to allow for analysis of the depth of the pick-up volume in each scenario.

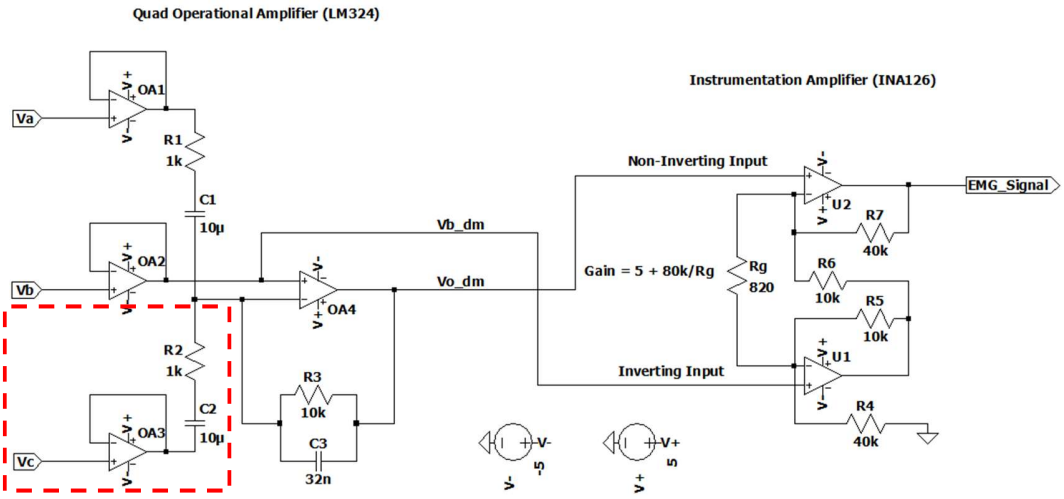

Figure 1: DD Circuit built in LTSpice. The circuit is based on the design provided by Guerrero et. al. in 2016 [7]. The circuit also includes the addition of an instrumentation amplifier at the end to collect the EMG signal and further amplify it before processing. The red dotted line box indicates the section of the circuit that is removed to change the proposed design from a DD circuit to a SD circuit.

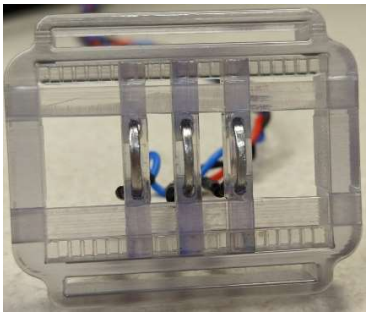

Figure 2: Electrode array designed by Amber Bollinger to adjust electrode spacing by 4mm at a time from 8mm to 40mm. The DD circuit used all three electrode bars. The SD circuit only used the two outer electrode bars, not the center one.

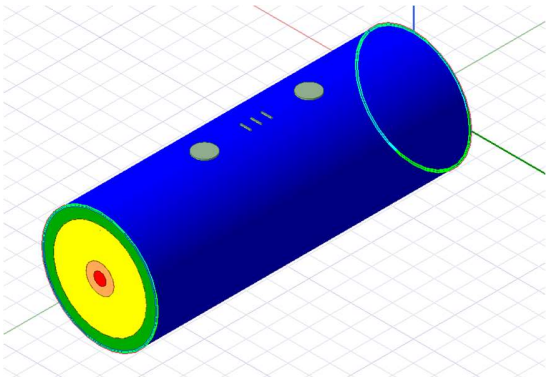

Figure 3: Idealized cylindrical model built in Maxwell 3D of an arm with two disk excitation electrodes and three bar recording electrodes. The model has cancellous and cortical bone, muscle (and a muscle fiber), fat, and skin. All parameters of these materials are described in the two articles by Lowery [8, 9].

CONCLUSION

From the pilot testing, it is clear there are specific benefits to each type of EMG detection circuit. The DD is more focal and so it can detect surface signals more readily; however, it cannot detect signals from muscles deep in the body. The SD circuit is less focal allowing for detection of signals deep in the body; however, too much crosstalk renders the surface EMG data unusable. From the data collected in pilot testing, suggestions to detect deeper or smaller signals from RPNIs could be through a combination of increasing pick-up volume through interelectrode spacing, increasing CMRR in the circuit design, and increasing gain to make the small signals more easily detectable. Further research will be done to elaborate on trends for these testing areas.

ACKNOWLEDGEMENTS

Weir Biomechatronics Development Laboratory

W81XWH-21-1-0771 (Kemp): Regenerative Peripheral Nerve Interfaces (RPNIs) for Surface Myoelectric Control of a Novel Powered Finger Partial Hand Prosthesis

This work was supported in part through funds from the Department of Veterans Affairs, Rehabilitation Research and Development Service, administered through the VA Eastern Colorado Health Care System – Rocky Mountain Regional VAMC

REFERENCES

[1] J. V. Basmajian & C. J. De Luca, “Muscles alive: Their functions revealed by electromyography” 5th ed. Williams & Wilkins, Baltimore, MD, 1985.

[2] J. V. Vugt & J. G. van Dijk, “A convenient method to reduce crosstalk in surface EMG,” *Clinical Neurophysiology*, vol. 112, pp. 583-592. DOI: https://doi.org/10.1016/S1388-2457(01)00482-5, 2001.

[3] R. C. Hooper, P. S. Cederna, D. L. Brown, S. C. Haase, J. F. Waljee, B. M. Egeland, B. P. Kelley, & T. A. Kung, “Regenerative peripheral nerve interfaces for the management of symptomatic hand and digital neuromas,” *Plastic and reconstructive surgery,* vol. 8, issue 6, e2792, DOI: https://doi.org/10.1097/GOX.0000000000002792, 2020.

[4] P. P. Vu, A. K. Vaskov, Z. T. Irwin, P. T. Henning, D. R. Lueders, A. T. Laidlaw, A. J. Davis, C. S. Nu, D. H. Gates, R. B. Gillespie, S. W. P. Kemp, T. A. Kung, C. A. Chestek, & P. S. Cederna, “A regenerative peripheral nerve interface allows real-time control of an artificial hand in upper limb amputees,” *Science Translational Medicine*, vol. 12, issue 533, DOI: https://doi.org/10.1126/scitranslmed.aay2857, 2020.

[4] V. A. Catacora, F. N. Guerrero and E. M. Spinelli, "Three-electrode double-differential biopotential amplifier for surface EMG measurements," *IEEE Transactions on Instrumentation and Measurement*, vol. 72, pp. 1-8, DOI: https://doi.org/10.1109/TIM.2023.3270975, 2023.

[6] T. M. Vieira, A. Botter, S. Muceli, & D. Farina, “Specificity of surface EMG recordings for gastrocnemius during upright standing,” *Scientific Reports*, vol. 7, DOI: https://doi.org/10.1038/s41598-017-13369-1, 2017.

[7] F. N. Guerrero, E. M. Spinelli, & M. A. Haberman, “Analysis and simple circuit design of double differential EMG active electrode,” *IEEE Transactions on Biomedical Circuits and Systems*, vol. 10, issue 3, pp. 787–795, DOI: https://doi.org/10.1109/TBCAS.2015.2492944, 2016.

[8] M. M. Lowery, N. S. Stoykov, A. Taflove, and T. A. Kuiken, “A multiplelayer finite-element model of the surface EMG signal,” *IEEE Transactions on Bio-Medical Engineering*, vol. 49, pp. 446–454, May 2002.

[9] M. M. Lowery, N. S. Stoykov, J.P. Dewald, & T. A. Kuiken, “Volume conduction in an anatomically based surface EMG model,” *IEEE Transactions on Bio-Medical Engineering*, vol. 51, issue 12, pp. 2138–2147, DOI: https://doi.org/10.1109/TBME.2004.836494, 2004.

CREATING PRESSURE AND THERMAL TACTILE SENSATIONS IN THE PHANTOM HAND USING NON-INVASIVE STIMULATION

Luke Osborn, Courtney Moran, Breanne Christie, Meiyong Himmtann, Rama Venkatasubramanian, Matthew Fifer, Robert Armiger

[1]*Research & Exploratory Development Department, Johns Hopkins University Applied Physics Laboratory, Laurel, MD, USA*

ABSTRACT

Invasive peripheral nerve interfaces have demonstrated the value of restored touch perceptions in the missing hand elicited by electrical stimulation after arm amputation. However, invasive interfaces may not be the preferred option for many prosthesis users. We explored the use of non-invasive mechanical stimulation, targeted transcutaneous electrical nerve stimulation (tTENS), and thermal stimulation of naturally occurring reinnervated nerve sites in the residual limb to restore multiple modalities of touch in the phantom hand. In two individuals with arm amputation, we reported tactile sensations of pressure, elicited by mechanical stimulation and tTENS, and cooling, elicited by thermal stimulation, in the phantom hand. Tactile perceptions and stimulation locations remained stable over multiple years. We observed that the activated regions of the phantom hand may by stimulation modality specific, in that tactile sensations did not always overlap when different stimulation modalities were used at the same location on the residual limb. These results may be useful in helping restore a broad range of touch feedback for prosthesis users through non-invasive stimulation approaches.

INTRODUCTION

Restoring the sense of touch to the missing hand after amputation can help improve prosthesis usage and function [1], [2], enhance decoding of electromyography prosthesis control signals [3], increase sensorimotor connectivity [4], and promote prosthesis integration into a user's body image [2], [5]. Invasive peripheral nerve stimulation techniques can directly excite sensory nerve fibers and elicit sensations of touch in the phantom hand [1], [2]. Non-invasive stimulation approaches have also restored touch perceptions in the missing hand after amputation.

Tactile sensations in the missing hand can be induced by mechanical stimulation of reinnervated sites in the skin of the residual limb in individuals both with [6] and without [7] targeted sensory reinnervation (TSR) surgeries. Targeted transcutaneous electrical nerve stimulation (tTENS) has also been used to restore sensations of touch in the phantom hand of individuals with arm amputation [8] and can be modulated to create pressure-related tactile sensations ranging from light touch to pain [9].

An important element of touch feedback for prosthesis users is being able to convey a useful range of tactile sensations. Perceptions from non-invasive mechanical and electrical stimulation are typically reported as being pressure, vibration, or tingling sensations in the phantom hand [3], [7]. Recently, sensations of temperature have also been restored through non-invasive thermal stimulation of reinnervated nerve sites in the skin [10], [11] and these thermal perceptions can be used to enable object identification during closed-loop prosthesis control [10].

In this study, we investigated the use of non-invasive mechanical, electrical, and thermal stimulation to elicit tactile sensations of pressure and temperature in the phantom hand of individuals with arm amputation. We quantified the resulting perception location and quality in addition to stimulation location for all three stimulation modalities.

METHODS

Two individuals with arm amputation participated in this study. Participant A1 had a left transhumeral arm amputation and participant A2 had a right transradial arm amputation. Neither participant had undergone targeted sensory reinnervation surgery (TSR); however, there were sites on the residual limb that, when stimulated, elicited

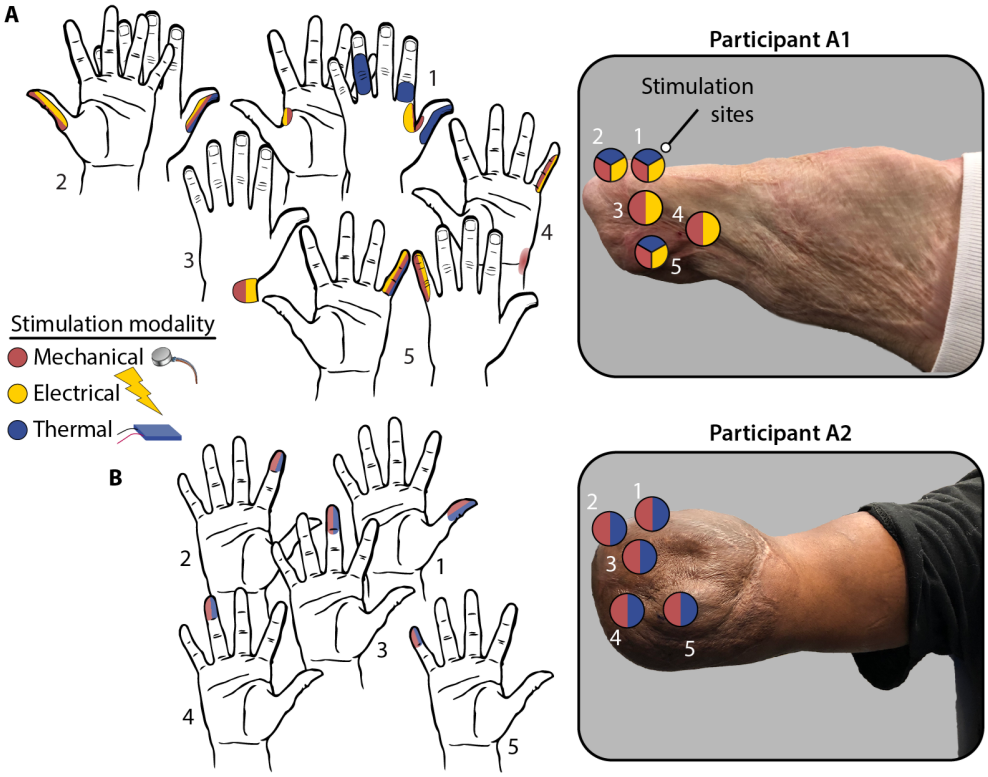

Figure 1: Tactile sensations in the phantom hand as a result of non-invasive skin stimulation. (A) Mechanical, electrical, and thermal stimulation of reinnervated nerve sites of participant A1 elicited sensations of pressure and temperature in the phantom hand. (B) Mechanical and thermal stimulation on the skin in participant A2's residual limb elicited sensations of pressure and temperature. Colors indicate stimulation modality and corresponding tactile perceptions.

sensations in the phantom hand. These sensory sites on the residual limb were identified based on prior sensory mapping studies with the participants [3], [10].

Three different stimulation modalities were used to elicit tactile sensations in the phantom hand. Mechanical stimulation was delivered through a 1 cm rounded plastic probe that was indented into the participant's skin by the experimenter. Electrical stimulation, tTENS, was delivered as a 4 mA biphasic square wave with a 0.5 ms pulse width (200 ms per phase with a 100 ms interphase interval) and a stimulation frequency of 4 Hz (DS8R, Digitimer). Thermal stimulation was delivered using a Bi_2Te_3 thermoelectric cooling (TEC) device with a surface temperature of 16 °C and an 11 mm x 11 mm surface area (Custom Thermoelectric).

Stimulation was applied to the stimulation sites on the residual limb and participants used a hand map to draw the activated regions of their phantom hand. Participants verbally reported the quality of tactile sensations from the stimulation. Participant A1 received stimulation from all three modalities (mechanical, electrical, and thermal) and participant A2 received mechanical and thermal stimulation. Participant A2 performed two follow-up sensory mapping experiments 11 and 23 months after the initial sensory mapping experiment. All experiments were approved by the Johns Hopkins Medicine Institutional Review Boards.

RESULTS & DISCUSSION

We found five unique locations on the residual limb for each participant that, when stimulated, produced tactile sensations in unique regions of the phantom hand (Figure 1). Sensations of pressure were elicited in the phantom hand by using mechanical stimulation of the reinnervated sensory sites on the residual limbs of both participants. The evoked tactile sensations from mechanical stimulation were described as being a "pressure" or "pressing" in the phantom hand.

For participant A1, tTENS also produced sensations of touch, specifically a pulsing pressure that matched the 4 Hz stimulation frequency, in the same regions of the phantom hand as did mechanical stimulation (Figure 1A). The evoked sensations from tTENS were described as being “pressure”, “pulsing”, and “tingling” in the phantom hand and tactile sensations were not perceived at stimulation site on the residual limb. Prior work suggests that the projected fields in the phantom hand from mechanical stimulation and tTENS of the same sensory site on the residual limb do not always overlap [7]; however, the projected fields for the two stimulation modalities did overlap for participant A1 (Figure 1A). Because every amputation is unique to each individual, it is reasonable that the projected fields may overlap for different stimulation modalities (e.g., mechanical and tTENS) in some individuals but not in others.

Sensations of temperature, specifically cooling, were reported in the phantom hand as a result of thermal stimulation on the residual limb from the TEC device. Three of the five stimulation sites on participant A1’s residual limb evoked cooling sensations in the phantom hand (Figure 1A) compared to all five stimulation locations on A2’s residual limb (Figure 1B). The thermal project fields did not all overlap with the mechanical and tTENS project fields for the same stimulation locations for A1. That is, one of the stimulation sites, when activated thermally, produced cooling sensations in the thumb and back of the index and ring fingers but elicited pressure sensations in between the thumb and index finger when the same location on the residual limb was activated with mechanical stimulation or tTENS (Figure 1A). The observations of non-overlapping projected fields in A1’s phantom hand based on stimulation modality align with prior results and have been reported across multiple individuals [7], [10]. For A2, thermal stimulation was perceived in the same region in the phantom hand as mechanical stimulation (Figure 1B). These sensory regions in the phantom hand remained stable over the two years of testing in that the stimulation locations on the residual limb and the corresponding regions of tactile activation in the phantom hand did not substantially change.

These results demonstrate that non-invasive stimulation can be used to activate underlying nerves in the residual limb and produce both pressure and thermal tactile sensations in the phantom hand after amputation. Interestingly, stimulating the same location on the residual limb with different modalities (e.g., mechanical, thermal) can produce sensations at different locations in the phantom hand.

CONCLUSION

Both pressure and thermal tactile sensations can be evoked in the phantom hand of individuals with arm amputation through the use of non-invasive stimulation of the residual limb. Having undergone TSR surgery is not a requirement to enable these tactile perceptions in the phantom hand through non-invasive stimulation of underlying sensory nerves in the residual limb. Mechanical and electrical stimulation enable sensations of pressure or pulsing in whereas thermal sensations or enabled by thermal stimulation of the sensory sites on the residual limb. The location of perceived tactile sensations in the phantom hand can be stimulation modality dependent. These results help demonstrate the possibility of restoring multiple modalities of touch to prosthesis users through non-invasive stimulation.

ACKNOWLEDGEMENTS

The authors thank the study participants for their contributions. This work was supported in part by internal research funds from the Johns Hopkins University Applied Physics Laboratory.

REFERENCES

[1] J. A. George *et al.*, “Biomimetic sensory feedback through peripheral nerve stimulation improves dexterous use of a bionic hand,” *Science Robotics*, vol. 4, no. 32, 2019, doi: 10.1126/scirobotics.aax2352.

[2] E. L. Graczyk, L. Resnik, M. A. Schiefer, M. S. Schmitt, and D. J. Tyler, “Home Use of a Neural-connected Sensory Prosthesis Provides the Functional and Psychosocial Experience of Having a Hand Again,” *Scientific Reports*, vol. 8, no. 1, p. 9866, 2018, doi: 10.1038/s41598-018-26952-x.

[3] L. E. Osborn *et al.*, “Sensory stimulation enhances phantom limb perception and movement decoding,” *J. Neural Eng.*, vol. 17, no. 5, p. 056006, Oct. 2020, doi: 10.1088/1741-2552/abb861.

[4] K. Ding *et al.*, “Towards machine to brain interfaces: Sensory stimulation enhances sensorimotor dynamic functional connectivity in upper limb amputees,” *Journal of Neural Engineering*, 2020, doi: 10.1088/1741-2552/ab882d.

[5] J. S. Schofield, C. E. Shell, D. T. Beckler, Z. C. Thumser, and P. D. Marasco, “Long-Term Home-Use of Sensory-Motor-Integrated Bidirectional Bionic Prosthetic Arms Promotes Functional, Perceptual, and Cognitive Changes,” *Front. Neurosci.*, vol. 14, Feb. 2020, doi: 10.3389/fnins.2020.00120.

[6] J. S. Hebert *et al.*, “Novel targeted sensory reinnervation technique to restore functional hand sensation after transhumeral amputation,” *IEEE Transactions on Neural Systems and Rehabilitation Engineering*, vol. 22, no. 4, pp. 765–773, 2014, doi: 10.1109/TNSRE.2013.2294907.

[7] L. E. Osborn *et al.*, “Phantom hand activation during physical touch and targeted transcutaneous electrical nerve stimulation,” in *MEC20 Symposium*, 2020, pp. 147–149. [Online]. Available: https://conferences.lib.unb.ca/index.php/mec/article/view/25

[8] L. Osborn *et al.*, “Targeted transcutaneous electrical nerve stimulation for phantom limb sensory feedback,” in *IEEE Biomedical Circuits and Systems (BioCAS)*, 2017, pp. 1–4. doi: 10.1109/BIOCAS.2017.8325200.

[9] L. E. Osborn *et al.*, “Prosthesis with neuromorphic multilayered e-dermis perceives touch and pain,” *Science Robotics*, vol. 3, no. 19, p. eaat3818, 2018, doi: 10.1126/scirobotics.aat3818.

[10] L. E. Osborn *et al.*, “Evoking natural thermal perceptions using a thin-film thermoelectric device with high cooling power density and speed,” *Nat. Biomed. Eng*, pp. 1–14, Jul. 2023, doi: 10.1038/s41551-023-01070-w.

[11] F. Iberite *et al.*, “Restoration of natural thermal sensation in upper-limb amputees,” *Science*, vol. 380, no. 6646, pp. 731–735, May 2023, doi: 10.1126/science.adf6121.

DEVELOPMENT AND ASSESSMENT OF AN AUGMENTED REALITY FEEDBACK SYSTEM FOR PROSTHESIS USERS

Lincoln Inglis[1] & Daniel Blustein[2]

[1]Department of Psychology, Western University, London, ON, Canada. [2]Department of Psychology, Acadia University, Wolfville, NS, Canada

ABSTRACT

Users of upper limb prostheses face a challenge when attempting to grasp fragile objects due to an impairment of naturalistic sensory feedback regarding grip strength. Augmented Reality (AR) has shown promise as a candidate in solving this issue. Here we present the implementation and testing of a novel AR application for the Microsoft HoloLens 2 and test it using an upper limb prosthesis simulator. Our novel AR software application displays a color overlay on top of a user's prosthetic hand that changes based on grip strength. Using a mechanical egg grasp-and-hold task, we compared grasp performance and learning between prosthesis users with and without AR grip force feedback. Using a mixed ANOVA, we observed no statistically significant difference in performance with and without AR feedback ($F(1,15) = 0.87$, $p = 0.37$) , though we did see improvement across three blocks of grasp trials ($F(2,30) = 6.58$, $p = 0.004$). The AR implementation as presented was not effective which could be explained by limitations of the HoloLens 2, our overlay visualization, a need for more user training, or the simplicity of the task. Emerging AR systems may be better suited to display useful sensory feedback for upper limb prostheses with reduced latency, higher resolution graphics, and improved hand tracking to better localize the visual overlay.

INTRODUCTION

The ability to grasp fragile objects is a key challenge faced by users of upper limb prostheses, at least partly attributed to a lack of naturalistic and intuitive sensory feedback. Without intact hand sensory structures, prosthesis users lose the valuable information that would typically be provided by the sense of touch and kinesthesia, forcing them to rely solely on visual perception when estimating how much force to apply to an object. While visual perception is a significant predictor of force perception [1], the altered internal models of prosthesis users result in inaccurate and especially variable predictions of the force required to successfully pick up a fragile object [2]. Seemingly trivial activities, such as picking up an egg without dropping or cracking it, can become quite difficult tasks.

Past research has sought to develop alternative sensory modalities by which grip force can be represented. Invasive solutions have been proposed in the form of neural interfaces, which directly stimulate peripheral sensory neurons [3], as well as reinnervation surgeries, which transfer residual nerves from the amputated limb to alternative muscle groups [4]. These solutions, however, can result in damage to peripheral nerves or unwanted tissue response [5]. Non-invasive solutions may be more widely accepted by patients with one study showing enhanced use of a prosthesis simulator when haptic feedback was applied to intact fingers [6]. However, this haptic feedback tends to be less incorporated when it is physically misaligned from its visual reference on the prosthesis [7]. Such findings suggest that this form of non-invasive feedback may not be as effective for users with more proximal amputations. Given these downsides, it may be worth investigating solutions which instead provide supplementary visual feedback.

Through Augmented Reality (AR), a visualization is superimposed over a person's view of the real environment around them, integrating digital information into a natural scene. The technology has been effective in educational [8] and stroke rehabilitation [9] settings. AR has also been proposed as an effective solution to the aforementioned grip strength perception problem. Grip strength information has been presented in the form of shape changing ellipses [10] or as visual progress bars [11]. As emerging prosthetic devices are often rejected as too much of a burden to use [12], one might fear that although effective, previous AR feedback systems may require too much attention and cognitive burden to provide real-world clinical benefit.

Our study sought to extend previous AR-based research by developing a more intuitive feedback system in which the visualized grip strength feedback is co-located with the prosthetic hand (i.e. the hand itself appears to change color). Using a between-subjects design, we investigated the effect of this system on motor learning and on grasp performance during a mechanical egg grasp-and-hold task.

METHODS

Augmented Reality Sensory Feedback System

We developed an Augmented Reality application in the Unity development platform for use with the Microsoft HoloLens 2 AR headset. The app places a colored sphere on the user's hand that tracks with hand movement. The location of the sphere can be moved between the right and left hand, and between the fingertips and the back of the hand, if desired. Every frame, or approximately 60 times per second, the application searches for incoming grip force data (in the form of keyboard input) from sensors on both the index finger and thumb. Originally two spheres were used per hand, one for each of the sensors, but this was determined to be confusing in pilot testing. The intensity of the cumulative grip force across both sensors is proportionally mapped to a color map of the visualized sphere. At no force applied, the sphere appears white. As the user applies force to an object, the sphere turns green, eventually shifting to red as maximal force is applied.

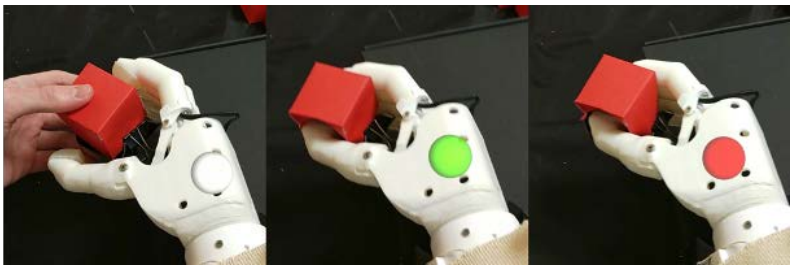

Figure 1: Augmented reality grip force display. Increasing grip force strength, from left to right, changes the visualized color across a gradient from white (no force) to green (low force) to red (high force).

Strain gauge sensors (Interlink Electronics FSR 400) on the pads of the index finger and thumb of a prosthesis simulator [13] measured force applied. The sensors interfaced with a 3.3V Arduino Micro microcontroller which converted the voltage input into the keyboard output necessary to bring data into the closed Microsoft ecosystem. The character string consisted of three digits for each finger (000 to 255), followed by a single-character delimiter, which was primarily used to signify the end of a given string, but could be altered to change user settings, such as enabling a color-blindness mode or switching the feedback location. A USB connection passed the output from the Arduino to the HoloLens 2 approximately once every 100ms, much slower than other AR prosthesis feedback systems [10], [11]. Faster transmission rates and Bluetooth transmission both resulted in data loss, a limitation of the Hololens 2.

Participants controlled the 3D-printed prosthesis simulator [13] via electromyographic (EMG) signals measured by a Thalmic Labs Myo armband. Flexor and extensor muscle activity during wrist movements was mapped to open and close the hand. EMG-driven velocity control of the prosthetic hand was calibrated using brachI/Oplexus software [14], with extreme velocities mapped to maximally comfortable wrist movement in both directions.

Participants

Seventeen participants were recruited from a research participant pool at Acadia University of undergraduate students who had intact limbs and corrected-to-normal color vision. Fourteen identified as female, two as male, and one as non-binary. The mean age of participants was 20.7 years (ranging from 18 to 32 years). Two participants indicated a left-hand dominance. Participants were compensated for their time with bonus credit towards their Psychology courses. All work was completed under the oversight of the Acadia University Research Ethics Board.

Experimental setup

The prosthetic hand simulator was mounted to the table and remained stationary throughout testing, with only one degree of freedom: hand open/close. Pilot testing with a donned simulator and multiple free degrees of movement led to tracking issues. The Hololens 2 could not automatically detect the prosthetic hand in certain orientations, leading to intermittent tracking of the visualization. Participants remained seated with their arm hanging at their side while controlling the prosthesis (Figure 2a) to grasp a mechanical egg (Figure 2b): a small paper cube (5cm x 5cm x 5cm) with two mechanical fuses inside, mounted perpendicularly between opposing graspable surfaces. The fuses were pieces of angel hair pasta that would 'break' if too much force were applied, generating an audible signal to indicate a failed grasp [15]. Each egg's mass was adjusted by attaching weights inside to equal two ounces.

Figure 2: Experimental setup. A. Participants wore the HoloLens 2 while controlling a prosthesis simulator. b. Mechanical egg in grasp-and-hold task. *Left*, participant view. *Right*, underside showing intact pasta fuses [15].

Procedure

After obtaining informed consent and demographic information, participants donned the Myo armband on their right forearm and completed the calibration procedure. Once the prosthesis' motor velocity maximum had been calibrated to match the strength of the participants' forearm muscles, participants donned the HoloLens 2 headset. Participants were randomly assigned to one of two conditions, as early testing indicated that the task was learned too quickly to use a within-subjects design. In one condition (unaided feedback, n = 9), the HoloLens headset was worn, but was not turned on. In the other (AR-assisted feedback, n = 8), the HoloLens was powered on with the AR application running. After being provided instructions, participants completed the grasp-and-hold task. In each trial of the grasp-and-hold task, participants were handed an intact mechanical egg on a spatula and were asked to hold the egg for two seconds, attempting to keep the egg intact. After two seconds, the participant was prompted to drop the egg intentionally, which represented a successful movement. Each movement block consisted of 20 egg holds, and participants completed three movement blocks, with a two-minute rest break between each block. The number of successful and unsuccessful (breaks and drops) egg grasps were recorded for each block.

Data analysis

We analyzed overall grasp performance with supplementary AR feedback and visual feedback only, as well as the change in performance across blocks. A mixed ANOVA was run with block number (within) and condition (between) as predictor variables, and the number of egg breaks+drops as the outcome variable.

RESULTS

A summary of results by block and condition can be found in Figure 3. Participants completing the first block failed an average of 7.25 egg grasps when using AR feedback (SD = 2.76), and an average of 5.56 without AR (SD = 2.13). In the second block, AR condition participants recorded an average of 6.12 egg failures (SD = 4.19), while their unaided counterparts failed an average of 4.22 (SD = 3.77). In the final block, participants using AR failed 4.25 eggs on average (SD = 2.25), while those without AR failed an average of 3.89 eggs (SD = 3.95).

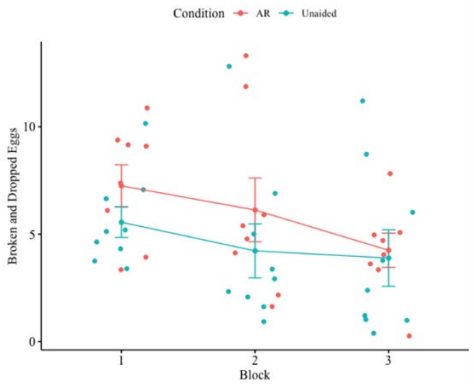

Figure 3: Failed egg grasps by feedback type and block. Error bars represent standard error of the mean.

Mauchly's Test for Sphericity showed no violations of the sphericity assumption, W = 0.98, p = 0.86. The mixed ANOVA showed a statistically significant main effect of Block, $F(2,30) = 6.58$, $p = 0.004$, and no statistically significant effect for Condition, $F(1,15) = 0.87$, $p = 0.37$, or the interaction between Block and Condition, $F(2,30) = 0.84$, $p = 0.44$. This suggests a statistically significant learning effect but does not provide support for the hypothesis that co-located AR feedback would change motor performance.

DISCUSSION

The HoloLens 2 implementation of an AR visual overlay conveying fingertip force feedback on a prosthetic hand did not significantly affect performance during grasping of a fragile object. These results are inconsistent with previous AR grip strength feedback systems [10], [11] using physically offset visualizations. Some possible explanations for why there was no improvement with our AR system include: 1) low resolution grip force feedback; 2) feedback latency issues; 3) graphical limitations of the HoloLens 2; and 4) a moving visualization relying on hand tracking (although movement was minimized due to a stationary hand, it did occur with participant head movement). Perhaps the task was too simple and the AR feedback added no useful information, as has been reported with haptic feedback systems [16]. We consider this work a pilot study to help inform future methodology and suggest using a more modern AR system to provide higher fidelity feedback. Many questions remain regarding the usability of AR feedback systems to improve user operation of prostheses and how to best implement it for maximum effectiveness.

ACKNOWLEDGEMENTS

Thank you to Aiden Fisk and Ahmed Shehata for technical support.

REFERENCES

[1] J. Diedrichsen, T. Verstynen, A. Hon, Y. Zhang, and R. B. Ivry, "Illusions of Force Perception: The Role of Sensori-Motor Predictions, Visual Information, and Motor Errors," *Journal of Neurophysiology*, vol. 97, no. 5, pp. 3305–3313, May 2007, doi: 10.1152/jn.01076.2006.

[2] P. S. Lum, I. Black, R. J. Holley, J. Barth, and A. W. Dromerick, "Internal models of upper limb prosthesis users when grasping and lifting a fragile object with their prosthetic limb," *Exp Brain Res*, vol. 232, no. 12, pp. 3785–3795, Dec. 2014, doi: 10.1007/s00221-014-4071-1.

[3] D. J. Tyler, "Neural interfaces for somatosensory feedback," *Current Opinion in Neurology*, vol. 28, no. 6, Art. no. 6, Dec. 2015, doi: 10.1097/WCO.0000000000000266.

[4] T. A. Kuiken *et al.*, "Targeted reinnervation for enhanced prosthetic arm function in a woman with a proximal amputation: a case study," *The Lancet*, vol. 369, no. 9559, Art. no. 9559, Feb. 2007, doi: 10.1016/S0140-6736(07)60193-7.

[5] K. A. Yildiz, A. Y. Shin, and K. R. Kaufman, "Interfaces with the peripheral nervous system for the control of a neuroprosthetic limb: a review," *J NeuroEngineering Rehabil*, vol. 17, no. 1, p. 43, Dec. 2020, doi: 10.1186/s12984-020-00667-5.

[6] C. Cipriani, J. L. Segil, F. Clemente, R. F. ff Weir, and B. Edin, "Humans can integrate feedback of discrete events in their sensorimotor control of a robotic hand," *Experimental Brain Research*, vol. 232, no. 11, Art. no. 11, Jul. 2014, doi: 10.1007/s00221-014-4024-8.

[7] D. Blustein, A. Wilson, and J. Sensinger, "Assessing the quality of supplementary sensory feedback using the crossmodal congruency task," *Scientific Reports*, vol. 8, no. 1, Art. no. 1, Dec. 2018, doi: 10.1038/s41598-018-24560-3.

[8] K.-E. Chang, J. Zhang, Y.-S. Huang, T.-C. Liu, and Y.-T. Sung, "Applying augmented reality in physical education on motor skills learning," *Interactive Learning Environments*, vol. 28, no. 6, pp. 685–697, Aug. 2020, doi: 10.1080/10494820.2019.1636073.

[9] X. Luo, T. Kline, H. C. Fischer, K. A. Stubblefield, R. V. Kenyon, and D. G. Kamper, "Integration of Augmented Reality and Assistive Devices for Post-Stroke Hand Opening Rehabilitation," in *2005 IEEE Engineering in Medicine and Biology 27th Annual Conference*, Jan. 2005, pp. 6855–6858. doi: 10.1109/IEMBS.2005.1616080.

[10] F. Clemente, S. Dosen, L. Lonini, M. Markovic, D. Farina, and C. Cipriani, "Humans Can Integrate Augmented Reality Feedback in Their Sensorimotor Control of a Robotic Hand," *IEEE Trans. Human-Mach. Syst.*, vol. 47, no. 4, pp. 583–589, Aug. 2017, doi: 10.1109/THMS.2016.2611998.

[11] M. Markovic, H. Karnal, B. Graimann, D. Farina, and S. Dosen, "GLIMPSE: Google Glass interface for sensory feedback in myoelectric hand prostheses," *J. Neural Eng.*, vol. 14, no. 3, p. 036007, Jun. 2017, doi: 10.1088/1741-2552/aa620a.

[12] E. A. Biddiss and T. T. Chau, "Upper limb prosthesis use and abandonment: A survey of the last 25 years," *Prosthetics and Orthotics International*, vol. 31, no. 3, Art. no. 3, Sep. 2007, doi: 10.1080/03093640600994581.

[13] E. Wells, S. Carpenter, M. Dawson, A. Shehata, J. Carey, and J. Hebert, "Development of a Modular Simulated Prosthesis and Evaluation of a Compliant Grip Force Sensor," *MEC20 Symposium*, Jul. 2020, Accessed: Jul. 20, 2020. [Online]. Available: https://conferences.lib.unb.ca/index.php/mec/article/view/74

[14] M. Dawson, H. Williams, G. Murgatroyd, J. Hebert, and P. Pilarski, "brachIOplexus: Myoelectric Training Software for Clinical and Research Applications," *MEC20 Symposium*, Jul. 2020, Accessed: Jul. 20, 2020. [Online]. Available: https://conferences.lib.unb.ca/index.php/mec/article/view/40

[15] F. Clemente, M. D'Alonzo, M. Controzzi, B. B. Edin, and C. Cipriani, "Non-invasive, temporally discrete feedback of object contact and release improves grasp control of closed-loop myoelectric transradial prostheses," *IEEE Transactions on Neural Systems and Rehabilitation Engineering*, vol. 24, no. 12, Art. no. 12, 2015, doi: 10.1109/TNSRE.2015.2500586.

[16] E. Raveh, S. Portnoy, and J. Friedman, "Myoelectric Prosthesis Users Improve Performance Time and Accuracy Using Vibrotactile Feedback When Visual Feedback Is Disturbed," *Archives of Physical Medicine and Rehabilitation*, vol. 99, no. 11, pp. 2263–2270, Nov. 2018, doi: 10.1016/j.apmr.2018.05.019.

EFFECT OF BIOMIMICRY ON PERCEIVED INTENSITY, NATURALNESS, AND PLEASANTNESS USING NON-INVASIVE ELECTRICAL STIMULATION

Robert Midura, Mark Brinton PhD

Elizabethtown College: Department of Engineering and Physics

ABSTRACT

This study focused on testing different non-invasive electrical stimulations for their perceived intensity, naturalness, and pleasantness. The eventual goal is to develop natural feeling, non-invasive electrical stimulation for prostheses. We found no difference between naturalness and pleasantness ratings; however, the 1st order biomimetic algorithms (amplitude or frequency modulation) felt stronger than the 2nd order (frequency modulation) stimulus while keeping the total charge constant.

INTRODUCTION

Limb-loss is a lifelong challenge with high-medical costs and often includes life-long use of painkillers, antidepressants, and other drugs. Up to 50% of upper limb amputees do not use their prosthetic [1], with their reasoning including high cost [2]–[4], ineffective controls [2], lack of sensory feedback [5], [6], and requires too much attention to control the prosthesis properly [7]. Invasive neurostimulation can provide a sense of touch with surgically implanted electrodes, but also comes with high-costs and surgical risks.

Electrocutaneous stimulation is similar to invasive neural stimulation in that it provides an intuitive form of sensory feedback with high spatial and temporal resolution [8]–[15]. Electrocutaneous stimulation has the added benefit of being inexpensive and compact; it can be readily implemented into commercial prosthetic sockets [14]. However, with traditional encoding algorithms the sensations feel unnatural, numbing or 'electrical' [16], [17]. Sharp, prickly sensations can occur at higher amplitude stimuli due to high electric field development at the edge of the electrode that are large enough to activate small, unmyelinated pain and itch fibres [18], [19]. The purpose of this research is to test non-invasive, biomimetic electrocutaneous stimuli and understand their effect on perceived intensity, pleasantness, and naturalness.

MATERIALS AND METHODS

Four different types of stimuli were tested: linear (i.e., amplitude proportional to applied force), 1st order biomimetic (amplitude modulation) [20], 2nd order biomimetic (frequency modulation) [20]–[22], and a combination of both amplitude and frequency modulation with 1st order biomimetic. Biphasic, pulsed stimuli were delivered using a MATLAB GUI and a custom high-compliance voltage constant current stimulator with updates to stimulation parameters occurring every 33 ms [23]. Participants first wet a small patch of skin on the upper arm where an electrode pad (1-cm diameter active electrode with a 0.75-cm diameter return electrode at each corner of a 9cm^2 quincunx pattern) was taped in place using Transpore™. A small dab of electro-gel was also applied to each electrode to ensure low-impedance connection.

Once connected the threshold of detection was identified using the method of ascending limits (2 second pulse train with 50µs pulse width at 150Hz). For the actual experiment, a 1.5-second force profile experienced during natural touch was played through each of the four algorithms. To ensure a fair comparison of intensity, the total charge for each type of stimuli was held the same using the 1st order, amplitude and frequency modulation algorithm as a reference (total charge depended on the individual threshold of detection and ranged from 12700 to 30700). For this algorithm, the amplitude varied between the threshold of detection and 6mA above the threshold, and frequency varied between 80Hz and 150Hz (all stimuli used biphasic pulses with 50µs for each phase). Using the total charge of this algorithm, the other stimulation parameters were modified to deliver a similar total charge. Linear had the frequency locked at 80Hz but amplitude varied from the detection threshold to the amplitude where the total charge equalled the reference. 1st order biomimetic set the amplitude range from detection to 6mA above and set frequency to the value that matched the total charge of the reference. The 2nd order biomimetic set the frequency range from 80Hz to 150Hz and set the max amplitude to the value that matched the total reference charge.

Each stimulation type was given three times in a randomized order. Participants were asked to rate each stimulation type on a scale of 1 to 10 for naturalness (0-"not natural" and 10-"very natural"), pleasantness (0-"I did not like this at all" and 10-"I really liked this"), and strength (0-"I did not feel the stimulation" and 10-"very intense"). The medians of the three ratings were normalized and then averaged across all participants and compared using a 1-way ANOVA and the Tukey-Kramer post

hoc comparison ($p < 0.05$ for significance). Participants also selected from a list of descriptor words to describe how each stimulation felt. All procedures were approved by the Elizabethtown Institutional Review Board and consent obtained for each participant (5 individuals with intact limbs).

RESULTS

This data can be seen in Figure 1. Figure 1 shows the ratings for naturalness, pleasantness and strength of each type of stimuli. There was no statistical difference between stimulation types for naturalness and pleasantness. However, the 2nd order (frequency modulation) was significantly weaker than the 1st order (amplitude modulation) and 1st order (frequency and amplitude modulation). A heat map showing how frequently each descriptor word was used by the five participants can be seen in Figure 2. Linear and 1st order (frequency and amplitude modulation) appeared to have the most unnatural/electrical descriptors listed while 1st order (amplitude modulation) and 2nd order (frequency modulation) appear to have a wide spread of both natural/physical and unnatural/electrical descriptors depending on the individual.

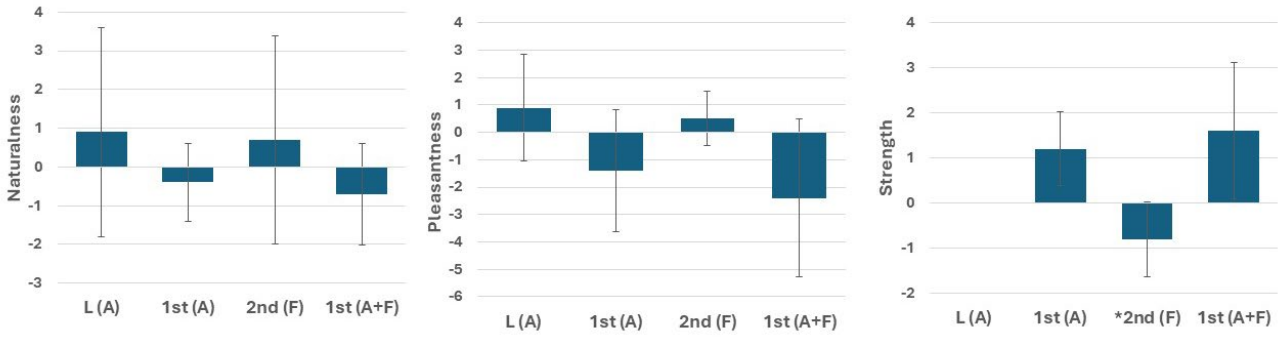

Figure 1: Normalized participant ratings for stimulus (a) naturalness, (b) pleasantness, and (c) strength for each stimulation type: linear (L, amplitude modulation); 1st order amplitude modulation (A); 2nd order frequency modulation (F); 1st order amplitude and frequency modulation (A+F). * Indicates statical significance indicated by 1-way ANOVA with Tukey-Kramer comparison, $p < 0.05$. Data are presented as the mean and standard deviation (both of which happened to be 0 for the normalized linear strength ratings).

DISCUSSION

We found that the 1st order biomimetic algorithms were perceived as stronger than the 2nd order algorithm even though the total charge delivered was the same. However, because the 2nd order algorithm only modulated frequency, it could also be that amplitude modulation feels stronger than frequency for the prototypical force profile played through each algorithm. Additionally, Likert data for naturalness and pleasantry show no statistically significant data that there is a difference between stimulation type. We expected that biomimetic algorithms might feel more natural than a traditional linear profile—however, the prototypical force profile included some elements of biomimicry (i.e., initial rapid rise on contact followed by a drop to a lower constant force during sustained contact) so the linear algorithm, which is proportional to the force, would have had some biomimicry as well. There may also be a trade-off between naturalness and strength as the 2nd order (frequency modulation) was the least strong and participants also used more natural descriptor words.

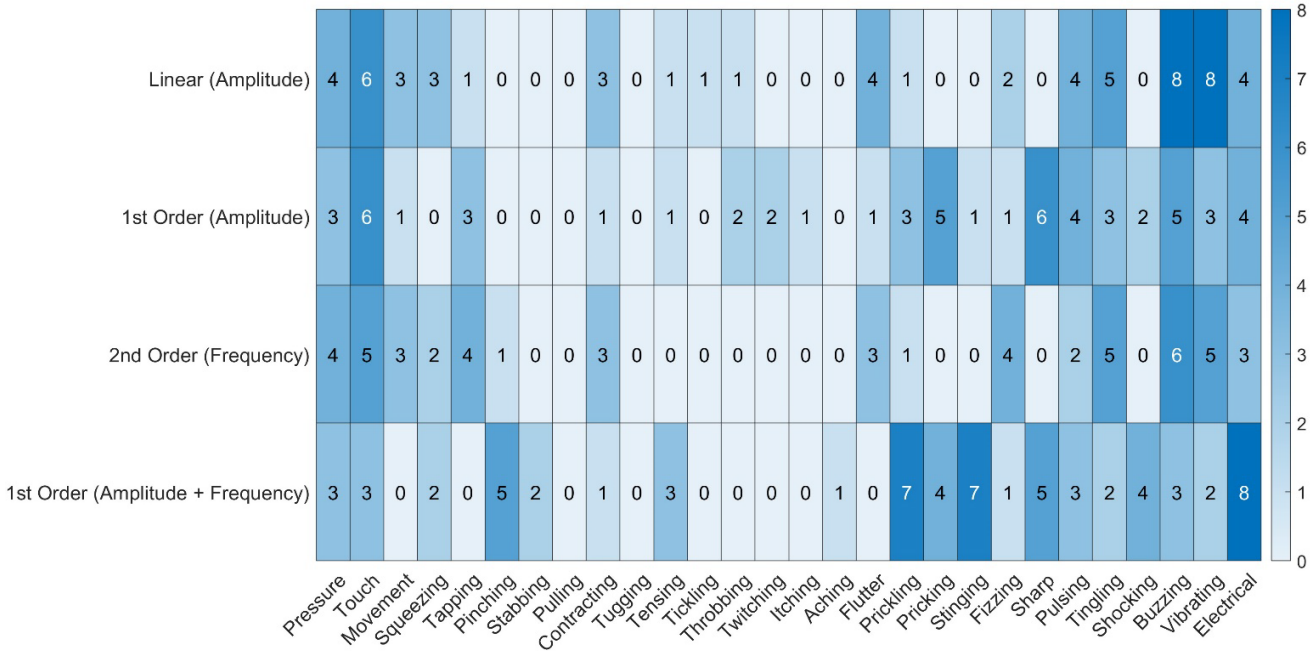

Figure 2: Number of times each descriptor word was used by participants for each stimulation algorithm. 2nd order algorithm had fewer unnatural and more natural descriptions.

References

[1] E. A. Biddiss and T. T. Chau, "Upper limb prosthesis use and abandonment: A survey of the last 25 years," *Prosthet. Orthot. Int.*, vol. 31, no. 3, pp. 236–257, 2007, doi: 10.1080/03093640600994581.

[2] E. Biddiss and T. Chau, "Upper-limb prosthetics: critical factors in device abandonment," *Am J Phys Med Rehabil*, vol. 86, no. 12, pp. 977–987, 2007, doi: 10.1097/PHM.0b013e3181587f6c.

[3] P. F. Pasquina, A. J. Carvalho, and T. P. Sheehan, "Ethics in rehabilitation: Access to prosthetics and quality care following amputation," *AMA J. Ethics*, vol. 17, no. 6, pp. 535–546, Jun. 2015, doi: 10.1001/journalofethics.2015.17.6.stas1-1506.

[4] L. Resnik *et al.*, *Advanced upper limb prosthetic devices: Implications for upper limb prosthetic rehabilitation*, vol. 93, no. 4. 2012, pp. 710–717.

[5] K. A. Raichle *et al.*, "Prosthesis use in persons with lower- and upper-limb amputation," *J. Rehabil. Res. Dev.*, vol. 45, no. 7, pp. 961–972, 2008.

[6] S. Lewis, M. F. Russold, H. Dietl, and E. Kaniusas, "User demands for sensory feedback in upper extremity prostheses," in *2012 IEEE International Symposium on Medical Measurements and Applications Proceedings*, 2012, pp. 1–4, doi: 10.1109/MeMeA.2012.6226669.

[7] D. Atkins, D. Heard, and W. Donovan, "Epidemiologic Overview of Individuals with Upper-Limb Loss and Their Reported Research Priorities," *J. Prosthetics*, vol. 8, no. 1, pp. 2–11, 1996.

[8] J. A. George, M. R. Brinton, P. C. Colgan, G. K. Colvin, S. J. Bensmaia, and G. A. Clark, "Intensity Discriminability of Electrocutaneous and Intraneural Stimulation Pulse Frequency in Intact Individuals and Amputees," in *Proceedings of the Annual International Conference of the IEEE Engineering in Medicine and Biology Society, EMBS*, Jan. 2020, vol. 2020-July, pp. 3893–3896, doi: 10.1109/EMBC44109.2020.9176720.

[9] J. L. Dideriksen, I. U. Mercader, and S. Dosen, "Closed-loop Control using Electrotactile Feedback Encoded in Frequency and Pulse Width," *IEEE Trans. Haptics*, vol. 13, no. 4, pp. 818–824, 2020, doi: 10.1109/TOH.2020.2985962.

[10] J. Dideriksen, M. Markovic, S. Lemling, D. Farina, and S. Dosen, “Electrotactile and Vibrotactile Feedback Enable Similar Performance in Psychometric Tests and Closed-loop Control,” *IEEE Trans. Haptics*, p. 1, 2021, doi: 10.1109/TOH.2021.3117628.

[11] M. A. Garenfeld, C. K. Mortensen, M. Strbac, J. L. Dideriksen, and S. Dosen, “Amplitude versus spatially modulated electrotactile feedback for myoelectric control of two degrees of freedom,” *J. Neural Eng.*, vol. 17, no. 4, p. 046034, Aug. 2020, doi: 10.1088/1741-2552/aba4fd.

[12] T. Boljanić *et al.*, “Design of multi-pad electrotactile system envisioned as a feedback channel for supernumerary robotic limbs,” *Artif. Organs*, vol. 00, pp. 1–10, Jun. 2022, doi: 10.1111/aor.14339.

[13] M. Štrbac *et al.*, “Integrated and flexible multichannel interface for electrotactile stimulation,” *J. Neural Eng.*, vol. 13, no. 4, 2016, doi: 10.1088/1741-2560/13/4/046014.

[14] Y. Abbass, M. Saleh, S. Dosen, and M. Valle, “Embedded Electrotactile Feedback System for Hand Prostheses Using Matrix Electrode and Electronic Skin,” *IEEE Trans. Biomed. Circuits Syst.*, vol. 15, no. 5, pp. 912–925, 2021, doi: 10.1109/TBCAS.2021.3107723.

[15] E. M. Dölker, S. Lau, M. A. Bernhard, and J. Haueisen, “Perception thresholds and qualitative perceptions for electrocutaneous stimulation,” *Sci. Rep.*, vol. 12, no. 1, 2022, doi: 10.1038/s41598-022-10708-9.

[16] D. W. Tan, M. A. Schiefer, M. W. Keith, J. R. Anderson, J. Tyler, and D. J. Tyler, “A neural interface provides long-term stable natural touch perception,” *Sci. Transl. Med.*, vol. 6, no. 257, p. 257ra138, 2014, doi: 10.1126/scitranslmed.3008669.

[17] S. J. Bensmaia, D. J. Tyler, and S. Micera, “Restoration of sensory information via bionic hands,” *Nat. Biomed. Eng.*, pp. 1–13, Nov. 2020, doi: 10.1038/s41551-020-00630-8.

[18] B. Wang, A. Petrossians, and J. D. Weiland, “Reduction of Edge Effect on Disk Electrodes by Optimized Current Waveform,” *IEEE Trans. Biomed. Eng.*, vol. 61, no. 8, p. 2254, 2014, doi: 10.1109/TBME.2014.2300860.

[19] X. F. Wei and W. M. Grill, “Current density distributions, field distributions and impedance analysis of segmented deep brain stimulation electrodes,” *J. Neural Eng.*, vol. 2, no. 4, p. 139, Nov. 2005, doi: 10.1088/1741-2560/2/4/010.

[20] J. A. George *et al.*, “Biomimetic sensory feedback through peripheral nerve stimulation improves dexterous use of a bionic hand,” *Sci. Robot.*, vol. 4, no. 32, p. eaax2352, Jul. 2019, doi: 10.1126/scirobotics.aax2352.

[21] H. P. Saal and S. J. Bensmaia, “Biomimetic approaches to bionic touch through a peripheral nerve interface,” *Neuropsychologia*, vol. 79, pp. 344–353, Dec. 2015, doi: 10.1016/j.neuropsychologia.2015.06.010.

[22] E. V. Okorokova, Q. He, and S. J. Bensmaia, “Biomimetic encoding model for restoring touch in bionic hands through a nerve interface,” *J. Neural Eng.*, vol. 15, no. 6, p. 66033, Oct. 2018, doi: 10.1088/1741-2552/aae398.

[23] M. A. Trout, A. T. Harrison, M. R. Brinton, and J. A. George, “A portable, programmable, multichannel stimulator with high compliance voltage for noninvasive neural stimulation of motor and sensory nerves in humans,” *Sci. Rep.*, vol. 13, no. 1, p. 3469, Mar. 2023, doi: 10.1038/s41598-023-30545-8.

EVIDENCE THAT A DEEP LEARNING REGRESSION-BASED CONTROLLER MITIGATES THE LIMB POSITION EFFECT FOR AN INDIVIDUAL WITH TRANSRADIAL AMPUTATION

Heather E. Williams[1,2], Jacqueline S. Hebert[1,3], Patrick M. Pilarski*[2,3], Ahmed W. Shehata*[1,3]

[1]Dept. of Biomedical Engineering, University of Alberta, Edmonton, Canada; [2]Alberta Machine Intelligence Institute (Amii), Edmonton, Canada; [3]Dept. of Medicine, University of Alberta
** These authors contributed equally to this work.*

ABSTRACT

Myoelectric upper limb prostheses provide wrist and hand movements to users yet remain somewhat unreliable and challenging to operate in high and cross-body limb positions. Hand and wrist movements are typically controlled sequentially and at a pre-set velocity. We have made significant inroads towards developing a novel controller that is reliable in multiple limb positions and offers fluid movements. Our recent work unveiled a promising *deep learning regression-based myoelectric control solution*. Herein we present results from our current study that tested device control using our solution versus a baseline (*classification*) alternative. A myoelectric prosthesis user with transradial amputation donned an experimental prosthesis and performed two functional tasks under each control option. The user exhibited superior device controllability across multiple limb positions using our regression-based solution. This work contributes evidence that a deep learning regression control approach can elicit accurate, simultaneous, and proportional device movements, while mitigating the limb position effect for a transradial prosthesis user.

INTRODUCTION

A myoelectric prosthesis connects to a user's residual limb via a socket and is normally controlled using electromyography (EMG) signals. EMG signals are generated by residual muscle contractions, detected by surface electrodes within the socket, and transmitted to the device's onboard controller. Pattern recognition-based controllers decode these signals to predict the user's intended movements and send corresponding commands to the device's motors. The most advanced controllers generally use a classification algorithm (model), which predicts one device action (or class) at a time [1]. The resulting prosthetic limb movements are somewhat robotic and are delivered at a pre-set velocity. That is, the wrist and hand cannot inherently move together simultaneously or with varied velocity.

Typically, individuals with transradial amputation are capable of reliably performing a limited number of residual limb muscle contractions [1]. These distinct contractions are selected to control predetermined device grasp patterns (such as hand open or close) and wrist rotation [1]. To initialize their pattern recognition-based control model for daily use, they must first perform a pre-determined series of muscle contractions, known as a training routine. Through training, patterns observed in captured EMG signals are associated with corresponding device actions [2]. A prevalent control problem, known as the "limb position effect", results when users attempt to use their devices in untrained limb positions [3]. Oftentimes, users struggle to regain control in response to this problem. To mitigate the effect, a control model must be trained in multiple limb positions [3].

Pattern recognition-based control models can be developed using a recurrent convolutional neural network (RCNN) approach. RCNNs are a type of network architecture for *deep learning*, capable of learning directly from and handling large amounts of multimodal data [4]. These capabilities lend themselves to the capture of limb position data for improved device control. In our prior work, we merged EMG data with accelerometer data from an inertial measurement unit (EMG+IMU) using an RCNN [5, 6]. We also tested an EMG+IMU regression-based control model (RCNN-Reg) [6] and found that regression models can yield smooth device movements, given that they can predict multiple movements at once, each proportional to muscle contraction intensity and across multiple limb positions [5]. In that study, we compared RCNN-Reg to a classification-based alternative that is commonly used in control comparisons (linear discriminant analysis, LDA-Baseline) [6]. Model testing involved participants without amputation (with a simulated prosthesis donned, a reasonable proxy for a person with amputation [7]) who performed two functional tasks—the Refined Clothespin Relocation Test (RCRT) [8] and the Pasta Box Task [9]. Our work 1) found that RCNN-Reg mitigated the limb position effect; 2) substantiated that participants could perform simultaneous wrist rotation and hand open/closed movements at varied velocities, as offered by RCNN-Reg; and 3) reported that RCNN-Reg yielded better predictive accuracy than LDA-Baseline [5, 10].

This current paper extends our earlier RCNN-Reg control model work by testing its translatability to those with upper limb loss. To accomplish this, one individual with transradial amputation donned an experimental myoelectric prosthesis that was controlled by RCNN-Reg in one session and then by LDA-Baseline in a separate session. All experimentation methods from our earlier research study ([6]) were followed. We were excited to find that RCNN-Reg indeed provided accurate, simultaneous, and proportional device movements for an individual with amputation, while mitigating the limb position effect. As such, RCNN-Reg might well offer a valuable control model alternative to traditional classification-based approaches for consideration in future myoelectric control research.

METHODS

One participant with amputation was recruited for this study. She was female, with an age of 50 years, a height of 167 cm, and corrected-to-normal vision. She was right-handed prior to amputation. Two years prior to this study, she had a right-side transradial amputation. Her residual limb was 18 cm long with a circumference of 21 cm at the widest point. The participant typically used a myoelectric hand. She also had some at-home commercial pattern recognition-based prosthesis control experience with two degrees of freedom (wrist rotation and hand) at an estimated usage of 6 hours/day over 3 weeks. She provided written informed consent, as approved by the University of Alberta Health Research Ethics Board (Pro00086557). The participant trained and tested RCNN-Reg in her first session and LDA-Baseline in her second session, with 28 days between the two sessions. An overview of our equipment, experimentation methods, and control analysis metrics is illustrated in Figure 1. Full protocol details can be found in our earlier works [6, 10].

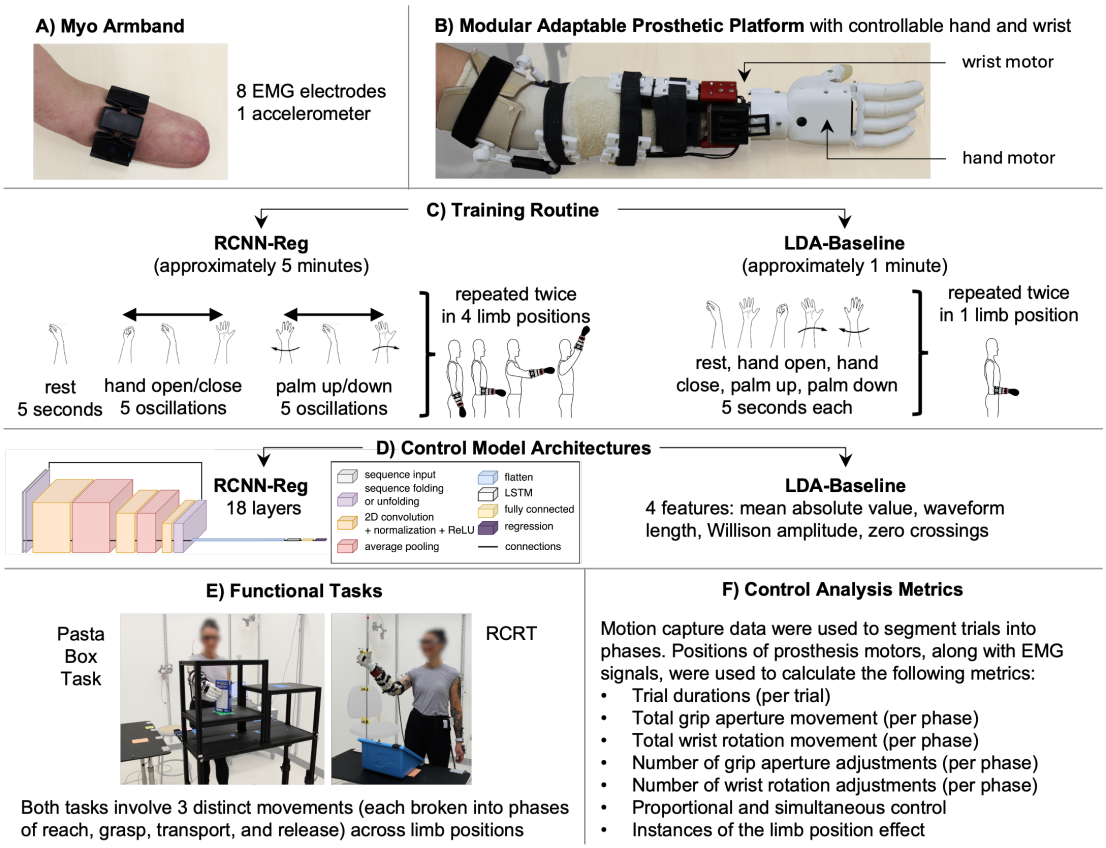

Figure 1: Equipment, experimentation, and analysis metrics in order of use: A) donned Myo armband, B) donned prosthesis [11], C) training routine employed for RCNN-Reg and LDA-Baseline models, including overall training durations [6], D) control model architecture details for RCNN-Reg and LDA-Baseline [6], E) functional tasks performed to test control—the Pasta Box Task [9] and the Refined Clothespin Relocation Test (RCRT) [8], split into RCRT Up and RCRT Down, and F) select metrics calculated for control analysis from our suite of metrics for comparative myoelectric prosthesis control [10].

RESULTS

RCNN-Reg yielded comparatively better myoelectric prosthesis control than LDA-Baseline. RCNN-Reg's improved control, barring a few exceptions, was evidenced by: 1) lower trial durations; 2) less total grip aperture and wrist rotation

movement (indicators of corrections in mm and degrees, respectively); 3) simultaneous control of the prosthetic hand and wrist; along with 4) fewer grip aperture and wrist rotation adjustments (number of corrections). Results are illustrated in Figures 2A–F, respectively, with Figures 2A–C,2E–F showing exceptions where *some* grip and wrist rotation corrections were made by the participant. It was also apparent that the participant took advantage of RCNN-Reg's proportional control capabilities during task execution. That is, her hand and wrist movements occurred at a less-than-maximal velocity 100% of the time.

In our previous work [6], *under LDA-Baseline control, the limb position effect was identified a total of 13 times* (as determined through analysis of median and interquartile range trends [10]). Ten instances were evidenced during the Pasta Box Task (in 1 reach, 1 reach-grasp, 4 grasp, 2 transport, and 2 release metrics) and 3 instances during RCRT Down (all in grasp metrics). Conversely, in this present work, *under RCNN-Reg control, the limb position effect was identified a total of 3 times*, all during the Pasta Box Task (determined using our earlier work's analysis methods [10]). Such instances were evidenced in 1 reach metric and 2 transport metrics.

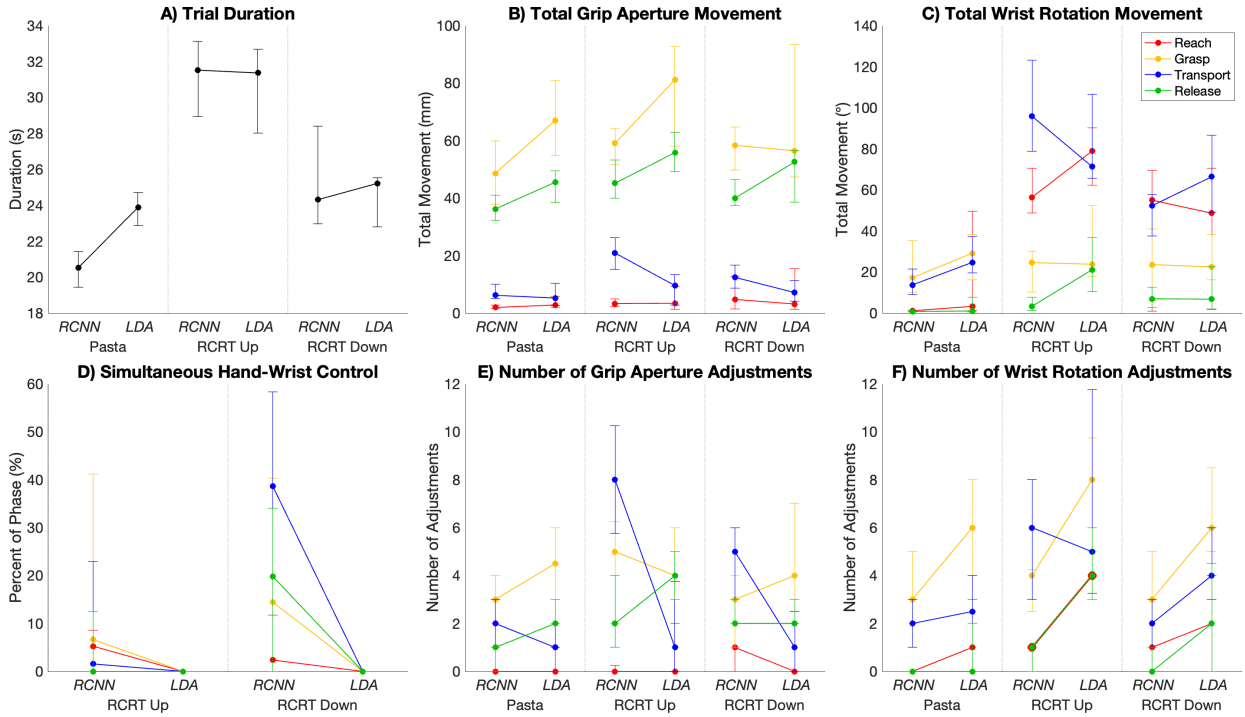

Figure 2: Controller comparison results (abbreviated as RCNN/LDA), including median A) trial duration, B) total grip aperture movement, C) total wrist rotation movement, D) simultaneous hand-wrist control, E) number of grip aperture adjustments, and F) number of wrist rotation adjustments. Medians are presented for each task, and for each phase (Reach in red, Grasp in orange, Transport in blue, and Release in green) where applicable. Interquartile ranges across trials are indicated with coloured error bars where applicable. Note that simultaneous hand-wrist control is only illustrated for RCRT Up/Down, as wrist rotation is not required in the Pasta Box Task (Pasta).

DISCUSSION & FUTURE WORK

Pasta Box Task Control Successes and Challenges: Although RCNN-Reg control was generally superior to LDA-Baseline, our participant exhibited some unexpected control challenges in the transport phases of the Pasta Box Task (Figure 2B,E's abovementioned control exceptions)—evidenced by increased total grip aperture movement and grip aperture adjustments. The Pasta Box Task requires a participant to transport a box in both cross-body and away-from-body limb positions (the specific instances where the limb position effect under RCNN-Reg control occurred). Notably, RCNN-Reg's training routine did *not* include these specific limb positions. Given these circumstances, the addition of cross-body and away-from-body limb positions to RCNN-Reg's training routine is advised. Future work should investigate which training positions improve device control.

RCRT Up and Down Control Successes and Challenges: When testing RCNN-Reg, our participant did not experience the limb position effect during execution of RCRT Up and Down. The effect was likely mitigated because RCNN-Reg's control model was trained in the same high limb positions required of these tasks. Despite this, the participant exhibited control challenges in transport phases of RCRT Up and Down (Figure 2B,C,E,F's abovementioned control exceptions)—evidenced

by increased total grip aperture and wrist rotation movement, along with more grip aperture and wrist rotation adjustments, versus under LDA-Baseline control. These outcomes indicated her need to perform movement corrections to maintain control. RCRT's transport phases require a participant to rotate their wrist while not dropping the grasped clothespin, an inherently difficult movement. Although our participant experienced challenges, she appreciated the simultaneous control capabilities offered by RCNN-Reg in transport phases, as verbally reported: "It's neat that you can do it at the same time [simultaneous control], because you feel like you're losing it [starting to drop the clothespin while rotating the wrist] and you can try and grab it [adjust grip during wrist rotation]." Based on our participant's appreciation of these capabilities, and the fact that progressive learning needs to be allocated for complicated hand-tasks [12], we believe she could master simultaneous control and exhibit fewer adjustments in RCRT's transport phases if afforded more controller-use practice.

Training Routine Implications: RCNN-Reg's 5-minute training routine might prove to be burdensome for a user if repeated multiple times throughout the day (for re-calibration purposes). Future work should be undertaken to shorten the training routine duration. For instance, reducing the number of oscillations performed might be feasible. The incorporation of dynamic limb positions might also reduce routine duration *and* provide richer training data [13].

Future Experimentation: We recognize that our work did not exhaustively investigate RCNN-Reg. To corroborate our findings, the experimentation must be repeated by more participants with transradial amputation.

CONCLUSION

Our case study contributes, for the first time, evidence that an RCNN regression-based controller offers a user with transradial amputation control of their prosthetic wrist and hand simultaneously across multiple limb positions, using varied velocities. *RCNN-Reg successfully mitigated the limb position effect during device use,* given that our participant was able to retain control of their myoelectric prosthesis throughout numerous re-orientations of their limb in space during different tasks. Although regression-based control solutions have not garnered as much research attention as classification-based counterparts, the merits of RCNN-Reg, as presented in this paper, suggest that it be strongly considered as a future prosthesis controller.

ACKNOWLEDGEMENTS

We thank Quinn Boser, Thomas R. Dawson, Michael R. Dawson, and Albert Vette for data collection, data processing and/or experimental design assistance. This work was supported by Amii, the CIFAR AI Chairs program, NSERC DG RGPIN-2019-05961, and NSERC RGPIN-2023-04450.

REFERENCES

[1] P. Geethanjali, "Myoelectric control of prosthetic hands: State-of-the-art review," *Medical Devices: Evidence and Research*, vol. 9, pp. 247–55, 2016.

[2] E. Scheme, K. Englehart, "Electromyogram pattern recognition for control of powered upper-limb prostheses: State of the art and challenges for clinical use," *J. Rehabil. Res. Dev.*, vol. 48, no. 6, pp. 643–59, 2011.

[3] E. Campbell, A. Phinyomark, E. Scheme, "Current trends and confounding factors in myoelectric control: Limb position and contraction intensity," *Sensors (Switzerland)*, vol. 20, no. 6, p. 1613, 2020.

[4] A. Phinyomark, E. Scheme, "EMG pattern recognition in the era of big data and deep learning," *Big Data and Cognitive Computing*, vol. 2, no. 3, p. 21, 2018.

[5] H. E. Williams, A. W. Shehata, M. R. Dawson, E. Scheme, J. S. Hebert, P. M. Pilarski, "Recurrent convolutional neural networks as an approach to position-aware myoelectric prosthesis control," *IEEE Trans. Biomed. Eng.*, vol. 69, no. 7, pp. 2243–55, 2022.

[6] H. E. Williams, A. W. Shehata, K. Y. Cheng, J. S. Hebert, P. M. Pilarski, "Myoelectric Prosthesis Control using Recurrent Convolutional Neural Network Regression Mitigates the Limb Position Effect," *bioRxiv*, 2024.

[7] H. E. Williams, C. S. Chapman, P. M. Pilarski, A. H. Vette, J. S. Hebert, "Myoelectric prosthesis users and non-disabled individuals wearing a simulated prosthesis exhibit similar compensatory movement strategies," *J. Neuroeng. Rehabil.*, vol. 18, p. 72, 2021.

[8] A. Hussaini, P. Kyberd, "Refined clothespin relocation test and assessment of motion," *Prosthet. Orthot. Int.*, vol. 41, no. 3, pp. 294–302, 2017.

[9] A. M. Valevicius, Q. A. Boser, E. B. Lavoie, G. S. Murgatroyd, P. M. Pilarski, C. S. Chapman, A. H Vette, J. S. Hebert, "Characterization of normative hand movements during two functional upper limb tasks," *PLOS ONE*, vol. 13, no. 6, p. e0199549, 2018.

[10] H. E. Williams, A. W. Shehata, K. Y. Cheng, J. S. Hebert, P. M. Pilarski, "A multifaceted suite of metrics for comparative myoelectric prosthesis controller research," *accepted to PLOS One*, 2024.

[11] B. W. Hallworth, A. W. Shehata, M. R. Dawson, F. Sperle, M. Connan, W. Friedl, B. Vodermayer, C. Castellini, J. S. Hebert, P. M. Pilarski, "A transradial modular adaptable platform for evaluating prosthetic feedback and control strategies," *Proc. MEC20*, pp. 203–6, 2020.

[12] J. M. Hahne, M. Markovic, D. Farina, "User adaptation in Myoelectric Man-Machine Interfaces," *Sci. Rep.*, vol. 7, p. 4437, 2017.

[13] A. Gigli, A. Gijsberts, C. Castellini, "Natural myocontrol in a realistic setting: A comparison between static and dynamic data acquisition," *Proc. ICORR*, pp. 1061–6, 2019.

FIRST EVALUATION OF AN INTEGRATED SONOMYOGRAPHIC PROSTHESIS IN INDIVIDUALS WITH CONGENITAL LIMB DIFFERENCE

Afsana Hossain Rima[1,2*], Zahra Taghizadeh[1*], Ahmed Bashatah[1], Abhishek Aher[1], Gabriel Gibson[1], Brian Monroe[4], Siddhartha Sikdar[1,3]

[1]Department of Bioengineering, George Mason University, Fairfax, VA
[2]Department of Electrical & Computer Engineering, George Mason University, Fairfax, VA
[3]Center for Adaptive Systems of Brain-Body Interactions, Fairfax, VA
[4]Hanger Clinic, Laurel, MD

([*]Afsana Hossain Rima and Zahra Taghizadeh are co-first authors)

ABSTRACT

Sonomyography (SMG) or ultrasound-based sensing of muscle deformation is an emerging modality for enhancing upper limb prosthesis control, offering the ability to spatially resolve muscle activity in both superficial and deep layers. Prior studies from our group as well as other groups have demonstrated the feasibility of SMG for prosthetic control using clinical ultrasound imaging systems and as well as miniaturized wearable ultrasound systems with several single-element ultrasound transducers for tracking muscle interfaces. However, the performance of SMG using miniaturized ultrasound sensors incorporated into a prosthetic socket has not been evaluated thus far. In this study, we incorporated single element ultrasound sensors into custom designed prosthetic sockets for two individuals with congenital transradial limb difference and evaluated the performance of classification and proportional control. Our work demonstrates the potential for SMG as well as highlights some challenges that need to be overcome.

INTRODUCTION

Despite the longstanding commercial availability of myoelectric prosthetics, there continue to be inherent limitations associated with surface Electromyography (EMG) signals. EMG signals suffer from poor amplitude resolution, a low signal-to-noise ratio, and crosstalk from adjacent muscles [1],[2]. So, achieving intuitive control of prosthetic hands is still an open problem. Sonomyography (SMG), an emerging modality that utilizes ultrasound for sensing muscle deformation associated with volitional motor intent and provides control signals that have the potential for significant improvement in prosthesis functionality. Prior work has shown that ultrasound can feasibly generate discrete control signals for a large set of unique hand grasps [3]. Our prior research demonstrated that sonomyography (SMG) can accurately differentiate hand grasps using supervised learning algorithms, achieving high accuracy in both individuals with and without upper limb loss, and showed the potential for using a miniaturized and compact wearable ultrasound system [4], [5]. However, it is currently not known how the miniaturized ultrasound transducers will perform inside a prosthetic socket, especially when the arm is moved in different positions within the reachable workspace, since ultrasound signal quality can be affected by sensor shift and loss of contact with the skin. Our objective in this study was to investigate these questions.

METHODS

In an ongoing study, we have recruited two individuals with congenital transradial limb difference. The first participant was an experienced myoelectric prosthesis user, while the second participant had never used a myoelectric prosthesis. Written informed consent was obtained under the guidelines and approval of GMU Institutional Review Board (IRB) prior to conducting the experiment. In this pilot phase of the study, we iteratively tested the performance of our prototype system in a variety of conditions to identify the challenges that need to be overcome. The first step of the process was to identify the sensor positions on the residual forearm. To identify suitable sensor placement locations, we palpated the participant's residual limb while they were attempting different volitional muscle contractions. The ultrasound transducers were then placed at these locations and held in place with adhesive tape. Subsequently, we recorded SMG data for each motion across multiple trials while the participant attempted different

volitional grasps, and we evaluated the classification accuracy. When satisfactory performance was obtained, the locations were documented and communicated to our prosthetist.

In collaboration with our prosthetist, custom sockets were for our participants with transducers incorporated. The sockets were created with a set of soft thermoplastics where the sensors are attached and a hard outer shell where the prosthetic hand is attached. We iteratively refined the transducer housing to ensure that the sockets could be donned and doffed without any discomfort.

(A)

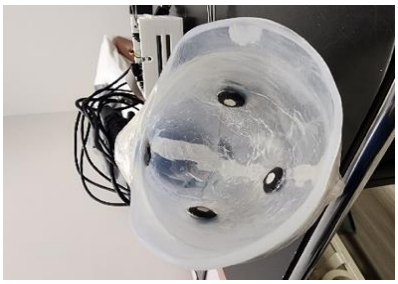

(B)

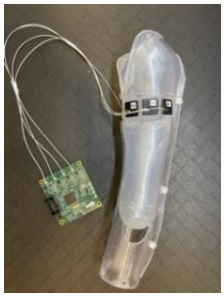

(C)

(D)

Figure.1. (A) SMG sensor location (B) Custom-fitted socket integrated SMG sensors for the second participant, (C) Custom-fitted socket integrated SMG sensors for the first participant, attached to our custom designed prototype ultrasound front end electronics circuit board, and (D) Our participant wearing the prosthetic socket with TASKA hand

In our study, we employed a supervised learning approach to test our prototype system. We utilized a dynamic training protocol that we have previously developed [6]. The dynamic training protocol takes less than 30 seconds and acquires data at multiple different arm positions within a large reachable workspace. Once the training data are obtained, the performance is then tested with different trials with the arm in different positions. Principal Component Analysis (PCA) was used for dimensionality reduction and Linear discriminant analysis (LDA) was used for classification of different motions. We also utilized Gaussian Process Regression (GPR) for classification and control. Our main goal in this study was to understand the impact of training method and the impact of dynamic movement on socket loading and sensor shift on classification performance. Through this investigation, we aimed to enhance our understanding of these critical factors in system performance and reliability.

RESULTS

The first participant was able to perceive three distinct volitional motions which were mapped to power grasp, pinch, and tripod. The second participant was able to perceive two distinct volitional motions which were mapped to power grasp and tripod. In addition, both participants were able to perform wrist rotation. Therefore, including rest as a separate class, we had 5 distinct classes for the first participant and 4 distinct classes for the second participant.

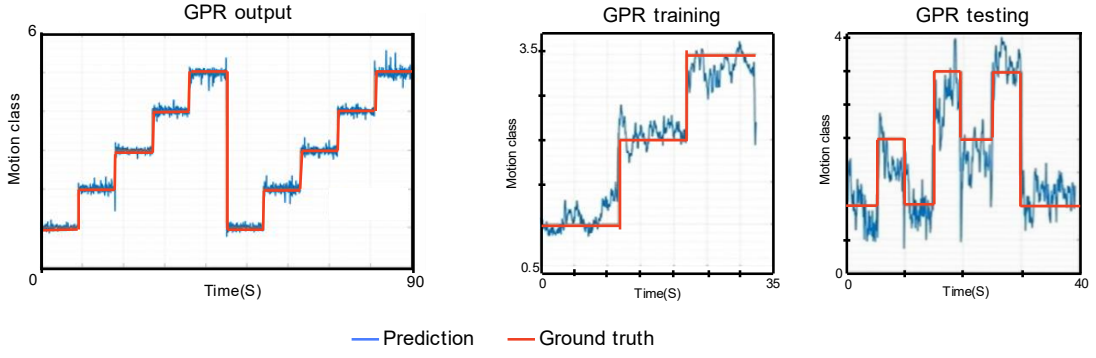

(A) (B.1) (B.2)

Figure. 2. (A) Test of 4-channel SMG system in the first participant. A Gaussian Process Regression was used to train and test with 2-fold cross validation. The participant repeated five movements (rest, power, tripod, wrist) and held each for 10 seconds. (B) Separate training and real-time testing of Gaussian process regression for three motion classes.

Using a dynamic training and dynamic testing paradigm, we obtained a classification accuracy of 81.6% for the first participant to differentiate between 5 classes. Using Gaussian process regression, we were able to demonstrate real-time transitions between three different classes (Figure 2).

Training data obtained from the second participant in three different arm positions (Figure 3A) exhibited a 100% cross-validation accuracy across all trials (Figure 3B). Furthermore, pooled data from four grasps performed at three different positions and projected onto Linear Discriminant Analysis (LDA) space showed consistent separation between the classes (Figure 3C).

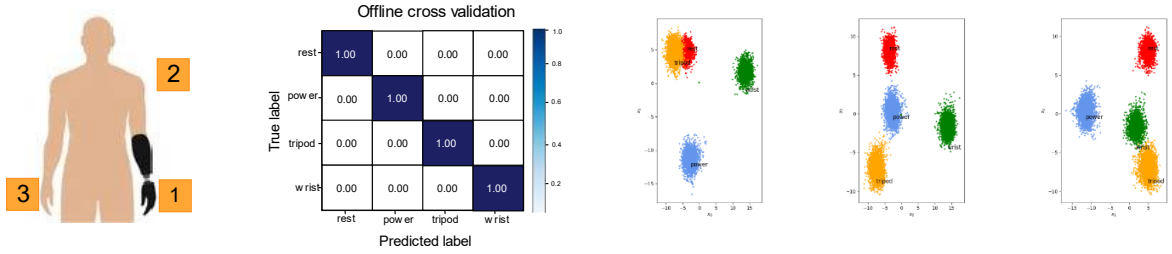

(A) (B) (C)

Figure. 3. (A) Evaluation of signal quality from our first myoelectric naive participant at different arm positions, (B) offline cross validation from data collected at positions 1,2 and 3 with a prosthetic socket loaded with the TASKA hand, and (C)Pooled data from four grasps at all three positions projected into LDA space showing spatially where data is located, each plot shows the location of a motion on 2 of the projected axes.

To evaluate the effect of training and arm position, a single DOF (power grasp) was compared to rest for the second participant. Data were collected for multiple training trials and analysed offline, both for static arm position, and while the arm was moved rapidly from a neutral position to shoulder level. For the static arm positions, an accuracy of 85% was obtained for the first trial, and the accuracy increased to 100% by the fourth trial. For the dynamic trials,

a peak accuracy of 94% was obtained, but the accuracy declined to approximately 60% with increasing trials. Analysis of the data from individual channels demonstrated that data were inconsistent from one of the sensors. Analysis of classification accuracy using one or combination of channels revealed that high classification accuracy could be obtained for both static and dynamic trials using a subset of channels. Table 1 presents the classification accuracy results from the session for static and dynamic training of rest and power motions, considering all four channels, subsets of channels, and each individual channel, respectively.

Table 1: Channel-wise classification accuracy

Static Trials							
Trials	**All Channels**	**Channel 2,3 & 4**	**Channel 2 & 4**	**Channel 1**	**Channel 2**	**Channel 3**	**Channel 4**
Trial_1	85%	70%	99%	90%	98%	53%	84%
Trial_2	89%	100%	99%	50%	90%	49%	86%
Trial_3	99%	100%	99%	61%	99%	86%	92%
Trial_4	100%	100%	100%	66%	99%	55%	94%
Dynamic Trials							
Trial_1	94%	97%	98%	56%	93%	62%	81%
Trial_2	55%	84%	79%	23%	62%	58%	70%
Trial_3	58%	70%	55%	46%	59%	60%	78%

DISCUSSION

To the best of our knowledge, this is the first report of the performance of a miniaturized SMG system incorporated into a prosthetic socket and tested with an attached end effector to evaluate the effect of socket shift and loading on SMG signal quality and classification performance. Preliminary results from two subjects with congenital limb difference indicate that SMG sensors incorporated into prosthetic sockets can be used to successfully classify between grasps with performance like that reported in the literature using clinical ultrasound systems, even for subjects who have never used a myoelectric prosthesis. However, our evaluation also revealed the challenges associated with sensor shift and coupling during dynamic movements. We anticipate that three strategies can be utilized to mitigate this challenge: (1) investigation of strategies to maintain adequate sensor contact, such as adjustable panels over each sensor that can be tightened with BOA cables; (2) utilizing signal analysis to automatically determine a subset of channels that provide adequate data quality and (3) incorporating a redundant number of sensors, or a to minimize the impact of any sensor shift on one or more sensors. We are currently investigating whether these strategies can lead to more robust functional task performance using SMG.

ACKNOWLEDGEMENTS

This work was supported by the Department of Defense under Award No. W81XWH-16-1-0722 and the National Institutes of Health under Award No. U01EB027601. Opinions, interpretations, conclusions, and recommendations are those of the authors and are not necessarily endorsed by the Department of Defense or National Institutes of Health.

REFERENCES

[1] Y.-K. Kong, M. S. Hallbeck, and M.-C. Jung, “Crosstalk effect on surface electromyogram of the forearm flexors during a static grip task,” *J. Electromyogr. Kinesiol.*, vol. 20, no. 6, pp. 1223–1229, Dec. 2010, doi: 10.1016/j.jelekin.2010.08.001.

[2] E. A. Clancy, E. L. Morin, and R. Merletti, “Sampling, noise-reduction and amplitude estimation issues in surface electromyography,” *J. Electromyogr. Kinesiol.*, vol. 12, no. 1, pp. 1–16, Feb. 2002, doi: 10.1016/S1050-6411(01)00033-5.

[3] V. Nazari and Y.-P. Zheng, “Controlling Upper Limb Prostheses Using Sonomyography (SMG): A Review,” *Sensors*, vol. 23, no. 4, p. 1885, Feb. 2023, doi: 10.3390/s23041885.

[4] S. Engdahl *et al.*, “ASSESSING THE FEASIBILITY OF USING SONOMYOGRAPHY FOR UPPER LIMB PROSTHESIS CONTROL”, *MEC Symposium, Aug. 22.*

[5] S. Acuña, S. Engdahl, A. Bashatah, P. Otto, R. Kaliki, and S. Sikdar, “A WEARABLE SONOMYOGRAPHY SYSTEM FOR PROSTHESIS CONTROL”, *MEC Symposium, Aug. 22.*

[6] S. M. Engdahl, S. A. Acuña, E. L. King, A. Bashatah, and S. Sikdar, “First Demonstration of Functional Task Performance Using a Sonomyographic Prosthesis: A Case Study,” *Front. Bioeng. Biotechnol.*, vol. 10, p. 876836, May 2022, doi: 10.3389/fbioe.2022.876836.

ICE IS NICE: A MODULAR GAMIFIED RESEARCH AND TRAINING PLATFORM FOR PEDIATRIC UPPER LIMB PROSTHETIC CONTROL

Joshua D McGinnis, Lana H Wong, Marcus A Battraw, Jonathon S Schofield

Department of Mechanical and Aerospace Engineering, University of California, Davis, Davis CA, USA

ABSTRACT

Training for children who are prescribed myoelectric upper limb prostheses presents unique challenges in maintaining attention, motivation, and ultimately providing an enjoyable experience that is effective in developing the core motor skills required for device operation. From a clinical perspective, patient engagement is critical for maximizing functional outcomes, and from a research perspective, it can be vital to ensuring the quality of collected data. Therefore, our goal was to develop a training and research platform designed to both collect high-quality data from actively engaged participants and to provide them with a fun and engaging way to practice actuating the muscles relevant to myoelectric prosthetic control. "*Ice is Nice"* is a side scrolling video game that prompts children to perform a variety of movements with their missing hand, and the game is controlled using real-time measurement of their muscular activity. Our system is agnostic to muscle measurement systems, capable of using electromyography, force myography, and ultrasound-based control, among many others. As the game is played, data is logged to capture metrics relevant to game proficiency, human motor learning, and machine learning performance. Therefore, we suggest *"Ice is Nice"* provides a research and training platform with significant potential to support numerous follow-on studies conducted with children and adults. These studies aim to develop robust prosthetic control strategies, understand the effects of motor learning on prosthetic operation, and examine the functional capabilities of individuals operating upper limb prostheses.

INTRODUCTION

The main goal of upper limb prostheses is to assist in the functional execution of everyday tasks, though they are also beneficial in the psychosocial domain as well by promoting social inclusivity and giving the user a greater degree of independence [1]. However, abandonment rates are high in pediatric populations and exceed those found in adult populations, with an estimated 35-45% of prescribed devices being abandoned [2].

Children present with challenges associated with prosthesis prescription and usage that differ from those faced by their adult counterparts. For example, the vast majority of upper limb deficiencies in children are congenital, in contrast to adult populations where the majority of upper limb amputations are acquired, resulting from trauma, disease progression, or infection [3]. These differences in etiology are particularly relevant to the use and potential abandonment of modern myoelectric prosthetic systems, which require the user to intentionally and skillfully control their residual muscles. As most pediatric prosthesis wearers will never have used the muscles in their affected limb to control an intact hand, the muscle activity from which prosthetic control signals are derived, may be very different in these groups of prosthesis wearers. In our previous work, we have shown that children born without a hand retain a motor representation of their missing limb that presents itself as coordinated patterns of muscle activation while attempting to make different hand movements [3], [4]. These findings were observed in children who had not undergone any prior training in envisioning their missing hand or performing imagery tasks. We argue that, like learning any new motor skill, training and practice will improve these children's coordination and proficiency in performing such tasks and ultimately provide tremendous potential towards improved dexterous prosthetic control and functional outcomes.

Modern myoelectric training encourages wearers to make muscle contraction patterns that are separable in feature space [5], [6]. This theoretically results in more accurate classifications for pattern recognition systems as the acceptable margin for error increases but does not necessarily reflect biomimetic control. The shortcoming associated with this form of training is that this type of instruction often leads to an internal focus of attention (focusing on one's own body movements, muscle contractions) rather than an external focus of attention (focusing on the effects of one's movements, prosthetic movement). Previous research has shown that having an internal focus of attention results in

less effective movements and motor learning, as it may impede with the body's natural and automatic control processes [7], [8]. In the context of prosthetic control, the end result is an observable decline in pattern recognition performance in the time following internally focused training [9].

Our objective was to develop a research and training platform intended for use among pediatric prosthesis wearers. "*Ice is Nice*" is a gamified platform which prompts users to practice making common grasping movements using their missing hand and uses the derived affected muscle activity as game control signals, thus providing the possibility for training with an external focus of attention. The long-term goal is to provide users with a low-stakes, yet engaging training environment that also enables researchers and clinicians to attain high quality data that quantifies training progression, game performance improvements, and the associated improvements in machine learning performance.

METHODS

Game Walkthrough

"*Ice is Nice*" is a side scrolling game that prompts children to perform different hand motions while recording relevant motor learning and machine learning metrics in the background. Upon starting the program, the user is brought to the main menu (Figure 1a). The user is then directed towards the administrator menu (Figure 1b). This interface allows the researcher to choose anywhere from two to five hand motions from a pool of ten that they wish the participant to practice. These motions were selected from the ten most commonly used in tasks of daily living [10]. The researcher is then directed towards the next screen (Figure 1c), where they may specify the total number of movement repetitions that the participant will be instructed to perform along with the frequency at which each occurs. This allows the researcher to emphasize specific hand motions, perhaps ones that the participant has difficulty performing. After completing this step, the researcher hands off control to the participant, allowing them to select their preferred character (a caribou or seal, Figure 1d, described further below). Following the character selection, the game begins. The character automatically walks across the screen and encounters an obstacle (an iceberg or hole in the ice, Figure 2a). The participant is then prompted to perform a movement and hold it. If held long enough, the character successfully jumps over the obstacle and walks towards the next one (Figure 2b).

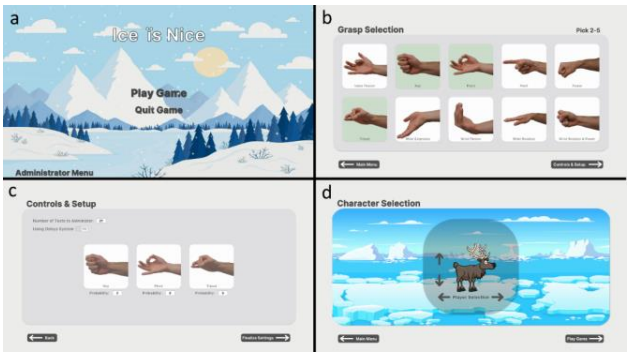

Figure 1: Upon program startup, the user first sees (a) the main menu. Next, the administrator menu is brought up for the researcher to (b) select desired motions and (c) specify how many total movements the participant will be instructed to complete along with the individual motion frequency. The participant may then (d) choose the character they wish to play as.

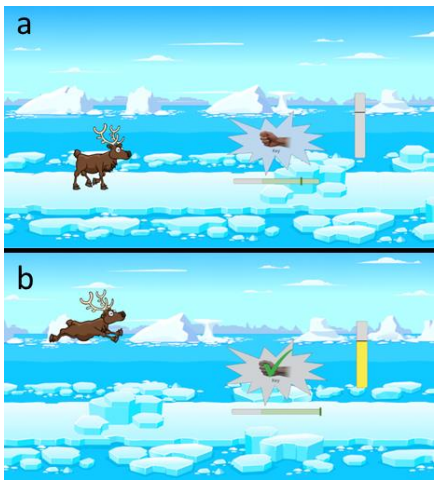

Figure 2: The user first (a) approaches an obstacle and is prompted to make a hand motion. Upon successfully holding the motion long enough, (b) the character jumps over the obstacle.

Game and Controller Design

Controlling one's affected muscles to operate a prosthesis, like any other learned motor skill, requires practice, repetition, and time. Our primary motivation was to ensure that this learning process is an engaging, motivating, and enjoyable experience. Several key design requirements shaped our final system.

Game control, involving the classification of hand movements, was designed to be hardware agnostic. This was achieved by integrating a real-time pattern recognition script with the game through a localhost TCP connection, using code written in MATLAB and Unity software. The latency of this connection was measured to be less than 1ms. The game received real-time input classification data from MATLAB representing predicted grasps as whole numbers ranging from zero to ten, inclusive (Table 1). A majority voting post-processing

technique was employed to improve classification stability, where each new prediction was placed into a buffer of length *n* and the prediction that occurred most frequent was the selected output control for the game. Thus, the game was able to take input derived from pattern recognition predictions in MATLAB based on a wide range of signals commonly used in the control of upper limb prostheses, including EMG, FMG, sonomyography, and others [11]. For example, to assess feasibility, we implemented a game control system that used surface electromyography (sEMG). Using our Delsys Trigno system, MATLAB recorded inputs from eight EMG electrodes at 2000Hz. We used a Linear Discriminant Analysis classifier that was trained on five features from the Hudgins feature set in the time-domain [12]. Hand grasp classifications were transmitted to Unity in real-time, and by using the majority voting scheme described above, the game successfully registered the attempted hand grasp to control the game. It was verified that this process retained communication response times below the commonly implemented maximum acceptable delay of 300ms [13].

Table 1: The provided numbering convention must be adhered to when connecting a custom real-time classification script to the game.

Grasp Name	Grasp ID
Index Flexion	0
Key	1
Pinch	2
Point	3
Power	4
Tripod	5
Wrist Extension	6
Wrist Flexion	7
Wrist Rotation	8
Wrist Rotation & Power	9
Rest	10

Promoting Engagement During Training

Particular attention was given to the game's design to maintain player engagement throughout. This is evident in the game's presentation and various mechanics, all designed to minimize the potential for player frustration and sustain engagement when misclassifications inevitably occur. For example, the game incorporates cartoonish graphics, lively animations, and vibrant color palettes to enhance visual appeal and retain attention. Additionally, players are provided with the opportunity to choose from a diverse range of characters and variations (Figure 3). A game mechanic designed to reduce the potential for frustration allows players to skip a prompted grasp motion by pressing the spacebar, ensuring they do not get stuck if they fatigue or are unable to perform a particular missing hand movement. Finally, the game provides ongoing positive feedback throughout.

Figure 3: A few of the character choices are shown in the above image.

Visual positive feedback was a key design criteria guiding game development. This was of particular importance as, in addition to fostering engagement beyond that of neutral or negative feedback[14], [15], the inclusion of visual feedback often results in the participant producing higher quality training and performance data [16]. One form of positive feedback employed throughout the game is a green checkmark displayed when the user successfully completes the required hand motion. This is paired with a horizontal progress bar and a vertical points bar (Figure 2). Together, the user is prompted to make the specified hand motion with an image of it, and a horizontal progress bar begins to advance, allowing the participant to prepare and time the start of their missing hand movement (muscle contraction). When this progress bar reaches the green colored region, the participant will begin receiving points for maintaining the appropriate missing hand movement. The vertical progress bar then gradually advances (fills up) as more points are required. Once a target amount is reached, a large green check mark is shown, the character jumps over the obstacle, and the game advances to the next hand movement.

Finally, to promote engagement and encourage the development and refinement of hand movement proficiency, the game provides the opportunity to adjust the difficulty of gameplay. Here, we implemented three adjustable parameters: one affecting the time a participant has to prepare for the required hand movement, another determining how long they must hold the movement (contract their muscles), and one more affecting the time between required movements. These settings were implemented to ensure that training sessions could be tailored to reflect the user's goals, whether it to emphasize making separable and consistent muscle contractions or to challenge the participant in terms of more rapidly achieving various hand movements.

DISCUSSION AND FUTURE WORK

"*Ice is Nice*" is a research and training platform designed for children (or adults) to practice the motor skills necessary for controlling pattern recognition-based prosthetic control systems. It enables researchers and clinicians to collect high-quality data that is captured in the background as the user interacts with a side-scrolling gameplay environment. It was designed to engage participants during training, which may be otherwise tedious, and also provide

opportunities to challenge participants through difficulty adjustments while minimizing the potential for frustration. Furthermore, the system was designed to be agnostic to prosthetic control systems, accepting number-coded hand grasp data. That is, any control system or software capable of exporting real-time movement predictions following our number-coded list can be accepted by "*Ice is Nice*" (in Unity). It can then be placed in its buffer, and use the built-in majority voting scheme to control the gameplay. We are now beginning testing with able-bodied cohorts and children with unilateral congenital below elbow deficiency operating the game using electromyography and ultrasound-based control systems. Additional game modifications that will be released in our next software update includes visually distinct, 'levels' of gameplay with preset degrees of difficulty, and alternative post-processing techniques. We aim to further evaluate the motor learning and training effects with use of our system, as well as refine it toward a stand-alone platform alongside a low-cost EMG band for take-home training applications.

REFERENCES

[1] M. A. Battraw, J. Fitzgerald, W. M. Joiner, M. A. James, A. M. Bagley, and J. S. Schofield, "A review of upper limb pediatric prostheses and perspectives on future advancements," *Prosthet. Orthot. Int.*, vol. 46, no. 3, pp. 267–273, Jun. 2022, doi: 10.1097/PXR.0000000000000094.

[2] E. A. Biddiss and T. T. Chau, "Upper limb prosthesis use and abandonment: A survey of the last 25 years," *Prosthet. Orthot. Int.*, vol. 31, no. 3, pp. 236–257, Sep. 2007, doi: 10.1080/03093640600994581.

[3] J. J. Fitzgerald, M. A. Battraw, M. A. James, A. M. Bagley, J. S. Schofield, and W. M. Joiner, "Moving a missing hand: children born with below elbow deficiency can enact hand grasp patterns with their residual muscles," *J. NeuroEngineering Rehabil.*, vol. 21, no. 1, p. 13, Jan. 2024, doi: 10.1186/s12984-024-01306-z.

[4] M. A. Battraw, J. Fitzgerald, M. A. James, A. M. Bagley, W. M. Joiner, and J. S. Schofield, "Understanding the capacity of children with congenital unilateral below-elbow deficiency to actuate their affected muscles," *Sci. Rep.*, vol. 14, no. 1, p. 4563, Feb. 2024, doi: 10.1038/s41598-024-54952-7.

[5] M. A. Powell, R. R. Kaliki, and N. V. Thakor, "User Training for Pattern Recognition-Based Myoelectric Prostheses: Improving Phantom Limb Movement Consistency and Distinguishability," *IEEE Trans. Neural Syst. Rehabil. Eng.*, vol. 22, no. 3, pp. 522–532, May 2014, doi: 10.1109/TNSRE.2013.2279737.

[6] A. D. Roche *et al.*, "A Structured Rehabilitation Protocol for Improved Multifunctional Prosthetic Control: A Case Study," *J. Vis. Exp.*, no. 105, p. 52968, Nov. 2015, doi: 10.3791/52968.

[7] B. Bruya, Ed., *Effortless Attention: A New Perspective in the Cognitive Science of Attention and Action*. The MIT Press, 2010. doi: 10.7551/mitpress/9780262013840.001.0001.

[8] G. Wulf, *Attention and motor skill learning.* in Attention and motor skill learning. Champaign, IL, US: Human Kinetics, 2007, pp. xi, 211.

[9] L. Resnik, H. (Helen) Huang, A. Winslow, D. L. Crouch, F. Zhang, and N. Wolk, "Evaluation of EMG pattern recognition for upper limb prosthesis control: a case study in comparison with direct myoelectric control," *J. NeuroEngineering Rehabil.*, vol. 15, no. 1, p. 23, Dec. 2018, doi: 10.1186/s12984-018-0361-3.

[10] J. Z. Zheng, S. De La Rosa, and A. M. Dollar, "An investigation of grasp type and frequency in daily household and machine shop tasks," in *2011 IEEE International Conference on Robotics and Automation*, Shanghai, China: IEEE, May 2011, pp. 4169–4175. doi: 10.1109/ICRA.2011.5980366.

[11] A. Marinelli *et al.*, "Active upper limb prostheses: a review on current state and upcoming breakthroughs," *Prog. Biomed. Eng.*, vol. 5, no. 1, p. 012001, Jan. 2023, doi: 10.1088/2516-1091/acac57.

[12] B. Hudgins, P. Parker, and R. N. Scott, "A new strategy for multifunction myoelectric control," *IEEE Trans. Biomed. Eng.*, vol. 40, no. 1, pp. 82–94, Jan. 1993, doi: 10.1109/10.204774.

[13] M. Asghari Oskoei and H. Hu, "Myoelectric control systems—A survey," *Biomed. Signal Process. Control*, vol. 2, no. 4, pp. 275–294, Oct. 2007, doi: 10.1016/j.bspc.2007.07.009.

[14] A. F. Lewis *et al.*, "Effects of positive social comparative feedback on motor sequence learning and performance expectancies," *Front. Psychol.*, vol. 13, p. 1005705, Jan. 2023, doi: 10.3389/fpsyg.2022.1005705.

[15] R. J. Klein and M. D. Robinson, "The negative feedback dysregulation effect: losses of motor control in response to negative feedback," *Cogn. Emot.*, vol. 33, no. 3, pp. 536–547, Apr. 2019, doi: 10.1080/02699931.2018.1463197.

[16] M. B. Kristoffersen, A. W. Franzke, C. K. Van Der Sluis, A. Murgia, and R. M. Bongers, "The Effect of Feedback During Training Sessions on Learning Pattern-Recognition-Based Prosthesis Control," *IEEE Trans. Neural Syst. Rehabil. Eng.*, vol. 27, no. 10, pp. 2087–2096, Oct. 2019, doi: 10.1109/TNSRE.2019.2929917.

Investigating The Speed-Accuracy Tradeoff in Discrimination of Electrotactile Stimuli

Felix Jarto[1], Sigrid Dupan[2]

[1]*School of Electrical and Electronic Engineering, University College Dublin, Ireland*

[2]*School of Public Health, Physiotherapy and Sports Science, University College Dublin, Ireland*

Abstract

Sensory feedback has been shown to improve the functionality of prosthetic devices in terms of increased control precision. This increase in control is related to the importance of sensory feedback in the context of motor control. To ensure precise control, ideal feedback should be recognized by the user both swiftly and accurately. Transcutaneous electrotactile stimulation is a prevalent choice for providing sensory feedback due to its non-invasive nature. However, it is not yet clear how to optimize this kind of stimulation for speed and accuracy of response. In this study, we set out to investigate how we can affect the Speed-Accuracy Tradeoff (SAT) during responses to an instantaneous change in electrotactile stimulation intensity. Nineteen participants completed an intensity discrimination task. Participants were asked to either prioritize speed or accuracy during specific blocks, while cognitive load, magnitude of intensity shift and direction of shift were manipulated. The results imply that the magnitude of intensity shift needs to be well beyond the just noticeable difference to ensure fast and accurate responses.

Introduction.

The noise in our motor system results in executed motions not necessarily aligning with the movements we planned. Sensory feedback allows us to perceive the difference between planned and executed motor actions and make small corrections on the fly [2]. In healthy individuals real-time, closed-loop movement control is enabled by the integration of tactile, proprioceptive and visual information [3], [4]. People with upper limb difference do not have access to tactile and proprioceptive information, and therefore mainly depend on visual feedback. The lack of feedback through other modalities results in users relying more on feedforward control processes [5]. In the case of prosthetics, this results in diminished control due to the loss of ability to make small movement corrections, such as spontaneously adjusting grip shape and force. In order to improve closed-loop sensorimotor control in prostheses, additional sensory information needs to be provided.

Providing extra feedback through additional modalities does not necessarily result in better control: if the feedback carries a high amount of uncertainty, its impact on control will be negligible. For this reason, additional feedback has to be easily recognizable and distinguishable [6]. It is also known that in any kind of closed-loop control environment, sensory feedback delays have to be minimized to improve control stability [7]. The necessity of having to be simultaneously both fast and accurate causes a speed-accuracy tradeoff (SAT) to appear [8], [9]. Due to the decision making process needing time to accumulate evidence necessary to make a judgment, the sensorimotor system is faced with a dilemma: it can make a fast decision which compromises the response accuracy or it can wait for more evidence, compromising the reaction time. In order to minimize the effect of this tradeoff on real-time control, it is not enough to provide sensory feedback through a faster modality, but the feedback also needs to include the same amount of information within a smaller timescale.

Transcutaneous electrotactile stimulation is an attractive choice for closed-loop feedback as it is non-invasive and energy efficient [10], on top of tactile stimuli registering faster than visual stimuli [11]. Electrotactile stimulation has been used before to close the loop during prosthetic control, either by conveying information regarding sense of touch (eg. grasping force [12], [13]) or proprioception (eg. finger positions [14]). These studies report improved control precision in both cases, further making electrotactile stimulation an appealing choice. Although electrotactile feedback has been investigated in the context of prosthetics, it is not yet clear how the choice

in parameters influences the SAT. Therefore, we investigated the SAT in a discrimination task, while varying both the perceived stimulation intensity and the cognitive load.

Methods

Participants

Nineteen participants (11 males, 8 females with mean age ± SD = 28 ± 5) without limb difference took part in the experiment. Participants provided written informed consent before the start of the experiment. The study was approved by the UCD Human Research Ethics Committee – Sciences (LS-22-46-Dupan).

Transcutaneous Electrotactile Stimulation

Electrotactile stimulation was provided using an analog stimulus isolator (A-M Systems Model 2200) which was controlled using an NI board (NI USB-6211) connected to the experimental PC running a Python script. Stimulation was provided as biphasic square waves, with frequency and amplitude fixed at 50Hz and 5mA respectively. Perceived stimulus intensity was modulated by increasing and decreasing the pulse width. Stimulator electrodes were placed above the flexor carpi radialis of the non-dominant forearm of the participants.

Experimental Protocol

Participants were asked to sit in front of a monitor and provide their responses using a numpad keyboard. The experiment consisted of 3 parts, which are represented in Fig. 1a. The experiment began with measuring the dynamic range (DR) of stimulation. The stimulation pulse width was increased from 50μs in 50μs increments, with the stimulus trains lasting 3 seconds. Participants were asked to press a button when they felt the stimulation, which resulted in the pulse width dropping by 100μs. The same intensity had to be matched 3 times in row for the detection threshold (DT) to be determined. Following that, the pulse width was increased to a point where the participant reported a feeling of pain or discomfort which corresponded to the pain threshold (PT). The DR was determined as the pulse width range between the DT to the PT.

The just noticeable difference (JND) was measured with respect to a stimulus set to 25% of the DR using a staircase procedure [15]. The participant was instructed to determine the stronger of two consecutive stimuli, with the compared intensity starting from 50% DR. The order of the reference and compared intensities was randomized. Every correct response resulted in the compared intensity dropping by 10μs and every incorrect one in the intensity rising by 20μs. JND was determined as the difference between the reference intensity and the average of the ten intensities, where a reversal has taken place.

During the experimental task, participants were asked to respond to an instantaneous shift in stimulus intensity via a button press indicating the direction of shift (higher or lower). The reference intensity was set at 25% DR and the magnitude of change in intensity corresponded to 1-4 times JND. The direction of intensity shift (rising/falling) was randomized over the trials. The first stimulus lasted between 2 and 4 seconds, while the second stimulus continued until the participants responded with the button press or timed out after 3 seconds. At the start of each block, participants were instructed to prioritize speed or accuracy in their response. To impose cognitive load, participants were asked to simultaneously listen to paragraphs from an audiobook (*Dr. Ox's Experiment* by Jules Verne) and answer a multiple choice question afterwards in half of the blocks [16], [17], [18]. Speed/Accuracy conditions were changed every block, while cognitive load conditions were changed every two blocks. The outcome variables of the task were response speed and response accuracy. A timeout was registered as an incorrect response with a reaction time of 3 seconds.

Results

Four-way ANOVA reveals that stimulus shift magnitude had a significant effect on both reaction times and response accuracies ($p < 0.001$ in both cases). In depth analysis revealed that a notable proportion of overall responses were timeouts at lower shift intensities (36.49% at 1xJND and 6.44% at 2xJND), most likely resulting from the participants not noticing the shift (Fig 1b.). Subsequent analysis shows significant differences between all shift intensities for reaction times ($p < 0.001$ in all cases); as shift intensities increase, the reaction times get faster

(Fig 1c). The presence of cognitive load only affected reaction times ($p < 0.001$, Fig. 1d), but not response accuracy ($p = 0.756$). In the case of shift direction, the analysis reveals an interaction effect with shift magnitude regarding both reaction times and response accuracies ($p = 0.0257$ and $p < 0.001$, respectively; Fig. 1e-f). Further analysis using a paired T-test revealed that a significant difference was only present for the lowest shift magnitude in both cases ($p = 0.0184$ and $p = 0.0012$ for reaction times and response accuracy respectively). Explicit instructions regarding focus on response speed or response accuracy did not have a significant effect on either reaction times ($p = 0.1945$) or response accuracies ($p = 0.0978$).

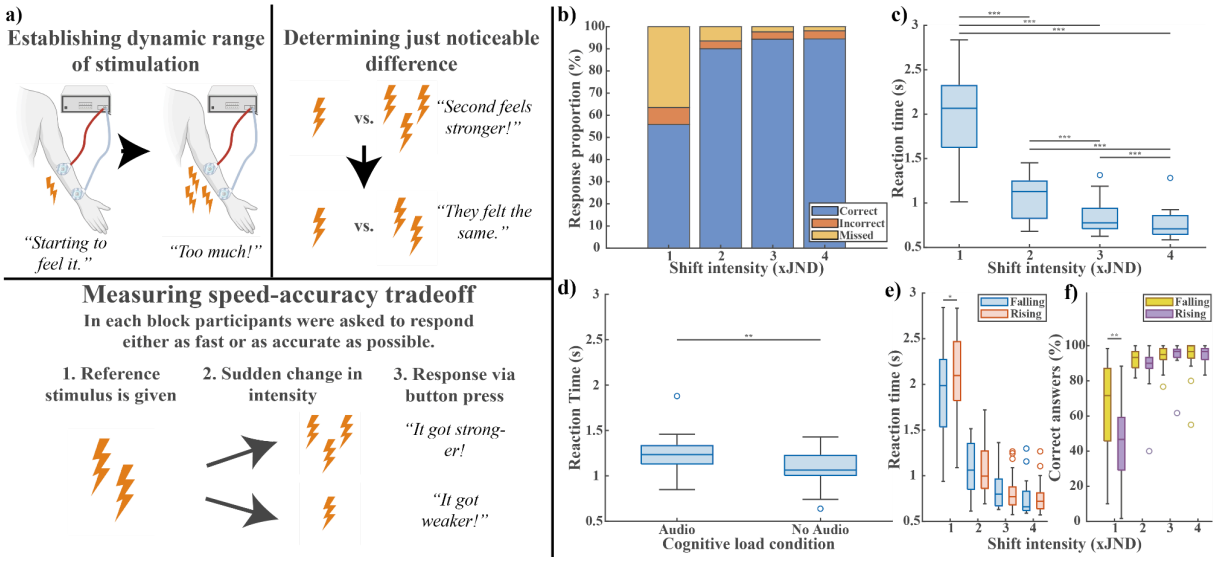

Figure 1: a.) Structure of experimental protocol. b.) Response proportions grouped by accuracy. c.) Average reaction times depending on shift intensities. d.) Average response times with and without the presence of cognitive load. e.) Interaction effect of shift direction and shift intensity regarding response times; a significant difference is only observable at the lowest intensity. f.) Interaction effect of shift direction and shift intensity regarding response accuracies; a significant difference is only observable at the lowest intensity.

Discussion

In this study, we investigated how stimulus-related and environmental variables affect the speed-accuracy tradeoff. We have shown that, during shifts in electrotactile stimulation, the intensity of shift significantly affects both response accuracies and reaction times. Higher shifts in intensity result in less missed shifts and overall significantly more correct responses. Reaction times also reduced significantly with increased shift intensity. Our results indicate that the presence of cognitive load only affects reaction times, but not response accuracies, which implies that accurate discrimination of electrotactile stimuli is possible even with divided focus. Additionally, we have shown that at lower shift intensities the response accuracy is affected differently depending on the direction of the shift, further reinforcing the importance of higher intensity shifts.

Previous research has shown that providing additional sensory information during prosthetic use eases the cognitive load on the user and allows for more precise control of the device [19], [20]. Sensory feedback is commonly used to inform the user on object interactions or hand/grip posture, replacing tactile or proprioceptive information, respectively [12], [13], [14]. We found that, for electrotactile stimulation, the stimulus shift intensity should be at least 3 times the value of the JND to ensure discrimination of the stimuli. Providing additional feedback which is both fast to register and easy to interpret could result in the decrease of cognitive load by alleviating the burden on the visual system, which in turn could improve sensorimotor control of the prosthetic.

Increased reaction times and decreased response accuracies at small shift intensities are in line with previous research regarding closed-loop error tracking using electrotactile feedback [21]. Continuous modulation of pulse-width along the DR - using small intensity shifts - resulted in high control delay during the task [21]. Based on our results, we hypothesize that the benefits of encoding information through higher intensity shifts are likely to carry over to closed-loop control in the form of decreased control delay.

References

[1] E. D. Papaleo *et al.*, 'Integration of proprioception in upper limb prostheses through non-invasive strategies: a review', *J. NeuroEngineering Rehabil.*, vol. 20, no. 1, p. 118, Sep. 2023.

[2] E. Todorov, 'Optimality principles in sensorimotor control', *Nat. Neurosci.*, vol. 7, no. 9, pp. 907–915, Sep. 2004.

[3] R. J. van Beers, A. C. Sittig, and J. J. D. van der Gon, 'Integration of Proprioceptive and Visual Position-Information: An Experimentally Supported Model', *J. Neurophysiol.*, vol. 81, no. 3, pp. 1355–1364, Mar. 1999.

[4] M. O. Ernst and M. S. Banks, 'Humans integrate visual and haptic information in a statistically optimal fashion', *Nature*, vol. 415, no. 6870, pp. 429–433, Jan. 2002.

[5] I. Saunders and S. Vijayakumar, 'The role of feed-forward and feedback processes for closed-loop prosthesis control', *J. NeuroEngineering Rehabil.*, vol. 8, no. 1, p. 60, Oct. 2011.

[6] J. W. Sensinger and S. Dosen, 'A Review of Sensory Feedback in Upper-Limb Prostheses From the Perspective of Human Motor Control', *Front. Neurosci.*, vol. 14, p. 345, Jun. 2020.

[7] T. G. Molnar, D. Hajdu, and T. Insperger, 'Chapter 10 - The Smith predictor, the modified Smith predictor, and the finite spectrum assignment: A comparative study', in *Stability, Control and Application of Time-delay Systems*, Q. Gao and H. R. Karimi, Eds., Butterworth-Heinemann, 2019.

[8] J. P. Gallivan *et al.*, 'Decision-making in sensorimotor control', *Nat. Rev. Neurosci.*, vol. 19, no. 9, pp. 519–534, Sep. 2018.

[9] R. P. Heitz, 'The speed-accuracy tradeoff: history, physiology, methodology, and behavior', *Front. Neurosci.*, vol. 8, Jun. 2014.

[10] K. Li *et al.*, 'Non-Invasive Stimulation-Based Tactile Sensation for Upper-Extremity Prosthesis: A Review', *IEEE Sens. J.*, vol. 17, no. 9, pp. 2625–2635, May 2017.

[11] M. Akamatsu, I. S. Mackenzie, and T. Hasbroucq, 'A comparison of tactile, auditory, and visual feedback in a pointing task using a mouse-type device', *Ergonomics*, vol. 38, no. 4, pp. 816–827, Apr. 1995.

[12] M. Isaković *et al.*, 'Electrotactile feedback improves performance and facilitates learning in the routine grasping task', *Eur. J. Transl. Myol.*, vol. 26, no. 3, Jun. 2016.

[13] M. A. Schweisfurth *et al.*, 'Electrotactile EMG feedback improves the control of prosthesis grasping force', *J. Neural Eng.*, vol. 13, no. 5, p. 056010, Oct. 2016.

[14] G. K. Patel *et al.*, 'Multichannel electrotactile feedback for simultaneous and proportional myoelectric control', *J. Neural Eng.*, vol. 13, no. 5, p. 056015, Oct. 2016.

[15] T. N. Cornsweet, 'The Staircase-Method in Psychophysics', *Am. J. Psychol.*, vol. 75, no. 3, p. 485, Sep. 1962.

[16] J. A. O'Sullivan *et al.*, 'Attentional Selection in a Cocktail Party Environment Can Be Decoded from Single-Trial EEG', *Cereb. Cortex*, vol. 25, no. 7, pp. 1697–1706, Jul. 2015.

[17] R. J. Nowosielski, L. M. Trick, and R. Toxopeus, 'Good distractions: Testing the effects of listening to an audiobook on driving performance in simple and complex road environments', *Accid. Anal. Prev.*, vol. 111, pp. 202–209, Feb. 2018.

[18] A. Atakanova *et al.*, 'Does listening to audiobooks affect gait behavior?', *BMC Sports Sci. Med. Rehabil.*, vol. 15, no. 1, p. 159, Nov. 2023.

[19] J. Park and M. Zahabi, 'Cognitive Workload Assessment of Prosthetic Devices: A Review of Literature and Meta-Analysis', *IEEE Trans. Hum.-Mach. Syst.*, vol. 52, no. 2, pp. 181–195, Apr. 2022.

[20] N. Thomas *et al.*, 'Neurophysiological Evaluation of Haptic Feedback for Myoelectric Prostheses', *IEEE Trans. Hum.-Mach. Syst.*, vol. 51, no. 3, pp. 253-264, June 2021.

[21] J. L. Dideriksen, I. U. Mercader, and S. Dosen, 'Closed-loop Control using Electrotactile Feedback Encoded in Frequency and Pulse Width', *IEEE Trans. Haptics*, vol. 13, no. 4, pp. 818–824, Oct. 2020.

INVESTIGATING THE UNIVERSALITY OF OPTICAL MYOGRAPHY

Simon Stuttaford, Jacopo Franco, Patrick Degenaar, Matthew Dyson

Newcastle University, School of Engineering, Microsystems Group

ABSTRACT

Optical myography, a lesser-known approach for monitoring muscle activity, may be influenced by factors such as skin tone, blood oxygenation, and the composition of the surrounding tissue. This study presents a preliminary investigation of optical myography across 20 limb-intact individuals with varying skin tones and one individual with limb difference. The findings underscore the approach's potential applicability across diverse populations, advancing its viability as a muscle monitoring technique.

INTRODUCTION

The vast majority of wearable systems designed to monitor muscle activity use electromyography, forcemyography or phonomyography [1]. Relatively little research has explored wearable photonic systems for monitoring muscles [1, 2]. As such, optical approaches are poorly understood [1]. Explanations for exact phenomenon measured are contradictory, ranging from changes in skeletal muscle oxygenation to movement of deep blood vessels [1, 3]. Additionally, the COVID-19 pandemic highlighted that optical biomedical sensors can have inherent ethnic biases; the accuracy of pulse oximetry having recently been found to depend on skin colour [4]. Furthermore, research in upper-limb prosthetics has stressed the importance of testing on end users, as conclusions drawn from studies using limb-intact individuals are not guaranteed to hold for individuals with limb-difference [5].

This research investigated the application of a novel photonic sensor to detect muscular movement in a residual limb and examined the impact of skin pigmentation on the recorded optical signal.

METHODS

Participants

One limb-different and twenty limb-intact participants took part in this study. Before participating in the study all participants provided written informed consent. Ethical approval was granted by the local committee at Newcastle University (ref: 21-029-FRA).

Recordings

Finger position: Finger position data were recorded using an Etee (TG0, UK) virtual reality (VR) controller at 100 Hz. For the participant with limb difference, finger position was recorded from the contralateral hand, and they were instructed to mirror finger movements with contractions in the residual limb.

Optical: Optical myography data were sampled at a rate of 500 Hz with a custom-made sensor [6]. For limb intact participants, the placement of the optical sensor targeted the flexor digitorum superficialis muscle which was located via palpation. For the limb different participant, the sensor was placed on, or close to, their EMG electrode site used for prosthesis control.

Electromyography: EMG data were sampled at 2000 Hz using a Trigno Quattro (Delsys, USA) sensor. Only recordings with the limb-different participant used EMG sensors. Two electrodes were placed on the muscle targeted by the optical sensor.

Protocol

Participants began at rest with their arm supported by a table. After a period of rest, the experimenter played a series of audible beeps for a total of 10 seconds at a time. The beeps played at a rate of 2.5 Hz and acted as a digital metronome. Participants were instructed to move their finger(s) in concert with the metronome, tapping the VR controller with the specified finger on each beep, and fully extending the finger between beeps. After the metronome had played for 10 seconds the beeps stopped, signalling the participant to relax. Participants were first given a practice run with the metronome before data collection began. A real-time plot of all sensor data was visible to the experimenter.

Analyses

Skin tone mapping: Skin tone data were collected using a digital camera (Canon EOS 1200D). Participants stood in a light-controlled room beside a colour correction palette commonly used in photography. Skin tone data were sampled from colour corrected images of the anterior forearm. Colour data were recorded using the CIELAB colour-space.

SNR calculation: The signal-to-noise ratio was calculated using the ratio of the signal power attributed to desired frequencies vs the power attributed to all other frequencies. The desired signal frequencies were taken to be below 5 Hz. Calculations were performed on optical data that had been filtered by a 4th order high-pass Butterworth filter at 1 Hz. Where statistical comparisons were used, SNR data across participants were assumed to be non-parametric.

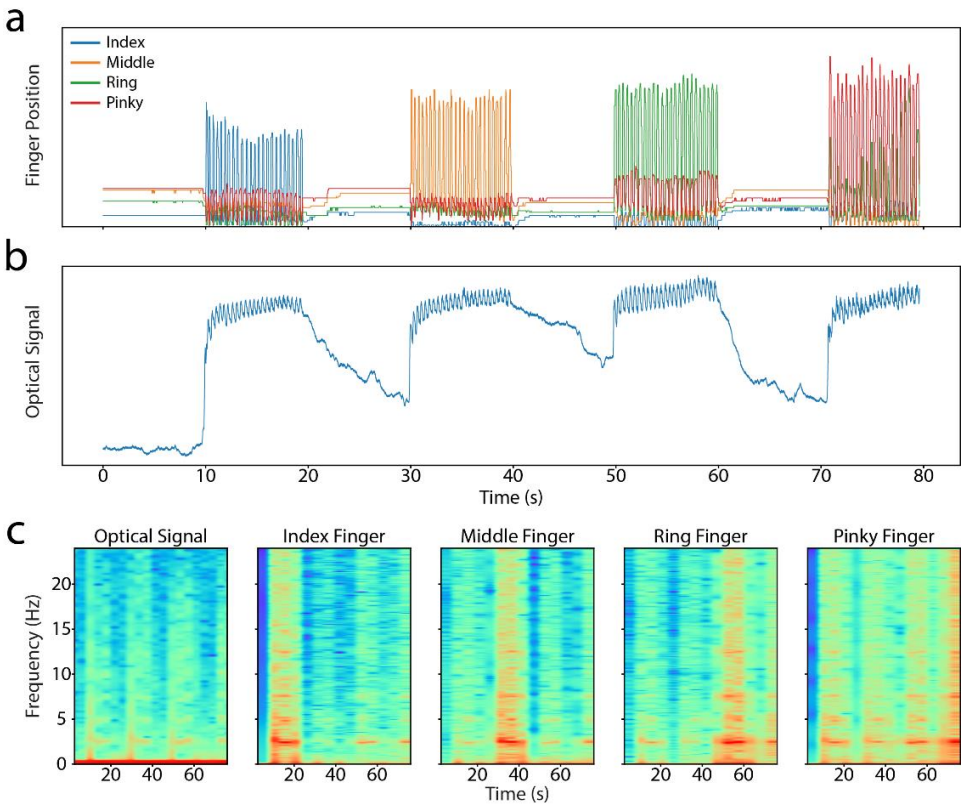

Figure 1: Finger movement detection using optical myography. The plots correspond to data collected from a single limb-intact participant. (a) Finger positions recorded from the VR controller. (b) Optical signal response. (a) & (b) are aligned on the time axis. (c) Time-frequency plots illustrating the detection of the 2.5 Hz finger movements across the optical sensor and VR controller.

RESULTS

Figure 1 shows the response of the optical signal during finger movement. Figure 1a shows that during the initial 12 seconds when the hand was at rest, the optical signal in Figure 1b is relatively stable. Once finger movement commences, an equally varying response is observed in the optical signal. When finger movement ceases, so do the rapid fluctuations of the optical signal. Then, the amplitude of the optical signal slowly decays, until the movement of the next finger, where the pattern repeats again. Figure 1c shows the time-frequency plots of the optical and the finger position data. For the optical signal, an increase in 2.5 Hz signal power can be seen repeating in concert with each finger's movement which is also confirmed to be approximately 2.5 Hz.

Figure 2 shows the effect of skin tone on the optical signal. No correlation was found between the skin tone and optical signal SNR (r = 0.06, p = 0.79), depicted in Figure 2a. Whereas, a strong positive correlation was found between skin tone and the baseline value of the optical signal when the participant is at rest (r = 0.63, p < 0.01).

Figure 3 shows an overview of the data collected from the residual limb of a single participant. Figure 3a & 3b shows a similar pattern, previously seen in Figure 1, between finger movement (on the intact limb) with the optical signal. In addition, a comparable pattern between the optical signal and EMG data can be seen in Figure 3b & 3d, with peaks of the EMG signal appearing to occur at similar points in time to the peaks of the optical signal. Finally, time-frequency plots of optical and EMG data are shown in Figure 3d & 3e. Increased optical signal power is evident around 2.5 Hz, and repeats in accordance with the metronome and finger movement. Likewise, the envelope of the EMG signal also has increased signal power at around 2.5 Hz. Both time-frequency plots show increased signal power occurring at the same moment in time, both aligning with the start and end of the metronome sound (and hence contralateral finger movement).

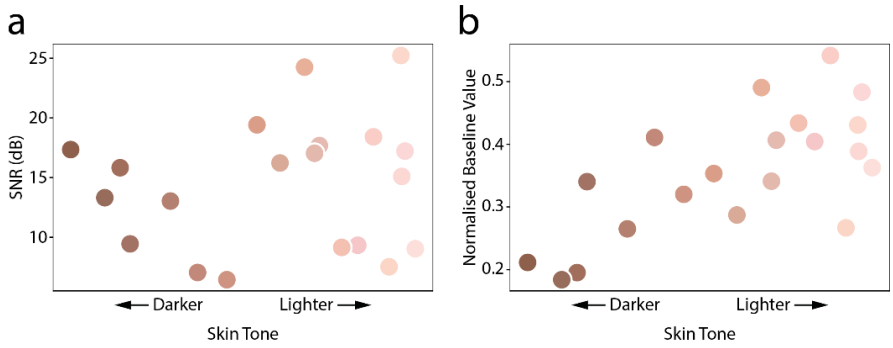

Figure 2: Effect of skin tone on optical signal properties. (a) Differences in signal-to-noise ratio across skin tones. (b) Differences in signal baselines across skin tones. Points correspond to individual participants. Point hues visually reflect the participants' measured skin tone.

DISCUSSION

Several theories have been proposed to explain the physiological source of optical myography signals, such as skeletal muscle oxygenation or blood vessel movement [1, 3]. This study showed that the optical sensor not only detected the onset and offset of movements with relatively little latency, but the frequency of the resultant optical signal also mirrored the physical rate of movement. This tight coupling between movement and signal response suggests that the optical signal reflects biomechanical changes associated with physical movement.

It has been shown that skin tone can affect properties of optical signals [4]. Furthermore, research in prosthetics has highlighted the importance of testing on individuals with limb-difference [5]. In order to assess the efficacy of the approach for a range of individuals, we tested participants with different skin tones or limb-difference. While a strong relationship was found between skin tone and the baseline optical signal, no relationship was found between skin tone and the SNR during finger movement. Testing on a limb different participant yielded similar results to limb-intact participants. Anecdotally, locating the ideal sensor placement on the residual limb was more challenging. This could be due to increased fatty tissue around the residual limb which may affect the SNR. However, to increase the certainty of our findings, we remain committed to expanding the sample size with the goal of enhancing diversity and inclusivity.

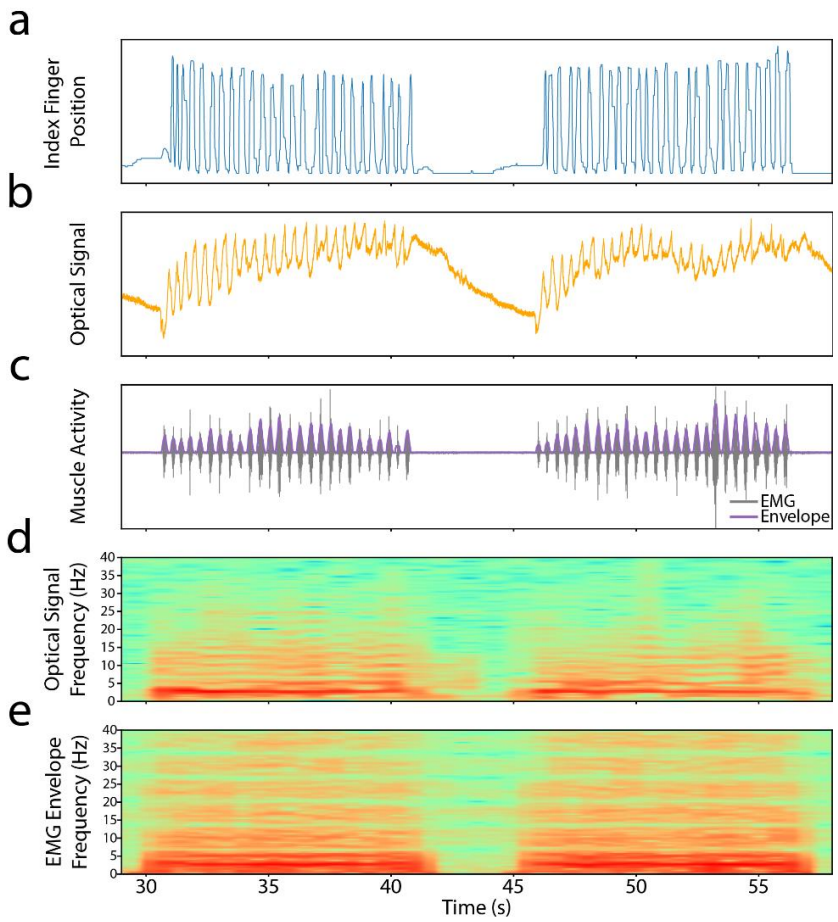

Figure 3: Overview of data collected from a residual limb. (a) Index finger position from the contralateral hand. (b – e) Recordings from residual limb. (b) & (c) Optical and muscle activity data, respectively. (d) & (e) Time-frequency plots of the optical signal and EMG envelope, respectively. Figures are temporally aligned on the x-axis.

ACKNOWLEDGEMENTS

This research was supported by Transformative Innovation in the Design of Assisted Living products and services (TIDAL N+) (Grant Number: EP/W000717/1).

REFERENCES

[1] H. Wang *et al*., "Wearable super-resolution muscle–machine interfacing," *Front. Neurosci.*, vol. 16, 2022.

[2] J. McIntosh, A. Marzo, M. Fraser, "SensIR: Detecting hand gestures with a wearable bracelet using infrared transmission and reflection," *submitted to J. Examples, in Proc. of the 30th Ann. ACM Symposium on User Interface Software and Technology*, 2017.

[3] M. Ferrari, M. Muthalib, V. Quaresima, "The use of near-infrared spectroscopy in understanding skeletal muscle physiology: recent developments," *Philos. Trans. R. Soc. A*, vol. 268, pp. 4577-4590, 2011.

[4] M. D. Keller, B. Harrison-Smith, C. Patil, M. S. Arefin, "Skin colour affects the accuracy of medical oxygen sensors," *Nature*, 2022.

[5] G. Li, A. E. Schultz, T. A. Kuiken, "Quantifying pattern recognition-based myoelectric control of multifunctional transradial prostheses," *IEEE*, vol. 18, pp. 185-192, 2010.

[6] J. Franco, S. Stuttaford, M. Dyson, P. Degenaar, "Optical sensing of muscle activity," *MEC Symp*., 2024. *(Submitted)*.

MEDIUM DENSITY DIGITAL ELECTROMYOGRAPHY SENSING SYSTEM

Eisa Aghchehli[1,2], Chenfei Ma[2], Matthew Dyson[1] and Kianoush Nazarpour[2]

[1]*School of Engineering, Newcastle University, UK.*

[2]*School of Informatics, The University of Edinburgh, UK.*

ABSTRACT

Surface electromyographic (EMG) signals are widely used for diagnostic and control purposes. Traditional EMG recordings typically use sparse electrode setups, limiting their use in dynamic environments like prosthetics or virtual reality. We propose a medium-density EMG armband design that leverages digital technology to capture EMG data from 21 channels. This system, designed to be more practical for everyday use and research, was tested against traditional single-channel methods for classifying six hand gestures using machine learning. Our results indicate the medium-density EMG system offers superior gesture classification accuracy, making it a valuable tool for real-world applications. We aim to further enhance this EMG recording setup and introduce it an open-source platform to the MEC community at the conference.

INTRODUCTION

Electromyography has emerged as a transformative technology in the area of human-machine interfacing, including prosthetics control, offering unique opportunities to bridge the interface between human neural activity and machine operations [1]. Its applications extend far beyond traditional diagnostics, leading into the development of advanced immersive virtual (VR) [2] and extended reality (XR) environments [3], rehabilitation programs [4], and myoelectric prosthetics [5,6]. The essence of EMG lies in its ability to decode the electrical signals generated by motor units during contraction, providing a direct pathway to understanding and harnessing human intent in real-time. This capability is pivotal in creating more intuitive and responsive systems that can cater to a wide spectrum of needs, from assisting individuals with mobility impairments to enhancing user experiences in digital realms.

In the domain of prosthetic development, EMG technology has the potential to be a game-changer and enable the development of limbs that can respond to the user's muscle signals with precision and fluidity. This not only restores a degree of lost functionality for amputees but also empowers them with a sense of autonomy and improved quality of life [6]. Similarly, in rehabilitation, EMG-based systems offer valuable insights into muscle performance and recovery progress. The integration of EMG into VR and XR applications [2, 3] opens new frontiers for interactive technologies, allowing users to control virtual environments through natural body movements.

However, the widespread adoption of EMG technology faces challenges, primarily due to the limitations of existing recording systems [7]. Traditional setups often require a trade-off between signal detail and system portability. High-density arrays [8] offer rich data at the expense of mobility and ease of use, while sparse configurations sacrifice detail for simplicity. Recognizing this gap, the proposed medium-density EMG recording system, implemented as an easily wearable armband, aims to overcome these obstacles. By utilising the principles of digital body area networks (BAN), this innovative approach seeks to provide a balanced solution that offers detailed signal acquisition without compromising on user comfort and mobility. This development not only stands to practically use the way multi-channel EMG is applied across various fields but also emphasises the potential for solid integration of human physiological signals into the rehabilitation and control systems.

We are excited to announce the introduction of our Medium Density System at the upcoming MEC Conference. Our platform will be presented alongside detailed designs and firmware, with the intention of enabling the community to reproduce it for further research. By openly sharing our work, we aim to foster collaboration and drive innovation within the research community. We look forward to engaging with fellow researchers and enthusiasts at the conference as we collectively advance the field.

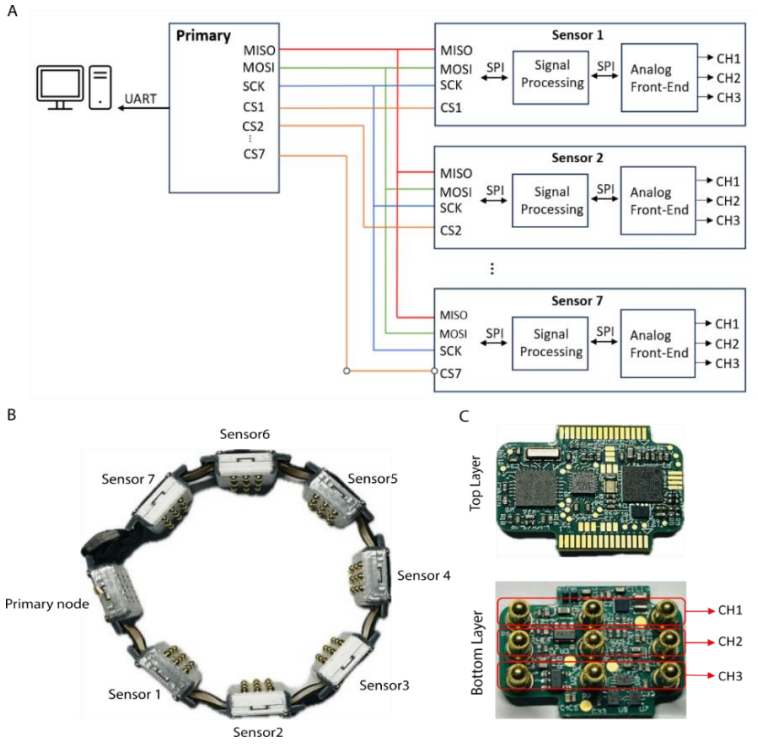

Figure 1: A) Overall block diagram of the system. B) The proposed armband. C) Two sides of sensor's PCB and number of channels on each PCB.

METHODS

Hardware

Figure 1A shows the overall diagram of the system. Each EMG sensor consists of two subsystems for analog front-end (AFE) amplification and EMG signal processing. The front-end circuit is built around an ADS1293 chip (Texas Instrument co., USA), with a built-in fixed gain amplifier and three channels, 24 bits analog to digital converter (ADC). Each channel is connected to two active electrodes for differential recording, along with a reference electrode, namely, E1, E2, and E0, respectively. The reference electrode is connected to the system ground. The EMG signals have been sampled at 1067 Hz. The EMG processing unit comprises an ARM CortexM4 based 32-bit flash microcontroller (STM32L433RCI3, ST Microelectronics). A 16MHz serial peripheral interface (SPI) connects the AFE subsystem to the signal processing subsystem. The EMG processing unit features a 2nd order infinite impulse response (IIR) Butterworth band-pass filter [25-350 Hz] which cancels undesired spectral components. Power-line interference is eliminated by a 2nd order IIR Butterworth notch filter, with cut-off frequency of 50 Hz.

For the sensor contacts, commercially available, gold-coated stainless steel has been used, which were housed in a 3D-printed case. The dimensions of the case met clinical standards and fitted comfortably around subjects' forearm as an armband. The design of the case was crafted using Fusion360, 3D designs and modelling software. To print the case, Bambu Studio software was employed to slice the model into printable layers. The case was then printed on a Bambu Lab P1S printer, with generic PLA (Polylactic Acid) as the printing material. Figure1B and 1C, show the final prototype armband and an 8-layer Printed Circuit Board (PCB) designed for the Primary and secondary nodes.

The network of EMG sensors is structured of two different types of nodes, namely, primary, and secondary. The former serves as a communication initiator and network synchronizer, and data handler and each sensor node acts as a secondary nodes. The SPI bus with a speed of 32 MHz enables data exchange between the primary and all secondary nodes. Each sensor is controlled with chip-select pin where the primary node request in sequence from each sensor. The primary node transfers data from all sensors through Universal Synchronous/asynchronous Receiver/Transmitter (USART) to a computer using USB to TTL Serial Cable (DSD TECH).

Experiment Design

The local ethics committee at Newcastle University (reference number: 20-DYS-050) approved this study. The experiment involved 10 participants, ranging in age from 19 to 43, including 2 females and 8 males. They signed an informed consent. They were tasked with performing six different movements: power grip, lateral pinch, tripod grip, pointer (extension), hand opening, and rest, with each movement repeated in 10 trials. During each trial, participants followed a structured sequence involving 3 seconds of the specified movement followed by 5 seconds of relaxation. Data collection and labelling were conducted automatically using the Axopy platform. The analytical models were developed in Python, utilizing the scikit-learn library for data processing and analysis. Programs ran on a DELL Latitude 5431 laptop, with 12th Gen Intel(R) Core™ i7-1270P, 2200MHz CPU, 32GB of memory.

Feature Extraction

Raw EMG data is too complex to be decoded with such a modest amount of data. Two features were adopted in the experiment, namely waveform length and log variance. They are commonly employed in the EMG experiment, meanwhile they are cost-efficient in terms of computation.

Machine Learning Modelling

Linear discriminant analysis (LDA) is one of the most adopted supervised machine learning algorithm, which exhibits a versatile mastery on both data dimensionality reduction and classification. The programming of the LDA model was implemented in Python, with scikit-learn library. 'Svd', or Singular Value Decomposition, was chosen as the solver for its efficiency with large feature sets. SVD reduces data dimensions by decomposing a matrix into three matrices, capturing the data's essential characteristics in a simplified form [9]. This method is ideal for processing extensive datasets, allowing for effective analysis and classification without significant information loss. The default number of components was set to 5 (n_class - 1), aiming to manage the substantial number of input features - 42 in total, calculated from 2 EMG features across 7 sensors and 3 channels. This approach to dimensionality reduction was intended to enhance the model's robustness while simultaneously lowering computational demands.

The data collection was partitioned into an 80% training set and a 20% testing set, shuffled and reapplied five times to facilitate a 5-fold cross-validation process. During this process, 80% of the data along with its labels were employed to train the LDA model, and the remaining 20% was used to evaluate the model's accuracy by comparing the predicted outcomes against the actual labels. This training and testing process was executed in parallel across five different conditions to ensure a comprehensive comparison. These conditions included the use of all three channels per sensor, three repetitions for each of the first, second, and third channels independently, and three repetitions using a randomly selected channel, applied consistently across all users.

RESULTS

Figures 2A and 2B show the experiment setup and the sample of raw EMG data have been recorded through all 21 input channels, respectively. Figure 2C presents the cumulative findings from a study involving 10 participants, where we explored the efficacy of five unique configurations for channel selection. These configurations include the use of three independent channels, as well as the first, second, and third input channels treated as separate entities, in addition to a scenario involving randomly chosen channels. The objective was to assess and compare their impact on classification accuracy. The data depicted in the graph reveals that the approach utilizing three independent input channels surpassed the performance of other configurations. This outcome suggests that medium-density electrodes, without expanding the spatial recording area, can significantly improve the precision of control systems in interpreting signals.

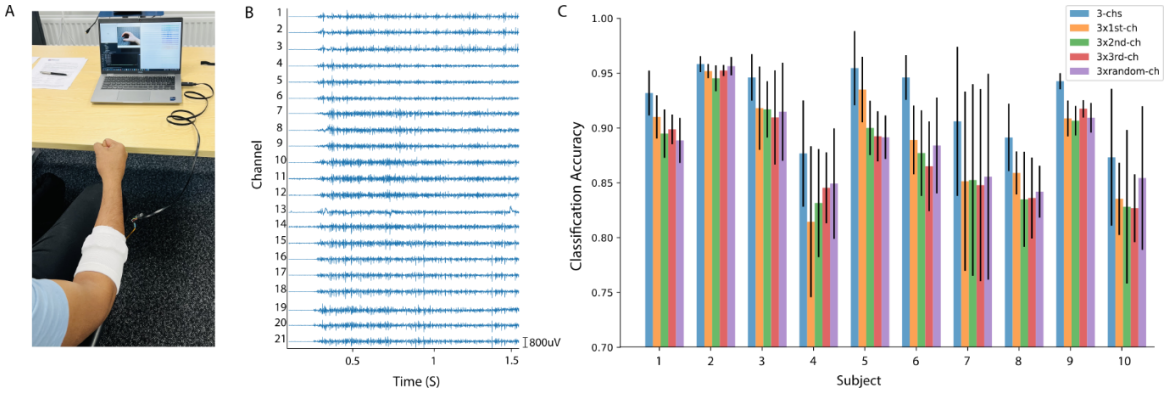

Figure 2: A) Experiment setup. B) Recorded raw EMG data over 21 input channels. C) Results on classification accuracy across subjects have been analyzed. Five distinct configurations to identify the optimal channel selection strategy have been examined.

ACKNOWLEDGEMENTS

This work was supported in part by funding from European Union's Horizon 2020 research and innovation programme under the Marie Skłodowska Curie grant agreement RISE–WELL (860173) and by funding from Engineering and Physical Sciences, UK (EP/R004242/2).

REFERENCES

[1] H. Wang, S. Zuo, M. Cerezo-Sánchez *et al.*, "Wearable super-resolution muscle–machine interfacing," *Frontiers in Neuroscience*, vol. 16, pp. 1020546, 2022.

[2] A. Dwivedi, Y. Kwon, and M. Liarokapis, "Emg-based decoding of manipulation motions in virtual reality: Towards immersive interfaces." pp. 3296-3303.

[3] A. Gaballa, R. S. Cavalcante, E. Lamounier *et al.*, "Extended Reality "X-Reality" for Prosthesis Training of Upper-Limb Amputees: A Review on Current and Future Clinical Potential," *IEEE Transactions on Neural Systems and Rehabilitation Engineering*, vol. 30, pp. 1652-1663, 2022.

[4] F. Zhang, L. Yang, and Y. Fu, "Development and Test of a Spasm Sensor for Hand Rehabilitation Exoskeleton," *IEEE Transactions on Instrumentation and Measurement*, vol. 71, pp. 1-8, 2021.

[5] S. Lee, and G. Saridis, "The control of a prosthetic arm by EMG pattern recognition," *IEEE Transactions on automatic control*, vol. 29, no. 4, pp. 290-302, 1984.

[6] M. Ahsan, M. I. Ibrahimy, and O. O. Khalifa, "Advances in electromyogram signal classification to improve the quality of life for the disabled and aged people," *Journal of Computer Science*, vol. 6, no. 7, pp. 706, 2010.

[7] N. Parajuli, N. Sreenivasan, P. Bifulco *et al.*, "Real-time EMG based pattern recognition control for hand prostheses: A review on existing methods, challenges and future implementation," *Sensors*, vol. 19, no. 20, pp. 4596, 2019.

[8] B. G. Lapatki, J. P. Van Dijk, I. E. Jonas *et al.*, "A thin, flexible multielectrode grid for high-density surface EMG," *Journal of Applied Physiology*, vol. 96, no. 1, pp. 327-336, 2004.

[9] A. Tharwat, T. Gaber, A. Ibrahim *et al.*, "Linear discriminant analysis: A detailed tutorial," *AI communications*, vol. 30, no. 2, pp. 169-190, 2017.

PATTERN SEPARABILITY VISUAL FEEDBACK TO IMPROVE PATTERN RECOGNITION DECODING PERFORMANCE

György M. Lévay[1*], Ruichen Yang[2*], Christopher L. Hunt[1], Megan C. Hodgson[1], Rahul R. Kaliki[1], and Nitish V. Thakor[2]

[1]Infinite Biomedical Technologies, LLC, Baltimore, MD, [2]The Johns Hopkins University, Baltimore, MD

* Equal Contribution

ABSTRACT

State-of-the-art myoelectric upper limb prostheses control often utilize pattern recognition (PR) systems that translate electromyograph (EMG) activity to a desired movement. As possible prosthesis movements increase, users have difficulty generating sufficiently separable EMG signals that reliably operate all possible degrees of freedom. Current training regimens attempt to increase the separability of a user's EMG signals through trial-and-error, where a therapist prompts a user to generate EMG signals and provides advice based on the strength and channel distribution of the EMG. In this work, we present a novel visual feedback interface that allows users to observe how their EMG signals affect PR output directly.

INTRODUCTION

Myoelectric control is a widely used method for the control of multi-articulated prosthetic devices. Myoelectric control operates by capturing electromyographic (EMG) signals generated during the user's muscle contractions and pattern recognition (PR) methods can be utilized to classify data into separate groups. Once these patterns of EMG activity have been established, they can serve as indicators for future EMG input, facilitating the identification of various movements [1]. While several factors contribute to the adoption of PR-based myoelectric control, low acceptance of prosthetic devices among individuals with upper limb loss (ULL) underscores significant challenges [2]. Experimental robustness does not necessarily equate to practical functionality and for novice users, there is often a steep learning curve to attain control proficiency [3]. Potential misclassifications can stem from a variety of environmental factors, including motion artifacts, electrode displacement, variations in limb positioning [4], and muscle fatigue. Furthermore, as the complexity and quantity of gestures employed in PR systems expand, the differentiation between each pattern becomes less discernible, leading to system confusion [5].

Previous literature has supported that human motor learning-based training plays a pivotal role in enhancing myoelectric PR-based prosthesis control, improving both accuracy and adaptability [6], [7], [8]. Existing training programs encompass various approaches, including motor imagery, which visually represents the picture of intended movements to the user, EMG training games that integrate proportional and derivative control into gameplay, and 2D virtual arm training that concurrently displays the user's movements on a screen [8], [9]. However, for a more defined separation of gesture classes, the core solution lies in either shifting the classes within the feature space to augment interclass distance or reducing intra-class variability [7]. Enhancing control strategy performance in the aforementioned training methods poses a challenge without insight into the underlying algorithm's performance, as users only have a 'black box' perspective of input-output interactions. This deficiency may obscure the understanding of a performance issue's origins, thereby limiting the users' ability to make informed, strategic adjustments, particularly as the complexity and number of gestures escalate [10].

In this work, we present a novel 3D visual feedback system designed to bridge the gap between the user and the pattern recognition system. Our system addresses the challenge of understanding the input-output control relationship in multi-gesture myoelectric control. PR training outcomes are showcased within a 3D interactive platform, wherein gesture relationships can be intuitively observed through their positioning in the feature space. Through this innovation, we aim to bolster the training-induced enhancement of control quality in myoelectric PR-based prostheses.

METHODS

This study was conducted in accordance with a protocol approved by the Johns Hopkins University School of Medicine Institutional Review Board. Twelve able-bodied participants, 6 males and 6 females, were recruited to take part in a 10-day longitudinal experiment. Participants varied in age from 18 to 22. No participants had previous experience with PR-based myoelectric control. Participant EMG signals were recorded using the 8 channel Myoband (Thalmic Labs, Ontario, Canada) positioned on the subject's dominant arm. Additionally, participants wore a bypass prosthesis to incorporate noise conditions from load and fatigue, and movements were performed in multiple spatial locations to incorporate the limb position effect.

Training Methods

Participants were provided one of two methods to visualize their control during the exploration period: (1) an experimental, 3D visualization of the pattern recognition decision-space; and (2) a controllable virtual arm (Figure 1).

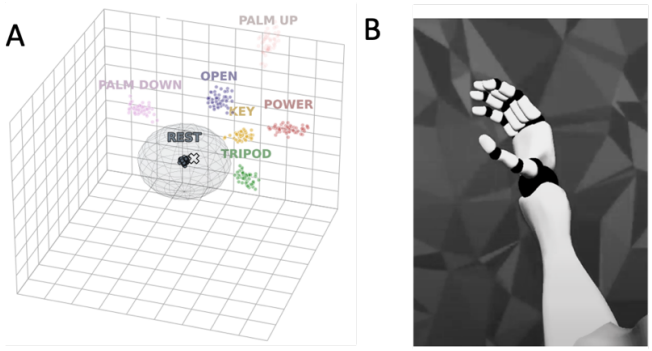

Figure 1. This figure shows the training methods employed in the study: (A) the 3D Visual System and; (B) the Virtual Arm.

The 3D control visualization projects the individual's incoming EMG data into the decision-space of the PR-based control method. This is accomplished by first undergoing a standard calibration regiment for PR-based control, where a calibration data set of EMG samples is collected on a class-by-class basis to generate a classifier. This calibration set is then projected into a 3-dimensional subspace, optimizing for low intra-cluster variability and high inter-cluster distance. During the evaluation periods, EMG activity of subjects was projected within the same training basis to represent where an individual's current EMG activity lies within the projection space. Within the visualization, the original training data is represented as coloured clusters of data points and the individual's current EMG activity is represented as a cursor. The cursor's position is modulated in real time by the user's EMG activity, allowing the participant to directly observe how their changing EMG patterns affect the proximity of their current pattern to the data the PR-based control method was calibrated with. In this way, participants receive direct visual feedback on the discriminability of their calibration data and the repeatability of their control as well as an opportunity to generate and observe how novel patterns of EMG activity map to regions of the decision-space (Figure 1a). In contrast, the virtual arm training method allows participants to operate a virtual model of an arm as if it were a real-world prosthesis (Figure 1b).

Experiment Protocols

Participants were evenly split into two groups of six, each comprising three males and three females: one experimental group utilizing the 3D visual feedback system, and a control group granted access to a real-time controllable virtual prosthesis. Each day, both participant groups underwent a calibration phase to capture EMG signals used for training the PR algorithm. From days 1 to 4, the participants performed a set of five gestures. This was increased to six distinct movements on day 5, and by day 7, they were executing a total of nine distinct movements (rest, open, power, pronation, supination, tripod, key, index point, pinch). Following the initial calibration phase, both participant groups were granted an exploration period to adjust their calibration data. Subjects had the flexibility to engage in practice sessions and refine their gestures if they found their control to be unsatisfactory and were allowed to recalibrate individual movements any number of times.

During this phase, the experimental group had access to real-time feedback from a 3D visual feedback system, while the control group had access solely to a virtual arm. To maintain consistency and fairness, time constraints were established for both groups: three minutes were allotted per movement (excluding rest). After the adaptation period, all participants' control proficiency was assessed following a Fitts Law assessment protocol (Figure 2c-d) [11].

During the testing phase, subjects were centrally positioned, with a display screen to their right and a numbered board to their left (Figure 2a). The screen presented the Fitts Law test and subjects were required to perform the task

with alternating limb positions, with classified hand grasps modulating the size of the ring and classified wrist movements modulating its orientation. Each task had a time limit of 15 seconds. The total number of tasks was determined by the total number of gestures: four movements correspond to 18, six movements to 36, and eight movements to 54 tasks. The control proficiency of subjects was evaluated based on four metrics of the Fitts Law test: completion rate, overshoot per trial (OT), path efficiency (PE), and throughput (TP) [11].

An 11th session was completed 30 days after the last session to gauge the long-term impact of the 3D visual system with the exact same setup.

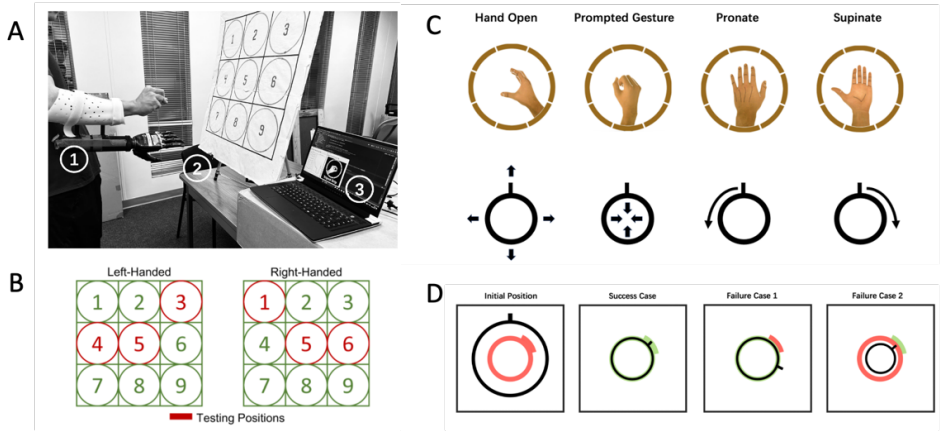

Figure 2. (A) Physical Setup for the Experiment: 1) a bypass prosthesis to emulate the weight-bearing experience; 2) a numbered board to achieve postural variance; and 3) a screen to display the Fitts Law Test. (B) An enumeration of the testing positions for the Fitts Law Tests. (C) In the Fitts Law Test, subjects will manoeuvre a black ring with open/close gestures, along with a protrusion on the ring with wrist rotation gestures. (D) Subjects are tasked with aligning to the red ring and protrusion. A trial is deemed successful only when both the ring and protrusion are aligned accurately within a timeframe of 15 seconds.

RESULTS

In this 10-day study involving twelve novice subjects, new movements were introduced in the first, fifth, and eighth sessions. As depicted in Figure 3a, the experimental group consistently outperformed the control group in terms of mean task completion rate.

A notable distinction between the two groups was observed in their ability to adapt to heightened control complexity. On the fifth day, the completion rate of the experimental group dipped from 0.97 ± 0.07 (mean $\pm$ standard deviation) to 0.83 ± 0.1 relative to the previous day, while the control group saw a more pronounced drop from 0.77 ± 0.23 to 0.51 ± 0.29. The divergence in performance was further amplified on the eighth day; the experimental group experienced a marginal decline in completion rate from 0.92 ± 0.12 to 0.86 ± 0.14 since day seven, whereas the control group exhibited a substantial decrement from 0.86 ± 0.07 to 0.46 ± 0.31. In both instances, the difference between the two groups was significant on the day following the introduction of new movements, a contrast to their previous day, where no significant difference was observed.

In terms of OT, PE and TP, the experimental group consistently outperformed the control group as shown on Figure 3b-d, although not at the rate indicated by the CR metric.

DISCUSSION

Throughout all sessions, the experimental group utilizing the 3D visual feedback system exhibited higher mean values for three metrics: CR, PE, and TP, and a lower mean for OT. This shows that the 3D system group surpassed the virtual arm group in all aspects of control proficiency. Based on feedback from participants, the experimental group reported less difficulty in modifying and fine-tuning movements and were able to refine their gestures effectively by observing overlaps in the visualization system. However, the results for OT, PE, and TP do not appear to align with the trend of increased control proficiency leading to increased differences between the two groups.

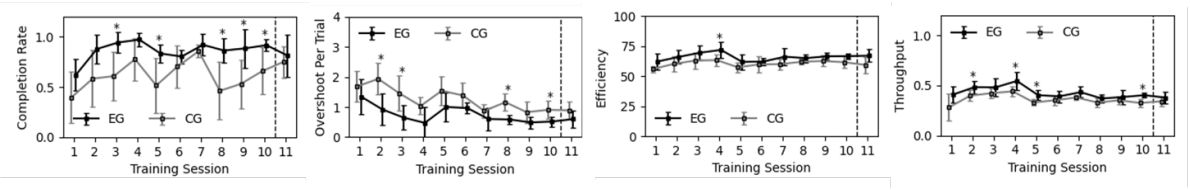

Figure 3. The results show the mean and standard deviation of the experimental group (EG) and control group (CG) over ten sessions, along with an additional return session conducted 30 days after session 10. In the span from session 1 to 4, four gestures were involved in calibration (excluding the resting position); in session 5, two additional movements were incorporated, and in session 8, two further movements were added. These movement differences separate the test into three segments. A dashed line delineates the return experiment results from the original test data. * indicate sessions wherein the difference between the experimental group and control group was statistically significant ($p < 0.05$).

The most plausible explanation for this affect is the decline in classification accuracy. Successfully executing the gestures required by the trial is crucial for task completion as well as incurring an overshoot, since overshoot is based on the over-application of the correct movement. This shows a limitation of this study, that a metric that captures failure to initialize an intended movement is missing.

The findings from the 11th session continue to highlight the experimental group's superior performance in all mean values, however the gains washed out over the 30-day period, suggesting a diminishing advantage conferred by the 3D system on subjects when training is suspended.

ACKNOWLEDGMENTS

This work was supported by the National Institutes of Health NIH U44NS119842.

REFERENCES

[1] Parajuli N, Sreenivasan N, Bifulco P, Cesarelli M, Savino S, Niola V, Esposito D, Hamilton TJ, Naik GR, Gunawardana U, Gargiulo GD. Real-time EMG based pattern recognition control for hand prostheses: A review on existing methods, challenges and future implementation. Sensors. 2019 Oct 22;19(20):4596.F.

[2] Atkins DJ, Heard DC, Donovan WH. Epidemiologic overview of individuals with upper-limb loss and their reported research priorities. Jpo: Journal of prosthetics and orthotics. 1996 Jan 1;8(1):2-11.\

[3] Bouwsema H, van der Sluis CK, Bongers RM. Changes in performance over time while learning to use a myoelectric prosthesis. Journal of neuroengineering and rehabilitation. 2014 Dec;11:1-5.

[4] Fougner A, Scheme E, Chan AD, Englehart K, Stavdahl Ø. Resolving the limb position effect in myoelectric pattern recognition. IEEE Transactions on Neural Systems and Rehabilitation Engineering. 2011 Aug 18;19(6):644-51.

[5] Scheme E, Englehart K. Electromyogram pattern recognition for control of powered upper-limb prostheses: state of the art and challenges for clinical use. Journal of Rehabilitation Research & Development. 2011 Sep 1;48(6)

[6] Kristoffersen MB, Franzke AW, van der Sluis CK, Murgia A, Bongers RM. The effect of feedback during training sessions on learning pattern recognition-based prosthesis control. IEEE Transactions on Neural Systems and Rehabilitation Engineering. 2019 Aug 20;27(10):2087-96.

[7] Bunderson NE, Kuiken TA. Quantification of feature space changes with experience during electromyogram pattern recognition control. IEEE Transactions on Neural Systems and Rehabilitation Engineering. 2012 Jan 12;20(3):239-46.

[8] Powell MA, Thakor NV. A training strategy for learning pattern recognition control for myoelectric prostheses. Journal of prosthetics and orthotics: JPO. 2013 Jan 1;25(1):30.

[9] Winslow BD, Ruble M, Huber Z. Mobile, game-based training for myoelectric prosthesis control. Frontiers in bioengineering and biotechnology. 2018 Jul 11;6:94.

[10] Castro MC, Arjunan SP, Kumar DK. Selection of suitable hand gestures for reliable myoelectric human computer interface. Biomedical engineering online. 2015 Dec;14:1-1.

[11] Scheme EJ, Englehart KB. Validation of a selective ensemble-based classification scheme for myoelectric control using a three-dimensional Fitts' law test. IEEE transactions on neural systems and rehabilitation engineering. 2012 Oct 25;21(4):616-23

Other

"INTEGRATING NOVEL COMPONENTS INTO BILATERAL PEDIATRIC SHOULDER DISARTICULATION PROSTHETIC FITTINGS: A CASE STUDY."

Brittney Carol Curcio, CPO, MSPO

Upper Limb Prosthetic Program, Hanger Clinic, San Antonio TX, USA

ABSTRACT

Pediatric amputees (both congenital and acquired) with above elbow limb loss have extremely limited prosthetic options. This often results in abandonment or no opportunity to use a prosthesis in childhood. In the absence of appropriately sized, commercially available components, repurposed and custom components were integrated in a series of fittings with a four-year-old patient with bilateral limb deficiencies at the shoulder disarticulation level. These included elbowless initial body powered prostheses, progression to 3D printed ratcheting elbow joints and repurposing of an electric wrist flexion unit as an electric pediatric elbow. Progressive enhancements to the prosthetic treatment plan led to increased prosthesis utilization and independence. Additional pediatric component options, especially electric components, are needed to address proximal limb deficiencies in these younger children.

INTRODUCTION

A recent retrospective analysis observed a prevalence of 23.5 congenital upper limb anomalies per 10,000 live births [1]. Of the 10,700 reported cases in this series, only 6 presented with complete congenital absence of one or both upper limbs [1]. Children with bilateral proximal upper limb congenital deficiencies find ways to adapt to the dexterous world around them [2]. They often surpass their abilities to function with traditional prostheses by compensating with alternative body mechanics to achieve their goals; thus making traditional body powered prostheses less valuable and irrelevant in regards to the majority of their activities of daily living. This case describes a series of prosthetic fittings for a 4-year-old female patient with congenital bilateral shoulder disarticulation, integrating both custom and repurposed components to facilitate increasing function.

PATIENT PRESENTATION

The patient presented with bilateral congenital limb deficiency at the shoulder disarticulation level at age 4. She had never been fit with prostheses as her family had been advised that there were no prosthetic options available that would make her more functional. With the expectation of starting kindergarten next year, there were several functional tasks that the patient, family, and therapist hoped she would be able to achieve with greater independence. At the time, the patient was extremely functional with her feet and incredibly determined to do everything independently. However, there were tasks that could not be completed efficiently or safely with her feet in which assistance would be required. Furthermore, she was diagnosed with hip dysplasia that required surgical intervention and left her with a leg length discrepancy. Otherwise, the patient was a healthy, lively, and strong willed 4-year-old girl.

INITIAL BODY-POWERED PROSTHESES

Recognizing the insurance limitations in the United States, a plan was made to initially provide body-powered devices to determine their functional impact. These initial body powered prostheses were fabricated as bilateral units (Figure 1). Pediatric Ottobock shoulder joints were directly laminated to "shoulder cap" style sockets with flexible inner liners. These friction shoulder joints allowed for pre-positioning in the sagittal plane. There was no elbow joint. Instead, a tube-shaped arm was laminated to a delrin wrist unit, where pediatric nylon coated hooks were fastened. The harness consisted of a single strap across her chest anteriorly, and elastic webbing that formed an "X" to connect the two sockets to one another in a criss-cross formation on her back. Control cables ran from her prosthetic hooks to the posterior distal aspect of the contralateral socket with housing retainers positioned at the approximate position of the elbows. With this configuration, the patient open the hook with scapular protraction and close the hook with scapular-retraction.

Figure 1: Initial body powered prosthesis

The initial impact of these devices was extremely positive. The patient was immediately able to open and close the hooks and she was soon able to donn and doff them independently. While they boosted her confidence, over time she learned of their many limitations. First, only one hook could be opened at a time due to the opposing forces on her back. This limited any chance at bimanual prehensile activities. Second, in the absence of an articulating elbow she could not lift the forearms to bring her hooks towards her mouth preventing her from feeding herself with her prosthetic hooks. Third, the amount of force experienced the anterior portion of the sockets with the excursion required to open her hooks caused much discomfort. Eventually the patient grew fatigued with the intensive effort required to use the prostheses and lost interest in them.

A second set of prostheses were later made to improve upon this design (Figure 2). The sockets were changed to "X Frame" designs to reduce localized pressure and improve comfort. The shoulder joints were replaced with universal ball and socket shoulder joints which allowed for friction resisted rotation, abduction/adduction and flexion/extension. Custom ratcheting elbow joints were 3D printed to connect the shoulder component to the wrists and hooks. The elbow joints could be passively positioned into various flexion positions. The locking cable was tied into a plastic tube that was routed along the anterior socket and towards the patients mouth so that she could bite and pull the tab cycle the elbow lock. The delrin wrists were replaced with passive flexion wrist units so that her hooks could be prepositioned for better access to midline reach. The hooks were cabled in a similar fashion to the previous prostheses.

Figure 2: Subsequent endoskeletal body powered prosthesis

Several functional improvements were observed with this second set of body powered prostheses. The force redistribution within the X frames reduced pain. The patient was able to unlock the elbow position with the bite straps but struggled to lock it again. While she required assistance to position the elbows, the family was happy that they could at least change the elbow position. Unfortunately, this socket set up required two straps for donning and doffing. While the patient was still able to do this independently, it increased the time and concentration for applying the prosthesis. She was still unable to operate both hooks at the same. Improvements included holding a wider object at waistline, carrying a bag over her forearm while walking, holding light weight foods in her hook which have been pre-positioned at her mouth, pushing open a door without having to use her feet and pulling large objects across the floor. Notably, the majority of the patient's activities could still be done faster with her feet.

Despite the functional gains that the prostheses provided there were limitations with both devices. The prostheses were bulky and changed her natural proprioception and understanding of spatial awareness. They took a lot of time to put on and take off independently and only provided her with a few functions. She would prefer to take the prostheses off in between functions while she was not needing them. Since the functionality was limited, this could mean between 15 minutes to several hours of time in between use. Over time the patient learned that she would rather ask for help or attempt to preform activities with her feet because it was faster and more efficient than to stop what she was doing to put the prostheses on and have someone preposition them for her.

MYOELETRIC PROSTHETIC INTERVENTION

Having established the limitations of body-powered designs for this patient, a myoelectric device plan was made. A unilateral left prosthesis was fabricated with a Sauter style socket (Figure 3). This allowed for the least amount of enclosed tissue and skin contact while maintaining a very stable socket fit. The proximal part of the socket, which contoured over her left shoulder provided vertical suspension. Medial suspension was provided by a single strap. A flexible inner socket was used to allow for adjustments of pressure and fit without disrupting the structural integrity of the socket frame. The Hosmer adult shoulder joint was turned upside down to better fit the small profile of the patient and the shape of the socket frame. The metal strut was contoured to fit the humeral section and provide protection to electrical wiring. The humeral section was laminated and left with a hollow opening. A delrin wrist was laminated to the distal end of the humeral section to provide a connection point to the elbow. Unfortunately, a pediatric myoelectric elbow is not available on the prosthetic market. Instead, a Motion Control powered wrist flexion unit was utilized. The powered flexion wrist which has a ½ inch threaded distal end was connected to the humeral section via the delrin wrist unit. A forearm was 3D printed and fastened to the articulating end of the powered flexion wrist. At the most distal end of the forearm, an Ottobock pediatric myoelectric wrist unit was epoxied to the forearm and the Ottobock Myolino hand was connected as the terminal device. The device was wired with a single site electrode, batteries and touch pad which would act as a switch (Figure 4). The electrode was placed at the patient's proximal pectoralis major. The switch was to be routed to the right side of her collar bone so that it could be accessed by her chin without interfering with the pectorals muscle movement.

Figure 3: myoelectric prosthesis

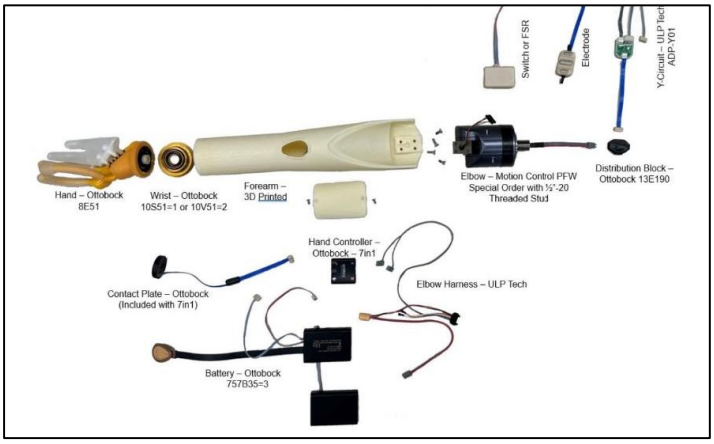

Figure 4: Components used in the myoelectric prosthesis

The patient was fit with the myoelectric prosthesis and operated it well. For simplicity and to prevent frustration, the integration of elbow function was initially deferred to later date to allow the patient to adapt to one component at a time.

The myoelectric prosthesis provided several opportunities that the body powered device could not offer for this specific patient presentation. First, it enabled the patient to operate the terminal device with very little force, excursion, and energy expenditure in comparison to the body powered cable devices. Second, she had the opportunity to flex the arm at the elbow which did not require any further force or excursion than what she was already using to control the terminal device. This allows for opportunities such as feeding herself, playing with toys in multiple dimensions, carrying objects, lifting them up to shoulder height and putting them as low as waist hight (Figure 5). All of this can now be done without gross movement of her spine and scapular deviation. It also reduces the amount of time that she must use her toes, foot, ankle, knee, and hip to bring something from the ground to the upper half of her body. The myoelectric system will also reduce the stress on her spine of having to be a flexed position as she would be able to maintain her posture while using prosthetic arms compared to the body powered prostheses and compared to using her feet.

Figure 5: powered prosthesis in use

ADDITIONAL OBSERVATIONS

The patient displayed right foot dominant. With the provision of the more functional prosthesis, we observed that she was able to use her prosthesis during bilateral engagement with her right foot. Fabricating a left upper extremity prosthesis allowed for her to use her right dominant foot to pass things from her foot to the hand of the prosthesis (Figure 6). A bilateral set of powered prostheses would have been both heavy and bulky and may have limited this functional capacity. The unilateral fitting allowed for open space and freedom to move enabled her to use her feet.

Figure 6: bilateral engagement of the prosthesis

CONCLUSION

The current options for pediatric components are limited. Additive manufacturing and creative repurposing of existing components represent alternate pathways to facilitate functional solutions within this small patient population. In the case of bilateral limb deficiency, consideration should be given to preserving existing function with any attempts towards prosthetic care.

ACKNOWLEDGEMENTS

A number of individuals and organizations contributed to this case including Jonathan E, Nottingham, CPO (Clinical and Fabrication Support), Bradford Illsely, (Fabrication Support), Jamey Waltermyer (Technology Support), Nate Sprunger (Manufacturer Support), Matt Mikosz, (developed 3D Printed Elbow), Annie Hess (Clinical Support), Hanger Fabrication Network (3D Printing) and Inner Wheel (donation of myoelectric parts)

"Written informed consent was obtained from the patient's guardian prior to the introduction of all non-commercial prosthetics components."

REFERENCES

[1] Y.H. Shin, G.H. Baek, Y.J. Kim, J.K. Kim. "Epidemiology of congenital upper limb anomalies in Korea: A nationalwide population-based study." *Plos One*, vol16(3), e0248105, 2021

[2] D.E. Krebs, J.E. Edelstein, M.A. Thornby. "Prosthetic management of children with limb deficiencies." *Phys Ther*. Vol 71(12), pp. 920-34, 1991.

PRELIMINARY EVALUATION OF VARIATIONS IN CONTROL STRATEGY FOLLOWING TRANSHUMERAL OSSEOINTEGRATION

Brian Monroe CP, Phil Stevens MEd, CPO

Hanger Upper Limb Prosthetic Program, Hanger Institute for Clinical Research and Education

ABSTRACT

While not as common as transfemoral applications, osseointegration at the transhumeral level has been performed across multiple clinical sites. Our experience with this amputation level has predominantly been with the use of the OPRA implant. We have followed a staged rehabilitation program inclusive of an early trainer to facilitate progressive positive and negative loading, a full-length, light weight, non-prehensile prosthetic arm and definitive arm prostheses. These have included both body-powered and externally powered definitive solutions. In the absence of a transhumeral socket, the facilitation of control strategies for both body-powered and myoelectric prostheses have required adaptation. For body powered systems, because of the direct attachment of a bone-anchored prosthesis, harnessing elements designed for suspension can be eliminated, while those that enable control of the terminal device, wrist or elbow most be modified and preserved. Accordingly, correct placement of the base plate and housing retainer for the control cable must be achieved in the absence of an external socket. This has been accomplished via external rigid outriggers for longer residual limbs or through their attachment to proximal endoskeletal or exoskeletal bridges with shorter residual limbs. For externally powered prostheses, the challenge lies in consistent placement of the surface electrodes that may be required over the residual limb, the ipsilateral chest wall or ipsilateral scapular region. This has been accomplished through outriggers, adhesive electrodes, non-custom electrode cuffs and custom silicone interfaces. These methods of facilitating traditional control strategies in the absence of the transhumeral socket will be described and discussed.

INTRODUCTION

While osseointegration has been predominantly performed and reported in transfemoral applications, several studies have reported upon its application at the transhumeral amputation level. In 2011, Jonsson et al reported upon their fitting protocols with 16 subjects. They describe their approach to staged prosthetic management with an early "trainer" device, a temporary light-weight, non-prehensile, long-arm prosthesis and ultimate definitive fittings of cosmetic, body-powered and myoelectric prostheses [1]. The 2- and 5- year survival rates for the implants in this cohort were subsequently reported at 82% and 80% respectively [2]. More recently, researchers have begun to explore the loads experienced in the transhumeral implant site across a range of physical movements and activities [3] as well as prosthesis types [4], both in vivo [3] and through mechanical simulation [4]. The prospective demand for osseointegration in this population appears to be high, with one survey suggesting 35% of those with unilateral transhumeral amputation would consider this procedure, with another 29% being undecided [5].

Notably, the factors that this group prioritized in considering this procedure included a capacity to do more activities with a durable, comfortable device [5]. These elements require consideration of an appropriate, consistent control strategy. For body-powered devices, harnessing is no longer indicated for suspension but remains necessary for cable-driven control the elbow, wrist and terminal device. Significantly, the base plate and housing retainer can no longer be mounted to the distal lateral aspect of the prosthetic socket but remain necessary for efficient cable-controlled activation of the prosthesis. For myoelectric devices, there is no longer a socket to house the surface electrodes. In this case series we will report upon our efforts and observations to date in establishing body-powered and myoelectric control strategies following osseointegration in the absence of a transhumeral socket.

TRAINING STAGES

Trainer

The use of the trainer is well described by Jonsson et al [1]. Its intent is to facilitate both positive and negative loading of the implant following surgical implantation. While patients are encouraged to move their limb in prescribed motions for recommended daily durations, as a static device, no control strategy is indicated during this phase (Figure 1)

Long Arm Trainer

The Long Arm Trainer is also suggested in Jonssen's original report [1]. This lightweight solution is an oppositional, non-prehensile prosthesis with no requirements for a control strategy. It is generally comprised of a friction or manual locking elbow and either a "passive static" hand or manually operated terminal device that does not required control cables or external powered componentry. The goal of the device is to increase torque loads from the trainer to a full-length prosthesis.

Figure 1: Trainer to facilitate positive and negative loading of the implant.

BODY POWERED ADAPTATIONS

Longer Arms

In socket-based body powered systems the harness/control cable provide both suspension and activation of the prosthesis. With osseointegration the harness no longer needs to suspend the prosthesis. This greatly increases user comfort as the harness no longer carries the weight of the prosthesis and does not need to be as tight. In many cases, this also allows increased functional range of movement of the extremity. However, the harness must still be designed to capture gross body motions, generating the required force and excursion to operate the prosthetic componentry. With friction or manual locking elbows, a figure-9 harness can be used. The application of a traditional cable-driven elbow lock requires a harnessing approach similar to the figure 8, with a superior harness strap running from the Northwestern ring over the contralateral shoulder where it attached to the elbow lock cable to facilitate cycling of the internal lock.

Figure 2: A rigid distal outriggers is used to mount the baseplate and retainer of a body powered prosthesis.

Ideally the proximal base plate location should keep the control strap along the distal ⅓ of the scapula to maximize available cable excursion generated from anatomic glenohumeral flexion without bridging clothing. With longer residual limbs, this proximal base plate location is over the residual limb. In such cased an outrigger can be designed and attached to the prosthetic elbow bridge. (Fig 2).

Shorter Arms

With shorter limbs if the ideal proximal base plate location falls within the length of the custom bridge, it can be mounted directly to the endoskeleton or exoskeletal segment. (Fig 3).

Figure 3: In the case of shorter residual limbs, the housing retainer is mounted to the proximal bridge segment of the prosthesis between the implant connection and the elbow table.

Bilateral applications

For bilateral OI harnessing the base plate location and mounting would be similar to the above examples. The harness can be designed to facilitate independent use of a single prosthesis or as a connected pair. In the case of the former the user can wear one prosthetic at a time by securing the control strap to the contralateral axilla via a figure-9 harness as described above. Another option is to join the harnesses together for bilateral use (Figure 4). The advantage of bilateral application is the elimination of axillary pressure caused by the axilla loop. Provided that the power required to operate the elbows and/or terminal devices of the two sides are similar, the inherent friction in the cable system allows the user to operate one side without inadvertent operation of the contralateral side.

While the harness is no longer required for suspension, it still plays a vital role in enabling cable excursion for both elbow & hook position and cycling of the elbow lock. Thus, the anterior suspensor straps continue to provide an anchor point for cycling the ipsilateral elbow lock as well as an anchor point for the contralateral control cable. The standard dacron anterior elbow lock strap, coupled with the anterior elastic webbing permits cycling of the elbow as observed in standard body powered transhumeral harnessing techniques.

Figure 4: Harnessing approach to a bilateral, body-powered transhumeral presentation.

MYOELECTRIC ADAPTATIONS

Currently we are limited to commercially available surface EMG sensors that were traditionally placed in the prosthetic socket. With osseointegration the socket is eliminated but there is still the need to use surface electrodes for control. These surface electrodes must maintain skin contact with the patient's limb throughout a significantly expanded functional range of motion. In the case of shorter limbs or limbs lacking usable myoelectric signal sites, the control sites may be moved to the chest wall or poster scapular region to capture available myolectric signals.

Outrigger

The outrigger approach was first described by Jonsson et al [1]. Outriggers are fabricated from a rigid material and attached distally at the laminated coupling that connects the elbow to the connection adaptor. This represents a simple method of providing consistent electrode location in dual site control (Figure 5).

Non-custom Electrode Bands

For more elaborate control strategies requiring multiple inputs, when the residual limb is long enough with a cylindrical shape, non-custom commercial electrode bands can be used. These systems may require frequent recalibration due to inconsistent placement during donning (Figure 6).

Figure 5&6: Two strategies for positioning electrodes of midlength and longer transhumeral limbs

Adhesive Electrodes

Adhesive electrodes represent an alternative for shorter limbs when the distance between the prosthetic elbow and the electrode placement is too long for outriggers and the limb is too conical for commercially available cuffs to stay in place without distal migration (Figure 7).

Custom Silicone Interfaces

An attractive alternative to adhesive electrodes is a custom silicone interface that accommodates the unique contours of the limb segment. This is especially desirable with the use of pattern recognition where multiple electrodes sites are required. (Figure 8).

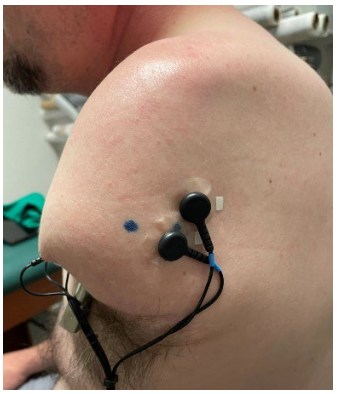

Figure 7&8: Two strategies for positioning electrodes with shorter transhumeral limbs.

CONCLUSIONS

As transhumeral osseointegration becomes more available, prosthetist will be confronted with the challenges of creating a consistent, comfortable control strategy. While our pilot observations in this space are limited, we have already encountered the need to adopt a number of strategies for both body-powered and myoelectric systems based on limb length, the complexity of the control system and the number of required inputs. Additional research is needed to understand the magnitude of the forces created by the control cables pulling against the housing retainers in the various required configurations. One solution to the challenges of maintaining elbow contact throughout an expanded range of shoulder motion is the promise of internal, surgically implanted myoelectrodes that better maintain their fidelity through shoulder movements.

ACKNOWLEDGEMENTS

The authors wish to acknowledge the clinical creativity of the treating prosthetists, Brittany Curcio CPO, Michael Duston CPO, William Fletcher CPO and John Boldt CPO.

REFERENCES

[1] S. Jonsson, K, Caine-Winterberger, R. Branemark. "Osseointegration amputation prostheses on the upper limbs: methods, prosthetics and rehabilitation. *Prosth Orthot Int,* vol 35(2), pp. 190-200, 2011.

[2] G. Tsikanylakis, O. Berlin, R. Branemark. Implant survival, adverse events, and bone remodeling of osseointegrated percutaneous implants for transhumeral amputees. Clin Orthop Rel Res, vol 472, pp 2947-56, 2014.

[3] P. Stenlund, K. Kulbacka-Ortiz, S. Jönsson, R. Brånemark. Loads on transhumeral amputees using osseointegrated prostheses. *Ann Biomed Eng*. Vol 47, pp. 1369-77, 201.

[4] C.E.Taylor, A.J. Drew, Y. Zhang, Y. Qiu, KN. Bachus, K.B. Foreman, H.B. Henninger. Upper extremity prosthetic selection influences loading of transhumeral osseointegrated systems. *PloS One*. Vol 15(8), e0237179, 2020.

[5] L. Resnik, H Benz, M. Borgia, MA Clark. Patient perspectives on osseointegration: a national survey of veterans with upper limb amputation. *PM&R,* vol 11(12), pp. 1261-71, 2019.

REFINEMENT OF NEW ITEMS IN THE ASSESSMENT OF CAPACITY FOR MYOELECTRIC CONTROL FOR MULTI-ARTICULATING HANDS

Kristi L. Turner, DHS, OTR/L [1], Wendy Hill, BScOT ,[2] Eric J. Earley, PhD[3,4], Maria Munoz-Novoa,[5] Liselotte Hermansson, PhD[6,7], Helen Lindner, PhD[8]

[1] *Center for Bionic Medicine, Shirley Ryan AbilityLab, Chicago, IL, USA*
[2]*Institute of Biomedical Engineering, University of New Brunswick, Fredericton, Canada*
[3]*Bone-Anchored Limb Research Group, University of Colorado, Aurora, CO, USA*
[4]*Department of Orthopedics, University of Colorado School of Medicine, Aurora, CO, USA*
[5]*Center for Bionics and Pain Research, Mölndal, Sweden*
[6]*Dept of Prosthetics and Orthotics, Faculty of Medicine and Health, Örebro University, Örebro, Sweden.*
[7]*University Health Care Research Center, Faculty of Medicine and Health, Örebro University, Örebro, Sweden*
[8]*School of Health Sciences, Örebro University, Örebro, Sweden*

ABSTRACT

This paper discusses the enhancement of the Assessment of Capacity for Myoelectric Control (ACMC) with the introduction of three new assessment items specifically designed for multi-articulating prosthetic hands. With the advent of these advanced prosthetics, assessing a user's capability to effectively operate them in functional tasks becomes crucial. The new ACMC items bridge the existing evaluation gap by focusing on the nuanced control skills required by users with upper limb loss or difference (ULL/D). This innovation, achieved through a collaborative effort among clinical and prosthetic researchers, utilizes video analysis and consensus to ensure these items accurately measure the adeptness in controlling multi-articulating hands during bimanual activities.

INTRODUCTION

Recent advancement in multi-articulating hands offer increased function to individuals with upper limb loss or difference (ULL/D) that have been previously using a single degree of freedom (DOF) prosthetic hand. While individuals with ULL/D generally prefer the enhanced functions and appearance of multi-articulating hands [1], several studies have reported challenges in learning to operate them and use in daily activities. Skills such as grip-switching, prepositioning various prosthetic components for grasping, and selecting the most secure grips require proper training and regular practice [2].

One way to monitor progress in learning multi-articulating hands is to use an assessment tool that captures different aspects of controlling a multi-articulating hand. The Assessment of Capacity for Myoelectric Control (ACMC) is an observation-based assessment that evaluates a person's ability to control a myoelectric prosthetic hand in bimanual activities [3]. Originally developed for conventional standard myoelectric hands with a single DOF, the ACMC items are not designed to capture the nuanced control of multi-articulating hands.

Here, we provide a brief report on the process of testing the degree to which the three new items capture several skills specifically related to the control of multi-articulating hands. Using video analysis and a consensus method, a group of clinical and prosthetic researchers used and refined the three new items to assess upper limb prosthesis users with various types of multi-articulating hands.

METHODS

Four raters (occupational therapists and researchers) with extensive clinical experience and knowledge of the ACMC participated in meetings to discuss areas not currently covered in the current ACMC. From these meetings, definitions were created with the intent to capture use and control strategies of multi-articulating hands [4]. After presenting these definitions at an ACMC training course, two certified raters (a physical therapist and an engineer), who were newly utilizing the ACMC in their research lab, provided feedback on the new items based on their experiences using the ACMC with their research participants [5], and were subsequently included in further discussions and refinement of item definitions, as described below (Figure 1).

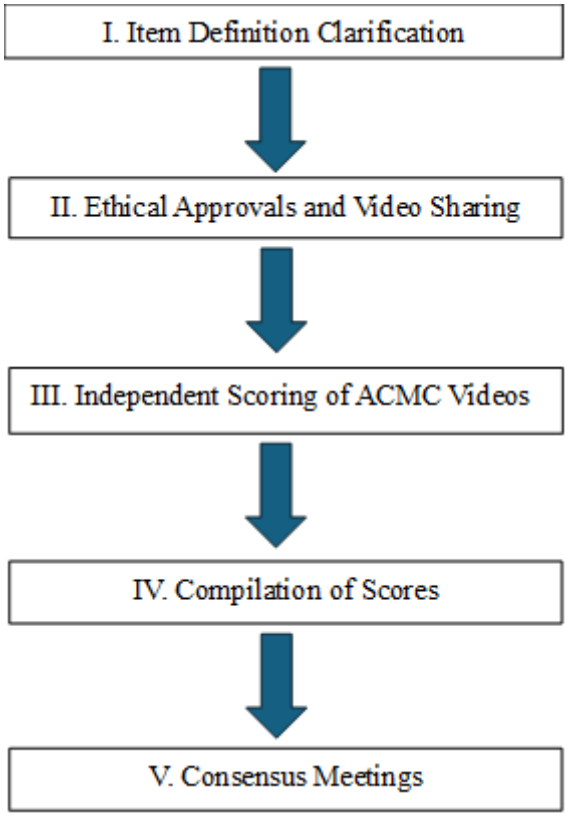

Figure 1: A flow chart to illustrate the process for definition refinement.

I. Initial meetings reviewed the item definitions and discussed any further clarifications. Raters engaged in detailed discussions to ensure a common understanding of the assessment items. The raters were in agreement that the refined name of each item was in accordance with their understanding:

Ability to switch grips

Positioning the hand appropriately for grasping

Choosing a secure grip for function

II. Ethical approvals were received by the respective raters to allow for sharing of ACMC videos. Subsequent meetings allowed for analysis of ACMC assessment videos from the raters' respective labs that captured a variety of control strategies, limb loss/ difference levels, components, and multi-articulating hands.

III. During each meeting, to prevent bias, ACMC videos were shared for each rater (n=5) to independently score the three new items without discussion with the other raters.

IV. After all videos were scored, each rater sent their ratings to the study facilitator who did not participate in the scoring meetings. Alongside the scores, raters provided justifications for each rating, offering insights into their decision-making process. The facilitator compiled the scores and justifications, allowing for a comparative review of the assessments.

V. At two consecutive meetings the study facilitator shared the results with the group of raters and chaired the discussion.

RESULTS

During the consensus meetings, the discussions focused on the individual scores in relation to the words of each item and rating scale definition. For example, the definition of "*Ability to switch grips*" before the consensus meeting read as "*about the mechanics of switching or accessing the grips available in the prosthetic hand. Is the person able to consistently and accurately switch between/access available grips*?" In the videos, often we saw inadvertent, **unintended**, or **delayed** switching of grips due to various reasons, such as unfamiliarity with the hand, the user's lack of ability to control, or the user not taking the opportunity to switch grips. As a result, raters initially rated this item 1 or 2 (Table 1) but after discussion all raters agreed to a score of 2.

Table 1. Initial individual scoring of one video of the item *Ability to switch grips*

	Rater 1	**Rater 2**	**Rater 3**	**Rater 4**	**Rater 5**
Score	2	2	2	1	1
Notes taken by rater from video	Slight delays when switching	Switched well but there were some delays	Slight delays when switching grips in particular at tabletop activities; significant delay when going to counter	Pick up suitcase with fine pinch. attempt to switch grip. grip shoes with fingers (good). Switching grip before packing toiletries bag. Change to lateral for shoe bag	Capable of switching, it is questionable whether it switches to the one he intended. Some delays in some task.

DISCUSSION

Using video analysis and a consensus method, we refined the new ACMC item definitions to evaluate the control of multi-articulating hands. The refined definitions include more comprehensive language, incorporation of examples, and additional details for scoring (e.g. number of reminders, specific descriptors) which improved the interpretability of the items. As an example, in the item "*Ability to switch grips"*, with the refined definition, the raters were able to reach consensus and agree on a common rating of this item.

This consensus process with raters of different backgrounds and experience with ACMC has strengthened the definitions and clarified the intent of capturing multi-articulating hand function. The next step is to validate the newly refined ACMC items together with the existing items with a sample of multi-articulating hand users.

REFERENCES

1. Widehammar C, Hiyoshi A, Lidström Holmqvist K, Lindner H, Hermansson L. Effect of multi-grip myoelectric prosthetic hands on daily activities, pain-related disability and prosthesis use compared with single-grip myoelectric prostheses: A single-case study. J Rehabil Med 2021.
2. Franzke AW, Kristoffersen MB, Bongers RM, Murgia A, Pobatschnig B, Unglaube F, et al. Users' and therapists' perceptions of myoelectric multi-function upper limb prostheses with conventional and pattern recognition control. PLoS One 2019;14(8):e0220899.
3. Lindner HYN, Linacre JM, Hermansson LM. Assessment of Capacity for Myoelectric Control: Evaluation of the construct and the rating scale. Journal of Rehabilitation Medicine 2009.
4. Hermansson, L, Turner, K, Lindner, H, Hill, W. Development of the Assessment of Capacity for Myoelectric Control Version 4 for use in Patients with Multi-Grip Prosthetic Hands. The 18th World Congress of the International Society for Prosthetics and Orthotics (ISPO), 1-4 November 2021.
5. Zbinden J, Sassu P, Mastinu E, Earley EJ, Munoz-Novoa M, Brånemark R, et al. Improved control of a prosthetic limb by surgically creating electro-neuromuscular constructs with implanted electrodes. Science Translational Medicine 2023;15(704):eabq3665.

THE EFFECTS OF LIMB POSITION AND APPLIED LOAD ON HAND GESTURE CLASSIFICATION ACCURACY USING ELECTROMYOGRAPHY AND FORCE MYOGRAPHY

Peyton R. Young[1], Eden J. Winslow[2], Giancarlo K. Sagastume[3], Marcus A. Battraw[1], Richard S. Whittle[1], Jonathon S. Schofield[*1]

[1]*University of California – Davis, Department of Mechanical Engineering*

[2]*University of California – Davis, Department of Biomedical Engineering*

[3]*University of California – Davis, Department of Electrical and Computer Engineering*

ABSTRACT

Modern mechatronic upper limb prostheses are controlled using surface electromyography sensors (EMG) that are typically embedded in the prosthetic socket. However, when the user moves their device in space or interacts with an object, changes in electrode contact pressure can occur that work to the detriment of consistent and effective prosthesis control. Yet, we suggest that these pressure changes offer unique information that can be captured using force myography (FMG) and decoded to help classify intended prosthesis movements. Thus, the goal of this work was to investigate the feasibility of combining FMG with EMG to classify hand grasping movements in an able-bodied cohort and compare this combination to EMG and FMG alone. We hypothesized that FMG will capture complimentary information to the EMG data and when combined, will produce more robust classification accuracies when the user's limb moves in space or grasps objects of varying loads. We used a custom EMG+FMG armband and instructed N=21 participants to grasp objects of different weights at a variety of different positions using 4 different hand grasp movements. The results demonstrated that the average classification accuracy of EMG+FMG was statistically different and of higher classification accuracy when compared to EMG and FMG. It was also found that position and load affect classification accuracy together suggesting that control techniques that adapt to these changes are likely to produce more effective prosthetic control performance.

INTRODUCTION

Modern upper limb prostheses (ULPs) are growing increasingly sophisticated with a variety of clinical and experimental systems offering individually articulating digits to perform a variety of hand movements, grasp force ranges similar to an intact limb, and proportional control of movements [1–3]. Operating these devices most commonly relies on surface electromyography (EMG) to measure residual muscle activity, decode the user's intended movements, and in turn actuate the corresponding prosthetic movement. However, even with these advancements, growing availability of advanced devices, and their increased prescription rates, abandonment rates remain as high as 23-26% [4]. Achieving effective and consistent device control is a major contributing factor [4]. One challenge is the fact that EMG sensors are embedded in the prosthetic socket (PS). When the device is moved or loaded (object interaction) the pressure distribution between the prosthetic socket and the residual limb can dramatically change [5] resulting in varying impedance, potential motion artifacts, and overall inconsistent electrode recordings that collectively work to the detriment of effective and consistent control [6, 7].

While these pressure changes add unwanted variability for EMG control systems, they may also offer unique information about the state of the prosthesis that can be useful for device control. For example, recent studies have recorded patterns of pressure changes inside the PS during residual muscle contractions, which were then classified using machine learning to infer intended prosthesis movements (force myography, FMG) [7–9]. We suggest that the measurement of pressures developed inside the PS may offer complimentary information to augment EMG-based control strategies. Thus, our objective was to investigate the feasibility of combining FMG with EMG to predict hand grasping movements across a variety limb positions and grasped loads. We hypothesized that EMG and FMG would demonstrate variable classification accuracies depending on the limb position and loading conditions and, when fused, EMG+FMG would perform more accurately than either system individually.

METHODS

Participants and Experimental Setup

We recruited N=21 able-bodied participants (14 male and 7 female, average age 24, SD 3.08). Research protocols were approved by the Institutional Review Board at the University of California, Davis and participants provided written informed consent. Participants wore our custom EMG+FMG armband which was comprised of our FMG system (8 Interlink Electronic FSR400 sensors) and our EMG system (8 EMG sensors from our Delsys Trigno EMG system) as shown in Figure 1. The sensors were arranged equidistantly onto a Velcro strap in an alternating sequence before they were tightened onto the muscle bulk of the participants' forearm. Sensor data was collected using two National Instruments USB6210 Data Acquisition Systems, one for the EMG data and one for the FMG data.

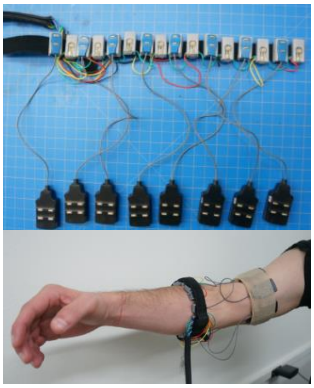

Figure 1: The EMG+FMG armband was comprised of 8 EMG and 8 FMG sensors which were housed in 3D printed casings which attach to the Velcro band.

Experimental Procedure

Participants grasped a weighted manipulandum (MPD) using a specific grasp configuration at various positions. This allowed us to examine how EMG, FMG, and their combination are affected by load and limb position. The MPD was loaded with 5 weights, including a no weight condition (the weight of the MPD, 53g), 250g, 500g, 750g, and 1000g. Participants stood in front of a 7-foot-tall shelf and grasped the MPD with 4 different hand grasps: Key, Pulp Pinch, Power and Tripod Pinch [10]. The shelf levels and standing 'zones' were adjusted for participant height such that their arm was fully extended when standing at zone 2 and reaching positions 5-8 (Figure 2a). The participants grasped the MPD using 4 different grasps, at 8 different positions, and under 5 different weights. Each trial consisted of the MPD being placed at one position, in line with the sagittal plane of the subject's dominant arm. They would then be queued to grasp and slightly lift the manipulandum with a specific grasp, hold it for 3 seconds, and then set it down and relax for 4 seconds. This was repeated 3 times at each position prior to moving on to the next randomized position, weight, and grasp combination. Randomization helped ensure that any potential muscle fatigue did not influence experimental results.

Data Analysis

Contraction data was first separated from resting data using time stamps before being parsed together and segmented using a 200ms window and a 50ms time increment [11]. We used the Hudgins' Set to create EMG features [12], the mean absolute value for FMG features [7] and combined both into a single feature vector for EMG+FMG [13]. We used linear discriminant analysis to classify hand grasps using leave-one-out cross validation to train the classifier and calculate classification accuracies. We analysed data in 3 cases: (1) Classification accuracy for a constant position (position 2) and varying weights, (2) classification accuracy for a constant weight (500g) and varying positions, and (3) training the classifier at a neutral position (position 2, no weight, as is done in numerous studies [13-15]) and testing the classifier with data from the most extended and loaded position (position 5, 1000g). We used multiple linear mixed effect models to examine statistical differences in classification accuracies of each modality (EMG vs. FMG vs. EMG+FMG) for each of the 3 cases, using modality as the fixed effect and participant as the random effect.

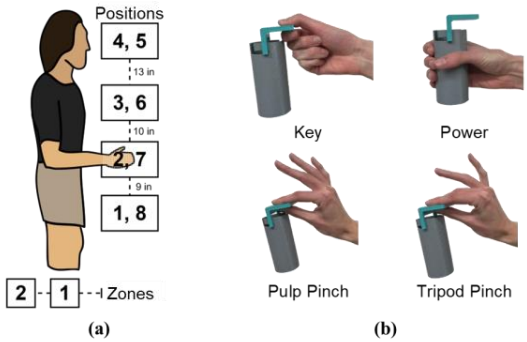

Figure 2: (a) The 8 positions and 2 zones for the test. The participant stood at zone 1 for positions 1-4 and zone 2 for positions 5-8. The participant's elbow was bent at 90º at position 2, between fully extended and bent at positions 1, 3, and 4, and fully extended at positions 5-8. (b) The manipulandum was comprised of two parts such that the weights can be top loaded and held with the 4 grasps.

RESULTS

The first two cases illustrated how varying either the load or position affected classification accuracy for each modality. The results are shown in Figures 3a and 3b, respectively.

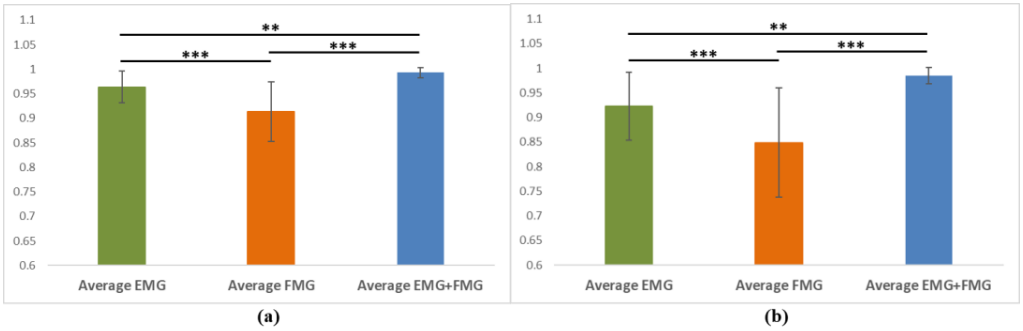

Figure 3. ** (P < 0.01) *** (P < 0.001) (a) Average classification accuracy for case 1 (constant position of position 2 with varying loads). (b) Average classification accuracy for case 2 (constant weight of 500g and varying positions).

For both cases, EMG+FMG was found to be the most accurate sensing modality while FMG alone was found to be the least accurate. Each sensing modality yielded an average classification accuracy of greater than 90% except for FMG in case 2 (84.9%, SD=11.1%). It was also found that each modality was statistically different from one another, as shown by Figures 3a and b. Furthermore, it was found that position and weight demonstrated an effect on EMG and FMG as shown by statistically different accuracies (P < 0.05) when comparing cases 1 and 2 while EMG+FMG was not affected (P > 0.05), indicating that the fusion of the two modalities may be more robust to these conditions.

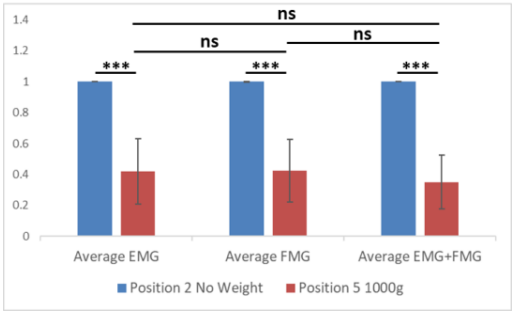

Figure 4: *** (P < 0.001) ns (P > 0.05) Case 3: Average classification accuracies at the neutral position (position 2 no weight) and at the extended and loaded position (position 5 1000g) after being trained at the neutral position.

For case 3, we first graphed the average classification accuracy of the classifier at the neutral position. We then trained the classifier at this neutral position and tested the classifier with data from the most extended and loaded position, illustrated in Figure 4. As shown, there are significant differences between the classification accuracies of the neutral and extended positions. Furthermore, there was no significant difference between each modality's classification accuracies at the extended and loaded position.

DISCUSSION AND FUTURE DIRECTIONS

We found that that position and grasped load affect classification accuracy muscle measurement modalities (EMG, FMG, EMG+FMG). As illustrated by the results of case 1 and 2, EMG outperformed FMG in both cases and yielded higher classification accuracies when the load and position was varied. This may have been a result of little change of radial muscle forces across the range of loads and positions, or alternatively large variability in these radial forces. Thus, it may be useful in the future to classify hand gestures under multiple combinations of varying weight and position to further define the nature of these relationships. Furthermore, as shown by the results of cases 1 and 2, the combination of EMG and FMG yields statistically different and nominally greater classification accuracies than either EMG or FMG could individually produce. This suggests that FMG produces complimentary information that can be paired with EMG data to more accurately classify hand gestures during varying position and loading conditions. Further, when comparing the results of the same modality across cases, accuracies for cases 1 and 2 for EMG and FMG were found to be statistically different whereas EMG+FMG demonstrated no difference. This indicates that the combination of the two provide a more robust classification accuracy during changes in position and load than the two modalities separated.

The results from case 3 further illustrate the effect of limb position and loading on classification accuracy for each modality. As shown in Figure 4, when the classifiers are trained and tested at the neutral position, as is typically done for ULPs, the classification accuracy of the four hand gestures approaches 100%. However, when trained in the neutral position and then tested in the extended and loaded position, the average classification of each modality decreases to 35-40%. Furthermore, these classification accuracies were found to be not statistically different from each other (P > 0.05), illustrating that each modality performed equally poorly when tested at the extended position. While the extended position was the most different from the neutral position, this illustrates the fact that limb position and

loading can work to the detriment of classification accuracies. As current ULPs are usually trained at a neutral position, the addition of weight and position would vastly decrease the effectiveness of the users control system. Furthermore, current literature does not provide a reliable consensus on if the combination of EMG and FMG adds any statistical value for hand gesture classification [13, 16, 17]. However, in our work, we demonstrated that when the limb is moved to various positions and loaded, as is more representative of real-world object manipulation, the addition of FMG adds significant improvements to current EMG classification systems. Thus, designing and implementing a control system that implements these combinations can account for or adapt to position and loading changes could aid in more effective device control.

The long-term goal of this work is to implement an EMG+FMG sensing system inside of ULPs for the purpose of more robust control. While this experiment begins to provide feasibility data to further explore this topic, future work is ongoing to investigate how combinations of position and load affect classification accuracy of grasping patterns along with how well the modalities can accurately classify positions and applied loads. This future work will illustrate the robustness of each sensing modality along with what conditions each sensing modality may be best suited to perform under. We further aim to begin to examine how in-socket prosthesis applications of our approaches may change relative to our able-bodied dataset and examine efficient machine learning training practices that incorporate and accommodate for position and grasped weight combinations.

ACKNOWLEDGEMENTS

The authors would like to thank the NSF for funding this work through the GRFP (award number 2036201). We would also like to thank our participants for their patience and cooperation during our experiment.

REFERENCES

[1] Scheme E, Englehart K. Electromyogram pattern recognition for control of powered upper-limb prostheses: State of the art and challenges for clinical use. J Rehabil Res Dev. 2011;48:643–660.

[2] Marinelli A, Boccardo N, Tessari F, et al. Active upper limb prostheses: a review on current state and upcoming breakthroughs. Progress in Biomedical Engineering. Institute of Physics; 2023.

[3] Segil JL, Huddle SA, Weir RFF. Functional assessment of a myoelectric postural controller and multi-functional prosthetic hand by persons with trans-radial limb loss. IEEE Transactions on Neural Systems and Rehabilitation Engineering. 2017;25:618–627.

[4] Biddiss E, Chau T. Upper limb prosthesis use and abandonment: A survey of the last 25 years. Prosthet Orthot Int. 2007. p. 236–257.

[5] Schofield JS, Schoepp KR, Williams HE, et al. Characterization of interfacial socket pressure in transhumeral prostheses: A case series. PLoS One [Internet]. 2017;12:e0178517-. Available from: https://doi.org/10.1371/journal.pone.0178517.

[6] Knapik JJ, Reynolds KL, Duplantis KL, Jones BH. Friction blisters. Sports Medicine 1995 20:3. 2012;20:136–147. Available from: https://link.springer.com/article/10.2165/00007256-199520030-00002.

[7] Radmand A, Scheme E, Englehart K. High-density force myography: A possible alternative for upper-limb prosthetic control. J Rehabil Res Dev. 2016;53:443–456.

[8] Gang Xiao Z, Menon C. A review of force myography research and development. 2019 [cited 2024 Feb 11]; Available from: www.mdpi.com/journal/sensors.

[9] Young PR, Hebert JS, Marasco PD, Carey JP, Schofield JS. Advances in the measurement of prosthetic socket interface mechanics: a review of technology, techniques, and a 20-year update. Expert Rev Med Devices. 2023; 20:729–739. Available from: https://www.tandfonline.com/action/journalInformation?journalCode=ierd20.

[10] Feix T, Romero J, Schmiedmayer HB, et al. The GRASP taxonomy of human grasp types. IEEE Trans Hum Mach Syst. 2016;46:66–77.

[11] Smith LH, Hargrove LJ, Lock BA, Kuiken TA. Determining the optimal window length for pattern recognition-based myoelectric control: balancing the competing effects of classification error and controller delay. IEEE Transaction on Neural Systems and Rehabilitation Engineering. 2011;19.

[12] Hudgins B, Parker P, Scott RN. The recognition of myoelectric patterns for prosthetic limb control. Proceedings of the Annual International Conference of the IEEE Engineering in Medicine and Biology Society Volume 13: 1991. 1991. p. 2040–2041.

[13] Nowak M, Eiband T, Castellini C. Multi-modal myocontrol: Testing combined force- and electromyography. IEEE International Conference on Rehabilitation Robotics. IEEE Computer Society; 2017. p. 1364–1368.

[14] Scheme E, Fougner A, Stavdahl Ø, et al. Examining the adverse effects of limb position on pattern recognition based myoelectric control. 2010 Annual International Conference of the IEEE Engineering in Medicine and Biology. 2010. p. 6337–6340

[15] Delva ML, Lajoie K, Khoshnam M, et al. Wrist-worn wearables based on force myography: On the significance of user anthropometry. Biomed Eng. 2020;19:1–18. Available from: https://biomedical-engineering-online.biomedcentral.com/articles/10.1186/s12938-020-00789-w.

[16] Jiang S, Gao Q, Liu H, et al. A novel, co-located EMG-FMG-sensing wearable armband for hand gesture recognition. Sens Actuators A Phys. 2020;301.

[17] Belyea A, Englehart K, Scheme E. FMG Versus EMG: A Comparison of Usability for Real-Time Pattern Recognition Based Control. IEEE Trans Biomed Eng. 2019;66:3098–3104.

Prosthetic Devices/Materials

A COMPACT 2-DOFS ACTUATED WRIST FOR IMPROVING DEXTERITY OF UPPER LIMB PROSTHETICS

N. Boccardo[*,1,2,†], M. Canepa[*,1,2,†], S. Stedman[1], L. Lombardi[1], A. Marinelli[1,†], D. Di Domenico[1,3,†], R. Galviati [1], E. Gruppioni[4,†], L. De Michieli[1,†] and M. Laffranchi[1,†]

1 Istituto Italiano di Tecnologia, Genova, Italy
2 Open University Affiliated Research Centre at Istituto Italiano di Tecnologia (ARC@IIT)
3 Department of Electrical, Electronics and Communications, Politecnico di Torino, Italy
4 INAIL Prosthetic Centre, Vigorso di Budrio, Italy
† IEEE Member
** These authors equally contributed to this manuscript*

ABSTRACT

This study tackles the challenges of developing an upper limb prosthetic system that accurately replicate the complexity of the human counterpart. Upper limb prostheses still present high abandonment rates, due to poor control intuitiveness and lack of dexterity. To address these issues, we introduce an anthropomorphic wrist prosthesis featuring active flexion-extension and pronation-supination capabilities, seamlessly integrated with the poly-articulated hand Hannes, with the goal of augmenting the dexterity and overall functionality in trans-radial and trans-humeral prostheses. Notably, the high dexterity and controllability observed when operated by amputees, using pattern recognition algorithms, based on a low-density EMG arrangement in a standard prosthetic socket, paves the way for future investigations and potential applications in home environment.

INTRODUCTION

The loss of the upper limb significantly impacts life quality for amputees, affecting manipulation and interaction abilities: in particular, the absence of wrist mobility forces amputees to perform unnatural movements, adding stress to shoulder and back during Activities of Daily Living (ADLs) [1]. Despite the importance of wrist mobility in naturally orienting the hand during grasping activities, there is a lack of multi-degrees of freedom actuated prosthetic wrists in the literature, with few commercial options offering limited active dexterity. To fill this gap, we developed and hereafter we present an innovative 2-DoFs prosthetic wrist, from both mechatronic and control perspectives [2]. The design aims at mimicking the ability of the intact human wrist during ADLs, in combination with our underactuated prosthetic hand Hannes [3]. The control exploits pattern recognition (PR) techniques to enhance both naturalness and intuitiveness of the multi-DoF prosthetic device. We provide a comprehensive overview of the project, starting with system requirements and then detailing the mechanical and control design. The experimental results and potential impact of the device in prosthetic applications are discussed, along with suggestions for future developments.

MATERIALS AND METHODS

The development of a prosthetic wrist device with 2 DoFs, incorporating flexion-extension (FE) and pronation-supination (PS), followed a user-centred design approach. We initially aimed at extracting the functional requirements, in terms of range of motion, torque, speed, robustness, anthropomorphism, weight, total length, and control latency. However, literature lacks valid estimates about wrist torque and speed during healthy subjects ADLs. Therefore, we conceived an experimental method to extract this information statistically. To estimate maximum power consumption requirements, we derived an average of 411 hand movements per day and set a worst-case of 1:1 ratio between hand and wrist movement from our previous clinical evaluation with Hannes [4]. Given the requirements, we designed a serial and modular mechanical architecture, creating two separate FE and PS wrist mechanism, with space to accommodate a standard Ottobock quick disconnect mechanism with electrical slipring, to transfer power and communicate to the hand. This modular design allows flexibility and compatibility with the existing prosthetic system, adapting to various amputation types and lengths. The FE wrist is designed with anthropomorphism in mind, minimizing misalignment between mechanical and anatomical rotation axes. Non-backdrivability is prioritized to prevent excessive battery consumption under static loads: this is achieved via a 3-stage gearbox, with an initial 4:1 planetary stage, an intermediate 2.1:1 spur gear and a final 40:1 worm gear (Figure 1A). This compact design achieves

82° range of motion (RoM), which is comparable to healthy subjects' requirements during ADLs. The FE mechanism has total length of 55 mm and total weight of 211 g. The PS is designed to be hollow shaft, to allow fitting of the standard slipring. It features a frameless 25 mm PMSM motor integrated with a 100:1 strain-wave reducer. The design allows the hand prosthesis to be attached and detached by the patient, whilst ensuring a robust connection between hand and socket. The resulting is an overall length of 65.1 mm and a 43 mm diameter (Figure 1D). From the control point of view, we exploited a previously developed, EMG based, Pattern Recognition control strategy, using Nonlinear-Logistic Regression (NLR), allowing users to control wrist PS, FE, and hand open and close in real-time [5, 6]. The control architecture presents two main layers: the joint selection layer, extracting from the NLR the classification of the action according to user intention and a joint control layer, computing the position references according to the RMS of EMG signal intensity. In this implementation, 6 standard dry surface EMG prosthetic sensors are used, to ensure compatibility with patient prosthetic socket.

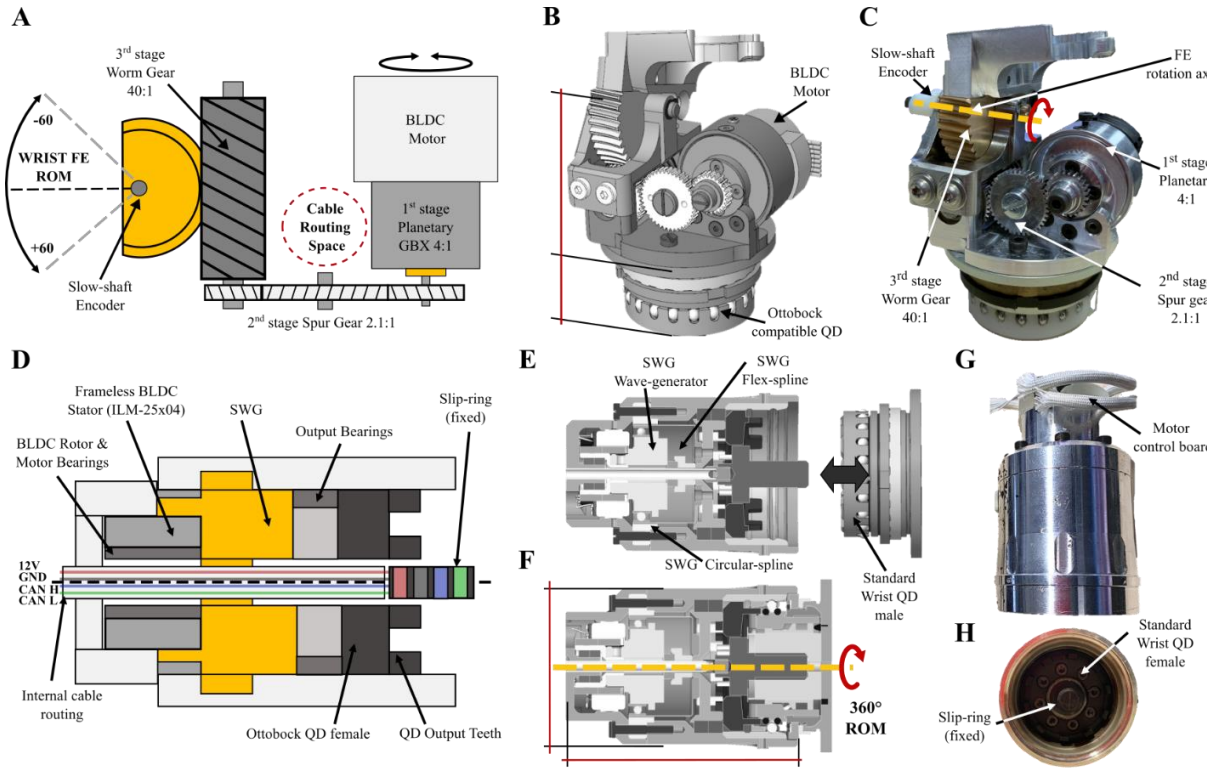

Figure 1: Wrist FE: **A)** Schematical representation of the adopted mechanism; **B)** Computer-aided design of the wrist device; **C)** Actual representation of the wrist device. Wrist PS: **D)** Schematical representation of the adopted mechanism; **E-F)** Computer-aided design of the wrist device; **G-H)** Actual representation of the wrist device.

RESULTS

We implemented a three phases testing methodology for assessing the prosthetic device capabilities [2]. In the dynamic tests phase, we aimed at estimating the mechanical bandwidth of the wrist actuators, applying a sequence of sinusoidal speed references from 0.25 to 4.5 Hz, resulting in 1 Hz for wrist PS and 2 Hz for wrist FE at -3dB in the complete Range of Motion. We performed then an able-body kinematics assessment, to extract the wrist speed profiles from healthy subjects during ADLs. The ROM and speed profiles were compared to the prosthetic wrist capabilities, simulating loads in realistic scenarios with the prosthetic wrist, such as lifting a heavy sphere of 532 gr in flexion and extension or pouring water from a 300 g jug with 500 ml water. Results showed a maximum torque of 5.27 Nm for PS joint during the glass jug pouring task and 2.38 Nm for FE joint during lifting of a heavy sphere, which were below

the maximum torque achievable by the actuators. The maximum speeds during healthy ADLs of 38.7 rpm for PS and 23.4 rpm for FE were extracted statistically from the data and compared with the maximum actuators' speeds, resulting in a superior performance of the mechanical wrist. Finally, we evaluated the PR control strategy with 10 healthy subjects and 3 mono-lateral amputees during ADLs. Written informed consent was obtained under the guidelines and approval of Bologna-Imola ethical committee (CP-PPRAS1/1-01) prior to conducting the experiments. An example of the EMG signals used to train the PR model is graphically represented in Figure 2. Preliminary results showed a good class separation and pattern discrimination, decoding the user intention and executing wrist movements in a repeatable manner at 300Hz. Since the control algorithm runs directly in the embedded control electronics, the resulting system is wearable and anthropomorphic, paving the way to the usage in a real clinical scenario. Moreover, we assessed power consumption in the worst case of 500 combined average wrist and hand movements, considering a 16 hours consecutive daily use, achieving a 56,2 % average battery usage with a small 11,1V, 2.5Ah prosthetic battery pack.

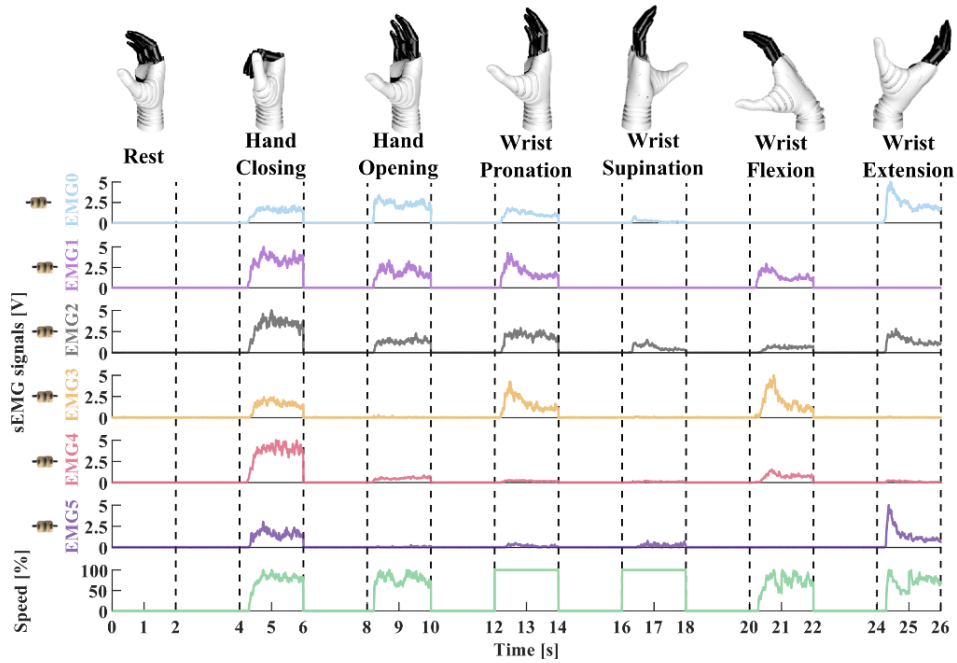

Figure 2: Representation of the 6 EMG signals used during the training of the Pattern Recognition model to control the 3 DoFs Hannes prosthetic system.

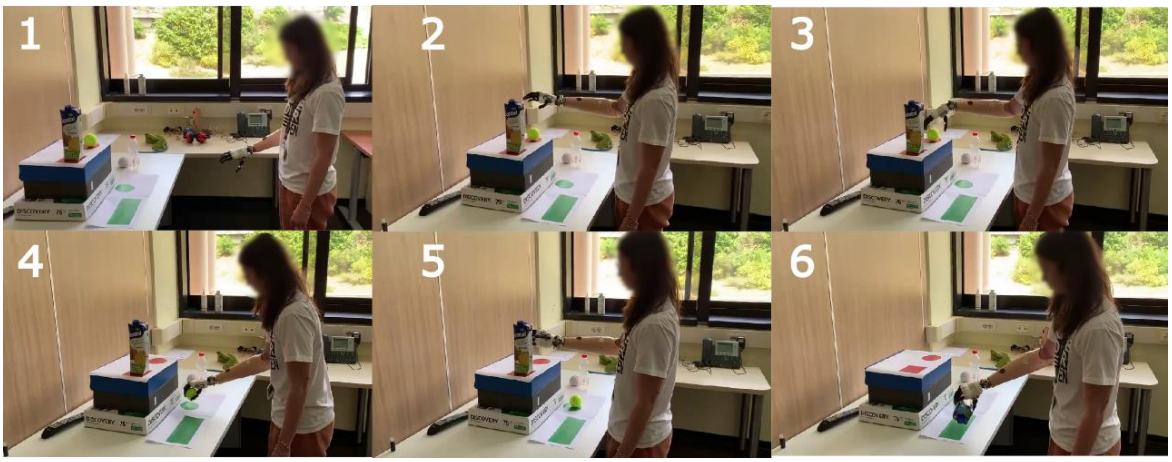

Figure 3: Time representation of a patient using the Hannes prosthesis during ADLs. Preparation of the wrist configuration to grasp an object (1), reaching the spherical object (2), adjusting the wrist FE to comfortably grasp the object (3), extend the wrist to place the object on the table (4), adjust the wrist PS to grasp a vertical object (5), adjust the wrist PS to place the object horizontally on the table (6).

DISCUSSIONS AND CONCLUSIONS

We introduced a prosthetic wrist with 2-DoFs [2], combined with the poly-articulated Hannes hand prosthesis [3], and evaluated its efficacy as a practical substitute for the natural counterpart. To achieve this goal, we conducted a variety of tests and validations: results show that this novel prosthetic system could mimic human movements and achieve satisfactory range of motions and mechatronics capabilities, providing potential benefits to patients due to an enhanced wrist dexterity. Statistical analysis confirms the 2-DoFs wrist's speed and torque performance exceeds average natural task requirements. We used the artificial wrist in combination to a machine learning based multi-DoFs control strategy, achieving low latency and a good usability, enabling an efficient control of wrist movements. Additionally, the compact prosthetic design promotes the overall anthropomorphism of the prosthesis, with a low impact on the energy budget. The promising results and performances pave the way for future studies to assess long-term use, robustness, and usability in clinical and at-home scenarios. As an example, Figure 3 illustrates a timeline depicting two distinct grasping scenarios that necessitate the utilization of the two DoFs in the wrist. The subjects in the study employed the PR model [5] to control the 3 DoFs of the prosthetic device during ADLs. In particular, the amputee was tasked with grasping and positioning both a spherical object and a vertical object using the developed prosthetic device. Notably, our observations indicated minimal compensatory movements at the shoulder level. The mechatronic system will enable usage of other advanced control strategies, including artificial intelligence, and has the potential for adaptation to trans-humeral prosthetic solutions, broadening its applicability.

ACKNOWLEDGEMENTS

This work was supported by the Istituto Nazionale Assicurazione Infortuni sul Lavoro, under grant agreements PPR AS 1/1 and PR19-PAS-P1. The Open University Affiliated Research Centre at Istituto Italiano di Tecnologia (ARC@IIT) is part of the Open University, Milton Keynes MK7 6AA, United Kingdom.

REFERENCES

[1] A. Marinelli *et al.*, "Active upper limb prostheses: A review on current state and upcoming breakthroughs," *Progress in Biomedical Engineering*, vol. 5, no. 1, p. 012001, 2023.

[2] N. Boccardo *et al.*, "Development of a 2-DoFs actuated wrist for enhancing the dexterity of myoelectric hands," *IEEE Transactions on Medical Robotics and Bionics*, 2023.

[3] M. Laffranchi *et al.*, "The Hannes hand prosthesis replicates the key biological properties of the human hand," *Science Robotics*, vol. 5, no. 46, p. eabb0467, 2020, doi: 10.1126/scirobotics.abb0467.

[4] M. Semprini *et al.*, "Clinical evaluation of Hannes: measuring the usability of a novel polyarticulated prosthetic hand," in *Tactile Sensing, Skill Learning, and Robotic Dexterous Manipulation*: Elsevier, 2022, pp. 205-225.

[5] D. Di Domenico *et al.*, "Hannes Prosthesis Control Based on Regression Machine Learning Algorithms," presented at the 2021 IEEE/RSJ International Conference on Intelligent Robots and Systems (IROS 2021), 2021.

[6] F. Egle *et al.*, "Preliminary Assessment of Two Simultaneous and Proportional Myocontrol Methods for 3-DoFs Prostheses Using Incremental Learning," in *2023 International Conference on Rehabilitation Robotics (ICORR)*, 2023: IEEE, pp. 1-6.

A TAXONOMY FOR COMMERCIALLY AVAILABLE MYOELECTRIC TERMINAL DEVICES

Eric J. Earley, PhD[1,2], Cristina Piazza, PhD[3], Kristi L. Turner, DHS, OTR/L[4]

[1]*Bone-Anchored Limb Research Group, University of Colorado, Aurora, CO, USA*

[2]*Department of Orthopedics, University of Colorado School of Medicine, Aurora, CO, USA*

[3]*Department of Computer Engineering, Technical University of Munich, Germany*

[4]*Center for Bionic Medicine, Shirley Ryan AbilityLab, Chicago, IL, USA*

ABSTRACT

The number of myoelectric prostheses available commercially has grown rapidly in the past decade, displaying a range of design philosophies and capabilities. As a result, the terms "myoelectric prosthesis," "bionic hand", or "multifunction prosthesis" commonly used to describe such devices fail to account for these different prosthetic designs. Here, we propose a myoelectric prosthesis terminal device taxonomy, which aims to describe the full span of prosthetic designs. We then categorize commercially available myoelectric prosthetic terminal devices to identify the subset of categories most frequently represented in the market, thereby expanding the ability to perform cross-study comparison and meta-analysis of myoelectric prosthesis performance.

INTRODUCTION

For people with limb loss or limb difference, myoelectric prosthetic hands represent the current standard of prosthetic care. While some prostheses are capable of only rudimentary opening and closing, reminiscent of the body-powered prosthetic hooks available throughout the 20th century, other modern "bionic" prosthetic hands are capable of emulating more complex hand movements, with features including thumb adduction and independent finger actuation. The number of myoelectric prosthetic hands entering the market has increased drastically in the past decade [1, 2]. While this provides a wealth of options for those with limb loss and limb difference, it also presents a challenge when it comes to comparing the capabilities of each hand, especially with respect to their degrees of freedom.

With the increased flexibility and versatility of these modern myoelectric prosthetic hands, the previous classifications of opening and closing the hand were insufficient to describe the new grasping styles that are now possible. There was a need for a grasping taxonomy which strove to classify the nearly infinite combinations of finger and hand positioning in a manageable number of prehensile patterns which are commonly used throughout daily life [3]. Related work near the end of the 20th century, namely the development of the Cutkosky grasping taxonomy [4] and postural synergy analysis [5], served as a foundation and inspiration for identifying the common grasp which multifunction prostheses would strive to mimic. While the control of individual fingers of a prosthetic hand can be done within research settings [6], most multifunction instead implement a subset of these grasping patterns as "presets", available for the user to access via pattern recognition control [7], gesture control, or a mobile app. These grasping styles subsequently influenced the development of several standardized outcomes to be able to characterize the benefits of the additional mechanical complexity (and cost) of these devices. For example, the Southampton Hand Assessment Procedure (SHAP) requires its various tasks to be performed using six specific grasps [8]. However, the ability for a prosthetic hand to achieve any of these grasps is wholly dependent on its mechanical design and its available degrees of freedom.

Given the vast difference in grasping capabilities across devices which share the label "myoelectric prosthesis," and the ever-expanding number of myoelectric prostheses available on the market, there is a clear need for a taxonomy which can categorize these devices based on their common functionality and their mechanical degrees of freedom. Thus, in this paper we propose such a terminal device taxonomy with two aims. First, we aim to describe the full span of possible prosthetic designs, such that any myoelectric prosthetic hand can be clearly classified. Second, we aim to perform a market analysis of commercially available myoelectric prosthetic terminal devices, to categorize these prostheses according to the proposed taxonomy, and to identify the most common categories. By identifying the subset

of categories most frequently represented in the market, we aim to expand the ability to perform cross-study comparisons and meta-analysis of myoelectric prosthesis performance according to common functionality, rather than grouping study outcomes by a growing list of individual devices.

METHODS

The genesis for creating the terminal device taxonomy arose during conversations regarding the development of a data entry sheet for the Assessment of Capacity for Myoelectric Control (ACMC) [9], wherein evaluators would be asked to indicate the prosthetic setup being used. In earlier iterations of this sheet, evaluators could select from a small number of myoelectric prosthetic hands commonly used in research. However, when revisiting this sheet for current use, we noted that it would become cumbersome to list every type of prosthetic hand; furthermore, doing so would also require frequent updates for the sheet to stay up-to-date with the latest technological developments. Instead, developing a smaller list of prosthetic hand categories that can broadly differentiate between the different types of myoelectric prostheses would both reduce the complexity of filling out the sheet for the evaluator, and also future-proof the list against requiring frequent updates to account for new prosthetic hands entering the market or research space.

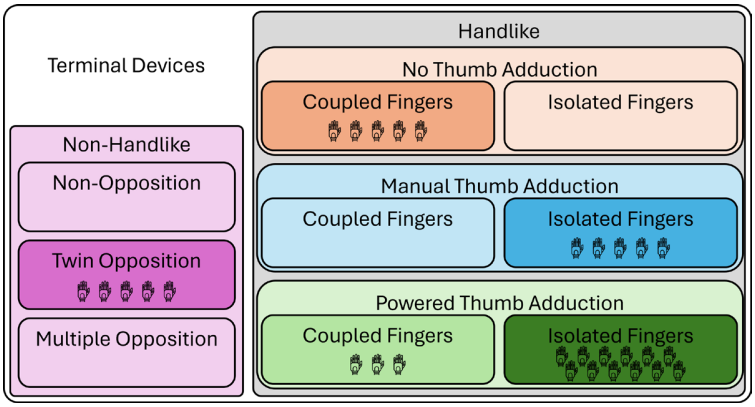

Figure 1: The proposed terminal device taxonomy features two higher-order taxa, *Handlike* and *Non-Handlike*, determined by the appearance and function of the device. Each higher-order taxon is further separated into several lower-order taxa. Icons within each taxon represent the number of commercially available prostheses categorized accordingly; taxa with greater representation are colored darker.

Development of the Taxonomy

Thematic analysis of common commercially available myoelectric prostheses provided a foundation for the taxonomy. We noted three broad categories that we wanted to account for in the taxonomy: prosthetic hooks and grippers, simple (open/close) prosthetic hands, and multifunction prosthetic hands. Next, particular focus was paid to grouping the different types of multifunction prosthetic hands, in which we noted two dimensions of categorization: thumb adduction and finger coupling. Finally, through a review of commercially available and research prostheses, we iterated upon the taxonomy as flaws were discovered which failed to categorize a prosthetic design.

The full taxonomy is shown in **Figure 1**. The following sections introduce the two overarching taxa (categorizations), followed by their unique lower-order taxa.

Non-Handlike Terminal Devices

Non-handlike terminal devices are prostheses which do not seek to emulate the appearance or function of the human hand, but instead performs grasping actions through other configurations. Non-handlike terminal devices can be separated into three categories:

- Twin opposition: two opposing surfaces are used to grasp objects, such as the traditional split-hook design.
- Multiple opposition: three or more opposing surfaces are used to grasp objects. Designs often take inspiration from industrial grippers.
- Non-opposition: objects are handled without opposition, instead employing other mechanisms such as suction or wrapping around the object.

Handlike Terminal Devices

Handlike terminal devices are prostheses which seek to emulate the appearance of the human hand, and to varying degrees emulate the natural function and degrees of freedom of the hand. Handlike terminal devices can be categorized

across two dimensions of mechanical degrees of freedom. First, devices can be separated into three categories describing the ability of the prosthetic thumb to adduct:

- No thumb adduction: the thumb is positioned in an abducted position, suitable for palmar grasping. It may flex, but cannot be rotated into an adducted position for lateral grasping.
- Manual thumb adduction: the thumb can be positioned in an abducted or adducted position, but must be rotated manually. Thumb flexion is still powered.
- Powered thumb adduction: thumb flexion and adduction are both powered.

Second, devices can be separated into two categories describing the coupling or independence of the prosthetic fingers:

- Isolated fingers: all five fingers are mechanically independent and could theoretically be adapted to actuate individual fingers, even if the fingers are normally controlled to move together (e.g. if using grasp-based pattern recognition).
- Coupled fingers: some or all fingers are mechanically coupled, such that they cannot be actuated independently.

Taxonomic Categorization of Commercially Available Prosthetic Terminal Devices

A list of commercially available prosthetic terminal devices is provided in **Table I**. The list was populated using an online database [10] supplemented by the authors' knowledge of devices that were omitted from the database. In total, 30 prosthetic terminal devices were identified; devices created only for research purposes, which are not commercially available, are not included.

Table I: Taxonomic Categorization of Commercially Available Prosthetic Terminal Devices

Non-Handlike Terminal Devices		
Fillauer MC Standard ETD	Twin opposition	
Fillauer ProPlus MC ETD	Twin opposition	
Fillauer ProPlus MC ETD2	Twin opposition	
Ottobock AxonHook	Twin opposition	
Ottobock Greifer	Twin opposition	
Handlike Terminal Devices	***Thumb Adduction***	***Finger Coupling***
Aether Biomedical Zeus Hand	Manual	Isolated
Atom Limbs Atom Touch	Powered	Isolated
BionIT Labs Adam's Hand	Powered	Isolated
BrainRobotics Prosthetic Hand	Powered	Isolated
COVVI Nexus Hand	Powered	Isolated
Fillauer MC ProPlus Hand	None	Coupled
Makers Hive KalArm	Manual	Isolated
MaxBionic MeHand	Powered	Isolated
Mobius Bionics Luke Arm	Powered	Coupled
Motorica Manifesto Hand	Powered	Isolated
Open Bionics Hero Arm	Powered	Isolated
Össur i-Limb Access	Manual	Isolated
Össur i-Limb Ultra	Powered	Isolated
Össur i-Limb Quantum	Powered	Isolated
Ottobock bebionic Hand	Manual	Isolated
Ottobock Michelangelo Hand	Powered	Coupled
Ottobock MyoHand VariPlus Speed	None	Coupled
Ottobock SensorHand Speed	None	Coupled
OYMotion OHand	Manual	Isolated
Prensilia MiaHand	Powered	Coupled
Psyonic AbilityHand	Powered	Isolated
Robo Bionics Grippy	None	Coupled
TASKA Hand Gen2	Powered	Isolated
Unlimited Tomorrow TrueLimb	None	Coupled
Vincent Systems Vincent Evolution	Powered	Isolated

RESULTS

Of the 30 identified commercially available prosthetic terminal devices, the majority (25) are handlike in design, and half (15) feature powered thumb adduction. Of these, most (12) feature isolated finger actuation, indicating the general trend for multifunction hands over the past decade. Although every hand with no thumb adduction or manual thumb adduction had coupled and isolated fingers, respectively, there was a subset of hands with powered thumb adduction and coupled fingers. This is likely intended to reduce the number of motors via underactuation, relying on the fact that prominent grasping synergies typically involve some degree of finger coupling [5].

DISCUSSION

Overall, we identified five categories which describe the commercially available prosthetic terminal devices:

- Non-handlike terminal device
- Hands without thumb adduction
- Hands with manual thumb adduction

- Hands with powered thumb adduction and coupled fingers
- Hands with powered thumb adduction and isolated fingers

The proposed taxonomy shown in **Figure 1** features several taxa which are not commercially represented. We do not recommend including these in the list of categories above, however we believe their presence in the taxonomy represents the possibility of prosthetic terminal device design. Indeed, examples of each of these taxa may be found in the literature, and have simply not been developed into a commercial product.

For handlike devices, a case can be made for the inclusion of *semi-coupled* fingers as a new taxa, which refers to devices where some, but not all, fingers are coupled. For example, the Mia hand couples the middle, ring, and little fingers, but the index finger actuates independently from these three fingers. However, for the purposes of a concise categorization listed above, we grouped all hands were finger coupling.

One aspect which is not considered in this taxonomy is the method used to control a prosthesis. For example, in a recent study, a prosthesis with fully isolated fingers (Ottobock bebionic) was set up to couple the middle, ring, and little fingers as one unit, and to control the index and thumb flexion independently [6]. The taxa for coupled and isolated fingers represent the limits of prosthetic function; A prosthetic hand designed with the ability to move fingers independently (isolated fingers) can be adapted to move them together (coupled) using the control system. However, a hand originally designed to move fingers only together (coupled) cannot be adapted to control the fingers independently.. For grasp-based pattern recognition, depending on the grasps available to the user, the distinction between coupled and isolated fingers may disappear, in which case the categories listed above could be further reduced from five to four.

ACKNOWLEDGEMENTS

We would like to thank Laura Miller, CP, PhD for her insights during the early development of the taxonomy.

REFERENCES

[1] C. Piazza, G. Grioli, M. G. Catalano, and A. Bicchi, "A Century of Robotic Hands," in *Annual Review of Control, Robotics, and Autonomous Systems* vol. 2, ed, 2019, pp. 1-32.

[2] C. Widehammar, A. Hiyoshi, K. Lidström Holmqvist, H. Lindner, and L. Hermansson, "Effect of multi-grip myoelectric prosthetic hands on daily activities, pain-related disability and prosthesis use compared with single-grip myoelectric prostheses: A single-case study," *Journal of Rehabilitation Medicine,* 2021, doi: 10.2340/jrm.v53.807.

[3] A. J. Spiers, J. Cochran, L. Resnik, and A. M. Dollar, "Quantifying Prosthetic and Intact Limb Use in Upper Limb Amputees via Egocentric Video: An Unsupervised, At-Home Study," *IEEE Transactions on Medical Robotics and Bionics,* vol. 3, no. 2, pp. 463-484, 2021, doi: 10.1109/tmrb.2021.3072253.

[4] M. R. Cutkosky and R. D. Howe, "Human grasp choice and robotic grasp analysis," in *Dextrous robot hands*, S. T. Venkataraman and T. Iberall, Eds., ed: Springer-Verlag New York, Inc., 1990, pp. 5-31.

[5] M. Santello, M. Flanders, and J. F. Soechting, "Postural hand synergies for tool use," in *The Journal of Neuroscience* vol. 18, ed, 1998, pp. 10105-10115.

[6] J. Zbinden *et al.*, "Improved control of a prosthetic limb by surgically creating electro-neuromuscular constructs with implanted electrodes," *Science Translational Medicine,* vol. 15, no. 704, p. eabq3665, 2023, doi: doi:10.1126/scitranslmed.abq3665.

[7] A. M. Simon *et al.*, "Myoelectric prosthesis hand grasp control following targeted muscle reinnervation in individuals with transradial amputation," in *Plos One* vol. 18, ed, 2023, p. e0280210.

[8] C. M. Light, P. H. Chappell, and P. J. Kyberd, "Establishing a standardized clinical assessment tool of pathologic and prosthetic hand function: normative data, reliability, and validity," in *Arch Phys Med Rehabil* vol. 83, ed, 2002, pp. 776-783.

[9] L. M. Hermansson, A. G. Fisher, B. Bernspång, and A. C. Eliasson, "Assessment of Capacity for Myoelectric Control: A new Rasch-built measure of prosthetic hand control," in *Journal of Rehabilitation Medicine* vol. 37, ed, 2005, pp. 166-171.

[10] W. Williams. "A Complete Guide to Bionic Arms & Hands." https:/bionicsforeveryone.com/bionic-arms-hands (accessed September 25, 2023 (archive.org).

AN APPROACH TO REPLICATING CLINICAL PROSTHETIC SOCKETS TO SUPPORT RESEARCH

Alix Chadwell[a,b,c], Laurence Kenney[b], Michael Prince[b], Jennifer Olsen[c], Matthew Dyson[c]

[a] University of Southampton, UK, [b] University of Salford, UK, [c] Newcastle University, UK

ABSTRACT

Research into upper-limb prostheses is often limited by access to prosthetic sockets, each custom-fitted by a prosthetist. Many technological advances in upper-limb prostheses come from engineering focussed labs. Unfortunately, with a global shortage of prosthetists, often, these labs cannot rely on access to a prosthetist to support experimental work, making it hard to undertake quality research reflective of clinical realities. We propose a process to replicate the internal shape of a clinical standard prosthetic socket and facilitate broader access to more representative research. Our proposed method uses a combination of silicone, alginate, and plaster. This proof-of-concept study demonstrates that the proposed new approach is feasible and accurate. This technique will facilitate improvements in the assessment of prosthetic technologies. The process is non-destructive, thus also opening opportunities for socket design and electrode placement research with the removal of confounding factors relating to socket shape. Improving access to prosthetic sockets for research purposes will undoubtedly have international impact.

INTRODUCTION

Studies requiring socket manufacture are often small, recruiting only people local to the research team/clinic. Manufacture of bespoke sockets on a larger scale is costly and puts excessive strain on an already stretched clinical service. Without a feasible and accurate approach to socket creation, many technical initiatives such as take-home training, real-world monitoring, and large-scale pattern recognition studies remain extremely challenging to deliver. We present a proof-of-concept for a socket replication process, which can be undertaken without a prosthetist present.

This research was in part inspired by the drive to upscale upper-limb prosthetics research to increase its impact [1]; one approach being to move research out of the lab and take it directly to participants. In cases where a bespoke research prosthesis is needed, this will require a mobile socket fitting process. Even where labs are fortunate enough to have access to in-house or local prosthetists, it is unlikely they will have capacity to spend significant time travelling to participants' homes; consequently, an alternative approach to socket manufacture is required.

One option is to replicate a participant's existing socket shape. Physical replication techniques are sometimes used clinically [2]; however, in all cases we could identify, the replication process is poorly documented, sometimes destructive, and mould removal can be difficult with narrow or long upper-limb sockets. The authors were also unable to identify any validation studies of such approaches. Photogrammetry, to digitally replicate internal socket surfaces, has been shown to have some success for lower-limb sockets [3], however, as an upper-limb socket is smaller and usually bent at the elbow, line-of-sight can be obstructed.

A reliable and accurate socket replication process would have wider impacts beyond simply enabling research studies to reflect clinical realities. Socket design and manufacture is rarely documented [4]. In the absence of a validated socket replication method, controlled studies of the impact of socket shape and local physical attributes, such as mechanical compliance, on fit and comfort are difficult to deliver. This is because the nature of casting means that no two sockets manufactured for a person will be the same.

Here we demonstrate the feasibility of accurately replicating a prosthetic socket's shape without damaging the original. A case-study is provided, using a myoelectric socket to demonstrate accurate capture of both socket shape and precise electrode position. This is key to the performance of the resulting prosthesis.

METHODOLOGY

Limbtex Limbcopy Silicone, Platsil Gel Silicone, and alginate were evaluated as materials to capture the negative mould from the socket. Our proposed approach uses the Platsil Gel Silicone which was easiest to work with and kept

its shape well for a prolonged period. We also trialled both full-fill and layer coating techniques; our proposed approach combines the compressibility and ease of extraction associated with the layer coating with the structural benefits of the full-fill.

Initial preparation of the socket involved covering the electrodes and any holes/rivets with Tegaderm film bandage to avoid damage or leakage of the moulding agent into the void between the inner- and outer- socket. A tape collar was built up above the socket trim lines. We added a tube into the mould ensuring it filled as much of the void as possible without touching the edges of the socket: Note that, to make it easier to remove later, the tube can be wrapped in a layer of clingfilm. The mould was then filled with silicone and left to cure. Once cured the tube was removed allowing the mould to be compressed and displaced from the socket walls. The tube was then re-inserted into the mould after extraction to ensure the shape was maintained. We recommend using Platsil Gel00 (a softer silicone) for ease of mould extraction although we have tested this method with different Shore hardnesses (A25-0030).

We converted the silicone negative (Figure 1a) into plaster (Figure 1b) via an alginate positive. As there is a risk of compound error, it is important to carefully avoid changes in the shape of the mould between steps. The plaster negative was carefully smoothed down to remove any bumps from bubbles in the alginate whilst avoiding any change in the shape or volume. The area above the trim lines was tidied so as not to tear the bag during lamination.

As can be seen in Figure 1, the electrodes leave an impression in the mould. When traditionally manufacturing a myoelectric prosthetic socket, electrode dummies are used. These are thinner than an electrode and designed to sit flat against the mould. To manufacture the clone socket these same electrode dummies are used, therefore the electrode indent must be infilled, restoring the shape in this area to match the mould for the original socket. The position of the electrodes needs to be identical for the replica sockets and original, so a plaster replica of the electrode was created via a silicone mould (Figure 1c). The depth of the plaster electrode was matched to the difference between the electrode and the dummy. The quality of the moulding process means that the plaster electrode could be easily aligned with the original electrode position by lining up the imprints of the metal contacts (Figure 1d). The web created by the protective Tegaderm must also be backfilled. To ensure the infill accurately reflected the original shape, the wet plaster was smoothed to the line of the plaster electrode and existing socket negative using a tongue depressor (Figure 1e). The plaster electrode was also coloured to help locate the dummy.

Once complete, the plaster mould was provided to prosthetics technicians to manufacture a prosthetic socket using their traditional approach to manufacturing a laminated socket.

To assess whether the clone socket accurately replicated the original, 3D scanning was used (Einscan-Pro 3D scanner). As it is difficult to accurately capture the internal shape of an upper-limb socket due to the small size and likelihood of occlusions, a silicone negative mould from the original socket was compared to another negative silicone mould from the clone socket. The alignment between the scans was assessed using CloudCompare software (v2.12.2). The meshes were aligned and the distance between the meshes computed using the ‘cloud-to-mesh’ function.

RESULTS

When comparing the silicone negative of the clone socket to the silicone negative of the original socket, the mean distance between points was 0.16mm (standard deviation 0.38mm). A positive difference suggests the clone is outside of the original reference scan (volumetrically larger), whilst a negative difference suggests the clone is inside (volumetrically smaller). Figure 2 shows a histogram of the distances between the sockets and highlights top right the areas where the difference was greater than 1mm. There are small areas on the posterior aspect of the socket and at the edge of the electrodes where the clone is 1-2mm larger than the original. Around the edge of the electrodes this will be caused by a new web being created by the Tegaderm which will not align perfectly with the original web. What is important to note is that the metal contacts of the electrode show very little error between the two moulds (<0.5mm) as shown in the close-up bottom right.

DISCUSSION

This study shows the recommended socket replication technique to be highly accurate. Although it has not been assessed quantitatively, we anticipate this technique will generate a significantly more accurate replica than a new socket manufactured from scratch using traditional casting or scanning techniques.

By removing the requirement for several socket iterations, this technique offers significant time, cost, and labour saving to researchers, technicians, and participants themselves. The process of taking the silicone mould may not be

quicker than casting due to curing time, however, only the prosthesis is required, thus freeing the participant up to continue with their activities. Most importantly, this process can easily be taken to the participant, without the requirement for a prosthetist. With the confidence that the final socket will fit, it also becomes more feasible to post sockets and moulds between labs [5].

This socket replication process can facilitate take-home trials of instrumented prostheses, thus opening a new opportunity to understand the impact of various factors relating specifically to socket fit. Additionally, by manufacturing sockets matching those prescribed clinically we can assess a range of socket types, originally manufactured by a broad pool of clinicians, rather than by one or two clinicians affiliated with the research, thereby reducing the risk of unconscious bias. These factors should all increase confidence in the validity of results. As the recommended process does not destroy or damage the original negative mould, this technique also opens new opportunities for us to evaluate socket design. We can manufacture several matching sockets with subtle changes, such as adjusting electrode positions or changing wall thickness. Additional electrodes may be added to form arrays, facilitating more applied pattern recognition research. Further, we can explore the impact of manufacturing the socket using emerging materials. By producing these sockets from identical plaster moulds, we can reduce the confounding factors in research.

CONCLUSION

This case study, focussing on an upper-limb myoelectric prosthesis, has demonstrated that the proposed new approach to replicating a clinical prosthetic socket is feasible and accurate (mean difference 0.16 mm). The non-destructive method involves shape capture using silicone and conversion into a plaster mould via alginate. This new method will facilitate the development of research prostheses without the requirement for an on-site prosthetist, opening up more opportunities for prosthetics research representative of the clinical realities. In addition, with an increased interest in real-world prosthetics research, this technique will enable engineering focussed labs to develop take-home versions of new technologies allowing exploration of the real-world practicalities of developments in prosthesis control. With the cost of novel prosthetic technologies increasing, funders require increased evidence of clinical and cost effectiveness. To generate this evidence base, research must represent the clinical population and their real-world use of their prostheses. This socket replication technique brings these studies a step closer to feasibility. Although the example socket presented here includes electrodes, this method would be similarly suitable for a non-myoelectric socket.

ACKNOWLEDGEMENTS

The authors would like to acknowledge the support of the prosthetics technicians at the University of Salford (Lee Willan, Bernard Noakes, and Daniel Fallon) in producing the sockets for this case-study.

Funding: This work was supported by the UK National Institute for Health Research (NIHR). Award. ID: NIHR201310.

REFERENCES

[1] C. van der Sluis, and R. Bongers, “TIPS for scaling up research in upper limb prosthetics”, *Prosthesis*, 2(4), 340-351, 2020.

[2] L. Diment et al., “Activity, socket fit, comfort and community participation in lower limb prosthesis users: a Cambodian cohort study”, *Journal of NeuroEngineering and Rehabilitation*, 19(42), 2022.

[3] A. Hernandez and E. Lemaire, “A smartphone photogrammetry method for digitizing prosthetic socket interiors”, *Prosthetics and Orthotics International*, 41(2), 210-214, 2016.

[4] J. Olsen et al., “The Impact of Limited Prosthetic Socket Documentation: A Researcher Perspective”, *Frontiers in Rehabilitation Sciences*, 3, 2022.

[5] J. Olsen, J. Head, L. Willan, S. Dupan, and M. Dyson, “Remote creation of clinical-standard myoelectric trans-radial bypass sockets during COVID-19”, *Annual International Conference of the IEEE Engineering in Medicine and Biology Society (EMBC)*, 2021.

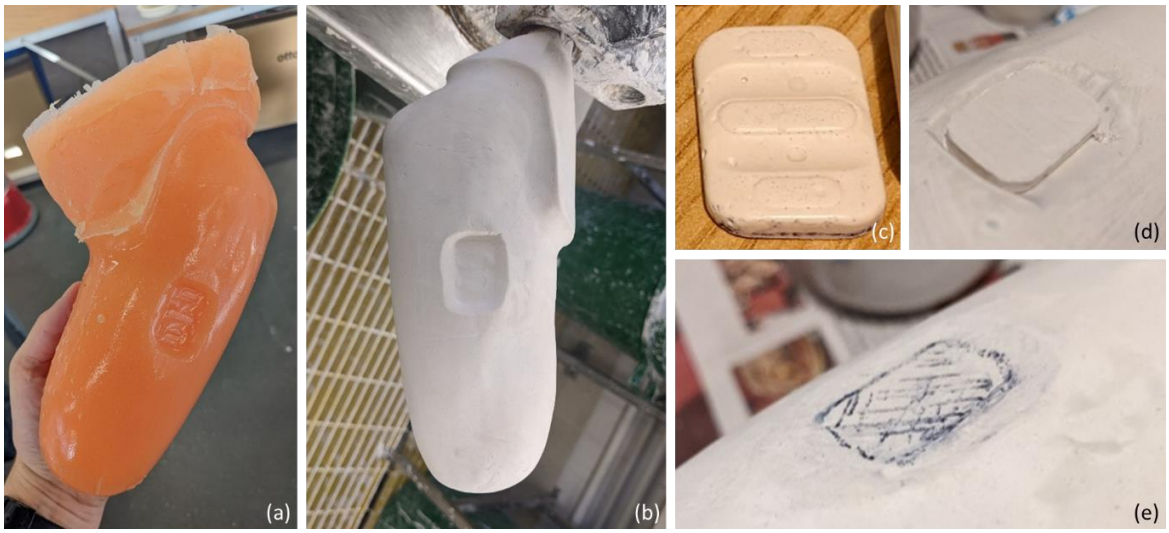

Figure 1: Examples of mould making process. (a) Silicone negative mould produced from original socket. (b) Smoothed plaster negative mould produced from silicone negative via an alginate positive. (c) A plaster electrode infill, shaped to match the front of the electrode, and at a thickness which when combined with the thickness of the dummy, matches the electrode. This is placed into the recess in the socket (d), seated in the correct location by the shaping from the metal electrode contacts, and coloured in to mark its position. The void around the edge is filled with wet plaster and flattened so as not to adjust the shape of the socket itself (e).

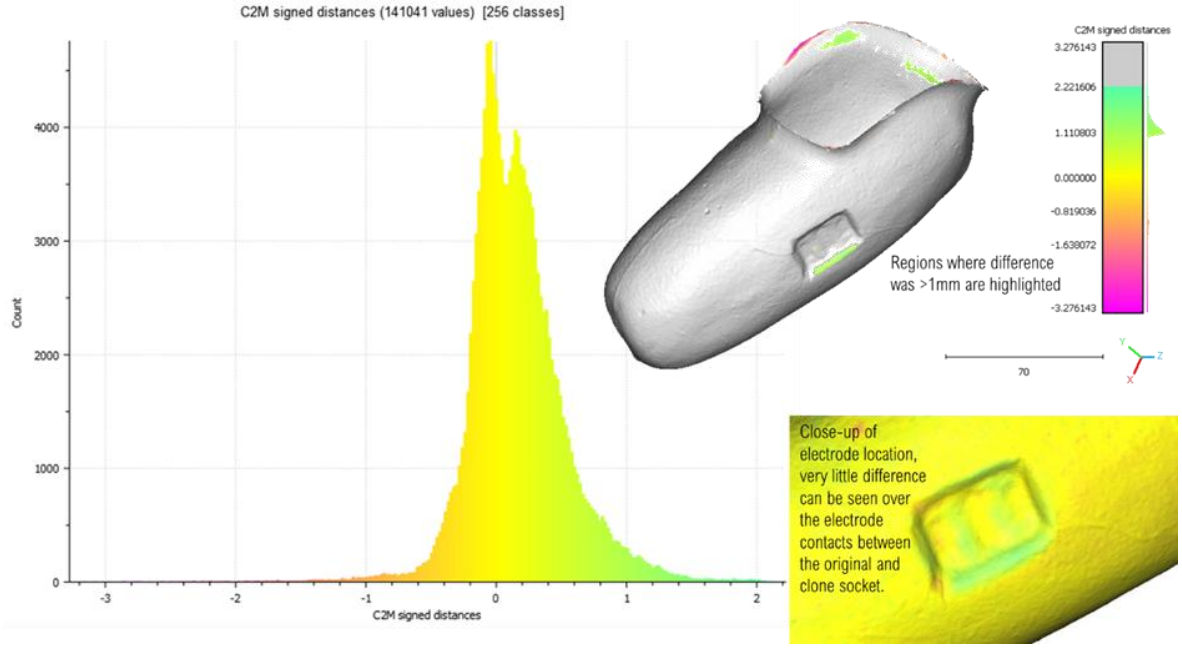

Figure 2: Histogram showing the distribution of Cloud to Mesh (C2M) distances (in mm) between the mesh of the silicone mould taken from the original socket and the mesh of the silicone mould taken from the replica socket. A positive difference indicates that the surface of the replica lies outside of the original reference scan, whilst a negative difference indicates the opposite. Top right any distances greater than 1mm can be seen highlighted on the socket. The discrepancy around the electrodes can be attributed to the Tegaderm web, but as can be seen bottom right, there is almost no discrepancy in the positioning of the electrode contacts.

DESIGNED FOR ADDITIVE MANUFACTURING: UPPER LIMB PROSTHESES

Chris Baschuk, MPO, CPO, FAAOP(D)

Point Designs, LLC

ABSTRACT

To mitigate high levels of prosthesis abandonment for upper limb difference individuals, new manufacturing methods and techniques, including additive manufacturing (AM), and the principles of design for additive manufacturing (DfAM) can be employed to improve the weight, bulk, comfort, and heat dissipation of upper limb prostheses. This project demonstrates how the principles of DfAM can be applied to upper limb prostheses to address each one of these specific areas. This case study of the design, development, and production of a shoulder disarticulation prosthesis not only exemplifies the practical application of AM in creating more effective and user-friendly prosthetic devices but also highlights the importance of material innovation in solving complex challenges. As this technology continues to evolve, it holds the promise of further breakthroughs in prosthetic devices, offering hope and improved quality of life for individuals with amputations. The success of this prosthesis underscores the transformative potential of combining advanced materials like PA12 and TPU with the precision and flexibility of additive manufacturing, paving the way for the next generation of prosthetic development.

INTRODUCTION

Additive manufacturing (AM), commonly known as 3D printing, is revolutionizing the field of prosthetics and orthotics. Unlike traditional methods which often require molds, casts, and extensive manual labor, additive manufacturing provides a more streamlined, customizable, and cost-effective approach [1]. There are three distinct areas in which additive manufacturing offers additional advantages over traditional prosthetic fabrication processes such as laminations and vacuum forming (Table 1).

Table 1: Benefits of 3D printing in prosthetic design and fabrication

Category	Benefits
Materials	Expansive array of materials, from flexible thermoplastics to strong polymers. Ability to layer or combine materials for desired textures, flexibility, and strengths. Nuanced material choices tailored to user needs.
Design Flexibility	Precise tailoring to the user's anatomy using digital software. Incorporation of advanced features like lattice structures for weight reduction. User-driven designs with aesthetic and functional preferences.
Manufacturing Methods	Customizability inherent in layer-by-layer additive manufacturing. Ability to create complex structures unachievable with traditional methods. Precise control over prosthetic socket wall characteristics. Digital simulation and validation prior to physical production. Ease of adjusting designs.

The success of a prosthesis hinges on the proper integration of materials, design, and manufacturing methods by the prosthetist. When balanced, these components yield a prosthesis that harmoniously merges technology with the user's daily life.

BACKGROUND

There are multiple compounding factors that can result in a high rate of prosthesis abandonment for individuals with upper limb loss or differences. These factors may include any, or a combination, of the following: excessive weight of the prosthesis, excessive bulk of the prosthesis to accommodate prosthetic components, lack of adequate heat dissipation, improper fit, and inability to perform the desired functionality [2]. The more proximal the amputation is on the arm, the greater the likelihood that this abandonment will occur [3][4]. There have been advances in prosthetic socket design and trim lines over the course of the past 20 years that have been meant to address some of these issues however these designs have still relied on the traditional fabrication methods of thermoforming plastic, custom silicone fabrication, and performing composite laminations. These processes are well described and understood within the prosthetic and orthotic profession. An externally powered shoulder level prosthesis requires a significant amount of clinical time and technical labor to produce. The process to construct a definitive shoulder level prosthesis from the diagnostic phase requires the design and fabrication of a flexible interface, a rigid frame type socket, a shoulder bulkhead, a humeral section, and a forearm section. Special care needs to be undertaken to maintain the alignment of the modular components in 3D space with respect to the socket. This requires the creation of special jigs and fixtures to accomplish. Not all prosthetic clinics have the capacity to perform this level of involved fabrication in their own facilities and therefore often rely on outsourcing this process. The definitive fabrication process for a shoulder level prosthesis can take several days or more to complete depending on the requirements and complexity of the design. Once the definitive prosthesis is completed, any adjustments or changes to the overall design and function of the prosthesis are very limited without having to completely redo the fabrication process.

METHODS

To address the five above-described contributing factors to prosthesis abandonment, the principles of design for additive manufacturing (DfAM) were applied to the design and production of a revolutionary multi-material shoulder disarticulation prosthesis. Through the application of DfAM, a shoulder level prosthesis was able to be produced that relied on well-established socket design principles [5], but that utilized new methods and materials to further improve upon the design. Additionally, a digital semi-automated workflow was created in the process of the design and development of this shoulder disarticulation prosthesis that allows these same techniques and principles to be easily applied to all other levels of upper limb amputations. The production process is streamlined, reducing the time and labor traditionally required to create a prosthetic. This efficiency not only makes the prosthetic more accessible but also opens the door for iterative design improvements based on user feedback, ensuring that the prosthesis continually evolves to meet the needs of its users more effectively [6].

This innovative approach leveraged the distinctive capabilities of additive manufacturing to address and overcome the longstanding challenges associated with conventional prostheses, including bulkiness, weight, discomfort, and the complexity of fabrication. Designed for a patient in Canada aiming to return to work as a commercial truck driver, this prosthesis highlights the potential of using specific materials and modern manufacturing techniques to enhance user comfort, functionality, and acceptance.

To address the weight, bulk, comfort, and heat dissipation of the prosthesis it was determined that a combination of PA12 (Polyamide 12) and TPU (Thermoplastic Polyurethane) would be the most appropriate materials. PA12 is known for its exceptional strength, rigidity, and resistance to many chemicals and abrasion, making it an ideal choice for the structural components of the prosthesis. Its use ensures durability and longevity, critical for a prosthetic that must withstand daily wear and tear. TPU, on the other hand, offers flexibility and resilience, qualities essential for parts of the prosthesis that require movement or are in direct contact with the user's skin. The combination of PA12 and TPU, each selected for their specific material properties, enables the creation of a prosthesis that is both strong and comfortable.

The main socket and inner flexible portion of the prosthesis are comprised of lattice structures as much as possible. A honeycomb lattice structure was selected for its strength as well as the ability to reduce the overall material volume required for the prosthesis by 50%. This ultimately reduces the weight of the prosthesis by 50%, the material consumption needed for the prosthesis by 50%, and therefore the overall cost to print the components of the prosthesis

by 50%. This choice in design and materials reduced the surface area of the body covered by the prosthesis by 50% because the perforations in the lattice on the inner flexible and the rigid outer frame are perfectly aligned.

Utilizing the principles of DfAM areas of the prosthesis that were meant to be rigid, such as the areas over the electrodes were able to be kept rigid while areas of the prosthesis that would benefit from having more flexibility were able to be designed to be more flexible through variable wall thickness. For example, the area around the shoulder girdle was kept more rigid whereas the area around the ribs was allowed to be more flexible. This allowed the prosthesis to better move with the user's body (Figure 1).

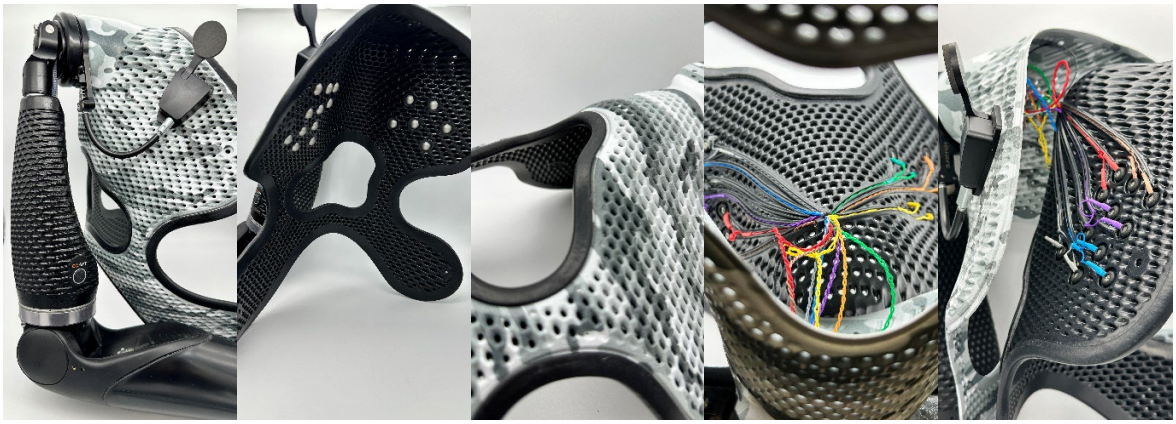

Figure 1: Images from left to right: outside of prosthesis; inside of prosthesis; close up of lattice structure and TPU overlap of rigid frame; wire organization of pattern recognition system; partially assembled prosthesis.

DISCUSSION

Utilizing AM, the prosthesis is custom fitted to the patient, ensuring a perfect match with their anatomical structure and functional needs. This technology allows for intricate designs that accommodate the electronic components necessary for advanced functionality, such as batteries, sensors, and wiring, without adding unnecessary bulk. Moreover, additive manufacturing significantly reduces the waste associated with traditional prosthetic fabrication methods, offering a more sustainable solution. This prosthesis utilized a pattern recognition system with 17 individual electrode domes. Because the inner flexible was printed from TPU it allowed for the electrodes and wires to be embossed into the material which significantly reduced the overall bulk and thickness of the prosthesis. Because the components of the prosthesis were all digitally laid out prior to the production of the prosthesis, clearances were able to be confirmed which allowed for the overall thickness and profile of the prosthesis to be kept as minimal as possible without sacrificing structural integrity. To significantly reduce the bulk along the trim lines the TPU inner flexible was designed to wrap around the edge of the rigid frame creating a seamless transition.

CONCLUSION

This project not only exemplifies the practical application of additive manufacturing in creating more effective and user-friendly prosthetic devices but also highlights the importance of material innovation in solving complex challenges. As this technology continues to evolve, it holds the promise of further breakthroughs in prosthetic devices, offering hope and improved quality of life for individuals with amputations. The success of this prosthesis underscores the transformative potential of combining advanced materials like PA12 and TPU with the precision and flexibility of additive manufacturing, paving the way for the next generation of prosthetic development.

REFERENCES

[1] L. Diment, M. Thompson, J. Bergmann, “Clinical efficacy and effectiveness of 3D printing: a systematic review,” *BMJ Open*, 2017;7(12): e016891.

[2] E. Biddiss, T. Chau, “Upper limb prosthesis use and abandonment: A survey of the last 25 years,” *Prosthetics Orthot Int,* 2007;31(3):236-57.

[3] C. Pylatiuk, S. Schulz, L. Döderlein, “Results of an Internet survey of myoelectric prosthetic hand users,” *Prosthetics Orthot Int,* 2007;31(4):362-70.

[4] F. Cordella, A. Ciancio, R. Sacchetti, A. Davalli, A. Cutti, E. Guglielmelli, et al, “Literature review on needs of upper limb prosthesis users,” *Front Neurosci,* 2016;10:209.

[5] T. Farnsworth, J. Uellendahl, M. Mikosz, L. Miller, B. Petersen, “Shoulder region socket considerations,” *Journal of Prosthetics and Orthotics*. 2008 Jul 1;20(3):93-106. doi: 10.1097/JPO.0b013e31817d8036

[6] C. Baschuk, “The synergistic potential of embracing 3D printing in O&P [Internet],” *LinkedIn,* [cited 2023 Aug 30]. Available from: https://www.linkedin.com/pulse/synergistic-potential-embracing-3d-printing-op-chris-baschuk/

ENHANCING UPPER LIMB PROSTHETIC FABRICATION WITH 3D PRINTING TECHNOLOGY: OPPORTUNITIES AND APPLICATIONS

Daniel DaFonseca RTP, Heather Daley, CP, Wendy Hill, OT

Atlantic Clinic for Upper Limb Prosthetics, Institute of Biomedical Engineering, UNB,

ABSTRACT

This study explores the transformative impact of 3D printing technology in the field of upper limb prosthetics, highlighting its pivotal role in customizing prosthetic devices to meet individual needs with precision and efficiency. Through detailed examination of practical applications ranging from musical playing devices to recreational implementation, we showcase the versatility of additive manufacturing in enhancing patient outcomes. Despite potential hurdles such as cost and the necessity for specialized expertise, the evidence underscores the substantial benefits of 3D printing, including significant improvements in prosthetic functionality, patient satisfaction, and overall efficiency and effectiveness. Our findings advocate for the integration of 3D printing into prosthetic fabrication, emphasizing its potential to revolutionize patient care by offering tailored solutions that cater to the unique requirements of individuals with upper limb differences.

INTRODUCTION

3D printing is a remarkably valuable tool for fabrication of upper limb prosthetic devices that is under-utilized in many areas. 3D printing is not as media tends to stereotype it as, an enormous cost saving, plug and play solution to the entire cost and process of prosthetic production. The material and fabrication cost of an upper limb prosthesis is just a fraction of the entire cost of a fitting [1]. Replacing this with additive manufacturing (AM) makes very little difference in this front, and if anything, it can increase costs as it requires specialized knowledge to utilize it at all.

The benefits of AM are substantial and include more accurate, repeatable, and higher quality end results, or devices that aren't possible with traditional fabrication methods [2], [3]. Time savings are also a benefit in many cases, where after a design is finished, the operator can work on something else while the product is being printed. Less waste is generated with AM and is less labour intensive in the long term [2], [4]. AM has the potential to be the means for many end use applications in the industry today, depending on the type of technology in question. Suitable methods for use in prosthetics include technologies such as selective laser sintering (SLS) nylon parts or multi jet fusion (MJF), selective laser melting (SLM) for metal parts as well as direct metal laser sintering (DMLS). Less suitable technologies for most end use parts really narrows down to the most accessible one, fused deposition modelling (FDM). This is the most commonly used form of 3D printing portrayed by the media for prosthetic arms, and people often are misled into thinking a functional prosthesis can be fabricated for just $50 with a printer that costs less than $1000[5] . Considering that FDM printing is essentially a smart hot glue gun that relies on interlayer adhesion for structural integrity, regardless of material properties, this makes this application not suitable for truly robust end use applications. FDM is more suitable for rapid prototyping, fabrication aids, dynamic alignment fixtures, and numerous unique uses that will be outlined as examples in this paper. Ultimately, since AM is typically not intended for high-volume production, but very complex and custom small production, it is ideally suited for this industry.

CASE EXAMPLES

The following cases (of which informed consent was obtained under the guidelines and approval of UNB's research ethics board prior to the study) demonstrate the value of 3D printing in an upper limb prosthetic clinic:

Case 1

Presentation

MS is a 37-year-old male who sustained a workplace injury in 2010 resulting in a transhumeral amputation of his right arm. He had been an avid musician and was previously in a band as a guitarist before his accident. Since his amputation

and prosthetic fitting, he has returned to work in a steel plant and has resumed many of his previous hobbies, including playing bass one-handed with the tapping technique as his fretting hand. He was hesitant to try any other stringed instrument as he did not want to learn to play in an adapted way. However recently, he inquired about the possibility of strumming a guitar again.

Treatment

After much discussion about positioning and breaking down the skills required for strumming a prototype guitar playing device was designed using FDM ABS, and the final versions were manufactured from FDM PA12 CF, and SLS Nylon12, and utilizing a pin lock liner for suspension. For the diagnostic phase, a 3D printed socket was made with a ball socket distal arm to determine the best strumming position with a wide range of adjustability. Once that was determined, a fine adjustment version was made with a solid arm piece in the ideal strumming position and a TRS guitar pic holder at the terminal end to allow for minor tweaks in pick position. This socket was made as a topology optimized design in order to reduce as much weight as possible while still maintaining adequate strength and stiffness.

Outcome

The outcome from this fitting was a very lightweight but durable device that the patient was very happy to use. He initially found it awkward to strum using shoulder movement rather than his wrist and hand but felt that with practice he would improve. He felt a smaller guitar would improve his positioning and give him better control of his strumming, so we took the trial device to a local music shop to try various sized guitars. See photos. He was able to trial multiple guitars for shape, size and sound which helped us fine-tune the positioning of the terminal device in the final design. After using it at home for several weeks, the patient reported that with extended playing times, he was initially experiencing soreness in his shoulder, though with more practice and repetition and rest, this problem has lessened. Additionally, a softer custom pick was requested and then fabricated from thermolyn to mitigate the aggressiveness of less accurate strumming.

Figure 1: custom transhumeral guitar device

Case 2

Presentation

NR is a 6-year-old girl who was born with a transmetacarpal limb difference on her left side. She has equal length arms to the wrist level and full range of motion in her wrist. She is able to complete most of her daily activities independently with no prosthesis but has requested an adaptation for several recreational activities such as riding her bike, holding a skipping rope, and most recently, swimming. She was starting swimming lessons, and her mom was concerned that she would not be able to swim laps in a straight line because of her smaller hand span in the water.

Treatment

We initially looked at commercial swim paddle products geared to swim training but could not find a suitable product to fit her small size or that could easily be adapted to remain secure on her hand in the water. Ultimately, we decided a 3D printed custom device with a pocket for her hand would be the best solution. A scan was taken of her hand and forearm and the swim paddle prototype was then printed with FDM PETG. PETG was the filament of choice as it is chemical and UV resistant with a higher heat deflection temperature than other materials. This made it suitable

for swimming pool and outdoor settings. With inspiration from commercial swim paddles, the design incorporated s perforations to allow water to move through it and not give complete resistance. The suspension was achieved with a 15-shore silicone strap made from a 3D printed mould that has notches to adjust tightness.

Outcome

The outcome from this device was well received by NR. She found it comfortable, it helped her with swimming symmetry during swimming lessons, and she was very proud to show off her special swim mitt in her favourite colour.

Figure 2: custom partial hand swim paddle

Case 3

Presentation

CG is a 39-year-old female with a left-sided congenital limb difference at the wrist level. She wears a passive prosthesis daily, mainly for aesthetics. She is independent in all of her daily activities, however she mentioned at a recent appointment that she was having trouble holding a drumstick when playing the drums at home. She is very musical and had adapted her method of playing many instruments, but the tape she was using to help hold the drumstick in place on her residual limb was causing some discomfort and skin irritation.

Treatment

CG asked if we could fabricate a simple device that could help hold the drumstick more securely but that would still give her some control over the rhythm while drumming. She did not want to wear a hard socket to accomplish this. We discussed positioning of the drumstick on her limb and options for materials. A trial device made with FDM TPU. With a long residual limb, this allowed for an abundance of surface area to work with for force distribution. . The device is a single piece flexible TPU print with an integrated lacing for a boa system to adjust tightness. The drumstick is friction fit into two sleeves that are 10% infilled to reduce rigidity to give a more natural hit and rebound on strikes.

Outcome

The outcome from this trial device was great. The patient was happy with the fit and comfort in the new device and has been able to continue playing drums more often and for longer sessions with improved comfort and control.

Figure 3: custom wrist disarticulation drumstick holder

DISCUSSION

These are just a handful of examples of AM use in an upper limb prosthetic clinic setting., AM is also a useful tool for creating full sockets, forearm shells, cosmetic covers, tools, foundations for lamination, adapters, moulds and so on. Looking forward, there is a potential to further explore fully 3D printed prostheses with SLS or MJF Nylon, custom printed metal terminal devices (TDs) with SLM/DLMS metal printing, and 3D printed silicone sockets and liners. While there are many benefits to these applications, cost savings is not the primary objective. The benefits of 3D printing in prosthetic clinic include material selections, material combinations, weight reduction by material choice and/or design, and aesthetics.

CONCLUSION

The exploration of 3D printing in upper limb prosthetic clinics reveals a landscape brimming with opportunities yet marred by underutilization. This paper demonstrates the transformative potential of additive manufacturing in enhancing prosthetic design, customization, and functionality, while also addressing the challenges of cost and requisite specialized knowledge. The case examples provided showcase the technology's capability to produce outcomes previously unattainable through traditional methods, showcasing 3D printing's role in advancing patient-centric solutions and opening avenues for innovation in prosthetic care. As we navigate the evolving intersection of technology and healthcare, it is beneficial to further integrate 3D printing into prosthetic fabrication, leveraging its unique features to meet the complex needs of patients, thereby heralding a new era of personalized and accessible prosthetic solutions.

REFERENCES

[1] J. ten Kate, G. Smit, and P. Breedveld, “3D-printed upper limb prostheses: a review,” *Disabil Rehabil Assist Technol*, vol. 12, no. 3, pp. 300–314, Apr. 2017, doi: 10.1080/17483107.2016.1253117.

[2] Baschuk CM, “Stakeholder perspectives 3D printing and the evolution of partial hand prostheses: my journey from theory to practice,” *Canadian Prosthetics & Orthotics Journal*, vol. 6, no. 2, 2023, doi: 10.33137/cpoj.v6i2.42139.

[3] K. F. Gretsch, H. D. Lather, K. V. Peddada, C. R. Deeken, L. B. Wall, and C. A. Goldfarb, “Development of novel 3D-printed robotic prosthetic for transradial amputees,” *Prosthet Orthot Int*, vol. 40, no. 3, pp. 400–403, Jun. 2016, doi: 10.1177/0309364615579317.

[4] A. Manero *et al.*, “Implementation of 3D Printing Technology in the Field of Prosthetics: Past, Present, and Future,” *International Journal of Environmental Research and Public Health 2019, Vol. 16, Page 1641*, vol. 16, no. 9, p. 1641, May 2019, doi: 10.3390/IJERPH16091641.

[5] “The Synergistic Potential of Embracing 3D Printing in O&P.” Accessed: Mar. 06, 2024. [Online]. Available: https://www.linkedin.com/pulse/synergistic-potential-embracing-3d-printing-op-chris-baschuk/?trackingId=7Bf1k07eQxWDnUdTvr%2Fa1A%3D%3D

FUNCTIONAL OUTCOMES OF A TRANSRADIAL PROSTHESIS WITH AND WITHOUT WRIST FLEXION AND EXTENSION

Laura A. Miller, PhD, CP,[1,2] Kristi L. Turner, DHS, OTR/L,[1] Kevin Brenner,[1] Levi J. Hargrove, PhD, [1,2]

[1] Center for Bionic Medicine, Shirley Ryan AbilityLab, Chicago, IL, USA; [2] Northwestern University, Chicago, IL, USA

ABSTRACT

This study explores the function of a 2-degree-of-freedom (DOF) prosthetic wrist compared to a single-degree-of-freedom wrist for people with below-elbow amputation. The study involves five participants who wore a custom-made 2DOF wrist system and an Ottobock Transcarpal hand, using pattern recognition-based control. Participants did in-lab tests in two conditions: wrist rotation only and wrist rotation with flexion/extension. Functional outcomes, including the Southampton Hand Assessment Procedure, Box and Blocks Test, Jebsen Taylor Test, Activity Measures for Upper Limb Amputees, Clothespin Relocation Task, and Assessment for Capacity of Myoelectric Control, were measured. Preliminary results show little difference between the two conditions, possibly due to the additional addition length, mass, or control complexity.

INTRODUCTION

The wrist plays a crucial role in human dexterity, positioning the hand for optimal grasping and facilitating tasks like reaching the mid-line for self-care. While both hand and wrist function contribute to overall function, a recent study involving able-bodied subjects revealed an interesting finding: combining a robust two degree-of-freedom (DOF) wrist function (flexion/extension and rotation) with a single hand grasp is just as effective as pairing a 22-DOF intact hand with a wrist that only provides rotation.[1]

In the field of prosthetics, many multifunctional dexterous hands are now commercially available, such as the Bebionic Hand, Ability Hand, i-limb Ultra, and Taska. These devices have the potential to perform several hand grasps, but their complexity can impact their durability and make them challenging to control. Surprisingly, prosthetic wrists have seen limited evolution. Currently, there are two powered wrist rotators available from Motion Control and Ottobock. Only Motion Control markets a powered wrist flexion/extension unit. A major challenge in developing 2-DOF wrists has been creating a device that is short and lightweight. A further challenge has been controlling additional degrees of freedom using conventional amplitude-based control systems. New lightweight motors and pattern recognition–based control have emerged as potential solutions allowing for wrist rotation, flexion/extension, and hand grasp restoration.

The primary objective of this project is to evaluate the functional importance of a multifunction wrist compared to a single degree-of-freedom wrist. This was accomplished through in-laboratory testing of a custom designed wrist system with integrated wrist rotation and wrist flexion and extension. Changes in performance were assessed with multiple outcome measures that include both quantitative and qualitative testing of prosthesis control and functional performance. We hypothesize that adding a wrist flexion/extension module to a wrist rotation module and a single-DOF terminal device will provide improvements in function for transradial amputees.

METHODS

Participants were recruited with a transradial level limb absence and were fit with a custom 2DOF wrist and Ottobock Transcarpal hand (Figure 1). The custom wrist system allows for 351 degrees of rotation and 100.5 total degrees of flexion (58 degrees) and extension (42.5 degrees). For each participant, the prosthetic components were connected to a custom fabricated flexible inner socket and a fiberglass casting outer socket. When possible, an individual's home prosthesis was duplicated and modified, if needed, to allow for 8 channels of EMG. For condition

1, the wrist flexor was disabled and locked in place at a neutral position relative to the hand connection plate. For condition 2, the wrist flexor was enabled. All degrees-of-freedom were controlled using pattern recognition. The pattern recognition controller was a custom designed system with 8 channels of EMG input using an LDA classifier. All participants began with condition 1 (wrist rotation only) and then progressed to condition 2 (wrist rotation and wrist flexion) to align with how degrees-of-freedom would be added in a clinical scenario.

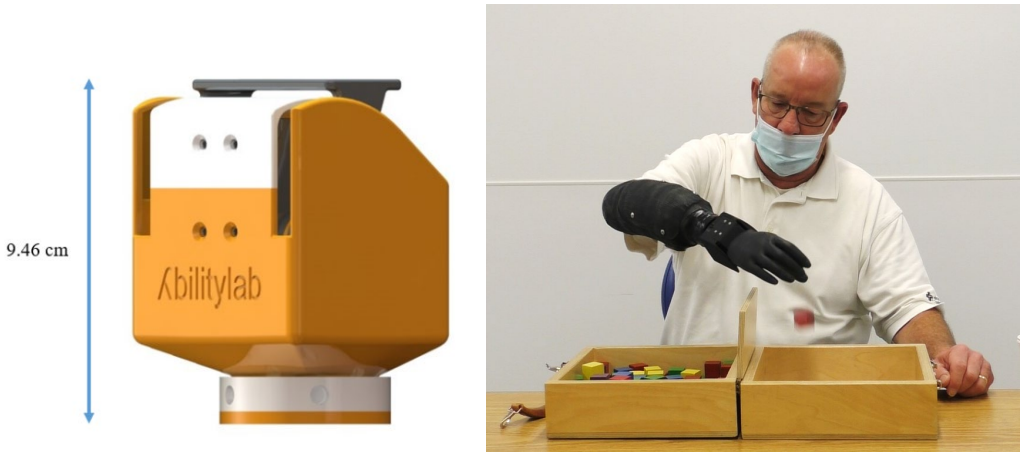

Figure 1: CAD image of wrist unit (left), participant wearing the prosthesis to complete the Box and Blocks test (right)

After participants were trained in the use of the system by an occupational therapist, they then completed outcome testing. These outcomes included the Southampton Hand Assessment Procedure (SHAP), Box and Blocks Test, Jebsen Taylor Test (total time in seconds for all tasks), Activity Measures for Upper Limb Amputees (AM-ULA), Clothespin Relocation Task (time to move 3 pins), and Assessment for Capacity of Myoelectric Control (ACMC).[2] Some participants completed a home trial with the device and repeated outcome testing before proceeding to the second condition. However, due to delays from Covid-19, not all participants completed home trials. Therefore, pre-home outcomes are presented for all participants. This study was approved by the Northwestern University IRB and all participants provided written consent.

RESULTS

Five participants, all with an amputation secondary to trauma, were recruited for this study. All participants had experience with myoelectric control but did not necessarily utilize a myoelectric prosthesis on a daily basis. Demographics are presented in Table 1.

Table 1: Participant demographics.

	Prosthetic side	TMR	Primary home device at time of participation	Age at time of enrollment	Home trial after Condition 1/2
P1	Right	N	Myo with 2-site control: Taska, passive wrist	55	Y/Y
P2	Left	Y	None: Abandon use	34	Y/N
P3	Left	N	Myo with 2-site control: Bebionic, passive wrist	28	Y/Y
P4	Right	N	Body powered: TRS Jaws	40	N/N
P5	Left	Y	Equal use of Body powered: 5x hook & Myo with Pattern recognition control: Bebionic hand and passive wrist	32	Y/N

Results of the functional outcomes are presented in Table 2. The results are the average and standard deviation for the 5 participants for pre-home outcome testing. The SHAP Index of Function is presented (higher scores indicate improved function). The Jebsen Taylor score is the total time to complete all tasks, summed and in seconds with lower scores indicating improved function. The AM-ULA is the total score with a higher value indicating a better score. Higher ACMC scores indicate improved function. The Clothespin Relocation Task result presented is the time, in seconds, to move 3 pins with 3 trials included per participant; a lower time would indicate faster performance. The Box and Blocks result is the number of blocks moved in 1 minute, with 3 trials included per person. More blocks would indicate improved performance.

.

Table 2: Results of functional testing for the 2 conditions, with and without wrist flexion. Average and standard deviation shown.

	SHAP		**Jebsen**		**AM-ULA**		**ACMC**		**Clothespin**		**Box & Blocks**	
	WR`	WR & WF	WR	WR & WF	WR	WR & WF	WR	WR & WF	WR	WR & WF	WR	WR & WF
Average	39.60	35.40	269.85	268.40	13.33	13.11	55.82	51.06	23.29	23.98	10.33	10.87
Std Dev	*6.90*	*5.01*	*25.37*	*27.63*	*0.68*	*0.74*	*4.54*	*3.31*	*2.27*	*2.79*	*1.42*	*1.88*

DISCUSSION

Overall results between the two conditions, wrist rotation only and wrist rotation with wrist flexion, are very similar. Though improvements in the outcomes were expected, the increased mass, length, and control complexity of the system likely did not allow for faster performance on the timed outcomes (SHAP, Jebsen, Clothespin and Box and Blocks). Though the addition of wrist flexion may have reduced some compensatory movements, the overall score of the AM-ULA is based on the multiple factors, including speed, compensation/awkwardness, and skillfulness, which did not appear to be sensitive to the change in components.

One major limitation is that only 2 of the 5 participants were able to complete all home trials due to delays in the study from Covid-19. Participants may have had additional improvements in function with this additional time to learn to use the device in a home environment. However, despite these limitations, the addition of this degree-of-freedom also did not appear to negatively impact function.

ACKNOWLEDGEMENTS

This work was supported by NIH 5R01HD094861-04

REFERENCES

[1] F. Montagnani, M. Controzzi, and C. Cipriani, "Is it Finger or Wrist Dexterity That is Missing in Current Hand Prostheses?," (in eng), *IEEE Trans Neural Syst Rehabil Eng,* vol. 23, no. 4, pp. 600-9, Jul 2015, doi: 10.1109/tnsre.2015.2398112.

[2] L. A. Miller and S. Swanson, "Summary and Recommendations of the Academy's State of the Science Conference on Upper Limb Prosthetic Outcome Measures,", *JPO Journal of Prosthetics & Orthotics,* vol. 21(9), no. Supplement, pp. P83-P89, 2009..

KINEMATIC CHANGES WITH POWERED WRIST FLEXION FOR TRANSRADIAL PROSTHETIC USERS COMPLETING THE GAZE AND MOVEMENT ASSESSMENT (GAMA) PASTA BOX TASK

Laura A. Miller, PhD, CP,[1,2] Quinn A. Boser,[3] Vikram Darbhe,[1,2] Jacqueline S. Hebert, MD,[3] Kevin Brenner,[1] Kristi L. Turner, DHS, OTR/L[1]

[1] Center for Bionic Medicine, Shirley Ryan AbilityLab, Chicago, IL, USA; [2] Northwestern University, Chicago, IL, USA; [3] University of Alberta, Edmonton, Canada

ABSTRACT

Many assessments used to evaluate prosthetic function primarily emphasize task completion time, overlooking the assessment of movement quality or the specific degree of freedom (DOF) activated during the task. For example, proper functioning of the wrist is crucial for accurate hand positioning, but the addition of this movement would likely add time to task completion. Unfortunately, only a limited number of available prosthetic wrists offer powered flexion and extension. As a result, users often need to rely on compensatory body movements, which can lead to injuries and even lead to abandonment of the device. In our study, we used the Gaze and Movement Assessment (GaMA) metric to compare task timing, endpoint trajectories, and 3D angular joint kinematics between a 1-DOF wrist and a 2-DOF wrist combined with a 1-DOF hand. Our hypothesis was that the 2-DOF wrist, though requiring more time, would yield kinematics closer to normative data and result in fewer compensatory movements compared to the 1-DOF wrist. Preliminary results on 4 individuals completing the Pasta Box task and utilizing a powered wrist flexion extension unit showed some changes in torso movements but large variability among the participants. Contrary to our hypothesis there was not a large difference in timing between the two conditions.

INTRODUCTION

Many functional assessments used to evaluate prosthetic function focus on task completion time without considering movement quality or the specific degree of freedom (DOF) activated during the task. To address this limitation, the Gaze and Movement Assessment (GaMA) metric was developed and validated at the University of Alberta under DARPA's Hand Proprioception and Touch Interfaces (HAPTIX) program. GaMA uses motion capture and eye tracking to quantify motion, including 3D angular kinematics and hand movements, as well as gaze behavior during simulated real-world tasks. The GaMA tasks, such as the Cup Transfer Task and the Pasta Box Task, simulate day-to-day functional requirements while challenging typical prosthetic limitations, such as reaching and transporting objects at varying heights and across the body. Each task can be subdivided into specific phases of reaching, grasping, transporting, and releasing objects. A performance aspect encourages the participant to work efficiently, and tasks are short to allow multiple repetitions within a reasonable testing time frame to assess performance consistency.[1, 2]

Previous work has highlighted the importance of wrist dexterity with individuals with intact limbs performing functional tasks while wearing braces to block certain wrist and hand movements.[3] In addition, both the type of terminal device and the presence of wrist motion have been found to impact compensatory movements in prosthetic users. For instance, a study comparing compensatory movements using two myoelectric hooks revealed a significant negative correlation between wrist flexion and shoulder abduction: greater wrist flexion was associated with less shoulder abduction, while ulnar or radial inclination of the wrist did not seem to influence shoulder abduction.

To address the need for wrist function, we designed a 2 DOF wrist that can be combined with a single DOF hand. We hypothesize that the time to complete some tasks would be slower when a wrist flex/extension (WFE) DOF is utilized but the trunk and shoulder compensatory movements, as measured by the GaMA metric, would be decreased.

METHODS

Five individuals have been enrolled and have completed testing with the 2 DOF wrist and Ottobock transcarpal hand controlled with 8 channels of EMG connected to a pattern recognition system.[4] For the Flexion Off condition, the wrist could be locked in a neutral position.

For each condition (Flexion On & Off), the users were trained on the use of the device, functional outcomes, and GaMA tasks by an Occupational Therapist. Functional outcomes included the Box and Blocks test, Southampton Hand

Assessment Procedure (SHAP), Jebsen Taylor Test of Hand Function, the Activities Measure for Upper Limb Amputees (AM-ULA) and the Clothespin Relocation Task. When possible, participants completed a home trial of at least 2 weeks for each condition, with the functional outcomes administered before and after the home trial, and GaMA tasks only administered after. Due to delays from Covid-19, some home trials were forfeit (Table 1). In this case, for each condition, the participant completed training, one set of functional outcomes, and the GaMA tasks.

Figure 1: S1 with device during calibration (Left). S4 completing the Pasta Box task (Right)

The GaMA tasks consist of object movements that are each divided into 4 phases: Reach, Grasp, Transport and Release. The data compared between Flexion On and Flexion Off included the timing for the reach, grasp, transport and release phases of each movement, the endpoint trajectory, and the joint kinematics. During the Flexion On condition, participants began trials with the wrist flexor in a neutral position. For all trials the hand was open and positioned with slight supination so that all motion capture markers were visible. For the current analysis, user data from 4 of the individuals were compared between conditions and to normative data for the Pasta Box task. For the Pasta Box task, participants begin with the hand on the front table in a "home" position. They then turn to the prosthetic side to pick up the pasta box and transfer it to the lower shelf, touch "home" then move the box from the lower shelf to the upper shelf, touch "home", transfer the box back to the starting position and end the trial when the hand returns "home". This allows for a cycle of movements that can be analysed by averaging multiple trials.

Conditions (Flexion Off and Flexion On) were not randomized. All participants completed the Flexion Off condition prior to continuing to the Flexion On condition, since this corresponds to how users would learn and build complexity in a clinical setting.

The remaining data continue to be processed. No statistical analysis has yet been performed; all conclusions reflect visual observation of trends in the metrics (averages across session trials). This study was approved by the Northwestern University IRB and the University of Alberta REB and all participants provided written consent.

RESULTS

Patient demographics are presented in Table 1. All 4 participants had experience with myoelectric prostheses, though S2 had abandoned use. The other 3 all utilized their 2-site system on a regular basis, 3-5 days per week.

Participants did engage the wrist flexor/extensor during the Flexion On condition. The most consistent activation was extension of the wrist during the first portion of the trial (Reach 1), in order to assist with positioning the grasp of the pasta box on the side table. There was otherwise large variability in wrist movements throughout the rest of the trial between participants, but on average the wrist stayed in an extended position. One participant (S1) also chose to rotate the wrist 180 degrees at the start of the trial (so the hand open/close faced away from the midline), however they still engaged the wrist into extension at the start of the trial.

Contrary to our hypothesis, the addition of wrist flexion did not appear to have a large impact on the overall timing of the task. One user did take a bit longer (S3: Off=19.3$\pm$2.7s, On=25.6$\pm$4.5s) but the other users did not show large changes (S1: Off= 29.9$\pm$2.9s, On= 30.4$\pm$2.8s; S2: Off= 27.6$\pm$6.9s, On= 30.7$\pm$7.3s; S4: Off= 29.0$\pm$2.0s, On= 27.8$\pm$2.1s). These times were much longer than normative trials (11.2$\pm$2.0s).

It was hypothesized that there would be reduction in the shoulder and trunk movements with the addition of wrist flexion and extension. However, a clear trend is not seen in the 4 participants analysed to date for the Pasta Box task. For example, Subjects 2 and 3 showed much larger trunk flexion/extension during the first phase of movement, picking up the pasta box from the side table, than Subjects 1 or 3.

Table 1: Participant demographics. * indicates condition was completed with a home trial

	Prosthetic side	**Primary home device at time of participation**	**Number of trials per condition**	
			Flexion OFF	***Flexion ON***
S1	Right	2-site myo: Taska, passive wrist	11 *	10 *
S2	Left	Abandon use	10 *	10
S3	Left	2-site myo: Bebionic, passive wrist	11 *	12 *
S4	Right	Body powered: TRS Jaws	10	10

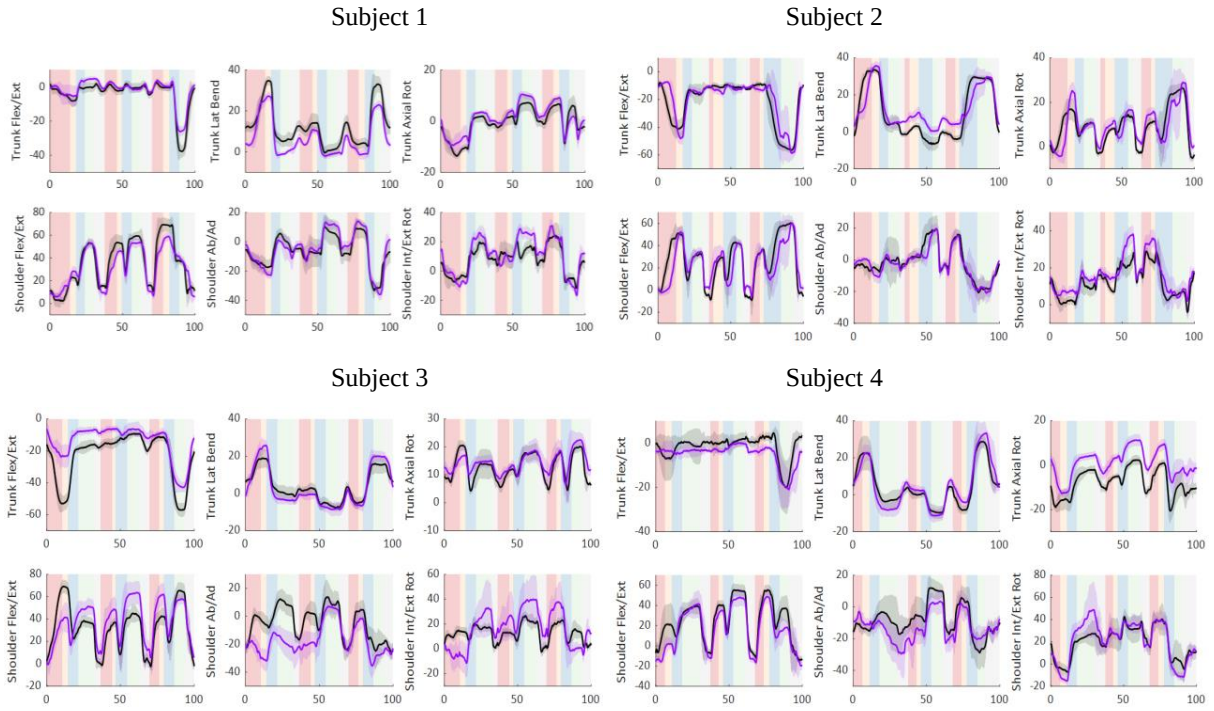

Figure 2: Kinematics for the Pasta Box task. For each subject: Top row- Trunk Flexion/Extension, Lateral Bend, & Axial Rotation. Bottom- Shoulder Flexion/Extension, Ab/Adduction, & Internal/External Rotation. Flexion Off is shown in Black, On is shown in Purple. Standard deviations are shown as a shaded band. Vertical shading indicates the timing of the task (Reach-pink, Grasp-yellow, Transport-blue, Release-green, Return Home-Gray).

The addition of Wrist Flexion/Extension resulted in decreased range of motion in some Trunk and Shoulder degrees of freedom, for two participants (S1 and S3). However, it also then resulted in increased Shoulder Internal/External rotation for S2 and S3 (Table 2). This increased internal rotation mostly occurred when the participants were placing or picking up the box at the second shelf, which may have been a consequence of the extended wrist position.

DISCUSSION

Despite initial expectations, participants did not, overall, take longer to complete the Pasta Box task with the addition of wrist flexion and extension. However, for both conditions, they were slower than the normative data. The participants did consistently utilize the wrist flexion and extension unit during the second condition to extend the wrist

at the beginning of the Pasta Box Task trials. After grasping the box on the side table, some participants continue to activate the wrist F/E throughout the task, while mostly holding the extended wrist angle. However, variability is high. There does not appear to be a consistent strategy for use of the wrist flexion and extension degree-of-freedom between or within participants. This variability is also reflected in the kinematics of the shoulder and trunk. Though the addition of wrist flexion and extension did result in a decrease in range of movement at the trunk and shoulder for two participants, increases were also seen in internal and external shoulder rotation. As previously mentioned, this increase occurred during the phase of the trial when the participant would place or pick up the pasta box on the highest shelf across the body. This may be because of additional compensation made from the extended position of the wrist or to stabilize the arm for better control of the hand grasp and release.

Table 2: Total Range of Motion for the Trunk and Shoulder for each condition: Average (Standard Deviation)

	Controls	S1		S2		S3		S4	
		Off	On	Off	On	Off	On	Off	On
Trunk Flex/Ext	10.2 (3.2)	44.3 (3.7)	32.6 (3.1)	51.4 (1.7)	55.6 (3.1)	51.3 (4.2)	42.6 (4.6)	29.4 (8.8)	28.9 (5.1)
Trunk Lateral Bend	17.7 (4.7)	36.6 (2.4)	30.7 (2.1)	41.9 (4.0)	36.8 (2.6)	29.7 (3.9)	36.9 (3.8)	40.2 (3.6)	48.1 (3.3)
Trunk Axial Rot	23.0 (5.4)	23.4 (2.5)	22.9 (1.7)	34.1 (2.0)	38.3 (2.5)	21.0 (1.5)	21.3 (6.5)	26.7 (3.7)	26.2 (2.4)
Shoulder Flex/Ext	86.3 (8.6)	74.1 (6.8)	58.7 (4.2)	76.9 (4.7)	73.7 (3.8)	80.3 (5.3)	76.5 (11.7)	83.1 (7.0)	77.3 (10.1)
Shoulder Abd/Add	27.7 (7.0)	50.7 (6.4)	53.2 (4.9)	47.4 (8.5)	49.6 (13.4)	56.9 (8.5)	51.6 (6.9)	50.8 (11.9)	48.3 (13.0)
Shoulder Int/Ext Rot	41.8 (7.9)	48.4 (6.8)	52.9 (3.4)	39.6 (3.6)	45.9 (4.5)	36.9 (5.4)	74.3 (18.7)	63.4 (11.9)	76.8 (20.1)

There are limitations to this current analysis. Currently only trials from four of the five participants have been processed. Once all trials have been completed a more in-depth evaluation of the results, including statistical analysis, can take place. We have also noted that wrist angles are also somewhat variable for normative data, and it may be that for the Pasta Box task it is more difficult to clearly identify the impact of wrist flexion. The GaMA metric also includes a second task, the Cup Transfer task. In that task, participants move small plastic cups from one of a table to the other and then back. One cup is picked up from the top and the other from the side. This task may show a more consistent use of the wrist flexion and extension movement that would allow a more direct analysis of the influence on shoulder and trunk compensation. As data analysis is completed, we expect that the GaMA metric will assist in evaluating use of additional DOF for prosthetic componentry, and compensatory movements. The kinematic analysis can serve as a supplement to other timed outcome measures, such as the box and blocks and the SHAP to quantify compensatory movements that are not well evaluated and scored in other measures.

ACKNOWLEDGEMENTS

This work was supported by CDMRP W81XWH1910863and NIH 5R01HD094861-04

REFERENCES

[1] A. M. Valevicius *et al.*, "Characterization of normative angular joint kinematics during two functional upper limb tasks," *Gait Posture*, vol. 69, pp. 176-186, Mar 2019, doi: 10.1016/j.gaitpost.2019.01.037.

[2] A. M. Valevicius *et al.*, "Characterization of normative hand movements during two functional upper limb tasks," *PLOS ONE*, vol. 13, no. 6, p. e0199549, 2018, doi: 10.1371/journal.pone.0199549.

[3] F. Montagnani, M. Controzzi, and C. Cipriani, "Is it Finger or Wrist Dexterity That is Missing in Current Hand Prostheses?," *IEEE Trans. Neural Syst. Rehabil. Eng.*., vol. 23, no. 4, pp. 600-609, 2015, doi: 10.1109/TNSRE.2015.2398112.

[4] L. A. Miller, *et al.*, "A Pilot Evaluation of Kinematic Changes With Powered Wrist Flexion for Transradial Prosthetic Users Using the Gaze and Movement Assessment (GaMA) Metric," in *Myoelectric Controls and Upper Limb Prosthetics Symposium (Proceedings)*, Fredericton, NB, CA, 2022: University of New Brunswick, pp. 132-135.

OPTICAL SENSING OF MUSCLE ACTIVITY

Jacopo Franco, Simon Stuttaford, Patrick Degenaar, Matthew Dyson

Newcastle University, School of Engineering, Microsystems Group

ABSTRACT

In recent years there has been an increasing interest in alternative muscle sensing methods. Optical myography is a relatively new field in muscle sensing techniques, which uses light to detect variation in the shape underlying muscle as it is contracted. We investigated the effect of finger motion and sensor placement on the resulting optical signal and compared it to clinical electromyography. Evidence suggests that the optical signal is strongly correlated to muscle activity and has high spatial accuracy.

INTRODUCTION

In upper-limb prosthetics research, methods of recording changes in muscle activity are commonly based on Electromyography (EMG), Mechanomyography and Sonomyography. Despite their attractive qualities, these sensors have limitations such as susceptibility to electrical noise, the influence of sweat, relatively high costs, and power requirements. An alternative approach known as 'optical myography', has gained increased interest in recent years [1, 2]. Typically, optical sensing involves shining a near-infrared (NIR) light source on the surface of the skin. The light travels through the derma, lipids, blood vessels and is partially reflected by the muscle's surface back to a photoreceiver. Contractions alter the geometry of the muscle which impact the intensity of light incident at the receiver. This can then be used to estimate muscle activation. This approach is like plethysmography (PPG) which estimates blood oxygenation. In contrast to PPG, rather than treating movement artefacts as noise, optical myography actively utilises this information. Exploring muscle activation from the optical domain introduces certain advantages. For example, while surface EMG captures the superposition of electrical activity over a given area, optical sensing may produce a finer spatial resolution, only detecting movement from areas below the photoreceiver [3]. However, being a less mature approach, the technique is not yet well understood [4]. We developed an NIR acquisition system to track subcutaneous changes from forearm muscles. The aim of this research was to explore the properties of optical myography and to investigate the relationship between sensor location and finger movement detection.

METHODS

We conducted two experiments involving closed-loop control of a one degree-of-freedom cursor via finger flexion Experiment A was run to characterise the response of the optical sensor across the lower arm of a single limb-intact participant. The optical data were compared to ground truth finger flexion data and gold standard EMG data. The aim of Experiment B was to investigate the relationship between finger flexion and optical signal response and to what degree individual fingers can be differentiated from one another.

Participants

Experiment A: One limb intact participant (male, 25 years old). Experiment B: 11 limb-intact participants (20-30 years old). All participants were free of any neurological or motor impairments and provided written informed consent. Ethics for this experiment was provided by the local committee at Newcastle University (Ref: 21-029-FRA).

Sensor design

Two LEDs at 640 nm and 850 nm are used as low-power emitters. The receiver consists of a photodiode (PD) and a transimpedance amplifier to convert the current generated into voltage. The analogue output is fed to a microcontroller which digitises the signal and relays it over a serial connection.

Recordings

Finger position: In experiment A, a flexible capacitive sensor (Bend Labs, Japan) was fixed on the middle finger providing the ground truth, the sensor was sampled at 500 Hz. In Experiment B, an infrared hand-tracking camera sensor (Leap Motion Controller, Ultraleap, USA) was used as the ground truth, approximating finger joint position at a sampling rate of 48 Hz. The Leap Motion sensor was placed on a desk around ~40 cm from the participant hand.

Electromyography: Two Trigno EMG sensors (Delsys, USA) were placed over the flexor carpi radialis (FCR) and muscle group and two sensors were placed over the extensor carpi radialis (ECR) muscle group. Sensors were sampled at 2000 Hz. Electromyography sensors were only used in Experiment A.

Optical: The optical sensor was mounted on the surface of the arm using an elastic strap. Note, there was no intentional air gap between the emitter-receiver components and the skin. The wavelength of light used during the experiments was 850 nm and the data was sampled at a rate of 500 Hz.

Protocol

Two experiments were performed. Experiment A recorded a high-density mapping of the participant's arm using the optical sensor. Experiment B explored how finger activity influences the optical signal acquired in a region around the wrist area. The participant sat in a comfortable position with their right arm and elbow supported. The participant was then shown the experimental task on a computer screen. The task consisted of a target moving up and down, following a cosine function. Finger position controlled the vertical height of a cursor on the screen. The goal was to keep the cursor inside the moving target.

Experiment A: The middle finger was placed inside an adapter ring which transferred the movement to the flexible sensor. Each trial lasted 10 seconds, with the vertical height of the target making one full cycle. There were 10 trials for each block. At the end of a block of trials, the sensor was moved to a new position on a 10 by 12 matrix. This approach was used to iteratively image the arm using a single channel sensor.

Experiment B: Participants were asked to follow the task on the monitor. At all times the silhouette of a hand highlighted which finger was to be moved during the trial. After 5 trials the participant was prompt by an image to use the next finger. Fingers were tested in order: Index, Middle, Ring and Pinky. After a block was completed, the optical sensor was moved along a row of 10 positions from the inside to the outside of the arm, at a distance around 4 cm from the wrist. The distance between each position was 1 cm.

Statistical analysis

Experiment A: Muscle activity was calculated using the mean absolute value (MAV) of the raw EMG output. A correlation value for each sensor position against the optical signal was estimated. This results in a 12x10 matrix, which was interpolated by a factor of 7. Correlation values were calculated for each sensor position over two windows, corresponding to flexion and extension of the finger. Correlation between optical and flex data were calculated trial by trial, and the mean correlation calculated.

Experiment B: The optical signal obtained during flexion and extension of the index finger was compared to that obtained during movement of the middle finger. A Bonferroni corrected statistical analysis was run, correcting for three comparisons. The calculation was performed over a period corresponding to peak flexion of the finger.

RESULTS

The results of Experiment A are shown in Figure 1. The block average was plotted to account for small variations in the participant performance, expected between trials. Some high frequency noise is showed in the EMG sensors, whereas the optical sensor shows environmental light switching frequencies (~100 Hz) and motion artifacts from changes in blood flow. As shown in Figure 1, the optical sensor output at distinct sensor sites is highly correlated to

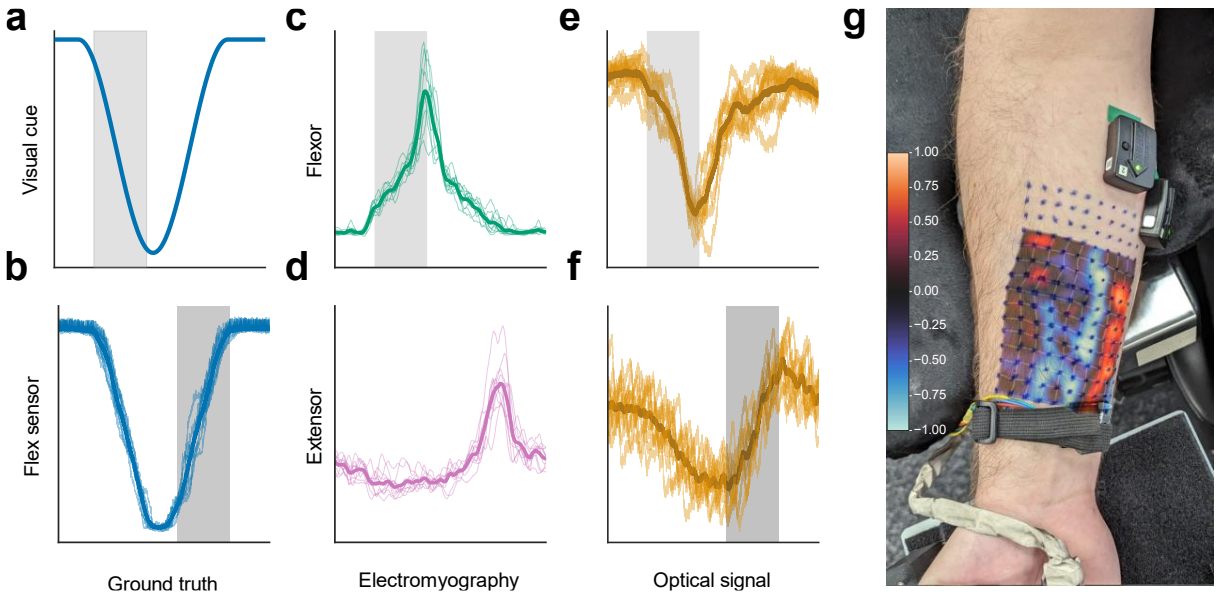

Figure 1: Exemplar timeseries of the sensors' output. The two time periods of interest are highlighted. Light grey indicates finger flexion, dark grey indicates extension. (a) Visual prompt for the participant. (b) Flex sensor providing the data for the ground truth. (c) & (e) Timeseries plots corresponding to the period of maximum negative flexor use correlation across the MAV from the EMG Flexor sensor, and the optical sensor, respectively. (d) & (f) timeseries analysis on the period of maximum positive correlation of respectively, the MAV of the EMG extensor, and the optical sensor. (g) Experiment A setup with resulting optical against flex sensor correlation heatmap conformed to participant arm. Axis intersections represent probe points, as indicated on the participant's arm.

the EMG envelope associated with flexion and extension of the finger. The arm image in Figure 1g indicates in red where a positive correlation exists between the optical signal and the flex sensor during flexion of the finger, suggesting a high degree of spatial acuity over the flexor muscle and tendons. A negative correlation is noted directly adjacent to the positive correlation, likely to also reflect muscle displacement. The intersection between the row and columns are indicative of the sensor position.

The results of experiment B are shown in Figure 2. An example showing the sensor tape guide in show in Figure 2a. The marks are posed 1 cm apart and indicated sensor positions to test. Note that 9 and 10 are wrapped around and are not visible in the image. The statistical significance map in Figure 2b estimates where statistical differences exist between activity produced by individual fingers, in this case the Index-Middle finger combination, across the ten sensor locations for each participant. Several areas reach statistical significance, predominantly on the ventral side of the arm towards the ulna. These are not limited to the inner portion of the wrist.

DISCUSSION

Slow variations in the optical sensor output are attributed to oxygen levels in the muscle tissue varying after repetitive activations. The timeseries shown in Figure 1 demonstrate that with appropriate filtering, this has relatively little impact on the ability of the optical sensor to sample the underlying muscle activity, with an accuracy comparable to the flex sensor and electromyography. Blood flow appears to be the larger source of noise in optical systems as presented in the timeseries. Since the cosine wave used as visual prompt in these experiments was relatively slow (0.14Hz), we anticipate a higher relative signal power for more rapid movements, with a bandpass filter appropriate to decrease blood flow artefacts.

Figure 1d shows EMG corresponding to participants use of antagonist muscles to bring the finger to a relaxed or straight position. It is interesting to note that the optical sensor produces a similar signal, Figure 1f, on the inner arm.

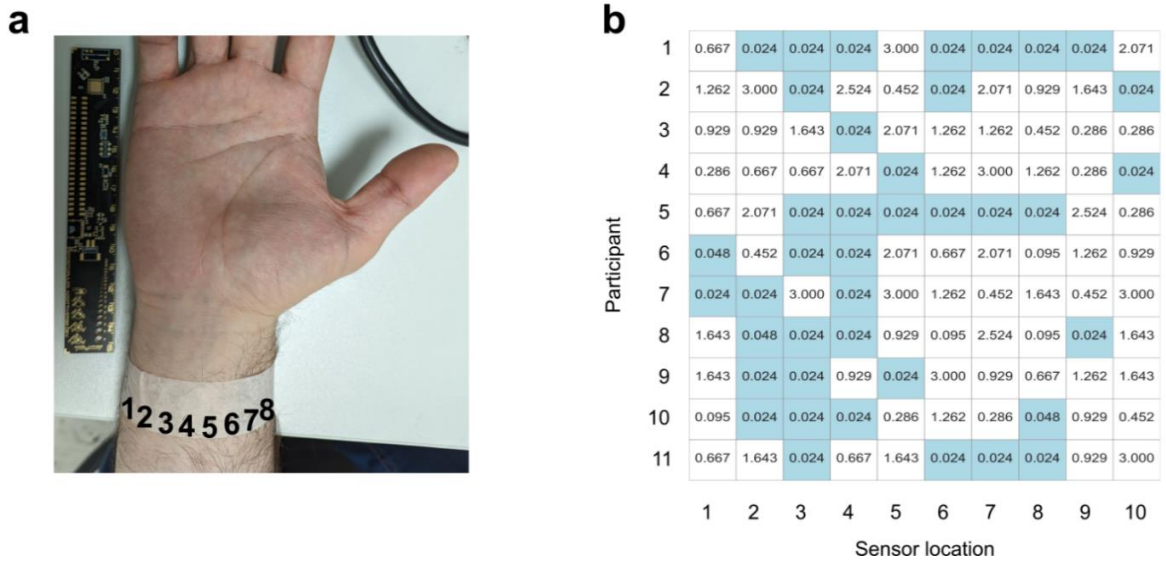

Figure 2: (a) Sample image showing sensors locations. (b) Bonferroni corrected statistical significance map showing where Index-Middle finger activity is significantly different ($p < 0.05$) at each sensor position across participants. The numerical value represents the Bonferroni statistical significance for the finger pair. Blue indicates statistical significance.

We assume this corresponds to the extensor group muscle returning from a contracted position back to a relaxed one. The correlation image shown in Figure 1g shows an extended area of positive correlation which may coincide with flexor digitorum superficialis. An area of inverted correlation lies directly adjacent to this area, it is possible that this corresponds to muscle moving away from the sensor as a contraction is made. The results presented in Figure 2 suggest activation from individual fingers are likely to be distinguishable using optical sensing. Most sites are located on the ventral side of the arm towards the ulna, again corresponding broadly to flexor digitorum superficialis. This muscle group is likely to play a role in the significance map, because it extends primarily on the inner and middle side of the forearm. We note quite a high variance between participants which may be connected to the individual biological differences in arm size and also of fat tissue. The conclusions which we can draw from an analysis based on a single sensor are however, limited. Future studies will utilise an increased density of sensor sites to ascertain more information about the spatial resolution of optical sensing. In a separate study we are utilising faster contracts to investigate how the signal changes compared to muscle activation, and we are also characterising how skin tone and other physiological factors impact on sensor output [5].

ACKNOWLEDGMENTS

The project was funded by the EPSRC, the UKRI Research Council Training Grants number 2595462 and EP/W000717/1 (TIDAL+).

REFERENCES

[1] A. Chianura and M. E. Giardini, ‘An electrooptical muscle contraction sensor’, Med Biol Eng Comput, vol. 48, no. 7, pp. 731–734, Jul. 2010, doi: 10.1007/s11517-010-0626-x.

[2] W. Guo, X. Sheng, H. Liu, and X. Zhu, ‘Development of a multi-channel compact-size wireless hybrid sEMG/NIRS sensor system for prosthetic manipulation’, IEEE Sens J, vol. 16, no. 2, pp. 447–456, Jan. 2016, doi: 10.1109/JSEN.2015.2459067.

[3] A. K. Bansal, S. Hou, O. Kulyk, E. M. Bowman, and I. D. W. Samuel, ‘Wearable organic optoelectronic sensors for medicine’, Advanced Materials, vol. 27, no. 46, pp. 7638–7644, Dec. 2015, doi: 10.1002/adma.201403560.

[4] E. Nsugbe, C. Phillips, M. Fraser, and J. McIntosh, ‘Gesture recognition for transhumeral prosthesis control using EMG and NIR’, IET Cyber-Systems and Robotics, vol. 2, no. 3, pp. 122–131, Sep. 2020, doi: 10.1049/iet-csr.2020.0008.

[5] S. Stuttaford, J. Franco, P. Degenaar, and M. Dyson, ‘Investigating the universality of optical myography’, MEC 2024 (Submitted)

POWER CONSUMPTION, LATENCY, AND MAXIMUM NUMBER OF SUPPORTED NODES FOR BLE BIOSENSOR APPLICATIONS

Kiriaki J. Rajotte[2], Anson Wooding[1], Todd Farrell[1], Jianan Li[2], Xinming Huang[2], Edward A. Clancy[2], Benjamin E. McDonald[1]

[1] *Liberating Technologies, Inc., Holliston, MA, USA*

[2] *Worcester Polytechnic Institute, Worcester, MA USA*

ABSTRACT

Wearable wireless physiological monitoring devices have emerged as powerful tools in healthcare, facilitating continuous monitoring of vital signs and physiological parameters in real-time. Many of these applications require small profile, and low-power battery operated devices. Bluetooth Low Energy (BLE) is a commonly selected wireless communication protocol as it provides fast data transfer, low cost, and low power. Physiological monitoring applications do not have as strict real-time latency requirements as control applications. For control use-cases, such as prosthesis control, real-time latency has a direct impact on user experience. In this work we explored various BLE parameter configurations in a multi-channel sensor node system to determine their relationship to power consumption, the number of supported peripheral nodes, and latency. Data collected during these experiments indicates that using longer connection intervals leads to a decrease in power consumption and that shorter event lengths allows for support of more peripheral sensor nodes for a given connection interval. It was observed that the typical latency between the application of an input signal at a peripheral node and its detection on the central node is approximately one connection interval. Future work should continue to investigate techniques to optimize power consumption, extend the number of supported peripheral nodes, and minimize latency through the system specifically for control applications.

INTRODUCTION

There has been considerable growth over the last decade in the adoption of wireless and wearable biopotential sensors for a variety of applications, including: remote patient monitoring and diagnostics [1] and human-machine interfaces for robotic or prosthesis control [2, 3]. To support this wide spectrum of applications, robust, reliable and low power wireless communications are required. One of the most used communication protocols for these applications is Bluetooth Low Energy (BLE). BLE is ideal for wearable systems because of its small form factor, low power, affordability, and interoperability across a variety of platforms, making it easy to integrate with existing systems (smart phones, computers, etc.).

The goal of this work is to explore the use of BLE in a wireless biopotential system; specifically, how the BLE parameters of connection interval, maximum transmission unit (MTU) size, and event length influence power consumption, the number of sensing nodes supported, as well as the impact on latency. Real-time biomedical applications such as multi-site monitoring of electromyograms for gait analysis, rehabilitation, or prosthesis control typically require low-latency (100 ms or less) communication protocols [4] and multiple peripheral nodes communicating with a single central node. Understanding how the important BLE transmission parameters of connection interval, event length, and MTU size influence system operation can be instructive in designing a robust and reliable wireless system.

BACKGROUND

BLE has been used in various wireless communications applications across disciplines. BLE offers a compelling combination of low power consumption, small form factor, affordability, interoperability, fast data transfer up to 2 Mbps [5], and security features, making it well-suited for a wide array of wireless wearable applications. Additionally, BLE offers flexibility in selecting the transmission event length, length of the connection interval, and size of the transmission. Understanding how these factors influence power consumption and number of supported sensor nodes is critical when developing reliable, wearable, battery-operated systems. In the case of medical devices, where there may be multiple sensor nodes, the data these sensors generate are critical to proper diagnostics and patient monitoring.

BLE Parameter Definitions

The following BLE definitions have been included to aid in understanding the parameters studied in this work.

- **Connection Interval (CI):** time between consecutive connection events between central and peripheral devices [6].
- **Maximum Transmission Unit (MTU):** the maximum packet size to be sent between connected devices [6].
- **Event Length:** allocated time within a CI for the data transfer to occur between a central and peripheral device [7]

Prior Works

Connection interval, MTU size and event length have been studied in prior works, but under different test conditions and in different combinations than those considered here. Additionally, BLE version 5.0 or earlier was used in many of these prior works. In this work, BLE version 5.3 was used as it specifically has upgrades that enable lower power consumption, improved reliability, and reduced latency through new features such as enhanced periodic advertising, connection subrating and improved channel classification [8].

Tipparaju et al. [9] used two peripherals and a single central node (different central nodes were used to study the influence of OS: iOS-based device, Android device, and Raspberry Pi) to study data loss and its relationship to MTU size and the influence of the external environment and interference on data loss (distance between central and peripheral nodes, physical obstacles in the path, other wireless signals, etc.). They proposed a mitigation protocol that reduces frequency of transmission and bundles the data with a timestamp to detect lost packets. If a lost packet is detected, their re-request routine is run to recover the lost data. Work conducted by Brunelli et al. [10] explored the use of BLE 4.1 operating on Texas Instruments' CC2650 BLE microcontroller in a wireless acquisition system for surface EMG signals. In their BLE experiments, they looked specifically at the relationship between connection interval and nominal throughput, interference and environmental influences, and the current consumption profile during a connection event. Tosi et al. [11] present an overview of the BLE protocol and how various parameters are related such as the maximum number of peripherals per central node and the influence of connection interval on throughput and power consumption. They also review other BLE-based studies, both theoretical and experimental, whose results are derived from a mix of simulation and measurement on different platforms. In this work, we utilize BLE version 5.3 and extend our analysis to more than two peripherals.

METHODS

Experimental Apparatus

The goal of this work was to measure power consumption, maximum number of supported peripheral devices, and latency as a function of connection interval, MTU, and event length. Combinations of connection interval values between 10–100 ms, and event length values between 2500–7500 µs were considered. These values were selected as appropriate for real-time control applications such as prosthesis/orthosis and robotic control. The MTU value was scaled to maximize the number of analog-to-digital converter (ADC) samples sent for a given connection interval. An additional twenty bytes of each BLE data packet were reserved for timing and header information.

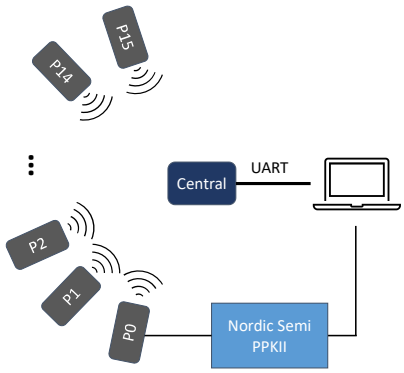

Figure 1 - Diagram of experimental setup.

Both the central and peripheral devices (up to 16) used a nRF52840 System-on-Chip (SoC) from Nordic Semiconductor running BLE version 5.3. All measurements were taken with a transmit power of 0 dBm. The peripheral nodes were placed in a semicircle 0.5 m away from the central node in an equidistant fashion (Figure 1). A single channel of the internal 12-bit ADC was enabled and continuously converting at 1 kHz to account for its power consumption. On the central node, the received packets are sent via UART to the host PC for off-line processing (although, unused in this study). The number of peripherals varied depending on the configuration used.

Determining Number of Supported Peripheral Devices and Measuring Power Supply Current

A separate set of trials measured both number of supported peripheral nodes and current consumption. All combinations of BLE parameters (connection interval, MTU, and event length) were investigated. In a trial, the number of peripherals was increased from a single device in increments of one until the central device was no longer able to accept additional incoming data. All non-connected peripherals were then powered off. Once the maximum number of connections has been established, data received by the central node were streamed for 10 minutes on the PC to observe sustained connections.

Once per minute during this 10 minutes of streaming, current consumption was measured from a single (connected) peripheral device using the Nordic Power Profiler Kit II (PPK2). The PPK2 device is placed in series with the power supply output and power input of the nRF52840. The Nordic Semiconductor Power Profiler application (v3.5.4) was used to control

the PPK2 device and log measured current consumption each trial. Average current was measured over 7 seconds (default measurement time window of the PPK2 device).

Measuring Latency

A logic analyzer was used to measure the time latency between the application of an analog signal to the ADC of one peripheral node and the arrival of its digital samples at the central node via BLE. To do so, a step input is applied to the ADC input of a peripheral node. The rising edge of the step input triggers the beginning of the measurement. Software edge detection is implemented on the central node to determine when the step input edge was detected in a received BLE packet. This software detection was used to emit a hardware logic signal on the central node. For each combination of event length and connection interval tested, 10 trials were completed.

RESULTS

Power Consumption

As shown in Table I, current consumption decreased as connection interval increased, with the largest decrements occurring at the shortest connection intervals. This trend was observed across all event lengths and absolute power consumption only differed substantially at a connection interval of 100 ms. Power reduced ~8% when increasing the connection interval from 10 to 20 ms and ~18% when increasing the connection interval from 10 to 100 ms, both for an event length of 2500 µs.

Table 1 - Average power consumption and number of supported peripherals for each parameter combination tested. Each cell shows the mean of the average current consumed across 10 trials in mA and the maximum number of supported peripherals at a distance of 0.5 m.

Event Length (µs)	Connection Interval (ms), Scaled MTU Value (bytes)					
	10, 40	20, 60	30, 80	40, 100	50, 120	100, 247
2500	2.84, 4	2.56, 8	2.50, 11	2.46, 12	2.35,12	2.33, 10
5000	2.85, 2	2.59, 4	2.47, 6	2.41, 8	2.45, 10	2.38, 10
7500	2.78, 1	2.58, 2	2.49, 4	2.47, 5	2.43, 6	2.38, 11

Number of Connected Devices

Figure 2 shows the number of connected peripherals vs. connection interval and event length. As the event length increases from 2500 µs to 7500 µs, the number of connected peripherals decreased by more than 50% for connection intervals of 10, 20, 30, and 40 ms. For a connection interval of 50 ms, a less drastic decrease (40%) in the number of connected peripherals was observed as event length increased. For a connection interval of 100 ms, an event length of 2500 µs provides a very narrow time window for the data transmission to occur which results in fewer successful transmissions under these conditions. In this case, increasing the event length to 5000 and 7000 µs allows for more successful transmissions to occur and in turn a greater number of sustained peripheral connections. Using the smallest possible event length of 2500 µs enables a greater number of peripheral devices to be connected in each connection interval, except for a connection interval of 100 ms. When selecting the event length, ensure that the event length chosen provides sufficient transmission time to send the data desired within a single event.

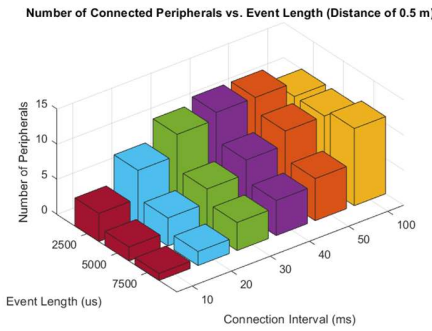

Figure 2 - Comparison of number of connected devices vs. event length and connection interval.

Latency

As connection intervals increased, the latencies also increased for a given configuration. To directly compare latency across the different configurations tested, each measurement was normalized by dividing the latency value by its connection interval. Figure 3 shows histograms of the normalized latency measurements, pooling all six connection intervals and three event lengths. Latency from application of the analog input on the peripheral to digital sample arrival on the central shows a triangle-like distribution with a mean of 1.14 connection intervals and variance of about 0.21 connection intervals. This triangle-like distribution is consistent with summing two, independent, uniformly distributed latencies, each of one connection interval duration [12]: (1) the delay from analog signal arrival at the peripheral node to completion

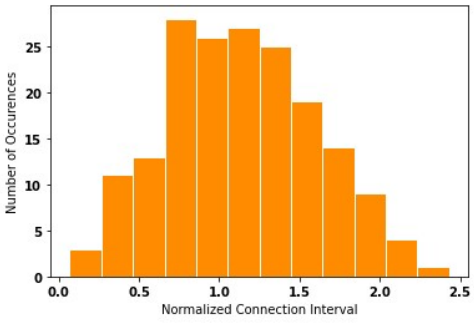

Figure 3 – Normalized latency: Edge detected in BLE data on Central.

of acquiring a full block of ADC samples, and (2) BLE transmission delay between the peripheral and central nodes. Some additional small delays were observed as expected to account for intermediate data processing as the data moves through the system.

DISCUSSION

Nordic Semiconductor's nRF52840 SoC was used to study the relationships between power consumption, the number of supported peripheral connections, and latency for different BLE configurations. In applications where power is constrained, longer connection intervals are recommended — when latency concerns permit. If aiming to maximize the number of peripheral sensors in the network, smaller event lengths allow for more data transfers to occur in each connection interval. This assumes the selected event length provides sufficient time for the data to be transferred. Overall system latency scales directly with connection interval, thus low latency requires short connection intervals. It is important to note that results may vary between different manufacturer's devices, firmware, software development kits (SDK) and the specific implementation of the biopotential application. Future work should look at potential performance improvements that may come from use of different hardware and software development kits, software optimization and upgrading to BLE version 5.4 [8]. Future work could focus on developing software optimized for power savings, such as implementing our patented power savings technique (U.S. patent #11,154,408, 2021) which reduces wireless transmissions during intervals of bio-signal inactivity to improve battery life.

CONCLUSION

The release of BLE 5.x has allowed for the development of larger and lower power wireless, biopotential sensor networks. It is critical to understand how selection of BLE parameters such as connection interval and event length influence power consumption, number of peripheral devices that the sensor network can reliably support, and latency. This experimental work tested different BLE configurations to study their influences on sensor network performance to guide application development. It was observed that power consumption decreased by as much as 18% by increasing connection interval from 10 to 100 ms. To increase the number of supported peripheral sensor nodes, designers should select the minimum event length required to successfully transmit their data. Finally, when looking at latency, it was found that on average, 1.14 connection intervals lapse between the application of a step response on the peripheral node and when it is detected in the received BLE data by the central node. Future work should consider the addition of power optimization methods and latency in the microcontroller's firmware as well as the use of the latest BLE versions.

ACKNOWLEDGEMENTS

This material is based upon work supported by the DoD STTR Program under Contract No. W81XWH-22-C-0049. Any opinions, findings and conclusions or recommendations expressed in this material are those of the author(s) and do not necessarily reflect the views of the U.S. Army Medical Research and Development Command (USAMRDC).

REFERENCES

[1] L. C. Fourati and S. Sai, "Remote health monitoring systems based on Bluetooth Low Energy (BLE) communication systems," The Impact of Digital Technologies on Public Health in Developed and Developing Countries, vol. 12157, pp. 41-54, 2020.
[2] P. Parker, K. Englehart and B. Hudgins, "Myoelectric signal processing for control of powered limb prostheses," Journal of Electromyo. And Kinesiol., vol. 16, pp. 541-548, 2006.
[3] Farina et al., "The extraction of neural information from the surface EMG for the control of upper-limb prostheses: Emerging avenues and Challenges," IEEE Trans Neural Syst Rehabil Eng., vol. 22, no. 4, pp. 797-809, 2014.
[4] T. R. Farrell and R. F. Weir, "The Optimal Controller Delay for Myoelectric Prostheses," IEEE Transactions on Neural Systems and Rehabilitation Engineering, vol. 15, no. 1, pp. 111-118, 2007.
[5] F. J. Dian, A. Yousegi and S. Lim, "A practical study on Bluetooth Low Energy (BLE) throughput," in 2018 IEEE 9th Annual Information Technology, Electronics and Mobile Communication Conference (IEMCON), Vancouver, 2018.
[6] K. Townsend, C. Cufi, Akiba and R. Davidson, Getting started with Bluetooth Low Energy, Sebastopol: O'Reilly, 2014.
[7] Nordic Semiconductor, "Connection timing with connection event length extension," 2 Sept. 2019. [Online]. Available: https://infocenter.nordicsemi.com/topic/sds_s140/SDS/s1xx/multilink_scheduling/extend_connection_event.html.
[8] Nordic Semiconductor, "What's new in Bluetooth 5.3?," Nordic Semiconductor, 20 August 2021. [Online]. Available: https://devzone.nordicsemi.com/nordic/nordicblog/b/blog/posts/bluetooth-5-3.
[9] V. V. Tipparaju, K. R. Mallires, D. Wang, F. Tsow and X. Xian, "Mitigation of data packet loss in Bluetooth Low Energy-based wearable healthcare ecosystem," Biosensors, vol. 11, no. 350, p. 17, 2021.
[10] D. Brunelli, E. Farella, D. Giovanelli, B. Milosevic and I. Minakov,"Design considerations for wireless acquisition of multichannel sEMG signals in prosthetic hand control," IEEE Sensors Journal, vol. 16, no. 23, pp. 8338-8347, 2016.
[11] J. Tosi, F. Taffoni, M. Santacatterina, R. Sannino and D. Formica, "Performance evaluation of Bluetooth Low Energy: A systematic review," Sensors, vol. 17, no. 2898, p. 34, 2017.
[12] A. Papoulis, "Functions of two random variables," in Probability, Random Variables, and Stochastic Processes, New York, McGraw-Hill Book Company, 1965, p. 190.

User Experience

A PORTABLE MYOELECTRIC PATTERN RECOGNITION-DRIVEN VIRTUAL TRAINING SYSTEM FOR PHANTOM LIMB PAIN MANAGEMENT

Zachary A. Wright[1], Blair A. Lock[1], Kristi L. Turner[3], Andrea Ikeda[3], Katie Cai[1], Xavier Oberhelman[1], Carlos Martinez[2], Levi J. Hargrove[3,4]

[1]Coapt, LLC, Chicago, IL, USA [2]Liberating Technologies, Inc., Holliston, MA, USA [3]Center for Bionic Medicine, Shirley Ryan AbilityLab, Chicago, IL, USA [4]Department of Physical Medicine and Rehabilitation, Northwestern University, Evanston, IL, USA

ABSTRACT

Individuals with limb absence commonly suffer from phantom limb pain (PLP), a debilitating condition with poorly understood mechanisms and limited treatment options. Current approaches to treat PLP have broadly proven unsafe or ineffective, leaving patients searching for alternative, long-term options. Recent studies have demonstrated the potential of phantom motor execution therapy, aided by myoelectric pattern recognition software and virtual reality systems, in alleviating PLP. However, widespread clinical adoption has been hindered by limited accessibility, especially for the lower limb absent population. This paper presents the design and development of a portable, myoelectric pattern recognition–driven virtual training system, tailored for at-home use by individuals with upper or lower limb absence to safely and effectively manage and reduce PLP.

INTRODUCTION

Phantom limb pain (PLP) can present a significant challenge for individuals with upper or lower limb absence, with a notable impact on their quality of life. PLP often manifests as sensations of discomfort or pain in the missing limb despite its physical absence highlighting the complex nature of this phenomenon. PLP affects a considerable proportion of the limb absent population, with approximately 79.9% reporting symptoms, among which 38.9% rate the pain as severe [1]. Symptoms of PLP can occur immediately after amputation and often remain during chronic stages of recovery, emphasizing the need for effective treatment options that can alleviate or help manage PLP long-term.

Current treatment approaches for PLP often involve pharmacological or surgical interventions, which may carry risks or prove ineffective for some individuals [2]. Non-invasive therapies, such as motor imagery and mirror therapy, provide safer alternative treatment. These neuroplasticity-based approaches ultimately aim to restore normative brain circuitry to alleviate pain. While both techniques activate similar brain regions, mirror therapy has shown greater effectiveness, likely due to the requirement for patients to activate different muscle groups in the residual limb, instead of mentally simulating movement of their phantom limb [3, 4]. Active engagement of residual limb muscles could possibly explain why regular use of a prosthesis has also shown to help reduce PLP [5, 6].

Most modern upper limb prostheses use muscle activity measured from residual limb muscles to control motorized arm components. Advanced myoelectric-controlled prostheses employ machine learning algorithms, such as pattern recognition, to decode the user's muscle activity patterns, enabling more intuitive control of their prosthesis. Recently, researchers have proposed a more advanced approach to mirror therapy that leverages pattern recognition technology to better capture, and perhaps, enhance user engagement by combining it with virtual reality systems. Such systems offer a more dynamic and immersive platform for individuals to actively engage movements that mimic those of their missing limb, termed phantom motor execution therapy. While myoelectric-controlled virtual reality systems have shown promise for PLP management [7], its widespread clinical implementation has remained limited, particularly for the lower limb absent population which has a higher prevalence of PLP [8].

This paper describes the design of a portable myoelectric, pattern recognition-driven virtual training system, referred to as the Phantom Limb Pain Management System (PLP-MS), which is suitable for individuals with either upper or lower limb absence who have chronic PLP. The PLP-MS consists of an expandable EMG-embedded cuff worn on the residual limb and a cloud-connected mobile software application featuring interactive virtual games played using phantom motor execution. With an aim to provide an accessible and effective treatment solution, the

PLP-MS provides users the flexibility to manage PLP virtually anywhere and as needed. Another key feature is its integration into a connected health platform, enabling remote delivery and monitoring of device training and therapy and thus facilitating a telerehabilitation application for PLP management.

HARDWARE DESIGN

EMG-embedded cuff: The main mechanical component of the PLP-MS includes a semi-rigid and expandable electrode-embedded arm/leg cuff (Figure 1). The cuff was made to fit comfortably with two different size options to accommodate most residual limb sizes. The standard-sized cuff has a minimum circumference of 17 cm (a cross-arm diameter of 5.4 cm) and maximum circumference of ~35 cm when fully expanded. It is suitable for upper residual limbs (above- or below-elbow) and fits most below-knee residual limbs. A larger version of the cuff has a minimum circumference approximately the maximum circumference of the standard-size cuff and can fit residual limb sizes up to ~60 cm.

Fig. 1: A standard and larger sized EMG-embedded arm/leg cuff embedded with bi-polar electrode sensors for convenient acquisition of up to 8 muscle activity signals.

Both sized cuffs were designed using CAD software and fabricated with 3D printed material. The cuffs comprise of 9 pods (8 EMG sensor pods and 1 main pod) which are adjoined radially by linkages attached to each pod. The linkages have a novel hinge mechanism to allow the cuff to expand when donned on the residual limb. For the larger-sized cuff, the linkages were made thicker which effectively increases the distance between the pods when not expanded.

Each of the EMG pods has two dome-shaped electrode sensors (one on each end, spaced 5 cm apart) such that 2 bands of 8 electrodes are equally spaced around the inner part of the cuff. A reference/ground electrode is in the middle of the main pod. Connection wires transmitting the EMG signals to the signal processing unit housed inside the main pod run along inner channels of the linkages. Enclosed on the face of each EMG pod are colored LED lights that illuminate at different intensities based on the underlying EMG muscle amplitude.

Controller Hardware: The main pod of the cuff houses the necessary hardware for amplifying and digitizing EMG signals and a microcontroller to translate recorded EMG signals into motion output commands using pattern recognition. This control system features enhanced digital filtering for optimal EMG signal quality, Bluetooth Low Energy communication, expandable data storage capacity, and power management and USB-C fast charging capabilities, among other functionalities. The charging circuitry, compatible with a 3.7V lithium-ion battery, includes undervoltage detection to safeguard against battery depletion below 3V. To ensure user safety, the power management circuitry disengages the system load during battery charging, preventing any risk of exposure to mains voltage from the USB-C port. The top of the main pod features a power button accompanied by a light indicator to convey power status, charging progress, and low battery notifications.

SOFTWARE DESIGN

Pattern recognition: The PLP-MS controller performs on-board signal processing and translates recorded EMG signals into motion output commands using an adaptive pattern recognition control algorithm [9]. Users are required to train (i.e., calibrate) the system by inputting representative EMG data for each selected limb motion to control. Users can train the system at any time to improve and personalize controller performance.

Mobile App Software: The PLP-MS controller communicates wirelessly via Bluetooth Low Energy to a custom interactive and user-friendly mobile application, called Control Companion™ (Figure 2). The mobile app was developed in Unity and is available on both iOS and Android platforms. It is compatible with Coapt's commercial Complete Control Gen2 pattern recognition system developed for controlling upper limb powered devices. Compatibility with the PLP-MS required some modifications such as adding lower-limb specific configuration elements. The controller streams recorded EMG signals and motion output commands to the mobile app. The main environments in Control Companion™ include:

Myoexplorer: A visualization tool that allows users to view their muscle activity in real-time using color-coded and dynamic representations of the EMG amplitudes recorded by the sensors (Figure 2, left). Myoexplorer can be used as a training tool to help visualize similarities and differences between muscle activity patterns corresponding to each motion and to explore the virtual space to train new patterns.

Configuration: Users can configure their controller according to limb loss side (right/left) and level (below- or above-elbow and below- or above-knee) and select the limb motions they want to train and use while playing virtual games (Figure 2, middle). Available motions include hand open/close, wrist supination/pronation and elbow flexion/extension for the upper limb users and ankle inversion/eversion, ankle flexion/extension and knee flexion/extension for the lower limb users.

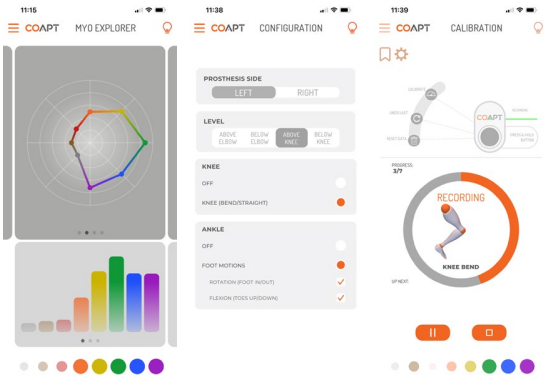

Fig. 2: The Control Companion™ mobile app allows users to view their EMG signals (left), configure the controller (middle) and calibrate selected limb motions (right).

Calibration: Virtual limb animations guide users through a motion calibration sequence to train their pattern recognition control system for each selected limb motion (Figure 2, right). Alternatively, users can also add additional EMG input data to any individual motion. Feedback about the quality of their calibration data and suggestions for improvement are provided through the AI-driven Control Coach® [10].

Training and Games: The app includes a range of virtual training and practice games (Figure 3) which are tailored to the user's limb loss level and side using custom virtual limbs and icons to prompt them to perform specific limb motions during gameplay. Simon Says tests their ability to isolate individual motions by requiring them to control the movement of a virtual limb until it matches a target position (Figure 3A). In-the-Zone tests their ability to modulate their muscle contraction intensity using proportional control by requiring users to match and hold their contraction intensity to a target level (Figure 3B). Zap It tests their ability to perform a sequence of prompted motions (Figure 3C). Each of these games allow users to select their preferred difficulty level (Beginner, Intermediate, Advanced) which changes game parameters (e.g., size of target, amount of time to hold in target) to make them more challenging and game performance metrics are displayed on the screen upon game completion. Additional games offer users greater freedom, such as Paper Flyer where they can hone their movement coordination skills by controlling the flight path of a paper airplane along two axes, navigating it through virtual rings (Figure 3D), Flick It Golf where they command motions to aim and shoot a ball into a hole, avoiding or using virtual objects to their advantage (Figure 3E), and Raceway where they navigate a car through an obstacle course trying to capture objects that provide a boost (Figure 3F).

Pain Assessment Tools: Interactive clinical tools allow for convenient collection of user-reported pain ratings. These include a Numerical Pain Rating Scale where users are prompted to rate their PLP on a standard 11-point scale (0 – no pain to 10 – very severe) (Figure 3G) and a Visual Analog Scale where users are prompted to move a slider on a vertical scale from "Zero Pain" to "Most Pain" (Figure 3H). The tools can be accessed at any time or pre-set to be presented to users at specific time intervals (e.g., every 24 hours).

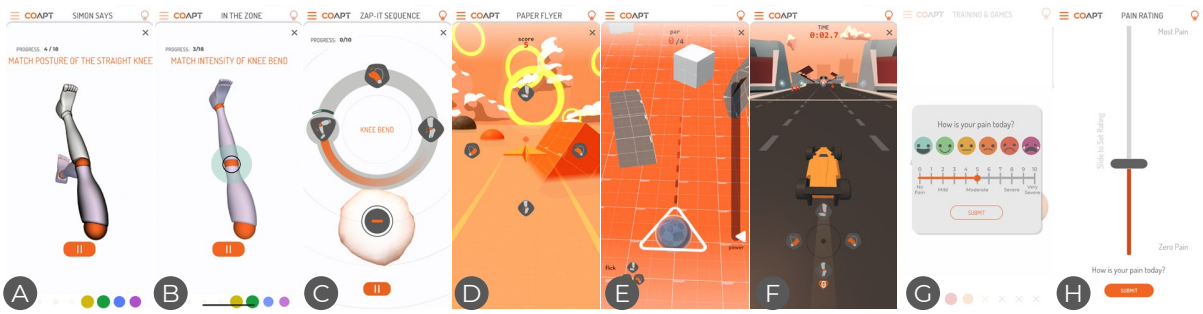

Fig. 3: The Control Companion™ mobile app offers a variety of virtual games and self-report pain rating tools.

Cloud-Connected Software: The Control Companion™ mobile app has cloud-connected data storage capabilities to remotely record a wide range of user data from connected devices; including calibration data, virtual game data and self-reported pain scores. Data is uploaded to a HIPAA-compliant cloud storage database hosted on Microsoft Azure Cloud Platform. Integration into a Connected Health Platform offers a convenient resource for researchers and clinicians to monitor device use and diagnostic information and to track user performance. User data can be viewed in a web-based software application containing real-time EMG signals, virtual game performance and aggregated data insights.

CLINICAL IMPLEMENTATION

Development of the PLP-MS was performed under a rigorous design process with clearly defined user and device specifications and testing procedures. This included gathering user and clinician feedback on hardware and software components in collaboration with the Shirly Ryan AbilityLab (Chicago, IL) who completed in-lab pilot usability and functionality testing with limb absent subjects (Figure 4). Feedback was used to iteratively refine and improve the PLP-MS prior to deployment for an ongoing at-home clinical trial evaluating its efficacy in reducing pain across 48 upper and lower extremity patients.

Fig. 4: A below knee (left) and above knee (right) limb absent subjects donning an cuff and playing virtual games.

ACKNOWLEDGEMENTS

This work was supported by the Assistant Secretary of Defense for Health Affairs, through the Defense Health Program, Congressionally Directed Medical Research Programs, Defense Medical Research and Development Program, Joint Program Committee 8 / Clinical and Rehabilitative Medicine Research Program, Restoring Warfighters with Neuromusculoskeletal Injuries Research Award under Award No. W81XWH2010873. Opinions, interpretations, conclusions, and recommendations are those of the author and are not necessarily endorsed by the Department of Defense.

REFERENCES

[1] P. L. Ephraim, S. T. Wegener, E. J. MacKenzie, T. R. Dillingham, and L. E. Pezzin, “Phantom pain, residual limb pain, and back pain in amputees: Results of a national survey,” Arch. Phys. Med. Rehabil., vol. 86, no. 10, pp. 1910–1919, 2005.

[2] H. Flor, “Phantom-limb pain: Characteristics, causes, and treatment,” Lancet Neurology, vol. 1, no. 3. Lancet Publishing Group, pp. 182–189, 01-Mar-2002.

[3] B. L. Chan et al., “Mirror therapy for phantom limb pain [15],” New England Journal of Medicine, vol. 357, no. 21. Massachussetts Medical Society, pp. 2206–2207, 22-Nov-2007.

[4] S. B. Finn et al., “A randomized, controlled trial of mirror therapy for upper extremity phantom limb pain in male amputees,” Front. Neurol., vol. 8, no. JUL, Jul. 2017.

[5] M. Lotze, W. Grodd, N. Birbaumer, M. Erb, E. Huse, and H. Flor, “Does use of a myoelectric prosthesis prevent cortical reorganization and phantom limb pain? [2],” Nature Neuroscience, vol. 2, no. 6. pp. 501–502, Jun-1999.

[6] C. Dietrich et al., “Leg prosthesis with somatosensory feedback reduces phantom limb pain and increases functionality,” Front. Neurol., vol. 9, no. APR, Apr. 2018.

[7] M. Ortiz-Catalan et al., “Phantom motor execution facilitated by machine learning and augmented reality as treatment for phantom limb pain: a single group, clinical trial in patients with chronic intractable phantom limb pain,” Lancet, vol. 388, no. 10062, pp. 2885–2894, Dec. 2016.

[8] P. U. Dijkstra, J. H. B. Geertzen, R. Stewart, and C. P. Van Der Schans, “Phantom pain and risk factors: A multivariate analysis,” J. Pain Symptom Manage., vol. 24, no. 6, pp. 578–585, Dec. 2002.

[9] M. M. C. Vidovic, H. J. Hwang, S. Amsuss, J. M. Hahne, D. Farina, and K. R. Muller, “Improving the robustness of myoelectric pattern recognition for upper limb prostheses by covariate shift adaptation,” IEEE Transactions on Neural Systems and Rehabilitation Engineering, vol. 24, no. 9, pp. 961–970, Sep. 2016, doi: 10.1109/TNSRE.2015.2492619.

[10] N. Brantly, A. Feuser, F. Cummins, L. Hargrove, B. Lock, and S. R. Abilitylab, “Pattern Recognition Myoelectric Contol Calibration Quality Feedback Tool To Increase Function,” MEC 17 - A Sense of What’s to Come, pp. 2–4, 2017.

ASSESSING CONTROL AND FEEDBACK IN VIRTUAL REALITY FOR MYO-ELECTRIC PROSTHESIS TRAINING

Samantha G. Rozevink[1], Bart Maas[1], Alessio Murgia[1], Raoul M. Bongers[1], Corry K. van der Sluis[2]

1. University of Groningen, University Medical Center Groningen, Department of Human Movement Sciences, Groningen, The Netherlands

2. University of Groningen, University Medical Center Groningen, Department of Rehabilitation Medicine, Groningen, The Netherlands

ABSTRACT

Training a myo-electric prosthesis could benefit from a virtual reality environment (VRE) as a training tool, however it should match the wishes and needs of prosthesis users and therapists. We investigated whether an existing VRE, developed for exploration of prosthesis use, complied with the needs and wishes of the end-users, regarding control and feedback. The VRE simulated a coffeehouse where different types of cups of coffee needed to be grasped. A preliminary sample of eight prosthesis users and eight therapists tried out the VRE and subsequently filled out a 7-item numeric rating scale questionnaire. Prosthesis users were not very satisfied with the control in the VRE, mainly due to the delay between the muscle impulse and the prosthesis movement. Therefore, they felt that the control did not correspond to a daily life experience with their own prosthesis. End-users agreed that sparse visual feedback was used and, then, only when needed. Negative feedback was however present in the game, which was only noted by therapists. Prosthesis users and therapists agreed with most items of the questionnaire, indicating that they experienced most factors of the framework in the VRE. However, the observed differences in experiences between end-users showed that both prosthesis users and therapists should be involved in the assessment of training tools.

INTRODUCTION

People with a limb deficiency can use a prosthesis to assist them in daily life tasks. From the majority of the available active prostheses, the myo-electric prostheses, which are controlled by the muscle signals of the user, are the most difficult to learn to control. Due to the lack of function and comfort, they are often abandoned [1]. Training can help a user to learn how to successfully control the prosthesis, however this is time consuming and often experienced as dull [2]. New ways of training are emerging due to the use of virtual reality environments (VRE), where a person can immerse themselves in a digital environment. VREs provide multiple advantages, such as adaptable environments, multiple possibilities in exercises, different types of feedback and the ability to include game elements in the training [3,4]. These can all help to improve the learning experience for prosthesis users.

Previous research from our group investigated the important design characteristics of a VRE to adhere to the needs and wishes of prothesis users and therapists [5]. Using a combination of a literature review and focus groups, the important characteristics of a VRE were detailed in a framework. The framework, consisting of four main domains and 46 factors, could be used during the development of a VRE or to verify whether an existing VRE adheres to the framework. The latter was explored for the first time in this study using the barista game (The Simulation Crew, Nijmegen). The framework was rewritten as a questionnaire to investigate the opinion of the user with regards to the current system. Here, we report on the domains control and feedback, since the use of feedback in VR could benefit the learning process for prosthesis control. Our research questions were as follows: 1) can the framework be used as a questionnaire to assess an existing VRE?; 2) does the VRE of the barista game include the needs and wishes of the end-users (users and therapists) according to the VRE framework domains control and feedback?

METHODS

The study was approved by the central ethics review board of the University Medical Center Groningen (RR1147). Participants signed an informed consent before participation.

The domains control and feedback, each containing 3 subdomains and 8 factors, were investigated in this study (Figure 1, A). We rephrased the factors of the framework into statements, where participants could indicate on a numeric rating scale from 1 (strongly disagree) to 10 (strongly agree) how much they agreed with the statement. Factors which either did

not exist in the current game or were clearly available, were removed beforehand for conciseness of the questionnaire. The factors that were removed concerned co-contraction and switching commands, control for lack of weight, audio and vibration feedback, as these were not implemented in the current VRE and could therefore not be assessed. Factors regarding calibration in different arm positions, proportional control, feedback on electromyography (EMG) and force, and animation as instruction of movement were clearly evident in the VRE and therefore also removed. Descriptive data such as mean and standard deviation was reported. Due to the small sample size and explorative nature of the study, no statistics were performed.

The 7-item questionnaire was used to evaluate whether an immersive VRE, which was developed to provide myoelectric training, contained the factors of the framework. The commercially available Oculus Rift was used in combination with a Bluetooth-connected Myoband (Otto Bock Healthcare Products GmbH, Wien, Austria) containing four active electrodes (Figure 1, B). A calibration was performed in three different arm positions, where the user trained the system the muscle signals for hand-open and hand-close movements. In the VRE, the participant immersed themselves in a Mediterranean café to work as a barista, where coffee orders had to be completed (The Simulation Crew, Nijmegen). The task was to grasp the correct cup with the prosthetic hand, place it under the coffee machine and press the correct button for the right drink (Figure 1, B). The cup had to be placed on the serving tray, subsequently. Higher levels resulted in more difficult game play, such as breakable cups that had to be grasped using proportional control or cups placed on high and low shelves. Participants played for approximately 15 to 30 minutes, depending on how fast they could complete the orders. In the game, feedback was provided on the force and EMG signal.

A

Control

Goal of the training regarding the control
- Training of co-contraction/switching commands *
- Training of single muscle activation
- Train separability and consistency of patterns

EMG
- Control for the lack of prosthesis weight in VR *
- Include proportional control *
- Prevent lagging of EMG signals

Calibration
- Calibrate in different arm positions *
- Difficulty of the control comparable to daily life

Feedback

The way feedback is provided to the user
- Mainly visual feedback, but used sparsely
- Audio feedback for specific actions *
- Vibration feedback for specific actions *

Topic on which feedback is provided
- EMG signal *
- Force production *

Type and moment of feedback
- Solely positive feedback
- Extra feedback during learning phase, later only when needed
- Animations as instruction of the movement *

B

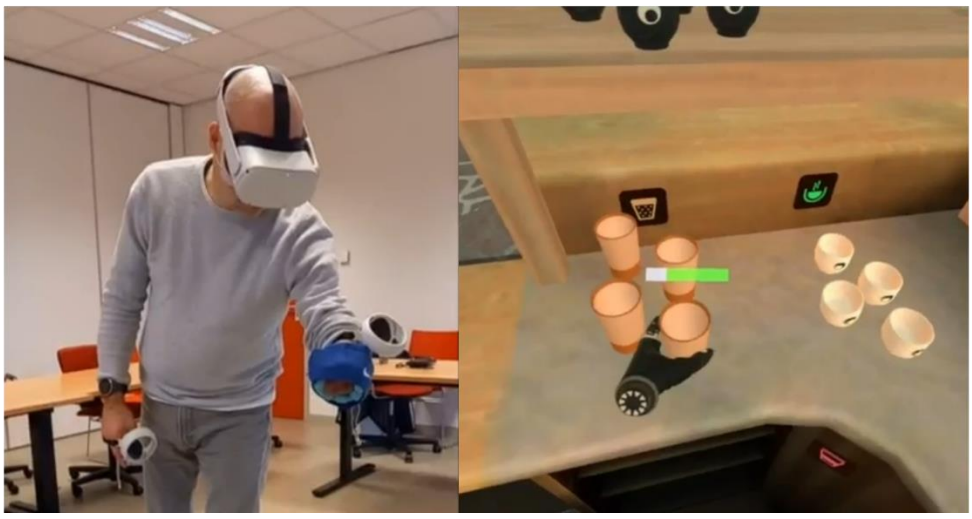

Figure 1: A: The domains ‘Control’ and ‘Feedback’ of the framework, which was developed based on a narrative review and focus groups with prosthesis users and therapists. Factors marked with an asterisk were not included in the questionnaire since they either did not exist of were clearly available in the VRE. B: the setup of a prosthesis user wearing the VR headset and Myoband around the stump (left photo). The task is to grasp cups to fulfil the coffee order (right photo).

RESULTS

A preliminary sample of eight prosthesis users (six males and two females, mean age 61.8 years) and eight therapists (one male and seven females, mean age 49.6 years) participated in the VR experience. The majority of the prosthesis users had a congenital deficit (N=5), the others (N=3) had an amputation due to trauma. Most of the participants had a previous VR experience (N=10).

Prosthesis users seemed to rate the control in the VRE lower than therapists, providing a mean score (±standard deviation) of all questions of 6.5±3.4 and 7.4±2.5, respectively (Figure 2). This was mainly visible in the items "lag between EMG and prosthesis movement" (prosthesis users=5.4±4.0; therapists=7.3±2.7) and "comparability to daily life prosthesis use" (prosthesis users=4.9±3.8; therapists=6.6±2.6). For the "control of a specific muscle" (prosthesis users=7.8±2.7; therapists=8.1±1.7) and "the training of separable muscle patterns" (prosthesis users=8±2.4; therapists=7.8±2.9), end-users generally agreed with these statements.

Prosthesis users provided a higher score on the feedback items (mean score of all questions=8.0±2.2) compared to therapists (mean score of all questions=7.0±2.4). Therapists noted that not only positive feedback was provided, since the waitress would respond displeased if participants did not prepare the right order (prosthesis users=7.9±2.4; therapists=5.3±2.7). All end-users seemed to agree that "the visual feedback was not too much" (prosthesis users=8.4±2.4; therapists=8.0±1.8) and that "extra feedback during the learning phase" (prosthesis users=7.6±2.1; therapists=7.9±2.0) were present.

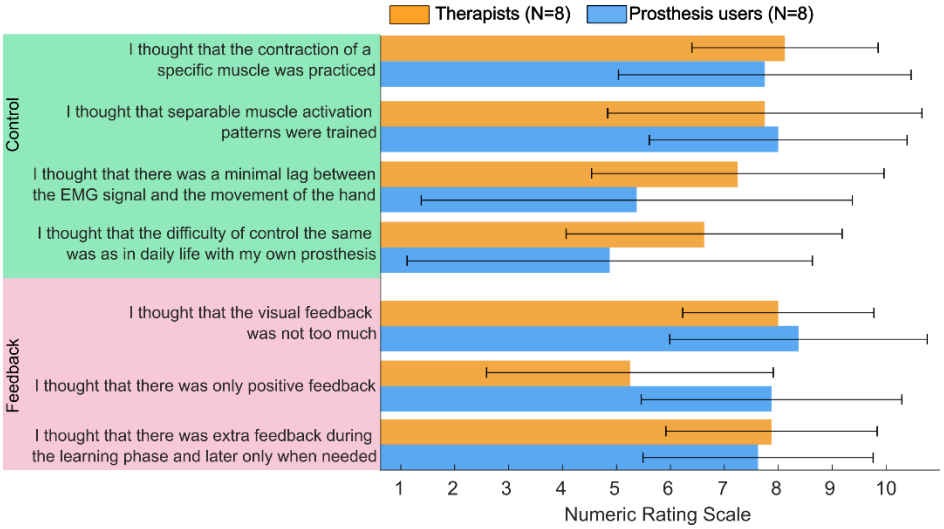

Figure 2: Questionnaire related to the framework of important design characteristics that should be part of a VRE to train prosthesis control, and the ratings of the therapists (orange) and prosthesis users (blue). Mean scores are represented by the bar graphs, whiskers represent the standard deviation

DISCUSSION

We investigated whether a previously developed framework describing the important design characteristics of a VRE for prosthesis control training could be used as a questionnaire and to investigate whether an existing VRE adhered to the framework. Results showed that the questionnaire could be used to assess adherence to the framework, although there were some limitations (see limitations). The prosthesis users and therapists agreed with most statements in the questionnaire, indicating that most factors were present in the barista game. We also noted that that the experiences of prosthesis users and therapists sometimes seemed to differ. Prosthesis users addressed that the control was often more difficult compared to their daily life prosthesis, in most cases this was caused by the delay between muscle activation and prosthesis movement. Note the large standard deviation in these questions, which indicates that some users agreed with the statements while others strongly disagreed. Furthermore, therapists might be less capable to judge whether control in VR is comparable to daily life, due to their lack of prosthesis experience.

Prosthesis users seemed to provide a higher score compared to therapists on the statement that "there was only positive feedback", a possible explanation is the unfamiliar term of positive feedback to patients. In the game, negative feedback would mean that the waitress would respond displeased with an incorrect order or when a glass was dropped, it shattered on the ground. These feedback visuals were negative, in the sense that they highlight something that the user did wrong.

According to the data logs, prosthesis users did encounter these experiences, but they were not perceived as negative. It is therefore questionable whether negative feedback should be avoided, as is mostly advised in learning studies [6]. The different experiences between prosthesis users and therapists shows that both types of end-users should be involved in the usability studies of training tools, since each group pays attention to different aspects of the system.

Limitations: The framework factors from previous research were translated into a questionnaire. Some questions could be interpreted in different ways. For example, the statement “control of the prosthesis is the same as daily life”. A low score on this item could mean that prosthesis control was either easier or harder compared to their own prothesis. Therefore, the information in the questionnaire provides limited information. The formulation of the questionnaire should be formally validated to be more informative. Another limitation is that in this study we chose not to rate all the items from the framework, for the conciseness of the questionnaire. In the future, all items could be rated, leading to more information on how end-users experienced the VRE and where improvements can be made in the design. Future research could use the framework as a questionnaire to assess VRE, however, the factors that are incorporated and the framing of the questions are important to reconsider.

Conclusion: Prosthesis users and therapists agreed with most items in the questionnaire, indicating that they experienced most factors of the framework in the VRE.

ACKNOWLEDGEMENTS

We thank the following rehabilitation centres for their participation in this research: De Hoogstraat Revalidatie Utrecht, Libra Eindhoven, Rijndam Revalidatie Rotterdam and Revalidatiecentrum Roessingh Enschede.

REFERENCES

[1] Smail LC, Neal C, Wilkins C, Packham TL. Comfort and function remain key factors in upper limb prosthetic abandonment: findings of a scoping review. Disabil Rehabil Assist Technol 2021;16:821–30. https://doi.org/10.1080/17483107.2020.1738567.

[2] Franzke AW, Kristoffersen MB, Bongers RM, Murgia A, Pobatschnig B, Unglaube F, et al. Users’ and therapists’ perceptions of myoelectric multi-function upper limb prostheses with conventional and pattern recognition control. PLoS One 2019;14:1–13. https://doi.org/10.1371/journal.pone.0220899.

[3] Hashim NA, Abd Razak NA, Shanmuganathan T, Jaladin RA, Gholizadeh H, Abu Osman NA. On the use of virtual reality for individuals with upper limb loss: a systematic scoping review. Eur J Phys Rehabil Med 2022;58:612–20. https://doi.org/10.23736/S1973-9087.22.06794-6.

[4] Papaleo ED, D’Alonzo M, Fiori F, Piombino V, Falato E, Pilato F, et al. Integration of proprioception in upper limb prostheses through non-invasive strategies: a review. J Neuroeng Rehabil 2023;20:1–22. https://doi.org/10.1186/s12984-023-01242-4.

[5] Rozevink SG, Murgia A, Bongers R, van der Sluis C. Users ’ and therapists ’ perspectives on the design of a virtual reality environment to train prosthesis control : a narrative review and focus group study (preprint). Res Sq 2023:1–26. https://doi.org/10.21203/rs.3.rs-3675534/v1.

[6] Wulf G, Lewthwaite R. Optimizing performance through intrinsic motivation and attention for learning: The OPTIMAL theory of motor learning. Psychon Bull Rev 2016;23:1382–414. https://doi.org/10.3758/s13423-015-0999-9.

EXPLORING USER COMPLIANCE IN THE TRAINING OF REGRESSION-BASED MYOELECTRIC CONTROL

Christian Morrell[1], Evan Campbell[1], and Erik Scheme[1]

[1]*Institute of Biomedical Engineering, University of New Brunswick, Canada*

ABSTRACT

Regression-based myoelectric control is promising because it could enable simultaneous independent control over multiple degrees of freedom. However, limitations in the robustness of online control and the added complexity of acquiring labelled training data have hindered its adoption. The scattered mix of prompting methods, visualization styles, and speeds used in the literature to collect labelled regression training data has obfuscated how these different prompting styles may affect the performance of regression-based myoelectric control. This work thus begins to investigate the potential effects that different visualizations may have on user behaviours and the quality of acquired training data for myoelectric control. Two distinct behaviours, referred to as *all or nothing* and *anticipation*, emerged when comparing the training data of three different prompting styles. Subsequently, 6 subjects were coached to emulate each of these behaviours during training and then completed a 10-trial Fitts' Law to assess the online usability of two different support vector regression (SVR) models. Results show that both user behaviours and the choice of regression model can have profound impacts on the usability of regression-based myoelectric control. Notably, real-time performance was severely degraded by the *anticipation* behaviour when using a linear kernel SVR, resulting in a 70% reduction in completion rate. These preliminary results motivate future work into how best to prompt users when training for supervised regression-based myoelectric control.

INTRODUCTION

Despite high levels of abandonment, many commercial upper-limb prostheses still employ decades-old control strategies [1]. Sophisticated coordination between the hand and wrist is needed for advanced tasks, yet even current prosthetic devices rely on sequential control schemes [1]. Regression-based control offers the potential of simultaneous independent control, but questions about the robustness of online regression control (e.g., challenges with quiescence, drift, susceptibility to confounds) and the increased complexity of acquiring labelled training data remain [1, 2].

A variety of training protocols have been used to acquire training data for regression-based systems, ranging from the use of force transducers, to limb kinematics tracking, to purely visual prompting styles [2–5]. Although the use of force and position mappings have been effective [3], they are not viable for users with upper limb differences, leading researchers to focus on visual prompts [2]. Unlike in classification tasks, however, the use of visual prompting in regression not only assumes that the user is performing the correct contraction, but also that they are tracking the amplitude of the degree of freedom closely over the entire progression. Given the likelihood of deviations in compliance and timing, however, this may not always be the case, potentially resulting in a discrepancy between the elicited contractions and the ground truth labels used to train the model. Furthermore, a variety of prompting methods, visualization styles, and speeds have been used in the literature, without clarity about how they may affect user behaviours or model training, or what role they may have on the online usability of regression-based myoelectric control [2, 4]. Consequently, this work describes an early exploration of the potential differences in user behaviours based on changes in prompting for regression-based myoelectric control.

METHODS

Data collection and preparation

Eight subjects participated in this exploratory pilot work (5 male, 3 female, 22 - 31 years old) as approved by the University of New Brunswick's Research Ethics Board (REB 2022-122). EMG data were collected from the forearm using the EMaGer cuff, a 64-channel high-density electromyography (HD-EMG) device comprised of a stretchable 4 x 16 array of EMG electrodes [6]. LibEMG, an open-source Python library for processing EMG, was used to facilitate data streaming, the creation of visual prompts, and real-time myoelectric control [7]. EMG data were bandpass filtered from 20-450 Hz to remove motion artefacts and notch filtered at 60, 120, 240, and 360 Hz to remove power-line interference. The filtered signals were then normalized to unit variance and zero mean to improve visualizations and standardize data for model training. The EMG time series were then enframed using 250ms windows with 50ms overlap, from which the Hudgins' Time Domain feature set were extracted [8].

Prompting styles

Three different prompting approaches were explored, based on their prevalence in the literature [4, 9, 10] and as distinct presentation styles. Contractions corresponding to two degrees of freedom (DOF), hand open/close and forearm

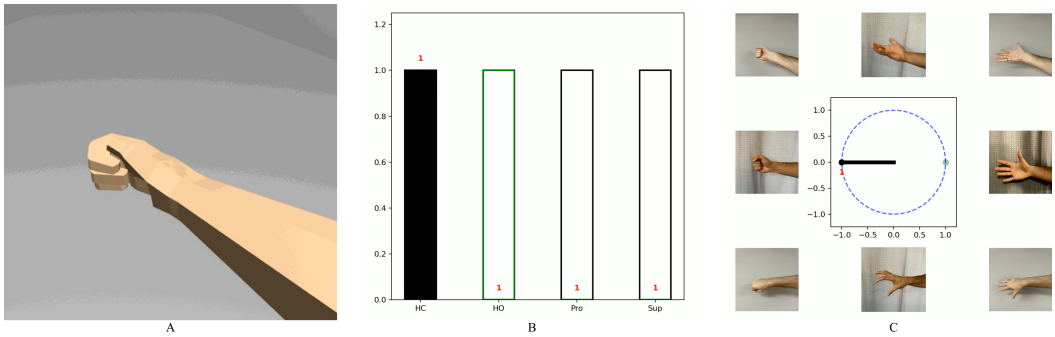

Fig. 1: Example of the Anthropomorphic (A), Bar plot (B), and Cartesian (C) visualizations used for prompting the user during training. For the Bar plot and Cartesian visualizations, countdowns were shown in red during periods of constant amplitude and the next destination of the target was shown in green.

pro/supination, were prompted as shown in Fig. 1. Briefly, the anthropomorphic approach (A) involved following a moving virtual limb, displayed from the user's perspective [10]. The bar plot (B) displayed the desired activation level and direction of a given direction DOF (similar to the prompting of classification based approaches, but with a target intensity [9]). Finally, the Cartesian approach (C) denoted the desired contraction and intensity via mappings to spatial locations, as often done in Fitts' Law testing [4].

Five subjects participated in this portion of the study, completing 5 repetitions of each DOF for each prompting style. Each repetition comprised of the sequence: no motion, to DOF -ve direction (e.g., pronation), to DOF +ve direction (e.g., supination), to no motion, to DOF +ve direction, to DOF -ve direction, to no motion. Every movement segment involved a ramp up (2 seconds), steady state (2 seconds), and a ramp down (2 seconds) and periods of no motion lasted 3 seconds. The order of visualizations was randomized for each participant. In all cases, users were asked to map the intensity of their contractions to the corresponding position of the prompt.

User behaviours

After analyzing the data from the prompting styles described above, a second pilot study was performed. Six subjects completed a training session emulating specific behaviours that had been observed consistently across subjects (anecdotally), followed by an online usability study. The goal of this portion was therefore not to evaluate the specific prompting styles, but to assess the impact of observed behaviours on the usability of the trained regression models. Subjects were coached to elicit two distinct behaviours; *all or nothing* and *anticipation*(explained below in *Results - Prompting styles*), and a baseline case, where they were asked to follow the prompt to the best of their ability. The order of these three cases was randomized for each participant, and 5 repetitions of each DOF were collected in each case. A Cartesian-style prompt was used in this phase due to its prevalence in the literature and similarity to the downstream task [4]. After each round of training, participants performed a 10-trial Fitts' Law-style target acquisition test, as provided by LibEMG [7], to assess the usability of the resulting regression model. To probe the impact of model linearity, three subjects used a support vector regressor (SVR) with a linear kernel, whereas the other three used a SVR with a non-linear radial basis function (RBF) kernel. A *deadzone* threshold of 0.25 was used for both models to reduce inadvertent activation (i.e., predictions with magnitude less than 0.25 did not elicit movement of the cursor) [2]. Online usability was assessed using effective throughput, path efficiency, and the number of target overshoots [11]).

RESULTS

Prompting styles

Fig. 2 shows a representation of how users reacted to the different prompting styles, using trends in the observed mean absolute value (MAV) of their EMG signals. The median MAV across channels was used to approximate the strength of the contraction for a given window and the median value across subjects was used to observe the consistency of user behaviours.

These behaviours were consistent enough across subjects that two distinct, anomalous behaviours emerged. The first behaviour, here called anticipation, is exemplified by a preemptive increase in MAV prior to reaching the 0 point of the Cartesian visualization in Fig. 2, and as later simulated in Fig. 3. The anticipation behaviour occurs when the user transitions from one end of the DOF to the other too early, meaning that they begin ramping up the other end of the DOF (e.g., hand close) while the prompt (and thus labels) indicate they should be still be ramping down from the previous end of the DOF (e.g., hand open). This occurred more often when the participants travelled from one extreme of the DOF to the other than when beginning from the rest position. This mismatch between behaviour and prompt, particularly around the rest position, may cause model confusion at low amplitudes and thus problems with quiescence.

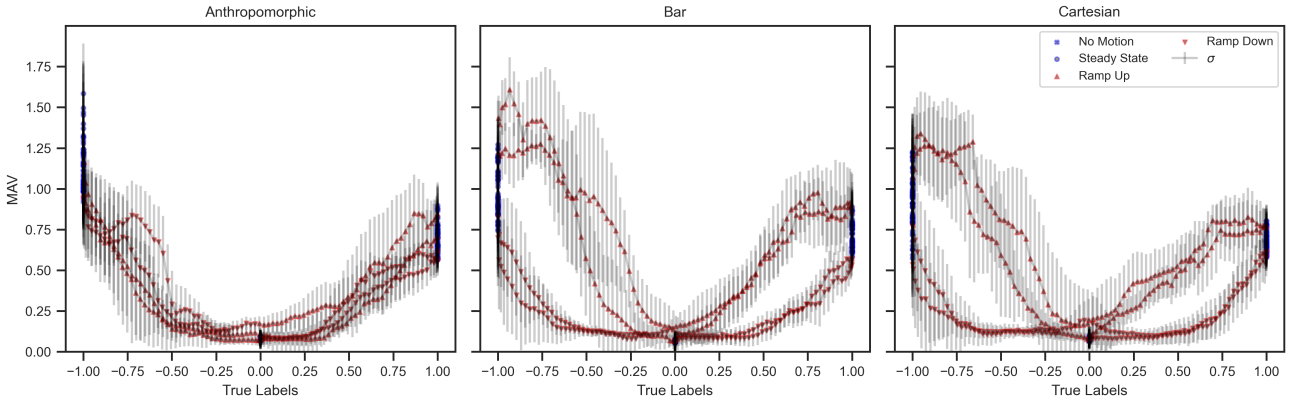

Fig. 2: Scatter plot of the strength of elicited contraction across subjects as prompting varied for each visualization style during collection of the hand open / close DOF. Each point represents the median MAV across channels and subjects for a single window. The segment of the movement (e.g., ramp up) is determined based on the ground truth labels at that window.

The second behaviour, here called *all or nothing*, is exemplified in Fig. 2 in the Anthromorphic and Bar visualizations, and later simulated in Fig. 3. From the Anthromorphic case, we see a wide band around 0 where there is no real activation. In the Bar plot case, we see cases where the users goes from rest very quickly to high levels of activation. These combined behaviours represent a lack of gradual modulation from low to high, or high to low. The all or nothing behaviour, in contrast to linearly increasing or decreasing prompts, may lead to poor model fitting and problems with proportional control.

User behaviours

Based on the previous observations, we explored how these two distinct behaviours may affect the training and usability of the resulting models. To emphasize their effect in this small pilot set, subjects were coached to elicit the identified behaviours, as shown in Fig. 3. The emulated behaviours exhibited by participants were purposely exaggerated to observe the potential effects of these behaviours on online performance in extreme cases. The MAV trends shown in Fig. 3 highlight these behaviours, described previously as observed more subtly in *Prompting styles*, including a wider deadzone during the all or nothing emulated behaviour and early ramping up during the anticipation emulated behaviour.

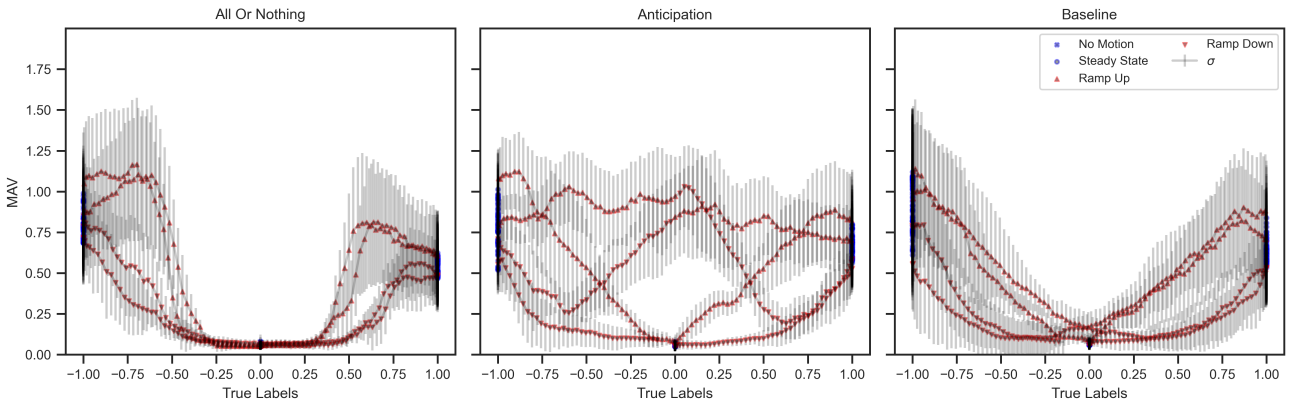

Fig. 3: Scatter plot of the simulated (and emphasized) behaviours illustrating the strength of contraction across subjects as prompting varied for each observed behaviour during data collection along the hand open / close DOF.

The results of the Fitts' Law testing for each of the behaviours are shown in Fig. 4. The anticipation behaviour was found to destroy the performance of the linear SVR model, as indicated by the fact that 24 of the 30 total trials could not be completed before the 30 second timeout. Because, the other performance metrics reported in Fig. 4 cannot be computed unless a trial is completed, this model cannot be fairly compared to those of the other behaviours / models. The linear SVR model also degraded when facing the all or nothing behaviour, though not nearly as badly. Contrarily, the non-linear RBF SVR appeared to be quite resilient to the anticipation and all or nothing behaviours.

DISCUSSION

This work describes the early pilot results of an ongoing study. Despite modest numbers of subjects, empirical evidence of the impact of prompting style on contraction behaviours was found. Anticipatory behaviours were seen that caused

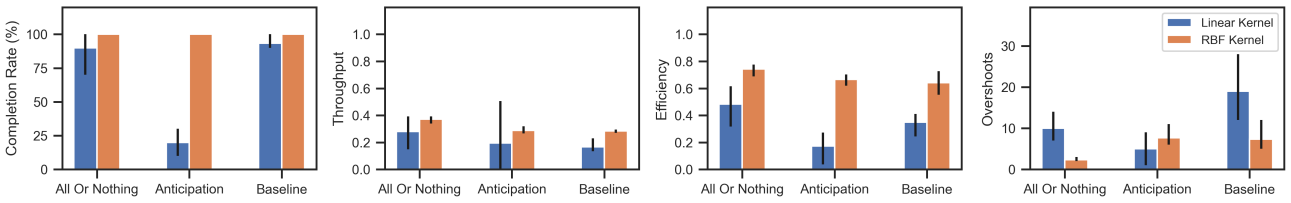

Fig. 4: Comparison of usability metrics captured via Fitts' Law test across user behaviours. Each bar represents the mean across subjects, error bars indicate the minimum and maximum values across subjects.

misalignment between the EMG and the given prompts. The observed all or nothing behaviours suggest user difficulties in slowly modulating DOF-specific contraction intensities in alignment with the prompts. The three prompting styles also tended to elicit different behaviours. For example, the clear spatial mapping of the Cartesian case, combined with the green "next destination" hint, caused more of the anticipatory behaviour. The limb position information implied by the Anthropomorphic style may have encouraged more of a position control behaviour leading to the all or nothing patterns of EMG. However, in addition to the impact of different prompting styles, many other factors could influence user behaviours, such as the speed at which contractions are prompted, the use of "next motion" hints, and the potential use of real-time feedback to help users better align. Although these results should not be taken as conclusive, they motivate further work on how to best to prompt users when training for regression-based myoelectric control.

The broader goal of this work is to explore the quality of training data and the impact that varying degrees of compliance has on regression performance. To wit, the behaviours that emerged from the prompting investigation led to notable differences in control when evaluated in an online Fitts-style test. Based on these preliminary results, some interesting observations emerged. The non-linear RBF SVR yielded better results than the linear model in general, and may thus be a more resilient solution in accounting for imperfection in training. The large number of timeouts of the linear SVR model with anticipation support this, but also highlight the interplay between model and behaviour. Paradoxically, it appears that the all or nothing behaviour actually led to better usability than the baseline behaviours. It was anticipated that this behaviour may result in a "skating" behaviour wherein the user is unable to stop. However, it is worth noting that a 25% activation threshold was employed across all models in this work, below which the controller would not move. While this was determined empirically to be necessary for usability (as in previous studies [2]), this may have masked the effects of the all or nothing behaviours.

Finally, it is important to acknowledge that this work represents only an initial examination of these effects. The user behaviours were emulated and exaggerated to better evaluated their effects for the small sample size. It also appears that user behaviours may have model-dependent impacts on usability. Consequently, this work serves mostly to highlight the potential implications of training compliance on model development, robustness, and usability, and warrants further examination.

REFERENCES

[1] A. D. Roche, H. Rehbaum, D. Farina, Oskar, and C. Aszmann, "Prosthetic Myoelectric Control Strategies: A Clinical Perspective," *Current Surgery Reports 2014 2:3*, vol. 2, no. 3, pp. 1–11, jan 2014.

[2] A. Ameri, E. N. Kamavuako, E. J. Scheme, K. B. Englehart, and P. A. Parker, "Support vector regression for improved real-time, simultaneous myoelectric control," *IEEE Transactions on Neural Systems and Rehabilitation Engineering*, vol. 22, no. 6, pp. 1198–1209, nov 2014.

[3] A. Ameri, E. J. Scheme, E. N. Kamavuako, K. B. Englehart, and P. A. Parker, "Real-time, simultaneous myoelectric control using force and position-based training paradigms," *IEEE Transactions on Biomedical Engineering*, vol. 61, pp. 279–287, 2 2014.

[4] J. M. Hahne, F. Bießmann, N. Jiang, H. Rehbaum, D. Farina, F. C. Meinecke, K. R. Muller, and L. C. Parra, "Linear and nonlinear regression techniques for simultaneous and proportional myoelectric control," *IEEE Transactions on Neural Systems and Rehabilitation Engineering*, vol. 22, no. 2, pp. 269–279, 2014.

[5] G. Hajian, E. Campbell, M. Ansari, E. Morin, A. Etemad, K. Englehart, and E. Scheme, "Generalizing upper limb force modeling with transfer learning: A multimodal approach using EMG and IMU for new users and conditions," *IEEE Transactions on Neural Systems and Rehabilitation Engineering*, 2024.

[6] F. Chamberland, É. Buteau, S. Tam, E. Campbell, A. Mortazavi, E. Scheme, P. Fortier, M. Boukadoum, A. Campeau-Lecours, and B. Gosselin, "Novel wearable hd-emg sensor with shift-robust gesture recognition using deep learning," *IEEE Transactions on Biomedical Circuits and Systems*, 2023.

[7] E. Eddy, E. Campbell, A. Phinyomark, S. Bateman, and E. Scheme, "LibEMG: An Open Source Library to Facilitate the Exploration of Myoelectric Control," *IEEE Access*, vol. 11, pp. 87 380–87 397, 2023.

[8] B. Hudgins, P. Parker, and R. N. Scott, "A new strategy for multifunction myoelectric control," *IEEE Transactions on Biomedical Engineering*, vol. 40, pp. 82–94, 1993, this is the reference for the HTD feature set.

[9] M. Barsotti, S. Dupan, I. Vujaklija, S. Došen, A. Frisoli, and D. Farina, "Online finger control using high-density EMG and minimal training data for robotic applications," *IEEE Robotics and Automation Letters*, vol. 4, pp. 217–223, 4 2019.

[10] A. M. Simon, L. J. Hargrove, B. A. Lock, and T. A. Kuiken, "The target achievement control test: Evaluating real-time myoelectric pattern recognition control of a multifunctional upper-limb prosthesis," *Journal of rehabilitation research and development*, vol. 48, p. 619, 2011.

[11] E. J. Scheme and K. B. Englehart, "Validation of a selective ensemble-based classification scheme for myoelectric control using a three-dimensional Fitts' law test," *IEEE Transactions on Neural Systems and Rehabilitation Engineering*, vol. 21, pp. 616–623, 2013.

LIMITATIONS TO THE SENSE OF AGENCY OVER MYOELECTRIC CONTROLLED MOVEMENTS

Sarah Mehigan[1], Sigrid Dupan[2]

[1] *School of Electrical and Electronic Engineering, University College Dublin, Ireland*

[2] *School of Public Health, Physiotherapy and Sport Science, University College Dublin, Ireland*

ABSTRACT

Prosthetic embodiment, the extent to which individuals perceive their prosthesis as an integral part of their body, is associated with lower prosthetic abandonment and is seen as a measure of how satisfied users are with their device. While there is no gold standard method to quantify embodiment, measurement techniques from the field of Human Computer Interfaces might allow us to quantify embodiment, and allow us to parse where reductions in embodiment originate. As muscle signals have a higher variance than movement patterns, it is possible that this increase in variance lowers people's sense of ownership over their actions when they use myoelectric control. Sense of agency is a measure that refers to the experience of feeling in control of one's actions, and the outcome those actions have on the environment. We compared the sense of agency over myoelectric and joystick controlled movements of 10 participants through a tracking task. While performing the tracking task, different levels of noise were added to the control signal before feedback was given to the participants, allowing us to impose different levels of control. We found that people rated their sense of agency over myoelectric controlled movements significantly lower than over joystick controlled movements ($p < 0.001$), and that this decrease was not only dependent on lower accuracies during the tracking task. These results suggest there might be an upper limit to the sense of agency over myoelectric controlled movements.

INTRODUCTION

Upper limb prosthetics aim to restore functionality and improve the quality of life of their users. One of the aspects of prosthetics that has been studied is 'embodiment', the extent to which individuals perceive their prosthesis as an integral part of their body. Embodiment is important as poor body image due to amputation is correlated with increased depression, and decreased life satisfaction, quality of life, activity and psychological adjustment [1]. Although embodiment serves as a metric for user acceptance and experience, no gold standard method has been established to quantify embodiment, with most studies relying on questionnaires [2-3]. The field of human computer interfaces could provide quantitative measures with a neuronal basis to study embodiment [4].

Sense of agency (SoA) refers to the experience of controlling one's actions, and through them, events in the outside world [5]. This sense of agency can be broken when your intended movement does not line up with either the movement of your body, or the outcome that you perceive. As a result, changes in how your body controls movement and changes to how it senses itself and the environment impact the SoA. To date, it is not clear if movements performed through myoelectric control can lead to the same SoA as those performed by people without limb difference. When performing goal-oriented movements, such as picking up an object, our brain and bodies will perform these movements in such a way that it minimises variance in the movement, and therefore error [6]. One of the strategies used to reduce variance is that movements will be controlled by more muscles than strictly necessary [6]. Not only will antagonists be activated to increase stiffness, and therefore lower variance, but agonist activity will be spread over multiple muscles due to signal dependent noise [6]. In essence, these strategies are adopted as the activity in our muscles is more noisy than the activity in our movement. As myoelectric control decodes movement from muscle activity, it is possible that it inherits some of that noisiness despite the signal processing filtering out most of the noise. If that is the case, then intended movements will not line up with executed movements more often, and lead to a reduction in SoA, representing a limitation to achieve high SoA and therefore embodiment.

In this study, we compared the SoA of joystick and myoelectric controlled movements. To investigate how sensitive the SoA is, we added noise to people's control signals before presenting them back to them.

METHODS

Participants

Ten participants (5 male, 5 female) without limb difference and free from neurological or motor disorders were recruited. The study was approved by the local ethics committee at University College Dublin (ref: LS-22-46-Dupan), and participants provided written informed consent prior to the start of the experiment.

Experimental setup

Participants performed a tracking movement on the screen through joystick control and 2-channel myoelectric control. Two EMG channels were placed on the extensor carpi radialis and the flexor carpi radialis of the right hand of participants. Signals were acquired using Trigno wireless EMG system (Delsys Inc, Natick, MA, USA), and signals were processed in real time using the AxoPy Python library. Muscle signals were sampled at 2000Hz, and updates were sent to the computer every 50ms. A fourth-order Butterworth bandpass filter (10-500Hz) was applied, after which the muscle signals were smoothed using the mean absolute value with a window length of 750ms. EMG channels were calibrated for each participant:

$$\hat{y} = (y - y_r) / (y_c - y_r)$$

where $\hat{y}$ is the normalized muscle activity, y the MAV, y_r the activity when the participant is at rest, and y_c represents a comfortable contraction. Participants controlled the position of a cursor on the screen, which was determined by subtracting $\hat{y}$ of the flexor muscle from $\hat{y}$ of the extensor muscle.

When participants controlled the cursor on the screen through the joystick (Flightstick pro, CH Products, Vista, California, USA), the position of the joystick was sampled every 50ms. The position of the joystick was calibrated so that moving the joystick fully to the right or left resulted in doubling the maximum necessary deviation on the screen.

Experimental design

Participants were tasked to perform a tracking task on the screen. A sinusoid function represented the goal line, and moved up over the screen, while the participant's cursor could only move in the left-right direction. Trials lasted 8s, and the sinusoid had a period of 4s and amplitude normalized to 1 (see the dotted black line in Fig. 1a). Participants performed 4 blocks of 20 trials, with blocks alternating between myoelectric and joystick control. Prior to starting the experiment, participants completed 4 familiarisation trials for each control method. If they had trouble completing the myoelectric controlled trials, then the calibration of the EMG channels was repeated.

Different levels of noise were added to the control signal of the participants. Noise signals were sinusoids with a period of 4s and amplitudes of 0, 0.1, 0.2 or 0.3 (see Fig. 1a). Levels of noise were randomised over the trials. Noise started 1s into the trial and ended at 7s, where the start and end of the noise were equal to 0, resulting in a phase shift of $\pi/2$ between the noise and the goal line. The noise was added to the control signal (both myoelctric and joystick control) before the data was presented on the screen. The choice of starting and ending the noise at 0 ensured that participants did not realise the visual feedback of the cursor did not represent their actual movement. Fig. 1b and 1c represent joystick and myoelectric trials where the dotted black line is the goal line, and the solid black line the feedback participants received. This feedback is a combination of their actual control (solid blue line) and the noise (dotted blue line).

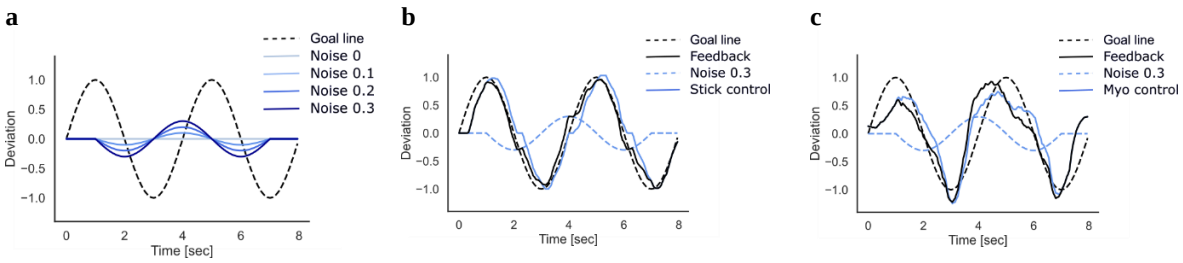

Figure 1. (a) Different noise levels added to the control signal. (b) Representative example of a trial for joystick control. (c) Representative example of a trial for myoelectric control.

After each trial, participants were asked to rate their SoA over that trial on a Likert scale from 1-9. Participants were reminded that this score should represent how much they felt in control of the cursor on the screen, not how well they performed the trial.

Analysis

The outcome measures of this study were participants' SoA and score. The score was defined as *1 – MAE*, with MAE the mean absolute error between the goal line and the visual feedback. We performed a 2-way ANOVA to investigate the effect of noise levels and control modality on SoA and scores, and post-hoc Tukey tests if any significance was found at group level.

RESULTS

The 2-way ANOVA presented in Fig. 2a tested the effect of the noise levels and control modalities on SoA. The test showed no interaction effect between the noise levels and control modalities ($p = 0.22$), but significant differences for the noise levels ($p < 0.001$) and control modalities ($p < 0.001$). Pairwise post-hoc Tukey tests showed that the SoA was significantly different for noise levels 0 vs 0.3 ($p = 0.001$), 0.1 vs 0.3 ($p = 0.001$) and 0.2 vs 0.3 ($p = 0.01$). These tests show that participants rated their SoA of myoelectric controlled movements lower than those controlled by the joystick. Additionally, participants gave lower scores to trials with high noise levels, even if conversations after the experiment made clear that none of them realised the feedback they received had additional noise added to it.

A similar story was present for the effect of the noise levels and control modalities on the score (Fig. 2b). The 2-way ANOVA showed no interaction ($p = 0.4$), and the mains effects showed significant differences in the score based on the noise levels ($p = 0.001$) and control modality ($p < 0.001$). Post-hoc Tukey tests showed that the only significant difference in score was between noise levels 0 and 0.3 ($p = 0.04$). This shows that participants were able to account for the noise that was added during the trials, and adjusted their myoelectric and joystick control accordingly.

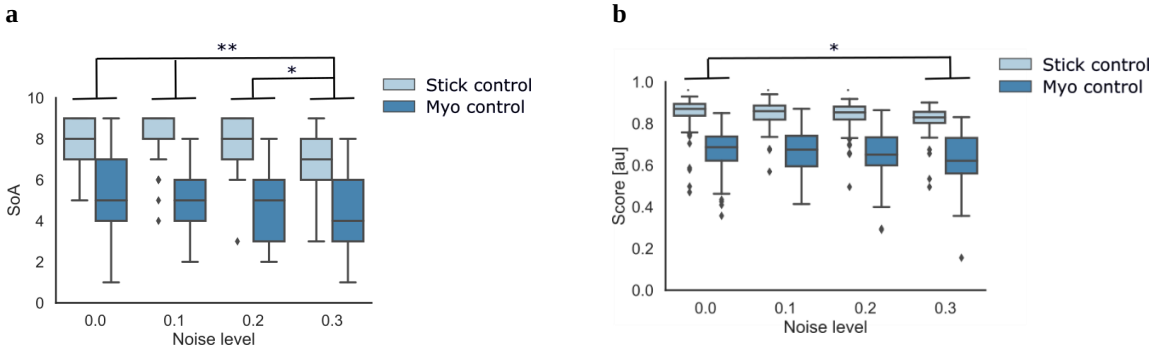

Figure 2. (a) Effect of noise levels and control modality on SoA. (b) Effect of noise levels and control modality on score.

While participants were asked to specifically rate their SoA and not how well they completed the tracking task, our results might still be biased through the difference in performance based on the control modalities. Therefore, we analysed how the SoA and control modality were related to the score, i.e. how well participants performed the task. Fig. 3a shows that decreases in reported SoA were related to decreases in score for both myoelectric control and joystick control. Two-way ANOVA analysis showed no interaction effect ($p = 0.3$), but significant differences based on reported SoA ($p < 0.001$) and control modality ($p < 0.001$). However, participants rated higher scoring joystick control trials with lower SoA than myoelectric control trials with a lower score. This suggests that participants did rate SoA and not how well they completed the tracking task. It is important to point out that the distribution of the reported SoA values was not even (Fig. 3b), so the current analysis of the relationship between reported SoA and scores should only be interpreted as a trend.

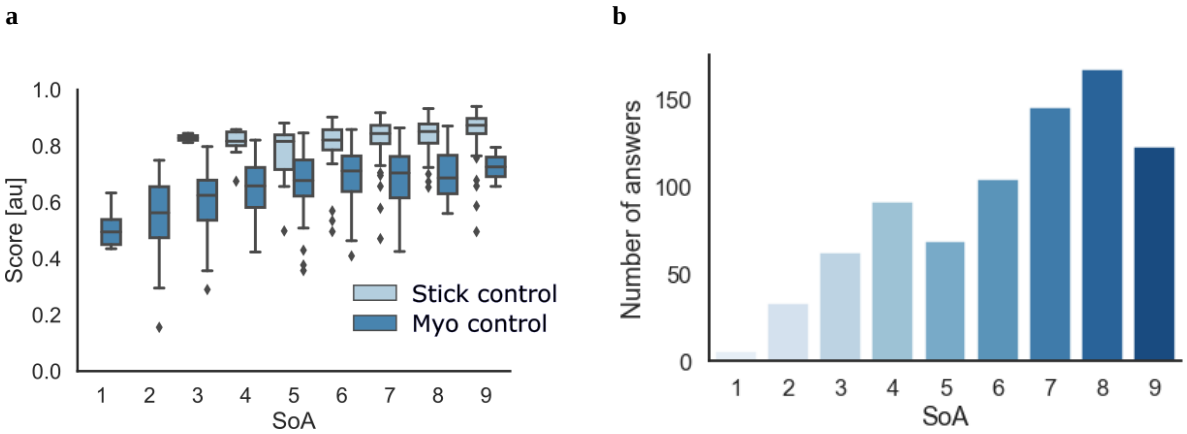

Figure 3. (a) Relationship between SoA and score for joystick and myoelectric control trials. (b) Amount of trials that received a certain value for SoA.

DISCUSSION

In this study, we investigated the SoA of movements that are controlled by joystick and myoelectric control. We found that (1) myoelectric control significantly lowered the SoA, and that (2) adding noise to the control signal before presenting it as visual feedback to the participants lowered the SoA. Participants were not aware that some trials had added noise, but the results showed they felt less in control of those trials. This was not only related to the actual performance in the trials, as trials with better performance in joystick control led to lower reported SoA than trials with myoelectric control.

This study used a tracking task to investigate SoA, a measure used previously to investigate SOA in stroke [7]. This approach allowed us to compare the SoA of joystick control and myoelectric control, and investigate how much the differences in SoA are related to tracking performance. Myoelectric control consistently led to poorer tracking performance, and people reported a significantly lower SoA over myoelectric control than joystick control. However, the reduction in SoA was not solely based on poorer performance, as joystick control trials received lower SoA ratings, even when performance was better. Therefore, it seems that myoelectric control inherently led to a lower SoA, which could be related to the difference in movement variance between joystick and myoelectric control [6]. As all participants in this study were naïve to myoelectric control, it is important to study SoA with experienced users as well. However, if the difference between joystick and myoelectric controlled movements holds, it might be an indication that there is an upper limit to the SoA one can feel over myoelectric movements. This might have repercussions on the level of embodiment people can feel over their myoelectric prostheses.

REFERENCES

[1] Rybarczyk, Bruce, and Jay Behel. "Limb loss and body image." *Psychoprosthetics*. London: Springer London, 2008. 23-31.

[2] D'Anna, Edoardo, et al. "A closed-loop hand prosthesis with simultaneous intraneural tactile and position feedback." Science Robotics 4.27 (2019).

[3] Page, David M., et al. "Motor control and sensory feedback enhance prosthesis embodiment and reduce phantom pain after long-term hand amputation." Frontiers in human neuroscience 12 (2018): 352.

[4] David, Nicole, Albert Newen, and Kai Vogeley. "The "sense of agency" and its underlying cognitive and neural mechanisms." Consciousness and cognition 17.2 (2008): 523-534.

[5] Haggard, Patrick. "Sense of agency in the human brain." Nature Reviews Neuroscience 18.4 (2017): 196-207.

[6] Diedrichsen, Jörn, Reza Shadmehr, and Richard B. Ivry. "The coordination of movement: optimal feedback control and beyond." Trends in cognitive sciences 14.1 (2010): 31-39.

[7] Miyawaki, Yu, Takeshi Otani, and Shu Morioka. "Agency judgments in post-stroke patients with sensorimotor deficits." Plos one 15.3 (2020): e0230603.

PRELIMINARY RESULTS OF A PORTABLE TAKE HOME PHANTOM LIMB PAIN MANAGEMENT SYSTEM

Kristi L. Turner[1], Andrea Ikeda[1], Zachary A. Wright[3], Blair A. Lock [3], Levi J. Hargrove [1,2]

[1] *Center for Bionic Medicine, Shirley Ryan AbilityLab, Chicago, IL, USA*
[2] *Northwestern University, Chicago, IL, USA*
[3] *Coapt, LLC, Chicago, IL, USA*

ABSTRACT

Phantom limb pain (PLP) is a common complaint in individuals with limb absence. PLP can persist chronically, necessitating effective management strategies beyond temporary pharmacological relief and invasive surgeries. Phantom motor execution, implemented through virtual reality (VR)-based therapy, has emerged as an effective alternative option to help manage PLP. This paper presents preliminary findings of an ongoing large-scale clinical study including individuals with upper or lower limb absence evaluating the effectiveness of a portable device for at-home PLP management as an accessible solution for VR-based therapy.

INTRODUCTION

Individuals with upper or lower limb absence often suffer from pain [1] that can severely impact their daily activities. This includes not only residual limb pain (RLP) but also phantom limb pain (PLP), which is prevalent following amputation [2]. PLP symptoms can start immediately post-amputation and frequently persist as a chronic problem throughout recovery. Classified as neuropathic pain, PLP typically leads to treatments that are pharmacological in nature, offering only temporary relief. While invasive methods or surgeries can provide some relief, they are generally considered only after less invasive options have failed [3]. There's a growing need for alternative PLP management strategies for individuals with limb loss.

Non-invasive treatments like motor imagery and mirror therapy, which are thought to leverage the brain's ability for neuroplasticity, have been developed to reduce pain. Motor imagery involves performing movements with the intact limb while visualising the same movements with the phantom limb. Mirror therapy involves performing movements with the intact limb while attempting to execute the same movements with the phantom limb as visual feedback is provided through a mirror. Interestingly, activities that engage the muscles in the residual limb, such as those used in mirror therapy, tend to be more effective, possibly due to the activation of muscle groups [4].

Therapy is advised for those with limb loss to improve muscle strength, educate on proper muscle contractions for prosthetic control, and educate different ways to carry out activities of daily living. The extent and quality of such training and therapy significantly impact rehabilitation success. Regularly wearing and using a prosthesis has been linked to better management of PLP, although RLP and PLP can influence the duration a prosthesis is worn [5],[6]. In addition, not all individuals with limb loss choose to regularly wear a prosthesis to help engage and strengthen residual limb muscles.

Virtual reality (VR) systems using muscle signals measured from the residual limb have emerged as promising tools for PLP management. Such systems promote muscle involvement by providing real-time task and game control practice, gaining acceptance as a practical clinical therapy option [7],[8]. Despite its potential benefits, VR-based therapy has lacked widespread at-home implementation and has not been evaluated extensively on the lower limb loss population which experience a higher prevalence of PLP [9]. Here, we present preliminary findings of an ongoing clinical study evaluating the effectiveness of a portable Phantom Limb Pain Management System (PLP-MS) developed for home use by individuals with upper or lower limb loss who suffer from PLP.

METHODS

Device: The Phantom Limb Pain Management System (PLP-MS) is a device that includes (1) an adjustable cuff with electrode sensors that attach to the arm/leg and measure EMG signals from the remaining limb muscles (Figure 1a), (2) a built-in hardware module that converts the user's EMG signal patterns into game commands using pattern recognition, (3) a custom mobile software application with a range of virtual training games (Figure 1b), and (4) a secure, HIPAA-compliant cloud-based storage system that allows study personnel to access user data remotely and monitor device activity and participant compliance with the study protocol. The device can be set up according to the side (right/left) and level (below- or above-elbow and below- or above-knee) of limb loss and can choose between 4-6 motions to control during virtual gameplay. These motions include hand open/close, wrist supination/pronation and elbow flexion/extension for the upper limb and ankle inversion/eversion, ankle dorsiflexion/plantar flexion and knee flexion/extension for the lower limb. The pattern recognition controller is trained by entering EMG data for each chosen motion during a calibration that the user initiates.

Participants: Individuals with limb loss/difference of upper, lower, or multiple limbs, who self-report PLP of 4 or greater on a 0-10 scale at least twice a month are enrolled. Although the trial is ongoing, we expect to enroll up to 48 individuals to participate in the clinical trial (ClinicalTrials.gov Identifier: NCT05915065). Informed consent is obtained under the guidelines and approval of the Northwestern University IRB prior to data collection.

Protocol: The study consists of: clinician-led instruction on how to use the PLP-MS, baseline outcome measurements, an 8-week home trial with the PLP-MS, post-home trial outcome measurements (week 8), and follow up outcome measurements at weeks 16, 24, and 32. The main outcome measure is the difference in the pain rating index (PRI), which is the total of the pain items on the Short Form McGill Pain Questionnaire (SF-MPQ) between baseline and post-treatment assessments. Other outcome measures include: a Visual Analogue Scale (VAS) for pain, the Patient-Reported Outcomes Measurement Information Systems (PROMIS) tools: a numerical rating scale (NRS) for pain (Pain Intensity 1a), Pain Interference 4a, and Sleep Disturbance 4a, PEG Scale (measuring pain intensity, interference with enjoyment of life, and interference with general activity), and Patient Health Questionnaire-2 (PHQ-2). Participants work with either a registered occupational therapist or a certified prosthetist for all parts of the study including training with the PLP-MS, outcome measurements, and all subsequent follow-up sessions.

Participants are sent the PLP-MS and receive up to four training sessions remotely via a secure Zoom link or in person (if local). Participants are provided with detailed instructions on setting up the system and navigating through the mobile software application which is downloaded onto their personal or provided mobile device. Training involves providing clinical guidance on how to perform muscular contractions to train the EMG-pattern recognition algorithms for controlling a virtual limb and instruction on how to play games within the mobile app. The number of training sessions for each participant is adjusted depending on their speed of learning how to independently use the PLP-MS.

a

b

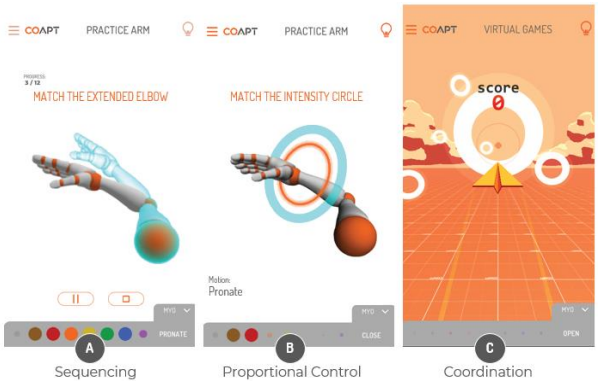

Figure 1: Phantom Limb Pain Management System a) EMG cuff that is donned on users' residual limb and includes 16 electrode sensors to record EMG (8 EMG pods – white, main pod – black) b) Screenshots of various virtual training games included in the mobile application.

After completing training and baseline outcome measurements, participants begin an eight-week home trial with the PLP-MS system, which requires a minimum total usage requirement of 1.5 hours per week and a recommended usage of 4-5 days per week for 20-40 minutes. Study personnel remotely monitor usage and device performance and contact participants as needed. Participants are also encouraged to contact study personnel for any concerns or troubleshooting throughout the home trial. Outcome measurements are collected after participants complete the home trial, and again at 16, 24, and 32 weeks to determine if changes in PLP persist.

RESULTS

To-date, thirty-one individuals with limb loss/difference of upper (below-elbow =5, above elbow = 5), lower (below-knee = 11, above-knee = 10) have been enrolled in the study. Seventeen participants have completed the 8-week home trial, post-home trial outcome measurements (week 8) and 13 participants have completed 16-week follow-up. Initial results of the primary outcome PRI indicate a decrease between Baseline (mean ± standard error; 15.2 ± 1.2) and post-home trial (week 8) (9.8 ± 0.9), indicating a potentially clinically meaningful change in PLP (suggested to be a change in PRI of at least 5 points) [10], [11] . The PRI increases towards baseline in 16-week follow-up (13.0 ± 1.5).

Secondary outcomes indicate a similar trend of improvement from Baseline to post-home trial (week 8) with two of the outcomes remaining lower than baseline at 16-week follow-up. Pain Intensity (NRS) scores show a decrease from Baseline (mean ± standard error; 5.7 ± 0.3) andpost-home trial (3.4 ± 0.5) with an increase towards baseline at week 16 (5 ± 0.5). Sleep Disturbance scores show a decrease from Baseline (mean ± standard error; 13.8 ± 0.6) and post home trial (10.2 ± 1.1) and increase almost to Baseline at week 16 post treatment (13.4 ± 1.1). PEG scores indicate a decrease from Baseline (mean ± standard error; 11.8 ± 1.0) and post home trial (5.9 ± 1.1) and increase in week 16 (8.6 ± 1.0). Pain Interference scores indicate a decrease between Baseline (mean ± standard error; 8.7 ± 0.5) and post home trial (5.6 ± 0.5) and remained lower than Baseline in week 16 (6.1 ± 0.5). This is also seen in PHQ-2 scores with a decrease between Baseline (mean ± standard error; 15.2 ± 0.3) and post home trial (0.6 ± 0.2) and in week 16 post treatment (0.9 ± 0.3). As this is an ongoing clinical trial, a statistical analysis will not be performed until the completion of the study.

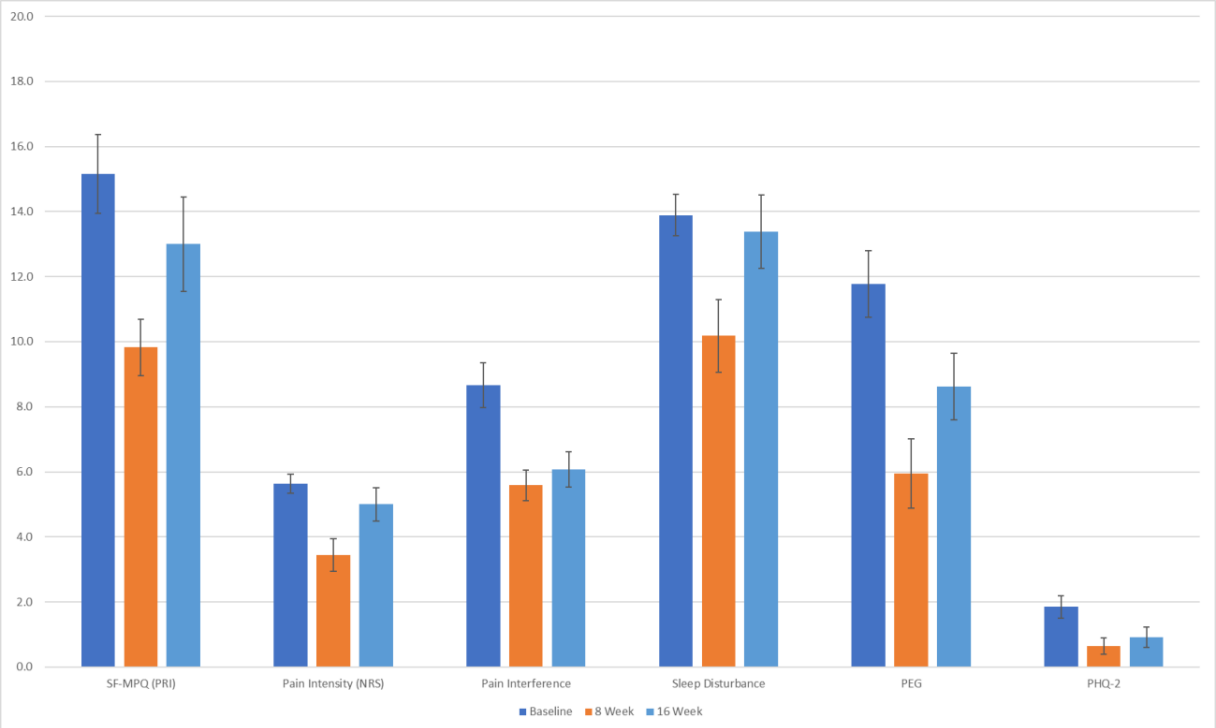

DISCUSSION

The initial findings suggest that the PLP-MS therapy may effectively lower PLP across participants with either upper or lower limb absence. It seems symptoms may recur after stopping the treatment, in line with previous studies [11]. Participants reported feeling less pain in terms of both intensity and frequency while using the PLP-MS, and many wanted to continue their treatment past the first 8 weeks. This clinical trial is still in progress and a thorough statistical analysis will be performed after it is completed. Further analyses will also examine how the outcomes may be influenced by different factors, such as the level of limb-difference and the frequency of device use. However, we are encouraged by the preliminary trends observed in the pain-related outcome measures and the initial feedback about the overall usability and functionality of the PLP-MS as a method of at-home PLP treatment that we've received from study participants.

A key and distinctive feature of this work is that it can be delivered remotely using telerehabilitation methods and adherence to device use can be tracked using the connected health platform. Clinicians can also monitor whether participants are using the device as instructed, and through quick inspection of their EMG signals recorded during user calibrations and virtual gameplay, they can confirm that they are trying to perform, rather than imagine, the specified movements. This study successfully demonstrates the accessibility of VR-based therapy for PLP management through the use of a portable system with cloud connectivity, allowing individuals to independently perform their own treatment, in their daily life. Additionally, the VR approach offers a safe alternative without drug-related side-effects, which could provide lasting relief for those who suffer from PLP.

ACKNOWLEDGEMENTS

This work was supported by the Assistant Secretary of Defense for Health Affairs, through the Defense Health Program, Congressionally Directed Medical Research Programs, Defense Medical Research and Development Program, Joint Program Committee 8 / Clinical and Rehabilitative Medicine Research Program, Restoring Warfighters with Neuromusculoskeletal Injuries Research Award under Award No. W81XWH2010873. Opinions, interpretations, conclusions, and recommendations are those of the author and are not necessarily endorsed by the Department of Defense.

The PLP-MS was developed jointly by research and development engineers at Coapt, LLC (Xavier Olberhelman, Katie Cai, MS) and Liberating Technologies, Inc. (Carlos Martinez).

REFERENCES

[1] "ASPN - Quantifying Pain Following Amputation: A Large Scale Outcomes Analysis From 768 Survey Respondents." [Online]. Available: https://peripheralnerve.org/meeting/abstracts/2018/PN106.cgi.

[2] P. L. Ephraim, S. T. Wegener, E. J. MacKenzie, T. R. Dillingham, and L. E. Pezzin, "Phantom pain, residual limb pain, and back pain in amputees: Results of a national survey," Arch. Phys. Med. Rehabil., vol. 86, no. 10, pp. 1910–1919, 2005.

[3] H. Knotkova, R. A. Cruciani, V. M. Tronnier, and D. Rasche, "Current and future options for the management of phantom-limb pain," Journal of Pain Research, vol. 5. pp. 39–49, 2012.

[4] D. Fernández-Espejo, S. Rossit, and A. M. Owen, "A thalamocortical mechanism for the absence of overt motor behavior in covertly aware patients," JAMA Neurol., vol. 72, no. 12, pp. 1442–1450, Dec. 2015.

[5] M. Lotze, W. Grodd, N. Birbaumer, M. Erb, E. Huse, and H. Flor, "Does use of a myoelectric prosthesis prevent cortical reorganization and phantom limb pain? [2]," Nature Neuroscience, vol. 2, no. 6. pp. 501–502, Jun-1999.

[6] C. Dietrich et al., "Leg prosthesis with somatosensory feedback reduces phantom limb pain and increases functionality," Front. Neurol., vol. 9, no. APR, Apr. 2018.

[7] M. Ortiz-Catalan et al., "Phantom motor execution facilitated by machine learning and augmented reality as treatment for phantom limb pain: a single group, clinical trial in patients with chronic intractable phantom limb pain," Lancet, vol. 388, no. 10062, pp. 2885–2894, Dec. 2016.

[8] B. N. Perry, A. L. Alphonso, J. W. Tsao, P. F. Pasquina, R. S. Armiger, and C. W. Moran, "A Virtual Integrated Environment for phantom limb pain treatment and Modular Prosthetic Limb training," in 2013 International Conference on Virtual Rehabilitation, ICVR 2013, 2013, pp. 153–157.

[9] P. U. Dijkstra, J. H. B. Geertzen, R. Stewart, and C. P. Van Der Schans, "Phantom pain and risk factors: A multivariate analysis," J. Pain Symptom Manage., vol. 24, no. 6, pp. 578–585, Dec. 2002.

[10] L. I. Strand, A. E. Ljunggren, B. Bogen, T. Ask, and T. B. Johnsen, "The Short-Form McGill Pain Questionnaire as an outcome measure: Test-retest reliability and responsiveness to change," Eur. J. Pain, vol. 12, no. 7, pp. 917–925, Oct. 2008.

[11] M. Ortiz-Catalan et al., "Phantom motor execution facilitated by machine learning and augmented reality as treatment for phantom limb pain: a single group, clinical trial in patients with chronic intractable phantom limb pain," Lancet, vol. 388, no. 10062, pp. 2885–2894, Dec. 2016.

PROSTHESIS RECEIPT IS ASSOCIATED WITH IMPROVED PARTICIPATION AND DECREASED PAIN FOLLOWING UPPER LIMB AMPUTATION

Dwiesha L. England, MS, Bretta L. Fylstra, PhD, Todd J Castleberry, PhD, Phillip M. Stevens MEd, Shane R. Wurdeman, PhD

Hanger Institute for Clinical Research and Education, Austin, TX, USA

ABSTRACT

Resuming activities of daily living and lifestyle participation are primary goals for patients following upper limb amputation. In many cases, an appropriately designed and fitted prosthesis can contribute to achieving these goals by increasing physical function and overall well-being. Pain interference constitutes another pervasive challenge experienced by this population. The objective of this study was to investigate the impact of first prosthesis receipt upon two health domains - Ability to Participate in Social Roles and Activities (APSRA) and Pain Interference (PI) as measured using the PROMIS suite of patient-reported outcomes. Univariate model results demonstrated a significant improvement in APSRA T-scores after first prosthesis receipt (Baseline: 41.6±7.82 and Follow-up: 47.2±9.70, p=<0.001). Additionally, there was a significant reduction in PI T-scores following receipt of first prosthesis (Baseline: 59.8±8.46 and Follow-up: 55.7±9.56, p= <0.001). Importantly, these significant differences persisted even after controlling for potential confounding effects of age, hours worn, sex, amputation level, time since amputation, and time from first prosthesis delivery to follow-up. APSRA and PI have previously been identified as being closely correlated with well-being in this population. The increased APSRA and decreased PI associated with first prosthesis receipt in this population appears to contribute to the larger goal of enhanced well-being following upper limb amputation.

INTRODUCTION

Upper limb amputation (ULA) has a profound and severe impact on one's well-being. Not only is it associated with immediate and obvious deficits in physical function, it is also visibly apparent, affecting body image and social stigma. Other areas of concern include pain in the affected side, over-use injuries in the unaffected side, psychological and emotional distress, and restriction with participation in social roles and activities [1]. Recently, the Patient-Reported Outcomes Measurement Information System (PROMIS) [2] designed generic instruments to assess a broad range of health care domains including the Ability to Participate in Social Roles and Activities (APSRA), Pain Interference (PI), and Physical Function. The latter has been investigated previously using the PROMIS-9 UE Physical Function specifically for individuals receiving their first prosthesis [3]. However, little is known about the longitudinal impacts of prosthesis receipt upon the domains APSRA and PI.

The provision of a prosthetic device can alter a patient's care pathway. In a recent cross-sectional study, patients who received an upper limb device showed significant improvement in their physical function scores compared to those who did not have a prosthesis [4]. In another cross-sectional study, both APSRA and PI were observed to be significant predictors of well-being in persons with ULA [5]. However, ability of the PROMIS APSRA to track differences before and after the provision of a prosthetic intervention is unclear. Tracking these outcomes longitudinally may provide valuable insights to the rehabilitation care team on patient progress in addition to the patient themselves, resulting in shared decision-making between patients and the rehabilitation team.

Pain is another health indicator that profusely affect persons with ULA. One study reported that out of 104 respondents with ULA, 90% reported pain in the first 6 months following amputation [6]. Furthermore, they concluded that these pain types are associated with disability and activity interference. In another cross-sectional study consisting of 250 respondents, PI was significantly and negatively associated with well-being [5]. The literature has mixed results on the impact of a prosthesis on pain after amputation, with some studies reporting decreased pain, while others report increased pain [7].

Therefore, the aim of this study was to assess the impact of the provision of first prosthesis on APSRA and PI scores. Comparisons were made between the baseline appointment (before prosthesis delivery) and at follow-up (after prosthesis delivery).

METHOD

Study design and participants

A retrospective longitudinal assessment of outcomes among patients with upper limb amputation was performed. Outcomes were included for patients who had an initial outcome collected before the initiation of a first prosthesis and had a follow-up outcome captured at least 2-weeks after the receipt of first prosthesis. There was no exclusion based on level of upper limb amputation, side of amputation, or device type. This database review was approved by the Western Copernicus Group Institutional Review Board (protocol #20170059) and designated to be exempt from informed consent.

Measures

The PROMIS v2.0 Ability to Participate in Social Roles and Activities 4a (APSRA), utilized in this study, assesses one's perceived ability to perform social roles and activities. The APSRA is comprised of 4 items evaluating respondent's ability to perform leisure activities, family activities, usual work, and activities with friends. The APSRA was scored using HealthMeasures Scoring Services, which uses response pattern scoring. Response pattern scoring accounts for item difficulty and missing data. In addition, raw scores are converted to T-scores with a T-score score of 50 represents the average for the general United States population. Higher T-score indicate better ability to perform social roles and activities and the standard deviation of the converted score is 10 points. PI was captured using question PAININ9 from the PROMIS v1.1 Pain Interference item bank. The question captures the magnitude of pain interfering with one's daily activities in the past 7 days. Similar to the APSRA, pain interference was scored using HealthMeasures scoring service. Raw scores were converted to T-scores, with higher scores representing worse pain experience.

Statistical analysis

Patient demographics were described using means, standard deviation, and frequencies. A paired t-test was used to compare APSRA and PI scores before and after first prosthesis receipt. Two subsequent multivariate mixed models were then applied to control for possible confounding effects such as, age, hours worn, sex, amputation level, time since amputation, and time from first prosthesis delivery to follow-up.

RESULTS

A final sample size of 75 patients with upper limb amputation were included in the analysis. From this sample, 68% were male, 87% had a below-the-elbow amputation, 76% had a body-powered device, and 56% had injury as the cause of amputation Results from our univariate analysis showed a significant improvement in APSRA scores after the receipt of first prosthesis (Baseline: 41.6±7.82 and follow-up: 47.2±9.70, p=<0.001). Similarly, there was a significant reduction in PI scores following first prosthesis delivery (Baseline: 59.8±8.46 and follow-up: 55.7±9.56, p= <0.001). Importantly after adjusting for the confounding effects of age, hours worn, sex, amputation level, time since amputation, and time from first prosthesis delivery to follow-up significant differences persisted for both models (table 1).

Table 1: Linear Mixed Effect Model for APSRA and PI (n=75)

	Estimate	**95% Confidence Interval**		**P**
		Lower bound	Upper bound	
Model 1: Linear Mixed Effect Model for APSRA				
First Prosthesis Intervention				
Baseline	ref			
Follow-up	5.60	3.84	7.361	< 0.001
Model 2: Linear Mixed Effect Model for PI				
First Prosthesis Intervention				
Baseline	ref			

Follow-up	-4.133	-5.952	-2.315	<0.001

DISCUSSION

The current study's main finding demonstrated that upper limb prosthesis users tend to report improvement in APSRA T-scores following first prosthesis receipt. In this study, the average increase in APSRA T-score was 5.6, which is comparable to the recommendation of a 5-point change in score as a reasonable Minimal Clinically Important Differences (MCID) for PROMIS instruments [8]. The use of a converted T-scores facilitates a recognition that prior to prosthesis receipt, affected individuals have, on average, activity and participation scores that are approximately one standard deviation below the population mean, placing them in approximately the 15th percentile for this construct among the population. With the receipt of their first prosthesis, the average APSRA scores improved to a level that approximates the mean levels of the general population. This increase in score may indicate engagement and satisfaction with device immediately following surgery among persons with ULA leading to the willingness of respondents to engage in activities involving leisure, family, friends, and work. While it is unknown how long patients will continue see improvement in APSRA or the impact of other factors to dampen this engagement across time, future studies may investigate longitudinal life trajectory of patients with ULP. These future findings can determine what device types can maintain or improve APSRA over a longer timeframe, which may be important for community re-integration following a major life event such as an amputation.

Our findings also indicate a reduction in PI among upper limb prosthesis. Before the receipt of an upper limb prosthesis, respondents reported an average pain interference score of 59.8±8.46. The use of a converted T-score facilitates a recognition that prior to prosthesis receipt, affected individuals report pain interferences levels that are approximately one standard deviation above the general population, placing them in approximately the 15th percentile for this construct. At least 2 weeks after the receipt of an upper limb prosthesis device the score decreased to 55.7±9.56, placing these individuals within one standard deviation of population averages. This change in score of an average of 4.1 points is approaching the MCID and future work should continue to track this change over a longer timeframe. Although it is unclear what factors may have caused this reduction in pain interference score, one study suggests that an increased use of a certain prosthesis types reduces certain pain types [9]. Alternate factors might include continued healing and recovery from the original injury and an additional area of cognitive focus as patients devote their thoughts to functional activity rather than their pain experience.

This study has a few limitations. Only persons who received an upper limb prosthesis were included, which means the study's findings may not be generalizable non-prosthesis users. Secondly, the time between prosthesis delivery and the follow-up assessment was not standardized. The follow-up assessment was collected as a part of routine clinical care. Because of this, some patients may have returned without any problems while other patients may have returned due to a problem. Therefore, there are no guarantees that the follow-up appointment represents the highest possible performance after prosthesis receipt. Lastly, while the exact estimate for MCID for APSRA and PI among persons with ULA is unknown, future studies can estimate the MCID using the distribution or anchor-based approaches for individuals in the upper limb amputation population.

CONCLUSION

The current study's findings support the use of the APSRA and PI assessment instruments to track changes following the provision of an upper limb prosthesis. Specifically, receipt of a first prosthesis is associated with greater participation in social roles and activities and decreased pain interference. Using these instruments can provide valuable insight to the rehabilitation on patient progress and aid in goal setting.

REFERENCES

[1] A. Hutchison, K. D'Cruz, P.Ross, and S. Anderson. "Exploring the barriers and facilitators to community reintegration for adults following traumatic upper limb amputation: a mixed methods systematic review." *Disability and rehabilitation* pp 1-14, 2023

[2] D. Ader, "Developing the patient-reported outcomes measurement information system (PROMIS)." *Medical care*, vol 45, no. 5, S1-S2, 2007: S1-S2.

[3] T. Castleberry, D. England, P. Stevens, A. Todd, S. Mandacina, S. Wurdeman. "PROMIS-9 UE Physical Function Demonstrates Good Responsiveness for Patients Following Upper Limb Prosthesis Intervention". Not yet published.

[4] DL. England, T. A. Miller, P. M. Stevens, J. H. Campbell, and S. R. Wurdeman. "Assessment of a nine-item patient-reported outcomes measurement information system upper extremity instrument among individuals with upper limb amputation." *American Journal of Physical Medicine & Rehabilitation* vol 100, no. 2, pp 130-137, 2021.

[5] PM. Stevens, D.L. England, A. E. Todd, S. A. Mandacina, and S. R. Wurdeman. "Activity and Participation, Bimanual Function, and Prosthesis Satisfaction are Strong Predictors of General Well-Being Among Upper Limb Prosthesis Users." *Archives of Rehabilitation Research and Clinical Translation* vol 5, no. 2, 100263, 2023.

[6] M.A. Hanley, D. M. Ehde, M. Jensen, J. Czerniecki, D. G. Smith, and L. R. Robinson. "Chronic pain associated with upper-limb loss." *American journal of physical medicine & rehabilitation/Association of Academic Physiatrists*, vol 88, no. 9, pp 742-779, 2009.

[7] K.A. Raichle, M. A. Hanley, I. Molton, N. J. Kadel, K. Campbell, E. Phelps, D. Ehde, and D.G. Smith. "Prosthesis use in persons with lower-and upper-limb amputation." *Journal of rehabilitation research and development* vol 45, no. 7, pp 961-972, 2008.

[8] K Khutok, J. Prawit, M. P. Jensen, and R. Kanlayanaphotporn. "Responsiveness of the PROMIS-29 scales in individuals with chronic low back pain," *Spine*, vol 46, no. 2. Pp 1-7-113, 2021.

[9] M. Lotze, W. Grodd, N. Birbaumer, M. Erb, El Huse, and H. Flor. "Does use of a myoelectric prosthesis prevent cortical reorganization and phantom limb pain?." *Nature neuroscience*, vol 2, no. 6, pp 501-502, 1999.

UN*LIMB*ITED WELLNESS: PROGRAM EXPANSION

Latour, D1,2; Hodgson, MC 2

Author Western New England University, 1; Handspring Clinical Services, 2

ABSTRACT

Individuals with upper limb absence face unique challenges, including limited access to specialized services and social support, contributing to pain, overuse, and isolation. The Unlimbited Wellness© program, developed to address these needs, utilizes telehealth to connect participants with peers and provide education and support. Implemented by occupational therapy students and practitioners, the program offers interprofessional interventions focusing on physical and psycho-social health, return-to-work, relationships, and recreation. Surveys and thematic analysis of pre- and post-surveys indicate improved perceptions of health, well-being, and prosthetic satisfaction among participants. Telehealth emerges as a viable option for reaching and empowering individuals with upper limb absence, reducing disparities, and improving quality of life. Clinical applications highlight the potential for telehealth to connect specialists and peers, improving care delivery and reducing disparity in access to specialized services.

INTRODUCTION

Individuals with upper limb absence are typically outnumbered by individuals with lower limb loss by a 1:4 ratio, and often require specialized services, including occupational therapy that may be difficult to access. Also, individuals are likely to encounter secondary conditions that include pain, overuse, perceptions of isolation, and social stigma. There is often a lack of access to specialized resources and medical care, or to meet peers. The Unlimbited Wellness© program was developed to meet the needs vocalized by the target population, offering a pathway using telehealth to access peers, and to become better informed about strategies that would help to prevent physical overuse, social isolation and facilitate improved self-advocacy skills with medical practitioners. Its ultimate aims were to promote health and well-being by educating, engaging and empowering people with upper limb absence. The program has expanded annually since 2021 through the efforts of 11 (3-5 students per year) entry-level doctor of occupational therapy students, who functioned with the mentorship of an occupational therapist and prosthetist to produce several series of interprofessional interventions. The students developed an on-campus telehealth center and collaborated with Handspring Clinical Services to implement the series with new components.

METHOD

Un***limb***ited Wellness© is based on results of ongoing needs assessments that specifically focus on the challenges experienced by this population. Participants of the Un***limb***ited Wellness© program interacted with peers via a telehealth model to learn about physical and psycho-social health conditions that may cause them disparity, prosthesis use/non-use, and to share strategies to prevent or manage them. Students expanded the original program to include additional topics and population subgroups. These include return-to-work, relationships and intimacy, fitness, and recreation including a hippotherapy ground program. Every iteration of Un***limb***ited Wellness© being reported has undergone the IRB process and been approved under exempt status as it is related to program expansion. Written informed consent was obtained under the guidelines and approval of AT Still University and Western New England University Research Ethics Boards prior to conducting these efforts.

Subjects: Approximately 30 adults with unilateral or bilateral upper limb absence

Apparatus: Surveys including the McGann Client Feedback Form, the Quick DASH; ADL questionnaires; educational materials

Procedures: Weekly meetings were held over the course of five to eight weeks per year addressing areas of physical overuse, prevention, medical conditions, awkward social experiences, intimacy and return to work. Participants were supplied with information and collaborative worksheets to advance engagement, knowledge and skill development.

Data Analysis: Thematic analysis of pre- and post-surveys; transcripts.

RESULTS

Effectiveness of the program was assessed via a survey of participant telehealth experiences and changes in perceptions of pain, ability, and quality of life as measured by the McGann Client Feedback Form, QuickDASH, Role Checklist, and custom surveys. Results suggest that the remote support group concept was effective to connect and to educate participants of all ages, levels of upper limb absence, and etiology. Overall, participant post-group perceptions of health, well-being, and prosthetic satisfaction, improved as compared to pre-group experiences. During the 1:1 interviews, all participants stated they felt empowered due to their engagement in peer discussions and collaborative exercises during the diverse foci of the Un***limb***ited Wellness© program.

DISCUSSION & CONCLUSION

Strengths of this study were the support of community partners, the passion of the investigators, and most importantly the interest and resilience of the participants. Weaknesses appeared in the challenge of engaging larger numbers of the population, probably complicated by COVID impact. Telehealth appears to be a viable option to reach unique population groups, educate them and engage them in peer and rehabilitative activity. Ultimately this effort serves to empower the population and to improve their perceived quality of life. The original Un***limb***ited Wellness© article has served as a foundation to other studies relating to the impact of care management for this population. The next iteration, planned for Spring 2024 includes occupational therapy students and practitioners who present with upper limb absence. New modules engage participants to address challenges related to the impact of stigma affecting work skills and professional relationships.

The program results indicate that a telehealth service delivery can be beneficial to enact health behavior change and empower individuals with upper limb absence.

CLINICAL APPLICATIONS

Clinical application is apparent in the discrepancy of adequate specialized practitioners to offer care to the population. Telehealth pathways can connect specialists, and peers to each other toward improved care, and reduction in disparity.

REFERENCES

[1]Braza, D.W. & Yacub Martin, J.N. Essentials of physical medicine and rehabilitation 2020.

[2]Kyberd, P. Assessment of Functionality of Multifunction Hands, Journal of Prosthetics and Orthotics; 2017.

[3]Latour, D. Un*limb*ited Wellness: Telehealth for Adults with Upper Limb Difference, Journal of Prosthetics and Prosthetics; 2019.

[4]Ostlie, K et al. Disability and Rehabilitation; 2011.

[5]Resnik, L.J., Borgia, M.L., Clark, M.A. Prevalence and Predictors of Unmet Need for Upper-Limb Prostheses; An Observational Cohort Study, Journal of Prosthetics and Orthotics; 2024

USER PERSPECTIVES ON FEATURES OF UPPER LIMB PROSTHESES: A QUALITATIVE CROSS-CASE COMPARISON

Melissa S. Schmitt[1-3], Alexandra Zanowick-Marr[1,2], Debra Kelty[4], Linda J. Resnik[4,5], Emily L. Graczyk[1,2]

[1] Department of Biomedical Engineering, Case Western Reserve University, Cleveland, OH
[2] Louis Stokes Cleveland Department of Veterans Affairs Medical Center, Cleveland, OH
[3] Francis Payne Bolton School of Nursing, Case Western Reserve University, Cleveland, OH
[4] Providence Department of Veterans Affairs Medical Center, Providence, RI
[5] Health Services, Policy and Practice, Brown University, Providence, RI

ABSTRACT

Researchers and prosthesis developers aim to add or modify the functional features of upper limb prosthetic devices, such as increasing the number of available movements, developing intuitive control schemes, and providing sensory feedback. However, user experiences with these features across currently available prosthetic devices are not well understood, nor do we know what the needs and perspectives of users are regarding prosthesis features. In this study, we collected in depth interviews with sixteen prosthesis users who had experience with a wide range of prosthesis types, including body-powered, single degree of freedom myoelectric, multi-degree of freedom myoelectric, and sensory augmentation. We used a qualitative case study design to examine experiences with and perspectives on the prosthesis features of movements, controls, terminal devices, and sensation. Study findings help to elucidate the current needs and preferences of upper limb prosthesis users and provide directions for future technology development.

INTRODUCTION

Upper limb amputation (ULA) can result in adverse outcomes, including chronic pain[1]–[3], anxiety, and depression[4], [5]. Though upper limb prosthesis use can mitigate adverse health outcomes by enhancing functional independence, reducing activity restrictions, improving community integration[6], and enhancing quality of life, approximately 21-44% of adults with ULA do not use prostheses at all [7], [8]. Studies to investigate the reasons for prosthetic abandonment have described dissatisfaction with weight, function[8], [9], and the lack of sensory feedback[10], [11].

The number and complexity of prosthetic device options available to individuals with ULA have increased significantly in the past decade[12]. To improve user experience and function, many research groups and prosthesis developers aim to increase the available features of upper limb prosthetic devices. These advanced prosthesis features span several domains, including prosthesis movements, control strategies, and sensory feedback. For example, devices have been developed that provide multi-articulated finger movements, multiple grasp types, intuitive control strategies via pattern recognition algorithms, powered wrist movements, and/or sensory feedback provided through wearable or implanted interfaces[13]. However, it is unclear which additional features users want and need, and which features will have meaningful impacts on functional and psychosocial outcomes.

Prior studies to assess participant experiences with and perspectives on prosthesis features typically focus on a single prosthesis feature or technology [11], [14], [15]. In addition, many user experience studies are purely hypothetical, in which participants are asked to imagine what a technology or feature might be like in the future. To address this gap, we performed a telephone interview study investigating the perspectives of sixteen participants with transradial or transhumeral limb loss who had experience using a wide variety of both commercial and research prosthetic technologies. We performed a qualitative analysis with multiple case series design to examine their personal experiences with the prosthesis features of control scheme, prosthesis movements, sensory feedback, and terminal device type. The participants perspectives and opinions on the features were informed by their personal experience. Improving our understanding of the connection between prosthesis features and the multifaceted experiences of prosthesis users will help guide prosthesis research and development efforts to better address user needs. Improved prosthesis designs could reduce prosthesis abandonment and improve quality of life after limb loss.

METHODS

Data for this study was collected by telephone interview as part of a larger, parent study which utilized a modified grounded theory approach. Participants were recruited through mailings, advertisements and referrals from prosthetists and rehabilitation health care providers. Eligible participants were at least 18 years old and experienced an transhumeral or transradial amputation

and had utilized a prosthesis for at least 6 months. A convenience sample of 16 individuals were enrolled into four groups of four participants each based on the prosthesis they used. The groups were: body-powered (BP) prosthesis, myoelectric single-degree-of-freedom (1-DoF) prosthesis, myoelectric multiple-degree-of-freedom (multi-DoF) prosthesis, and sensory augmented (SA) prosthesis. Written informed consent was obtained under the guidelines and approval of the United States Central Veterans Affairs Institutional Review Board prior to conducting the interviews.

Each participant was interviewed by telephone for two 45-60-minute sessions. The interviews were semi-structured with follow-up questions and probes to elucidate important concepts. Each interview was recorded with a digital audio recorder and transcribed verbatim. Data from the first four interviews were utilized to develop an initial code set. This code set was iteratively refined during the analysis of all interviews. Coding was conducted by M.S. and D.K. and auditing was conducted by L.R. and E.G. Analytic discussions within the team were used to identify sub-codes, determine central themes, and elucidate relationships between codes. The coding structure was iteratively fine-tuned during team meetings, leading to the final coding structure.

RESULTS

Users of BP devices used a body-powered cable system to control a voluntary open hook. The 1-DOF myoelectric users used two-site myoelectric control, with sensors embedded in their prosthesis sockets. The multi-DOF myoelectric users used either Co-apt or another pattern recognition system with 6-14 myoelectric sensors. All of the BP and 1DoF device users controlled the aperture of the terminal device. Six participants had powered wrist movements, with the remaining ten having passive wrist movements that could be made by manually turning the wrist with the intact hand. Individuals with trans-humeral amputation voluntarily operated their elbow via cabling or myoelectric power.

All of the participants with SA experienced the technology as a part of a research study, with most of these experiences occurring primarily in a laboratory environment. Two of the participants (P02 and P15) had taken part in a clinical trial utilizing implanted peripheral nerve cuff electrodes[16], [17]. By stimulating the nerve through different electrode contacts around the nerve, the participant was able to experience sensation at different locations on their missing hand[18], [19]. Additionally, P15 had implanted EMG recording electrodes. P10 and P14 had previously undergone targeted sensory reinnervation (TSR) and had participated in a trial using non-invasive SA delivered via transcutaneous stimulation and/or vibration[20], [21]. Three of the four SA users had experience receiving sensory feedback incorporated into a multi-DOF prosthetic device, while one SA user had a 1-DOF myoelectric device.

The interviews examined experiences with four prosthesis features: 1) prosthesis movements, 2) prosthesis control, 3) terminal devices, and 4) sensory feedback. The coding structure developed through our analysis revealed a total of 16 nodes across the four feature categories (Table 1).

Prosthesis Movements: Participants were asked to describe the movements of their prosthesis and how these movements played a role in the function of their prosthesis and their experience with the prosthesis. Three main themes emerged from these discussions. First, participants described the process through which they completed tasks with the prosthesis as generally consisting of multiple sub-steps, which sometimes required them to manually *pre-position* one or more joints of the prosthesis before beginning the task. Second, participants described the positions in space in which the prosthesis was most useful and most easily operated. This *functional workspace* of the prosthesis was generally limited to areas directly in front of their torso. Third, participants described the need for *compensatory movements* of the shoulder to make up for missing degrees of freedom in the prosthesis, such as a lack of wrist movements.

Prosthesis Control: Discussions about prosthesis control primarily centred on the participants' ability to control the opening and closing of the terminal device (rather than proximal joint movements). Participants spoke about their ability to *regulate the grasp force* produced by their terminal device to accomplish tasks and the *role of focus in controlling grasp force.* Additional themes that emerged included the *naturalness and ease* of their control scheme as well as the *reliability and precision* of their control.

Terminal Devices: Most participants had more than one terminal device or had previously used multiple types of terminal devices. They discussed the tradeoffs between different terminal devices or the reasons they would wear specific terminal devices. In general, participants across device categories compared hooks to hand-shaped terminal devices, and participants who used myoelectric devices also compared 1-DOF hands to multi-DOF hands.

Sensory feedback: Participants discussed whether they received any sensation from their prosthesis and their experiences with this sensory feedback. In general, participants who used multi-DOF myoelectric prostheses had the least sensation from their prostheses, while BP users expressed being able to perceive and utilize sensation from their shoulder to indicate the aperture or pressure exerted by the prosthesis. Participants who used prostheses with sensory augmentation received much more detailed and realistic sensory information than users of commercial devices. Participants also discussed the impacts of sensory feedback on their *prosthesis function*, *confidence* in using the prosthesis, *embodiment* of the prosthesis, *focus* required to use the prosthesis, and *naturalness* of the prosthesis. The SA users typically found the sensation to be functionally useful, as well as beneficial for increasing confidence, decreasing focus, and promoting prosthesis embodiment.

Table 1. Coding structure and exemplars. Participants were trans-radial (TR) or trans-humeral (TH) and used BP, 1DOF, or Multi-DOF prostheses. Four participants had prior experience using a prosthesis with sensory augmentation (SA) as part of a research study.

	Node	Definition	Exemplar
Prosthesis Movements	Functional Workspace	Comments on limb/body position impacting prosthesis operation and how the socket and/or harnessing impact range of motion or prosthesis operation in certain positions.	*Let's say I'm in an airplane and I'm reaching for the overhead container, I might have to alter my movement, just because of the way my muscles are different in an extended position. (P011, TR, Multi DOF)*
	Compensatory movement	Comments on compensatory movements needed to accomplish tasks.	*Rotating the wrist passively is task specific... I don't really use that one a whole lot. I compensate with my shoulder and elbow for that (P16, TR, 1DOF).*
	Preplanning-Prepositioning	Comments about strategies and/or series of movements to prepare the prosthesis or an object before performing a task with the prosthesis.	*You have to do everything in a consecutive manner. I'm doing this, but the [prosthetic] elbow has to be locked in order for that to happen, so I have to think about positioning, clicking in place, and then doing it. (P03, TH, BP)*
	Movement preferences	Comments about desired or preferred movements of the prosthesis.	*To be able to grab something with four fingers or something simulating fingers would be night and day. (P13, TR, 1 DoF)*
Prosthesis Control	Grasp force regulation	Comments about controlling the strength of grasp force, maintaining grasp, or varying the grasp force for a task.	*Yeah, if there's something a little loose [in the grasp of the prosthesis], I can squeeze [my muscles] where it'll tighten up the hand. (P04, TH, Multi DoF)*
	Role of focus in grasp force	Comments about how focus or visual monitoring is needed to maintain prosthesis control and how lack of focus or distraction contributes to unintended prosthesis movements.	*As long as I pay attention to what I'm holding and how hard I'm holding it, not a problem. Like I said, I can pick up a potato chip and not break it, or I can break up a glass and shatter it. It's just focus. (P06, TR, 1 DoF)*
	Naturalness of Control	Comments about the sense of naturalness of the prosthesis control system and similarities/differences between controlling the prosthesis and controlling an intact hand.	*I really am feeling like I don't have to think about the way that the muscles are doing [activating] more than what the prosthesis is doing. So when I'm using the prosthesis and it's doing what I'm asking it to do… I feel like it's almost a bit of like the natural motion now. (P9, TR, 1DOF)*
	Reliability and precision of control	Comments about the dependability of prosthesis control, situations that make control unreliable, and experiences with involuntary or unpredictable prosthesis movements.	*It's actually a sensor issue. So, for example, the TASKA and the COAPT is calibrated when your arms are at a certain position. So, as you're extending your arm, you're changing the sensor positions, and from extending your arm and bringing it back, there could be times where the sensors will read differently and release the grasp that you have. (P011, TR, Multi DoF)*
	Control preferences	Comments about features or capabilities of the control system that would make it more effective.	*I mean anything you can do to make the calibration process easier, to make the calibration process more robust so that the calibration lasts longer and is a little more tolerant of like if the socket shifts in your arm. (S07, TR, Multi-DoF)*
Terminal Device	Terminal Device Preferences	Comments about preferred terminal devices or trade-offs between terminal devices and any specialty attachments they used for task specific needs.	*"There's things that I can do with that hook that I couldn't do with my [prosthetic] hand, so the things that I do that I have done with my prosthetic hook, it would probably break my [prosthetic] fingers or my hand or wrist or something if I had the [prosthetic] hand doing the same task." (P1, TR, BP)*
Sensory Feedback	Sensation Experience	Comments about the location, modality, and intensity of the sensation provided by the prosthetic hand or prosthesis suspension/harnessing.	*I enjoyed getting that sensation back, sometimes as small as a pencil lead, and then it can be as much as my whole hand, depending on what kind and where I'm being stimulated on my nerve. (P15, TR, Multi DoF, SA)*
	Functional impact of sensation	Comments about the usefulness of information provided by sensation and how sensation helped (or did not help) with prosthesis task performance.	*I learned about how much pressure each different vibration was; it didn't take much concentration at all to be able to reach out 'cause you knew as soon as you hit that certain buzz, that was it. You just pick it up and go. (S10, TH, Multi-DoF, SA)*
	Role of sensation in confidence	Comments about how sensation enhanced confidence or how lack of sensation reduced confidence and contributed to task avoidance.	*It's [the sensory feedback] boosting my confidence, and then I know I can do this [task] where it's not going to frustrate me, and I can get it done. (P14, TH, Multi DoF, SA)*
	Role of sensation in focus	Comments about how sensory feedback impacts the need for focus and attention, and how sensory feedback reduces the need for visual monitoring during task performance.	*The sensory hand doesn't take as much focus as without it [sensation] because I can feel what I'm holding. I can feel that I'm squeezing tight enough to hold onto something, so I don't necessarily pay as much eye-contact attention as without it. (P02, TR, 1 DoF, SA)*

	Role of sensation in naturalness	Comments about how sensory feedback enhances the naturalness of the prosthesis experience and/or control. Comments about how sensation contributes to making the prosthesis feel like a real hand.	*When I've got it [sensation] on and I can feel, it feels like my hand is there. It feels like my hand's out where it should be, and I can feel when I'm touching, grabbing, and doing things, and without it, it feels like it's [my hand's] gone. (P02, TR, 1 DoF, SA)*
	Sensation preferences	Comments about preferences for the type, intensity, or amount of sensory feedback from the prosthesis.	*I don't have any sensory stuff that tells me [what my prosthesis is doing]. I wish I did. It's kind of weird; you shake someone's hand, and you can't feel it. (P04, TH, Multi DoF)*

CONCLUSION

This study is one of the first to compare user perspectives on functional features of upper limb prostheses across body-powered, 1-DoF myoelectric, multi-DoF myoelectric, and sensory augmented device groups. Use of semi-structured interviews enabled our participants to guide conversations and organically delve into topics they considered important to their lives. The themes that emerged within our analysis will help to elucidate the complex and multifaceted interplay between functional features and user experience across a diverse range of device types. Therefore, our findings provide invaluable insight into the expectations and experiences of prosthesis users and the practical utility of prosthesis functional features. Findings from this study will inform researchers, clinicians, and prosthesis developers about the impact of functional features on the use and adoption of prosthetic devices, and will enable future development of prostheses that better meet user needs.

REFERENCES

[1] E. Balakhanlou, J. Webster, M. Borgia, and L. Resnik, "Frequency and Severity of Phantom Limb Pain in Veterans with Major Upper Limb Amputation: Results of a National Survey," *PM R*, vol. 13, no. 8, pp. 827–835, 2021, doi: 10.1002/pmrj.12485.

[2] J. H. Davidson, K. E. Khor, and L. E. Jones, "A cross-sectional study of post-amputation pain in upper and lower limb amputees, experience of a tertiary referral amputee clinic," *Disabil. Rehabil.*, vol. 32, no. 22, pp. 1855–1862, 2010, doi: 10.3109/09638281003734441.

[3] M. T. Schley *et al.*, "Painful and nonpainful phantom and stump sensations in acute traumatic amputees," *J. Trauma - Inj. Infect. Crit. Care*, vol. 65, no. 4, pp. 858–864, 2008, doi: 10.1097/TA.0b013e31812eed9e.

[4] D. M. Desmond, "Coping, affective distress, and psychosocial adjustment among people with traumatic upper limb amputations," *J. Psychosom. Res.*, vol. 62, no. 1, pp. 15–21, 2007, doi: 10.1016/j.jpsychores.2006.07.027.

[5] P. S. Mckechnie and A. John, "Anxiety and depression following traumatic limb amputation: A systematic review," *Injury*, vol. 45, no. 12. Elsevier Ltd, pp. 1859–1866, 2014, doi: 10.1016/j.injury.2014.09.015.

[6] A. Hutchison, K. D'Cruz, P. Ross, and S. Anderson, "Exploring the barriers and facilitators to community reintegration for adults following traumatic upper limb amputation: a mixed methods systematic review," *Disabil. Rehabil.*, 2023, doi: 10.1080/09638288.2023.2200038.

[7] E. Biddiss and T. Chau, "Upper limb prosthesis use and abandonment: A survey of the last 25 years," *Prosthetics and Orthotics International*, vol. 31, no. 3. pp. 236–257, 2007, doi: 10.1080/03093640600994581.

[8] S. Salminger *et al.*, "Current rates of prosthetic usage in upper-limb amputees–have innovations had an impact on device acceptance?," *Disabil. Rehabil.*, vol. 44, no. 14, pp. 3708–3713, 2022, doi: 10.1080/09638288.2020.1866684.

[9] L. C. Smail, C. Neal, C. Wilkins, and T. L. Packham, "Comfort and function remain key factors in upper limb prosthetic abandonment: findings of a scoping review," *Disabil. Rehabil. Assist. Technol.*, vol. 16, no. 8, pp. 821–830, 2021, doi: 10.1080/17483107.2020.1738567.

[10] E. Biddiss and T. Chau, "Upper-Limb Prosthetics: Critical Factors in Device Abandonment," *Am. J. Phys. Med. Rehabil.*, vol. 86, no. 12, pp. 977–987, 2007, doi: 10.1097/PHM.0b013e3181587f6c.

[11] L. Jabban, B. W. Metcalfe, J. Raines, D. Zhang, and B. Ainsworth, "Experience of adults with upper-limb difference and their views on sensory feedback for prostheses: a mixed methods study," *J. Neuroeng. Rehabil.*, vol. 19, no. 1, pp. 1–18, 2022, doi: 10.1186/s12984-022-01054-y.

[12] A. Marinelli *et al.*, "Active upper limb prostheses: a review on current state and upcoming breakthroughs," *Prog. Biomed. Eng.*, vol. 5, no. 1, 2023, doi: 10.1088/2516-1091/acac57.

[13] T. J. Bates, J. R. Fergason, and S. N. Pierrie, "Technological Advances in Prosthesis Design and Rehabilitation Following Upper Extremity Limb Loss," *Curr. Rev. Musculoskelet. Med.*, vol. 13, no. 4, pp. 485–493, 2020, doi: 10.1007/s12178-020-09656-6.

[14] E. L. Graczyk, A. Gill, D. J. Tyler, and L. J. Resnik, "The benefits of sensation on the experience of a hand: A qualitative case series," *PLoS One*, vol. 14, no. 1, p. In press, 2019, doi: 10.1371/journal.pone.0211469.

[15] M. Luchetti, A. G. Cutti, G. Verni, R. Sacchetti, and N. Rossi, "Impact of Michelangelo prosthetic hand: Findings from a crossover longitudinal study," *J. Rehabil. Res. Dev.*, vol. 52, no. 5, pp. 605–618, 2015, doi: 10.1682/JRRD.2014.11.0283.

[16] D. W. Tan, M. A. Schiefer, M. W. Keith, J. R. Anderson, J. Tyler, and D. J. Tyler, "A neural interface provides long-term stable natural touch perception," *Sci. Transl. Med.*, vol. 6, no. 257ra138, pp. 1–12, Oct. 2014, doi: 10.1126/scitranslmed.3008669.

[17] E. L. Graczyk *et al.*, "The neural basis of perceived intensity in natural and artificial touch," *Sci. Transl. Med.*, vol. 8, no. 362ra142, pp. 1–11, 2016, doi: 10.1126/scitranslmed.aaf5187.

[18] M. A. Schiefer, E. L. Graczyk, S. Sidik, D. W. Tan, and D. J. Tyler, "Artificial tactile and proprioceptive feedback improves performance and confidence on object identification tasks," *PLoS One*, vol. 13, no. 12, pp. 1–18, 2018, doi: 10.1371/journal.pone.0207659.

[19] E. L. Graczyk, L. Resnik, M. A. Schiefer, M. S. Schmitt, and D. J. Tyler, "Home use of a neural-connected sensory prosthesis provides the functional and psychosocial experience of having a hand again," *Sci. Rep.*, vol. 8, no. 1, p. 9866, 2018, doi: 10.1038/s41598-018-26952-x.

[20] L. Osborn, J. Betthauser, R. Kaliki, and N. Thakor, "Targeted transcutaneous electrical nerve stimulation for phantom limb sensory feedback," *2017 IEEE Biomed. Circuits Syst. Conf. BioCAS 2017 - Proc.*, vol. 2018-Janua, p. 1, 2018, doi: 10.1109/BIOCAS.2017.8325101.

[21] L. E. Osborn *et al.*, "Sensory stimulation enhances phantom limb perception and movement decoding," *J. Neural Eng.*, vol. 17, no. 5, 2020, doi: 10.1088/1741-2552/abb861.